Neutrino physics and dark matter

A DISSERTATION PRESENTED

BY

SOFIANE M. BOUCENNA

TO

THE DEPARTMENT OF THEORETICAL PHYSICS

IN PARTIAL FULFILLMENT OF THE REQUIREMENTS

FOR THE DEGREE OF

DOCTOR OF PHILOSOPHY

IN THE SUBJECT OF

THEORETICAL PHYSICS

UNIVERSITY OF VALENCIA

VALENCIA, SPAIN

NOVEMBER 2014

Dr. José Wagner Furtado Valle, Professor de Investigación del CSIC.

CERTIFICA:

Que la presente memoria *Neutrino physics and dark matter*, ha sido realizada bajo su dirrección en el Departamento de Física Teórica de la Universidad de Valencia por Sofiane Mohamed Boucenna y constituye su tesis doctoral para optar al grado de Doctor en Física.

Y para que así conste, en cumplimiento con la legislación vigente, presenta ante el Departamento de Física Teórica, la referida memoria, firmando el presente certificado en Burjassot (Valencia) a 14 de Octubre de 2014.

Dr. José Wagner Furtado Valle

PhD Advisors:
Prof. José W.F. Valle
Dr. Stefano Morisi

Thesis Committee:
Prof. Stefan Antusch, Basel University — Switzerland.
Prof. Geneviève Bélanger, LAPTH — France.
Prof. Alejandro Ibarra, TUM — Germany.
Prof. Isabella Masina, Ferrara University — Italy.
Prof. Carlos Muñoz, IFT (UAM-CSIC) — Spain.
Prof. Sergio Pastor, IFIC (UV-CSIC) — Spain.

À mes parents.

Acknowledgments

I CANNOT EXPRESS ENOUGH GRATITUDE toward my advisor, and mentor Professor José Valle, for being so inspiring with his passion for physics, and so generous with his time. His ability to guide a work toward something more interesting without being overbearing, and to subtly drift me away from various intellectual pitfalls without being discouraging, created an environment of support and creative freedom which I have enjoyed tremendously. I owe this thesis to his mentorship.

To my co-advisor and friend Stefano Morisi, I am deeply grateful for his constant support, and for the hours and hours of discussions. Thanks for introducing me to the world of *model building*. With time, I have learned to embrace and tolerate the inherent messiness that accompany such an activity.

It is with great pleasure that I utter my gratitude to Martin Hirsch, for his constant availability to discuss and answer my questions —from the down to earth experimental ones up to the 'philosophical' ones. I have greatly benefited from such discussions. My warm thanks go also to Sergio Pastor for his pragmatic recommendations, and specially for his precious help and assistance during difficult bureaucratic situations.

I am indebted to the members of the committee of my thesis for generously accepting to review the manuscript.

I wish to thank the co-authors of all the papers that are listed below for the excellent collaborations. And to be fair, I have also to mention the co-authors of the *unwritten* papers. Whether the model had been mercilessly ruled out by data, or because of some particular life circumstance*, I thank Diego Aristizabal, Lotfi Boubeker, David Cerdeño, Nicolao Fornengo, Massi Lattanzi, Stefano Morisi, Daniel Schmidt, Marco Taoso, José Valle, Andrea Vittino, and Bryan Zaldivar for collaborating in various projects.

*In which case, there's still hope to finish the project!

As part of Astroparticle and High Energy Physics (AHEP) group, I have had the pleasure to meet excellent physicists. I am particularly grateful to Michal Malinský, Qaisar Shafi, David Cerdeño, Sandip Pakvasa, and Renato Fonseca for insightful discussions. I am also very grateful to the group for allowing me to go to many conferences and schools.

In the 'students sector', I thank all my colleagues and friends for sharing so many things. Avelino, Carolina, David, Laslo, Lucho, Urbano, and Valentina deserve special thanks.

During the thesis, I had the chance to do two long stays abroad:

- in California — USA: I thank Stefano Profumo for hosting me and for the excellent collaboration. I thank all the theory (SCIPP) group of UCSC, in particular Lorenzo Ubaldi and Sebastian Grab; and
- in Turin — Italy: thanks to Nicolao Fornengo for hosting me there. It is with pleasure that I thank the inhabitants of the 'bunker' of the physics faculty, specially Giulio and Andrea.

I also thank Michel Tytgat for generously inviting me for a short visit to Université Libre de Bruxelles, and the staff of KITPC — Beijing for having me there for a month.

Last but not least, I acknowledge financial support from the Spanish MICINN through grants FPA2011-22975 and Multidark CSD2009-00064 (MINECO), and PROMETEOII/2014/084 (Generalitat Valenciana). Special thanks to Prof. Carlos Muñoz for the financial support from Multidark.

Resumen

Neutrinos y Materia Oscura

El descubrimiento de las oscilaciones de neutrinos y la evidencia de la existencia de materia oscura, demuenstran la necesidad de una nueva física más allá del modelo estándar (SM). Sin embargo, la naturaleza detallada de la nueva física sigue siendo difícil de alcanzar. Por un lado, se desconoce el mecanismo responsable de generación de masa de los neutrinos y su estructura de sabor. Por lo tanto, la naturaleza de los neutrinos, su masa y parámetros de mezcla son todos impredichos en el SM. Por otro, la naturaleza de la materia oscura (DM) constituye uno de los problemas mas endémicos en la cosmología desde décadas, aunque recientemente algunos experimentos de detección directa e indirecta de DM están mostrando indicios que dan esperanza de una detección inminente.

La vinculación entre la generación de masa del neutrino y la naturaleza de la materia oscura, en un único marco, es teóricamente atractivo, y puede generar nuevas ideas sobre ambas cuestiones. La idea de la unificación en sí, o como Feynman solía llamarla *amalgamación*, es fundamental para la física, y en general para cualquier disciplina científica. Unificar es obtener nuevos conocimientos mediante la síntesis y generalización de los conocimientos.

Esta tesis está dedicada a la interacción entre la física de neutrinos y la materia oscura. Especialmente en el desarrollo y la comprensión de los modelos en los que la dinámica de la materia oscura y los neutrinos están relacionados. Mediante la conexión de la materia oscura con los neutrinos, es posible obtener información directa e indirecta sobre la nueva física. De hecho, los neutrinos ofrecen una manifestación notable de esta nueva física y varios experimentos nos proporcionan datos precisos sobre sus mezclas y masas. Estos datos revelan un fuerte contraste con el caso conocido de los quarks. Por las escalas de energía involucradas en el problema y la precisión de estas mediciones, la física de neutrinos ofrece una visión tentadora de uno de los problemas más profundos y duraderos del SM, a saber, el problema de sabor.

Plan de la tesis: Comenzaremos con una breve introducción del Modelo Estándar de la física de partículas y la notación que utilizaremos a lo largo de la tesis en el Capítulo (1). A continuación se presenta una introducción y una visión general de la física de la materia oscura y de los neutrinos en el Capítulo (2) y el Capítulo (3), respectivamente, y la revisión intentos de unificar su descripción en el Capítulo (4).

Empezamos la parte original de esta tesis en el Capítulo (5), donde se vinculan la materia oscura y los neutrinos a través de una simetría de sabor. Las simetrías de sabor, especialmente las basadas en grupos discretos no abelianos, proporcionan un motivo para abordar el problema de sabor a partir de primeros principios. La descripción unificada se consigue mediante la asignación de la DM a una representación irreducible del grupo de sabor. La ruptura de este grupo, que se requiere a fin de generar las masas y los patrones de mezcla, vincula la fenomenología de la DM con los neutrinos y estabiliza la DM al mismo tiempo. Presentaremos en detalle la fenomenología de un modelo que utiliza este mecanismo. El candidato de DM en el modelo emerge del triplete del grupo de sabor y se estabiliza por medio de una simetría remanente.

El Capítulo (6) está dedicado a un modelo más complejo, con una conexión aún más profunda entre los neutrinos y la materia oscura, siguiendo la misma filosofía de 'materia oscura discreta' del Capítulo (5). El modelo construido es compatible con los últimos resultados de Daya-Bay y su medición del último ángulo de mezcla desconocido, es decir, el ángulo de reactor.

Finalmente en el Capítulo (7), exploramos otra posible relación entre los neutrinos y la materia oscura: el majoron. El modelo mínimo, basado sobre el mecanismo de *seesaw*, tiene todos los ingredientes necesarios para tener en cuenta la posible observación directa de las ondas gravitatorias primordiales por BICEP2 y la confirmación del paradigma inflacionario. Si los resultados de BICEP2 se confirman despues del escrutinio de la comunidad científica, el impacto que tendrá en la cosmología y en general en la física, va a ser revolucionario.

Contents

Publications

This thesis is based on the following publications:

[1] **"Phenomenology of Dark Matter from A_4 Flavor Symmetry"**
S.M. Boucenna, M. Hirsch, S. Morisi, E. Peinado, M. Taoso, J.W.F. Valle
JHEP 1105 (2011) 037 (arXiv:1101.2874 [hep-ph])

[2] **"Predictive discrete dark matter model and neutrino oscillations"**
S.M. Boucenna, S. Morisi, E. Peinado, Y. Shimizu, J.W.F. Valle
Phys.Rev. D86 (2012) 073008 (arXiv:1204.4733 [hep-ph])

[3] **"Inflation and majoron dark matter in the seesaw mechanism"**
S.M. Boucenna, S. Morisi, Q. Shafi, J.W.F. Valle
Phys.Rev. D90 (2014) 055023 (arXiv:1404.3198 [hep-ph])

Other articles completed during the PhD only partially included here:

[4] **"Bi-large neutrino mixing and the Cabibbo angle"**
S.M. Boucenna, S. Morisi, M. Tortóla, J.W.F. Valle
Phys.Rev. D86 (2012) 051301 (arXiv:1206.2555 [hep-ph])

[5] **"The low-scale approach to neutrino masses"**
S.M. Boucenna, S. Morisi, J.W.F. Valle
Adv. in High Energy Physics, (2014) 831598 (arXiv:1404.3751 [hep-ph])

[6] **"Theories relating baryon asymmetry and dark matter: A mini review"**
S.M. Boucenna, S. Morisi
Front. Physics 1 (2013) 33 (arXiv:1310.1904 [hep-ph])

[7] **"Planck-scale effects on WIMP dark matter"**
S.M. Boucenna, R.A. Lineros, J.W.F. Valle
Front. Physics 1 (2013) 34 (arXiv:1204.2576 [hep-ph])

Other articles completed during the PhD but not included here:

[8] **"Direct and Indirect Singlet Scalar Dark Matter Detection in the Lepton-Specific two-Higgs-doublet Model"**
S.M. Boucenna, S. Profumo
Phys.Rev. D84 (2011) 055011 (arXiv:1106.3368 [hep-ph])

[9] **"Radiative neutrino mass in 331 scheme"**
S.M. Boucenna, S. Morisi, J.W.F. Valle
Phys.Rev. D90 (2014) 013005 (arXiv:1405.2332 [hep-ph])

[10] **"Small neutrino masses and gauge coupling unification"**
S.M. Boucenna, R. Fonseca, F. Gonzalez-Canales, J.W.F. Valle
arXiv:1411.0566 [hep-ph]

Abbreviations

$0\nu\beta\beta$	Neutrinoless Double Beta Decay
2HDM	2-Higgs-Doublet Model
BAU	Baryon Asymmetry of the Universe
BBN	Big Bang Nucleosyntesis
BEH	Brout-Englert-Higgs
BL	Bi-Large
CL	Confidence Level
CMB	Cosmic Microwave Background
CKM	Cabibbo-Kobayashi-Maskawa
$\mathcal{CP}$	Charge-Parity
DM	Dark Matter
DDM	Discrete Dark Matter
FCNC	Flavor Changing Neutral Currents
IDM	Inert Higgs Doublet model
IH (NH)	Inverted (Normal) Hierarchy
ΛCDM	Standard Model of Cosmology
LFV	Lepton Flavor Violation
(b)SM	(Beyond the) Standard Model
TBM	Tri-Bimaximal Mixing
vev	Vacuum Expectation Value
WIMP	Weakly Interacting Massive Particle

Experiments

ADMX	Axion Dark Matter eXperiment
AMS	Alpha Magnetic Spectrometer
ATLAS	A Toroidal LHC Apparatus
BICEP	Background Imaging of Cosmic Extragalactic Polarization
CAST	CERN Axion Solar Telescope
CMS	Compact Muon Solenoid
CDMS	Cryogenic Dark Matter Search
CoGeNT	Coherent Germanium Neutrino Technology dark matter experiment
DAMA	DArk MAtter
EXO	Enriched Xenon Observatory
Fermi-LAT	Fermi Large Area Telescope
LBNE	Long Baseline Neutrino Experiment
LEP	Large Electron-Positron collider
LHC	Large Hadron Collider
LUX	Large Underground Xenon experiment
MINOS	Main Injector Neutrino Oscillation Search
NOvA	NuMI Off-axis ν_e Appearance
PAMELA	Payload for Antimatter Matter Exploration and Light nuclei Astrophysics
PINGU	Precision IceCube Next Generation Upgrade
WMAP	Wilkinson Microwave Anisotropy Probe

Introduction and outline

The discovery of neutrino oscillations and the growing evidence for the existence of dark matter (DM) provide strong indications for the need of physics beyond the Standard Model. However the detailed nature of the new physics remains elusive. On the one hand, the mechanism responsible for neutrino mass generation and its flavor structure, as well as the nature of the associated messenger particle(s) are unknown. Consequently the nature of neutrinos, their mass and mixing parameters are all unpredicted. On the other, the nature of dark matter constitutes one of the most challenging questions in cosmology, though recently some direct and indirect DM detection experiments are showing tantalizing hints favoring a light WIMP-like DM candidate [11, 12] or keV dark matter [13] opening hopes for an imminent detection.

Linking neutrino mass generation to dark matter, two seemingly unrelated problems into a single framework, is theoretically appealing, and may bring us new insights on both issues. The idea of unification itself, or as Feynman used to call it *amalgamation*, is central to physics, and in general to any scientific discipline. To unify is to gain new insights by synthesizing and generalizing knowledge.

This thesis is dedicated to the interplay between neutrino physics and dark matter. Notably the development and understanding of models where the dynamics of dark matter and neutrinos are related to one another. By connecting dark matter to neutrinos, it is possible to obtain direct and indirect information on new physics beyond the Standard Model (bSM). Indeed, neutrinos offer a striking manifestation of bSM physics and various experiments provide us with precise data about their mixing and mass splittings. These data reveal a strong contrast with the known case of the quarks. By the scales of the problem and the precision of these measurements, neutrino physics offers a tantalizing insight into one of the deepest and most enduring problems of the SM, namely the flavor problem.

Outline

We will start by briefly introducing the Standard Model of particle physics and the notation we will use throughout the thesis in Chapter (1). Then we present a general introduction and overview of dark matter in Chapter (2). After giving an overview of neutrino physics in the next chapter, Chapter (3), the possible relation between dark matter and neutrinos will be the subject of the rest of this thesis, starting from Chapter (4), where we will review attempts to unify their description.

We start the original part of this thesis in Chapter (5) by linking dark matter to neutrinos via flavor symmetries. Flavor symmetries, particularly those based on non-Abelian discrete groups, provide a *rationale* to address the flavor problem from first principles. The unified description is achieved by assigning the DM to an irreducible representation (*irrep*) of the flavor group. The breaking of this group, which is required in order to generate the masses and mixing patterns, links the DM phenomenology to neutrinos and stabilizes the DM at the same time. We will present the phenomenology of a model realizing this mechanism in detail. The DM candidate in the model emerges from the triplet *irrep* of the flavor group and is stabilized by means of its remnant symmetry.

Chapter (6) is devoted to more complex, yet deeper links between neutrinos and dark matter following the same philosophy of "discrete dark matter" of Chapter (5). The constructed model is compatible with the findings of the Daya-Bay experiment and its landmark measurement of the last unkown mixing angle, namely the reactor angle (θ_{13}).

Finally in Chapter (7), we will explore another possible link between neutrinos and dark matter: the majoron. The minimal model, based on the seesaw mechanism has all the necessary ingredients to account for the possible direct observation of primordial gravitational waves by BICEP2 and the confirmation of the inflationary paradigm. If these results hold up to scrutiny, the impact on cosmology, and physics in general, will be quite revolutionary.

1

Preludio — the Standard Model and beyond

Never underestimate the joy people derive from hearing something they already know.

Enrico Fermi

A SERIES OF EXPERIMENTS AT HIGH-ENERGY PARTICLE COLLIDERS and a long process of accretion and synthesis of many theoretical ideas have established the Standard Model as a precise theory of particle interactions up to energies $\mathcal{O}(100)\,\mathrm{GeV}$, or in terms of length, down to distances $\mathcal{O}(10^{-16})\,\mathrm{cm}$. The SM includes the electroweak theory, formulated by S. Weinberg [14] and

A. Salam [15] in 1967, based on a model proposed earlier by S.L. Glashow in 1961 [16]; and quantum chromodynamics [17–21]. The model incorporates the Brout-Englert-Higgs (BEH) mechanism [22–24] at its core to provide masses to the matter and interaction fields. The edifice of the Standard Model as designed by its architects has been completed in 2012 after the discovery of the long-awaited Higgs boson by ATLAS [25] and CMS [26] collaborations (see Figure (1.1)) at the Large Hadron Collider (LHC)*.

Of all the ideas upon which the SM is built, the gauge principle [29] is without any doubt the most important insight gained in quantum field theory. Quantum Electrodynamics (QED), the very prototype of a successful physical theory since the end of the 40s, follows from the principle of invariance under local gauge transformations of the $U(1)$ group. This principle has been generalized to any compact Lie group to serve as the conceptual basis to construct quantum field theory models [30]†.

For a historical account of the genesis of modern particle physics, we refer to [32]. The history of the rise of the Standard Model has been discussed in these proceedings [33] and S. Weinberg's account of the making of the SM can be found in [34].

The rest of the chapter is devoted to a brief presentation of the SM and its shortcomings.

1.1 Bird's eye view of the Standard Model

Here we present a short overview of the Standard Model, as an excuse to introduce some notation and concepts that we will make use of in subsequent chapters. For more details we refer to the excellent books which describe the

*A nice account of the rise of colliders in particle physics can be found in [27] and [28].

†It is worth emphasizing also that while gauge theories offer extremely good description of Nature at its most fundamental level, as well as a guiding principle to constructing new theories, we still do not know why they work so well, although see [31] for a compelling explanation.

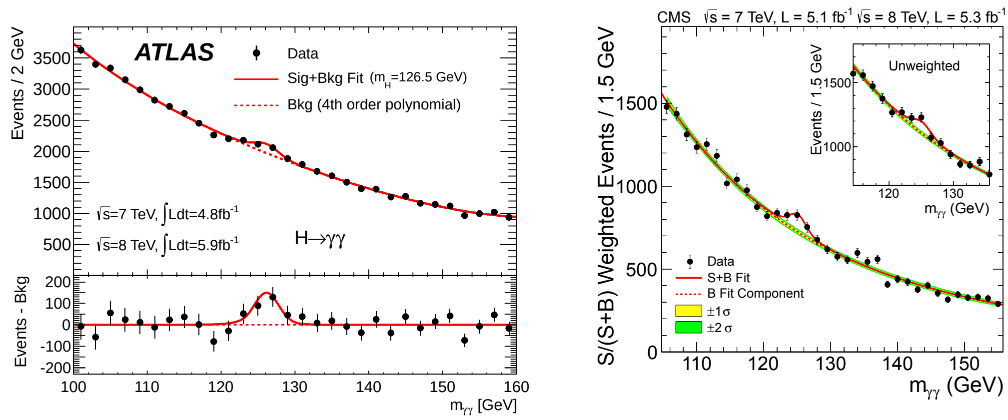

Figure 1.1: Higgs discovery in the $\gamma\gamma$ channel by ATLAS [25] and CMS [26] collaborations. $m_{\gamma\gamma}$ is the diphoton invariant mass distribution.

SM in great detail, for instance [35, 36].

The Standard Model is a renormalizable* gauge theory based on the $SU(3)_c \otimes SU(2)_L \otimes U(1)_Y$ group†. $SU(3)_c$ describes the strong interactions, quantum chromodynamics [17–21], and $SU(2)_L \otimes U(1)_Y$ describes electroweak interactions [14–16]. The SM contains three copies or families of fermions. Each family contains 15 chiral fermions: 2 charged leptons, 1 neutrino, and 12 quarks. Table (1.1) lists the fermions of the SM. Experiments in late 1950s established that (charged-current) weak interactions are left-handed, and this is understood by having only left-handed fermions transforming as doublets under $SU(2)_L$ local group. In addition to fermions, the model contains a spin zero scalar particle and 12 vector fields. Table (1.2) summarizes the particle

*The renormalizability of the SM was proved by G. 't Hooft and M. Veltman in 1971 [37].

†This is true at the local level, i.e., the Lie algebra is $\mathfrak{su}(3) \oplus \mathfrak{su}(2) \oplus \mathfrak{u}(1)$. In principle, the gauge group of the SM can be written as $SU(3)_c \otimes SU(2)_L \otimes U(1)_Y/\mathcal{Z}$ where $\mathcal{Z} = Z_6$ or one of its subgroups (Z_2 and Z_3). In general, we do not lose anything by representing the group G/N, where N is the kernel of G, instead of G — locally. One can even argue, in fact, that the 'true' group is G/N since it's the minimal choice. This issue is less of an academic exercise when we consider the global properties of the group, that is the group itself instead of its Lie algebra. The topological properties of the group can be seen for instance when the SM is embedded into a GUT group. Topological defects in the form of stable monopoles depend on the exact definition of the group and arise from the spontaneously broken symmetry of the unified model [38]. Such monopoles, if observed (or excluded by observation), could help us distinguish between the different version of the SM group [39]. See also [40–42].

	1^{st} Family	2^{nd} Family	3^{rd} Family
Leptons	ν_e e	ν_μ μ	ν_τ τ
Quarks	u d	c s	t b

Table 1.1: The Standard Model fermions.

content and representations of all the fields of the model.

The Lagrangian of the Standard Model embodies all our knowledge of strong and electroweak interactions. It can be decomposed into four conceptually distinct pieces: Dirac, Gauge (Yang-Mills), Yukawa, and Higgs interactions*:

$$\mathcal{L}_{SM} = \mathcal{L}_{Dirac} + \mathcal{L}_{Gauge} + \mathcal{L}_{Yuk} + \mathcal{L}_{Higgs} \,. \tag{1.1}$$

The gauge part controls the interactions of the vector bosons of the theory among themselves, namely the eight gluons of the strong interaction and the four electroweak bosons. It is given by:

$$\mathcal{L}_{Gauge} = -\frac{1}{2}\mathrm{Tr}(\mathrm{G}_{\mu\nu}\mathrm{G}^{\mu\nu}) - \frac{1}{2}\mathrm{Tr}(\mathrm{W}_{\mu\nu}\mathrm{W}^{\mu\nu}) - \frac{1}{4}\mathrm{B}_{\mu\nu}\mathrm{B}^{\mu\nu} \,, \tag{1.2}$$

where $G_{\mu\nu}$, $W_{\mu\nu}$ and $B_{\mu\nu}$ are the field strengths of $SU(3)_c$, $SU(2)_L$ and $U(1)_Y$, respectively. The Dirac Lagrangian encodes the kinetic term and the fermion-gauge bosons interactions in the covariant derivative:

$$\mathcal{L}_{Dirac} = \Sigma\psi i\gamma^{\mu}\mathcal{D}_{\mu}\psi \,, \tag{1.3}$$

where the sum runs over all the chiral fermions of the model. The covariant derivative is defined as $\mathcal{D}_\mu = \partial_\mu - ig_s G^a_\mu \lambda_a - igW^a_\mu \sigma_a - iYg'B_\mu$, where λ_a and σ_a are the generators of $SU(3)_c$ and $SU(2)_L$, respectively, in the representation of ψ, and Y is the hypercharge of ψ.

*We omit the gauge fixing terms and the ghosts interactions for simplicity.

The now-famous Higgs particle stems from the following Lagrangian:

$$\mathcal{L}_{Higgs} = \mathcal{D}_\mu H^\dagger \mathcal{D}^\mu H + \mu^2 H^\dagger H - \lambda (H^\dagger H)^2 \,, \tag{1.4}$$

with the prescription $\mu^2 > 0$ so that H acquires a vacuum expectation value (*vev*) and breaks the electroweak group, $SU(2)_L \otimes U(1)_Y$, down to the electromagnetic $U(1)_{em}$. The Higgs doublet can be written as:

$$H = \begin{pmatrix} H^+ \\ (v_{SM} + h + iA)/\sqrt{2} \end{pmatrix} . \tag{1.5}$$

After electroweak symmetry breaking[22–24], $H^\pm$ and A are identified with the three Nambu-Goldsone [43–45] bosons corresponding to the broken generators of $SU(2)_L \otimes U(1)_Y$. They are consequently eaten up by the gauge bosons, which acquire the masses

$$M_W = \frac{g}{2} v_{SM} \approx 80.39\,\text{GeV} \,, \quad M_Z = \frac{M_W}{\cos\theta_W} \approx 91.19\,\text{GeV} \,. \tag{1.6}$$

Where $v_{SM} = 246\,\text{GeV}$ is the *vev* of the Higgs (at 0 temperature) and θ_W is the (Weinberg's) weak mixing angle. The photon is of course massless, as a consequence of the preserved residual $U(1)_{em}$ symmetry. h is the recently discovered Higgs boson, whose mass is not predicted by the theory but is measured experimentally to be $M_h \approx 125.5\,\text{GeV}$ [25, 26], see Figure (1.1).

The interactions fermions-scalars are controlled by the Yukawa part of the Lagrangian:

$$\mathcal{L}_{Yuk} = \Gamma^e_{ij}\, \bar{L}_i\, H\, \ell_{j\,R} + \Gamma^d_{ij}\, \bar{Q}_i\, H\, d_{j\,R} + \Gamma^u_{ij}\, \bar{Q}_i\, \check{H}\, u_{j\,R} + \text{h.c.} \tag{1.7}$$

The indices i, j are generation labels. The couplings Γ_{ij} are 3×3 matrices. We denote the recurrent $i\tau_2 H$ (with τ_2 being the second Pauli matrix) as:

$$\boxed{\check{H} \equiv i\tau_2 H} \tag{1.8}$$

$\check{H}$ is pronounced 'H check'. We will use this notation throughout this thesis.

Fields	$SU(2)_L$	$U(1)_Y$	$SU(3)_c$
$L_a = \begin{pmatrix} \nu_{aL} \\ \ell_a \end{pmatrix}$	$\mathbf{2}$	$-\frac{\mathbf{1}}{\mathbf{2}}$	$\mathbf{1}$
ℓ_{aR}	$\mathbf{-1}$	$\mathbf{+1}$	$\mathbf{1}$
$Q_{aL} = \begin{pmatrix} u_{aL} \\ d_{aL} \end{pmatrix}$	$\mathbf{2}$	$+\frac{\mathbf{1}}{\mathbf{6}}$	$\mathbf{3}$
u_{aR}	$\mathbf{1}$	$+\frac{\mathbf{2}}{\mathbf{3}}$	$\mathbf{3}$
d_{aR}	$\mathbf{1}$	$-\frac{\mathbf{1}}{\mathbf{3}}$	$\mathbf{3}$
H	$\mathbf{2}$	$+\frac{\mathbf{1}}{\mathbf{2}}$	$\mathbf{1}$
B	$\mathbf{1}$	$\mathbf{0}$	$\mathbf{1}$
$W = \begin{pmatrix} W_1 \\ W_2 \\ W_3 \end{pmatrix}$	$\mathbf{3}$	$\mathbf{0}$	$\mathbf{1}$
g	$\mathbf{1}$	$\mathbf{0}$	$\mathbf{8}$

Table 1.2: The Standard Model of particle physics: charge assignments of the SM fermions, scalars and gauge bosons under the $SU(3)_c \otimes SU(2)_L \otimes U(1)_Y$ local symmetries. The index $a = e, \mu, \tau$ labels the three observed generations of fermions, see Table (1.1). We defined the electric charge as $Q = T_L^3 + Y$.

The Yukawa matrices can be diagonalized by means of bi-unitary transformations:

$$\Gamma^a = \mathcal{U}_L^a Y^a \mathcal{U}_R^{a\dagger} . \tag{1.9}$$

Because neutrinos are massless, we can consider Γ^e to be diagonal without loss of generality (we perform a simple redefinition of the fields L and ℓ_R). However, this is not possible for the quarks because the Higgs couples to both u and d types. This gives rise to a mismatch between flavor and mass bases and consequently to nontrivial mixing patterns among the quarks, best represented with the celebrated CKM, for Cabibbo-Kobayashi-Maskawa, matrix [46, 47]:

$$\mathcal{U}_{CKM} = \mathcal{U}_L^{u\dagger} \mathcal{U}_L^d . \tag{1.10}$$

The CKM matrix has 4 free parameters: 3 angles and a complex phase allowing for $\mathcal{CP}$ violation in the quark sector*. It can be parametrized as [50]

$$\mathcal{U}_{CKM} = \begin{pmatrix} 1 & 0 & 0 \\ 0 & c_{23} & -s_{23} \\ 0 & s_{23} & c_{23} \end{pmatrix} \begin{pmatrix} c_{13} & 0 & -e^{-i\delta} s_{13} \\ 0 & 1 & 0 \\ e^{i\delta} s_{13} & 0 & c_{13} \end{pmatrix} \begin{pmatrix} c_{12} & -s_{12} & 0 \\ s_{12} & c_{12} & 0 \\ 0 & 0 & 1 \end{pmatrix} . \tag{1.11}$$

Here, $s_{ij} = \sin\theta_{ij}$ and $c_{ij} = \cos\theta_{ij}$. The angles and the phase of the CKM matrix are found to be:

$$\theta_{12} \approx 13^\circ\,, \quad \theta_{23} \approx 2.4^\circ\,, \quad \theta_{13} \approx 0.2^\circ\,, \quad \delta \approx 59.7^\circ\,. \tag{1.12}$$

The masses of the fermions cannot be written explicitly because they violate the $SU(2)_L \otimes U(1)_Y$ symmetry. They emerge as a consequence of electroweak symmetry breaking triggered by the Higgs doublet — The BEH mechanism. For instance, from Equation (1.7) the electron's mass is given by

$$m_e = Y^e_{11} \langle H \rangle = \frac{1}{\sqrt{2}} Y^e_{11}\, v_{SM} \approx 0.511\,\text{MeV}\,. \tag{1.13}$$

That's essentially all we need to know about the architecture of the SM. The most precise physical model ever built is also a model of simplicity. A small number of clever theoretical insights joined together (Gauge principle, GIM mechanism, BEH mechanism, to cite but three examples) describe with astonishing accuracy the interactions of elementary particles. There are only 18 free parameters†: 3 gauge couplings, the Higgs quadratic mass coefficient and self-coupling, 9 quark and lepton masses, and 4 parameters in the CKM matrix. The model accounts for all collider experiments done at the Stanford Linear Collider (SLC), the Large Electron-Positron collider (LEP)‡, the Tevatron, and so far the LHC. It predicts or fits all the experimental data acquired in

*This was pointed out in 1972 by Kobayashi and Maskawa [46], building on previous work by Cabibbo where it had been shown that flavor mixing matrix for two generation models of the weak interactions is governed by a single angle, now known as the Cabibbo angle. Kobayashi and Maskawa were awarded the physics Nobel prize in 2008 following the confirmation of $\mathcal{CP}$ violation in the quark sector by BELL [48] and BaBar [49] experiments.

†19 if we include the QCD vacuum angle.

‡See [51] for a summary of SLC and LEP achievements.

the last 50 years — all but neutrino oscillations experiments and cosmological observations.

1.2 Going beyond

The SM description of Nature cannot account for three experimental facts: neutrino masses, the existence of dark matter and matter-anti-matter asymmetry*. These constitute striking experimental manifestations of new physics. But perhaps the biggest drawback of the SM is that it is but an effective theory. A phenomenological model necessarily leaves some questions unanswered. In the case of the SM, we do not know the answers to the following conceptual issues:

- Why is the gauge group $SU(3)_c \otimes SU(2)_L \otimes U(1)_Y$ and why is it a product of 3 different groups?
- Why are there three replicas of each family?
- How can we understand Electroweak universality (both left-handed leptons and quarks transform as $SU(2)_L$ doublets)?
- How are quarks and leptons related to each other (anomaly cancellation requires quarks and leptons)?
- Why don't the couplings unify at high energy?
- Why is charge quantized?
- What explains the hierarchy of fermion masses and their mixing?

On top of these questions, more 'aesthetic' considerations lead to the 'hierarchy problem' and the 'strong $\mathcal{CP}$ problem'. Thus the SM suffers from a series of conceptual problems and fails to account for some observations†. Numerous extensions of the SM have been put forward in the last decades to answer one

*We leave aside the problems of quantum gravity and dark energy.

†Or as B. Richter put it: "The experiments and theory of the 1960s and 1970s gave us today's Standard Model [...] a beautiful manuscript with some unfortunate Post-it notes stuck here and there with unanswered questions written on them."[52].

or more of these questions. None of these models has been as successful or satisfying as the SM, even if we did gain some new theoretical insights such as the idea of Grand Unified theories (GUT) [53–56], supersymmetry [57–60], or extra-dimensions [61, 62]. Hopefully, the next run of the LHC will give us some hints to point us in the right direction.

Among the problems listed above, the so-called 'flavor problem', namely why we have three families of fermions with the same Standard Model quantum numbers, but with very different masses, constitutes one of the most challenging open problems in particle physics. It is also phenomenologically interesting as it is directly testable. The mystery of the smallness of neutrino masses is the most pressing aspect of the problem. Indeed, the SM neither includes a mechanism that generates masses for the neutrinos, nor does it forbid them from acquiring one. While the discovery of the Higgs at LHC[25, 26] sheds light on the nature of electroweak symmetry breaking, the origin of neutrino masses remains elusive.

In the next two chapters we review the dark matter and neutrino mass problems in more details.

2
The dark Universe

L'anormal, logiquement second, est existentiellement premier.
Georges Canguilhem

A LITTLE MORE THAN 80 YEARS AGO, F. Zwicky studied the gravitational irregularities in the Coma cluster of galaxies [63]. What he found was surprising! There seemed to be a hidden mass that outnumbers the directly visible one nearly 400–to–1. He dubbed the mysterious mass *dunkle materie*: **dark** matter. His bold speculation, though, was largely ignored until the 1970's when V. Rubin pioneered the study of rotation curves of spiral galaxies [64]. Rotation curves remain until today a very strong evidence for the existence of dark matter.

By now we know that DM fills the Universe, accounting for most of its matter content, promotes structure formation, and explains the discrepancy between the visible and dynamical astronomical observations. Yet, barring a few observational and theoretical bounds we still know very little about its nature. After the spectacular discovery of the Higgs at LHC, the last piece of the Standard Model has been found. But as successful as it has been, the SM describes only a tiny fraction of the content of the Universe; stars, dust, galaxies, clusters of galaxies, black holes (including primordial ones), and even the Universe's graveyard (dead stars, brown dwarfs, etc.) represent but 5% of the energy content of the Universe. The remaining 95% is in the form of dark energy and dark matter, whose fundamental natures are completely unknown. However, the recent theoretical and experimental developments foreshadow that the next few years are going to be decisive for DM.

Here we will review the basics of the DM physics. In Section (2.1) we will review the evidence for DM. Next, the main candidates believed to solve the problem are described in Section (2.2). In Section (2.3) we describe the thermal production mechanism of DM particles in the early Universe. We will summarize the different possibilities of DM searches in Section (2.4). The link between DM and the baryon asymmetry of the Universe is briefly commented in Section (2.5). Finally, we will summarize the chapter and conclude in Section (2.6).

Since there's a significant number of excellent reviews and textbooks that are available, we will content ourselves by presenting the main ideas and results. For more details, we refer the reader to [65–68].

2.1 Evidence and requirements

There exists a wide variety of evidence in support of dark matter's existence. From sub-galactic scales up to cosmological scales. At sub-galactic and galactic

Component		68% CL limits
Symbol	Description	
$\Omega_{DM}h^2$	Dark matter	0.1199 ± 0.0027
$\Omega_B h^2$	Baryonic matter	0.02205 ± 0.00028
Ω_M	Total matter	$0.315^{+0.016}_{-0.018}$
Ω_Λ	Dark energy	$0.685^{+0.018}_{-0.016}$

Table 2.1: Density values for matter and dark matter in ΛCDM model from combined data of PLANCK and WMAP [77]. h is the Hubble parameter in units of $100\,\mathrm{km/sec/Mpc}$, $h \approx 0.67$ (The exact value of the Hubble parameter is model dependent).

scales, this evidence comes from galactic rotation curves [69], weak [70], and strong gravitational lensing [71, 72]. Moreover, observations of the velocity dispersion of individual stars in dwarf galaxies indicate a mass–to–light ratio (that is, the amount of dark matter with respect to visible matter) that can be as large as $\approx 10^3$. Galactic surveys (through observations of radial velocities of galaxies, weak lensing, and X-ray emission) indicate that at the scale of clusters of galaxies, the matter density is [73, 74]:

$$\Omega_M^{clusters} \approx 0.2 - 0.3\,, \tag{2.1}$$

far more important than the luminous matter density (baryons) $\Omega_B \approx 0.022$ [75]. At the scale of cluster of galaxies, the "Bullet cluster" [76] gives perhaps the strongest evidence for the existence of DM. Finally, at the cosmological scale, the robust observations of the anisotropies of the cosmic microwave background (CMB) lead to the precise determination of the total matter content of the Universe, both in the form of baryons and dark matter. We summarize the latest data from CMB observations in Table (2.1). In short, the dark matter hypothesis is so robust that it is a pillar of the Standard Model of cosmology, ΛCDM (where Λ denotes dark energy) or concordance model [78]. Figure (2.1) summarizes the matter and energy contents of the Universe.

Although the nature of DM is unknown, the various astronomical and cosmological observations that are available (including those which offer evidence for

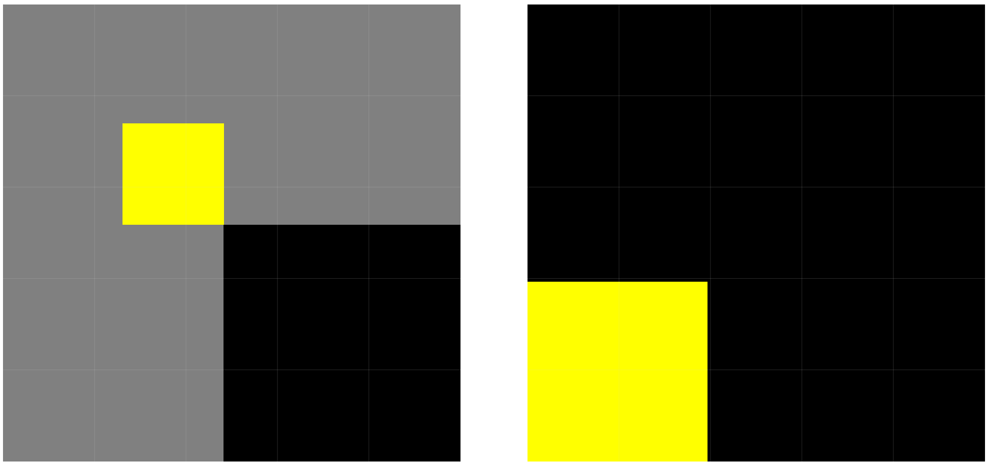

Figure 2.1: Visualization of the energy and matter content of the Universe. Gray, black and yellow areas represent respectively dark energy, dark matter and visible matter. Left: Total energy and matter budget of the Universe ($\approx$ 68% dark energy, $\approx$ 27% dark matter, $\approx$ 5% baryonic matter). Right: Matter content only ($\approx$ 85% dark matter, $\approx$ 15% baryonic matter). Normalizations were fixed from combined PLANCK and WMAP data [77] — c.f. Table (2.1).

its existence) reveal some aspects of its identity, or at least what it *should not* be like [79]. For instance, we know that an acceptable DM candidate should be:

- *neutral*: searches for heavy Hydrogen-like atoms and limits on strongly interacting DM [80–82] place very stringent limits on the (electric and color) charge of DM. As a result, dark matter must be neutral although there still exists open windows for milli-charged DM. For instance, for $m_{DM} \lesssim m_e$ the range $10^{-15} \lesssim Q_{DM} < 1$ is excluded [83] (Q_{DM} here is the electric charge of DM in units of e). But heavier DM masses see this constraint relaxed a bit and the allowed range is roughly $Q_{DM} \lesssim 10^{-7} \frac{M_\chi}{\text{GeV}}$ [84];

- *cold-ish*: the observed structure in the Universe [85] compared to results of dark matter simulations are in excellent agreement when DM is cold [86, 87], meaning it was non-relativistic well before the matter domination era (epoch of formation of galaxies, at $T \approx 1\,\text{eV}$). Warm dark matter gives also a good fit [88, 89]. The main difference with cold dark matter appears only at small scale, where warm dark matter is actually favored because its shorter *free-streaming* length suppresses galaxy formation (current cold dark matter simulations predict more satellite galaxies for the Milky Way than what is seen);

- *stable or very long lived*: since we see its effect today. In the case of decaying DM, the lifetime must be at least equal to the Hubble time ($\approx 10^{17}$s) in principle. In practice though, it must be several orders of magnitude larger than that if its decay products include 'visible' SM particles, for instance cosmic and gamma rays analysis constrain the lifetime of a DM candidate to be $\tau_{\rm DM} > 10^{26}\,$s [90–93];

- *consistent with Big Bang Nucleosynthesis (BBN)*: BBN [94] predicts the abundances of light elements produced in the first 3 minutes after the Big Bang with great accuracy. Since the energy scale of BBN is $\mathcal{O}$(MeV), DM in the mass range MeV is severely constrained in order not to spoil BBN;

- *collisionless*: in case the DM candidate has self-interactions [95], it must comply with several astronomical limits. For instance, the observed galactic halos in clusters would quickly evaporate if the cross section of self–interaction is too strong ($0.3 \lesssim \sigma/m_{DM} \lesssim 10^4\,\mathrm{cm}^2\mathrm{g}^{-1}$) [96].

And of course, it should account for the observed abundance $\Omega_{DM}h^2 \approx 0.2$ and be compatible with exclusion limits set by DM search experiments.

A Universe without darkness?

All the evidence for dark matter accumulated thus far are based on its gravitational influence. There's no evidence of a particle dark matter interacting non-gravitationally. It would certainly be reasonable to contemplate the possibility that all these gravitational anomalies are in fact signaling a departure from Newton's law (or general relativity in the case of lensing) instead of pointing toward the existence of a new form of matter. In 1983 Milgrom [97] proposed a phenomenological model known as modified Newtonian dynamics (MOND) to explain the observed galactic rotation curves without dark matter. The basic assumptions underlying MOND is that Newton's second law, $F = ma$, is modified to $F = ma \times \mu(a)$, where μ behaves as $\mu = a/a_0$ for very small accelerations and is almost unity otherwise (to recover Newton's limit). a_0 is a constant that is fitted from observations. MOND has been very successful in explaining the rotation curves of galaxies, however it fails with the other observations of dark matter, in particular CMB anisotropies.

Even the relativist formulation of MOND, known as Tensor-Vector-Scalar gravity, or TeVeS [98] cannot explain cluster-scale observations without the introduction of dark matter [99]. Finally, the observation of a collision between two clusters (the 'bullet cluster') gave the *coup de grâce* to modified gravity models by giving a strong direct empirical evidence in favor of DM*[76]. Indeed the bullet cluster reveals a clear separation between baryonic matter (seen by X-ray observations) and the gravitational potential of the system (determined using weak lensing). The existence of dark matter is an inescapable consequence of cosmological and astronomical observations.

2.2 Dark matter candidates

There have been many particles proposed as dark matter candidates throughout the years. The list of candidates is so long now that it is commonly referred to as a *zoo*. This includes: axions, gravitinos, superWIMPS, non-thermal dark matter, neutralinos, sterile neutrinos, Q-balls, WIMPzillas, sneutrinos, majorons, etc. From the most 'exotic' to the most 'natural' candidate, the mass of the particle and its interactions vary widely. Indeed, the proposed masses range from $10^{-6}\,\mathrm{eV}$ to up to $10^4\,\mathrm{M}_\odot$ (where $\mathrm{M}_\odot$ is a solar mass). That's 75 orders of magnitude! We sketch some of these DM candidates in Figure (2.2). Here we will briefly present some of the most popular and well motivated can-

*The title of the paper announcing the discovery even calls it a *proof*: "A Direct Empirical Proof of the Existence of Dark Matter".

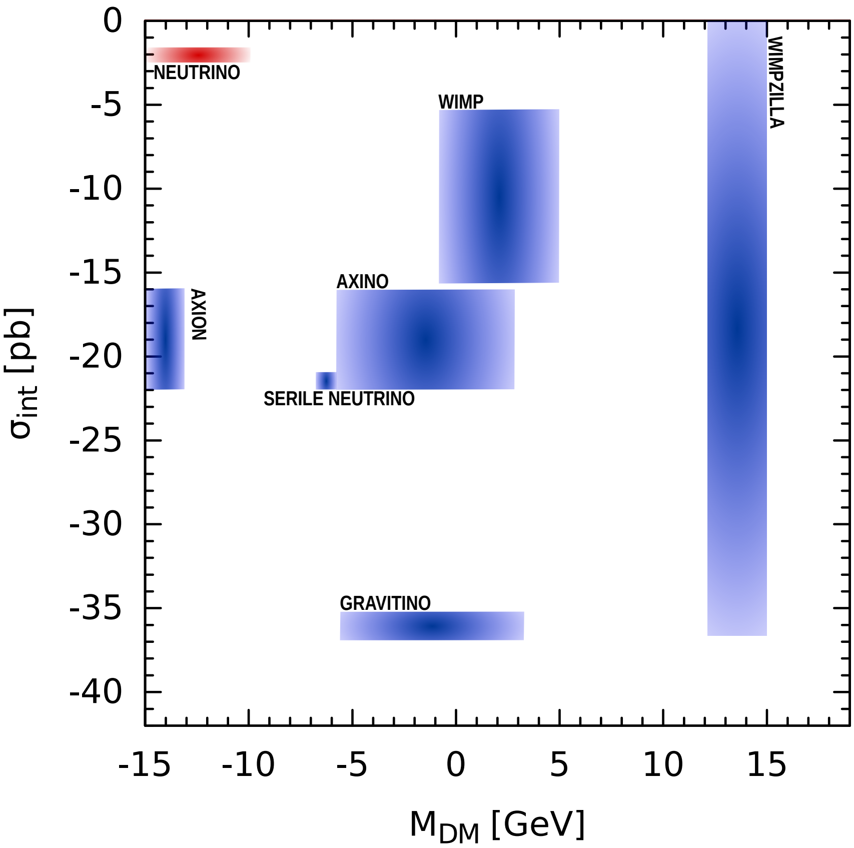

Figure 2.2: A schematic representation of some dark matter candidates. σ_{int} represents a typical order of magnitude of interaction strength with ordinary matter. The neutrino is shown for comparison purposes. Figure reproduced and updated from original sketch in [100].

didates:

‣ **Axions:** Axions were fist proposed to solve the so-called strong $\mathcal{CP}$ problem [101–104]. The latter is essentially a fine-tuning problem. In the quark sector of the SM, there's a parameter θ related to the vacuum topology of the theory that must be put to values smaller than 10^{-9} by hand. This is seen as unnatural for a dimensionless parameter. Peccei and Quinn proposed to solve the problem by postulating a new symmetry, $U(1)_{PQ}$. The axion is the pseudo-Goldstone boson associated with this symmetry. The fact that axions emerge from a theory that solves a problem of the SM that is unrelated to DM makes them particularly attractive and well motivated DM candidates.

Axions are stable and cold (non-relativistic at production) dark matter particles that satisfy the conditions listed in Section (2.1). There are a number of axion production mechanisms, but the easiest and more natural way to produce them is through non-thermal coherent oscillations of the axion field near the QCD phase transition [105]. Their mass is then given by [106–108]:

$$m_a \approx 6 \times 10^{-6} (\frac{10^{12}\,\text{GeV}}{f_a})\ \text{eV}\,, \tag{2.2}$$

where $10^9\,\text{GeV} \lesssim f_a \lesssim 10^{12}\,\text{GeV}$ is the axion decay constant and m_a its mass. Axions are also a testable hypothesis, experiments such like ADMX and CAST are currently searching for them. For a review, see [109] for instance.

▸ **Gravitinos:** The gravitino is the fermionic partner of the graviton in supersymmetric theories [110]. It is one of the first proposed candidates for DM [111]. Its couplings to ordinary particle are strongly suppressed, by a factor $\mathcal{O}(M_W/M_P)$ (where M_P is Planck's constant), making it *extremely* weakly interacting, which renders its direct detection completely hopeless although it can be seen indirectly [112–114]. The gravitino can be produced from thermal as well as non-thermal processes (or both at the same time). The mass of gravitino DM is strongly model depends on how supersymmetry is broken [115–117].

▸ **Weakly-interacting massive particles (WIMPs):** The name of this class of candidates [118] is self-explanatory, massive particles with interactions around the weak scale M_W. These candidates are remarkable for several reasons: (i) they appear naturally in various extension of the SM, notably supersymmetric extensions (neutralinos and sneutrinos are typical WIMPs) [66]; (ii) weak scale interactions naturally lead to the correct abundance via thermal production (insensitive to initial conditions); and last but not least (iii) they are testable by laboratory and satellite experiments [119]. WIMPs are cold dark matter with masses ranging in general from few MeV to $\mathcal{O}$(TeV)

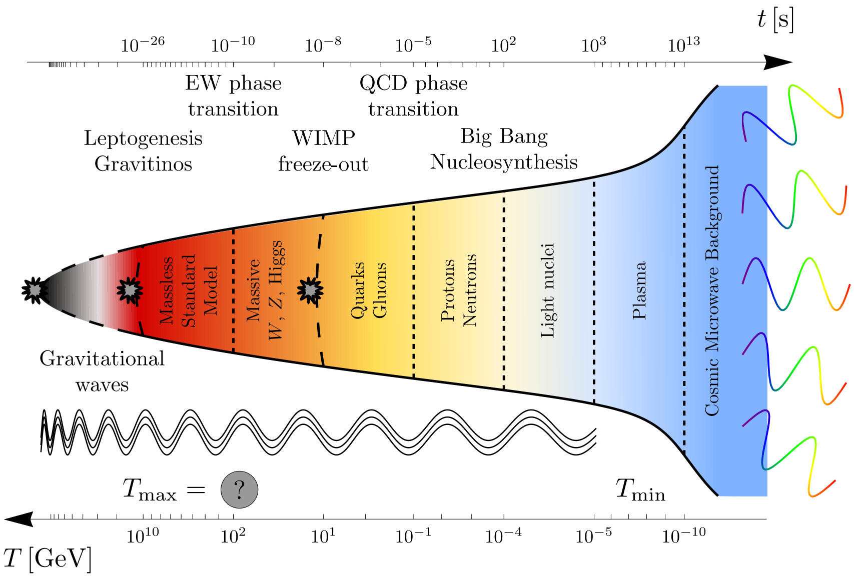

Figure 2.3: Time line of the hot thermal phase of the early Universe (from [121]).

(unitarity constrains the mass of a WIMP to be $\lesssim 130\,\text{TeV}$ [120]), although for a strict interpretation of 'weakly' (i.e., for interactions mediated by $W^{\pm}$ and Z bosons only) the mass scale is of $\mathcal{O}(100\,\text{GeV})$.
Because of their importance and the fact that they are central to this thesis (the candidate of Chapter (5) is a WIMP), we look into the WIMP class of particles in more details, particularly the production mechanism.

2.3 Thermal genesis of dark matter

The theoretical paradigm in cosmology —the Big Bang— provides a historical account of the evolution of the Universe. According to this paradigm, the Universe began from an isotropic and quasi-homogeneous (homogeneous up to a degree of $\approx 10^{-5}$) hot plasma some fifteen billion years ago, then started expanding rapidly. The expansion cools down the Universe and provides the necessary conditions for structure formation. Figure (2.3) summarizes the history of the Universe. It is in the hot phase of the Universe that the DM was produced.

The question *"How is dark matter produced?"* is one of the first ones to be addressed when proposing a DM candidate. In general, production mechanisms can be divided in two categories: thermal and non-thermal. Non-thermal mechanisms include for instance the direct production from inflaton decay or from coherent oscillations [122] (for a review, see e.g., [123]). They are model-dependent and usually fine-tuned to reproduce the correct abundance. In contrast, thermal production offers a simple, calculable, and model-independent mechanism to create DM from thermal processes alone. In general, there are four principal ways of creating DM from SM fields through a portal [124]. Here, we will summarize the key ingredients and results of the thermal production of DM via the *freeze-out* mechanism.

WIMP candidates offer the advantage of having a well defined production mechanism in the early Universe. Indeed, the hot primordial soup of SM particles gives as a byproduct a DM relic abundance that closely matches observations without any fine-tuning [125, 126].

Let χ denote a generic particle of mass M_χ interacting with SM fields ψ through an unidentified process $\chi\bar{\chi} \leftrightarrow \psi\bar{\psi}$ [*]. In the very early Universe, $T \gg M_\chi$ (T is the temperature of the Universe), the processes of creation and annihilation of $\chi\bar{\chi}$ were in equilibrium with SM processes, and the number of χ particles was as large as that of SM species. However, as the temperature falls below the DM mass, $T \lesssim M_\chi$, the processes of creation become exponentially suppressed while the annihilation should in principle continue. If that was the case, the number density of χ particles would be given by:

$$n_{\chi,\,\mathrm{eq}} = g_\chi \left(\frac{M_\chi T}{2\pi}\right)^{3/2} e^{-M_\chi/T} \,, \tag{2.3}$$

where g_χ is the number of internal degrees of freedom of χ. It is clear that χ would quickly become irrelevant. Fortunately, there's an ingredient that can save χ from disappearing: the expansion of the Universe. Indeed, the Hubble expansion acts as a friction term for annihilation processes and helps containing it. We can understand the mechanism in the following way: when the expansion starts dominating over the annihilation rate, it becomes increasingly

[*] This is just illustrative. Of course, any 2-to-N (with $N > 1$) process is possible.

hard for χ particles to find each other to annihilate. Their comoving density then *freezes* and survives until today. More formally, the opposed effects of expansion and annihilation are described by the Boltzmann equation:

$$\frac{dn_\chi}{dt} + 3Hn_\chi = -\langle\sigma_{\chi\bar{\chi}}|v|\rangle\,(n_\chi^2 - n_{\chi,\,\mathrm{eq}}^2)\,, \tag{2.4}$$

where n_χ is the number density of WIMPs, $H \approx T^2/M_P$ is the expansion rate of the Universe, and $\langle\sigma_{\chi\bar{\chi}}|v|\rangle$ is the thermally averaged $\chi\bar{\chi}$ annihilation cross section multiplied by the relative velocity. The cross section encodes the creation process of DM. For WIMPs this usually proceeds through a portal between the SM and the hidden DM sector, like the so-called 'Higgs portal' [127]. The two previously discussed limits ($T \gg M_\chi$ and $T \lesssim M_\chi$) are easy to identify in Equation (2.4). Indeed, at high temperatures (relativistic regime) the density of WIMPs is given by the equilibrium value, $n_{\chi,\,\mathrm{eq}} \approx T^3$, whereas in the opposite limit ($T \ll M_\chi$), the equilibrium density is very small, given by Equation (2.3), due to the depletion caused by the terms $3Hn_\chi$ and $\langle\sigma_{\chi\bar{\chi}}|v|\rangle\, n_\chi^2$. The condition of freeze–out, that is the temperature at which the density of DM freezes, can be expressed roughly as $H \approx n_{\chi,\,\mathrm{eq}}\langle\sigma_{\chi\bar{\chi}}|v|\rangle$, that is when the expansion rate is comparable to the annihilation rate. In Figure (2.4) we depict the evolution of the comoving number density of a stable species as it evolves with temperature for various values of $\langle\sigma_{\chi\bar{\chi}}|v|\rangle$. The exact temperature of freeze-out is found by solving the Boltzmann equation numerically. An analytic approximation of the solution is given by (we define $x \equiv M_\chi/T$) [67]:

$$x_{\mathrm{FO}} \equiv \frac{M_\chi}{T_{\mathrm{FO}}} \approx \ln\left[c(c+2)\sqrt{\frac{45}{8}}\,\frac{g_\chi}{2\pi^3}\,\frac{M_\chi M_P(a + 6b/x_{\mathrm{FO}})}{g_\star^{1/2} x_{\mathrm{FO}}^{1/2}}\right]. \tag{2.5}$$

Here $c \approx 0.5$ is a numerical factor, $g_\star$ is the number of external degrees of freedom available*, and a and b are terms in the non-relativistic expansion, $\langle\sigma_{\chi\bar{\chi}}|v|\rangle = a + b\langle v^2\rangle + \mathcal{O}(v^4)$. The term a comes from the s-wave annihilation, whereas $b\langle v^2\rangle$ comes from both s- and p-wave annihilations. The appearance of the Planck mass M_P can be traced back to the definition of the Hubble rate $H \equiv \dot{R}/R = (8\pi^3\rho/3M_P)^{1/2}$. The ensuing relic density of WIMPs today is

*For example, in the SM, $g_\star \approx 120$ at $T \approx 1\,\mathrm{TeV}$ and $g_\star \approx 65$ at $T \approx 1\,\mathrm{GeV}$.

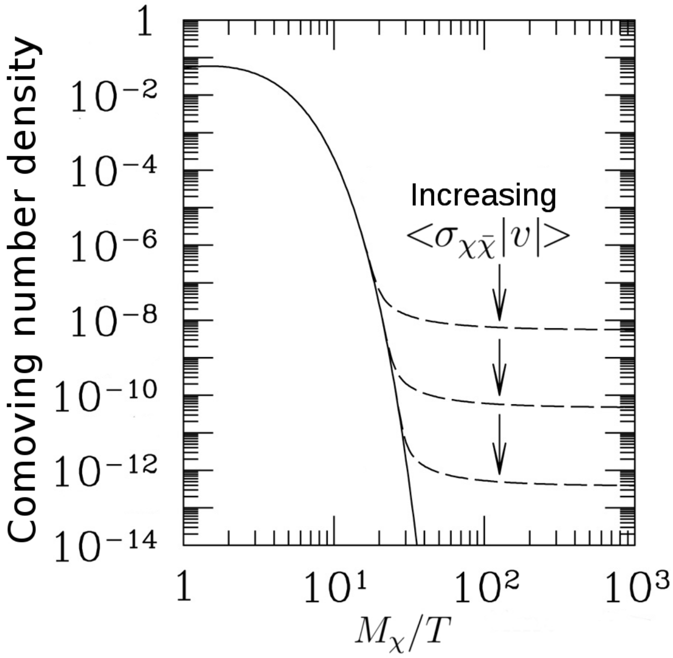

Figure 2.4: Thermal freeze-out: a schematic of the comoving number density of a stable species as it evolves with temperature and for various values of $\langle\sigma_{\chi\bar{\chi}}|v|\rangle$.

approximately given by:

$$\Omega_\chi h^2 \approx \frac{1.04 \times 10^9\,\mathrm{GeV}^{-1}}{M_P} \frac{x_{\mathrm{FO}}}{g_\star^{1/2}(a + 3b/x_{\mathrm{FO}})}. \tag{2.6}$$

For $M_\chi \approx$ GeV$-$ TeV and an annihilation cross section around the weak-scale, freeze-out occurs at $x_{\mathrm{FO}} \approx 17 - 25$, and the resulting relic abundance is:

$$\Omega_\chi h^2 \approx 0.1 \left(\frac{x_{\mathrm{FO}}}{20}\right)\left(\frac{g_\star}{80}\right)^{-1/2}\left(\frac{a + 3b/x_{\mathrm{FO}}}{3 \times 10^{-26}\,\mathrm{cm}^3\mathrm{s}^{-1}}\right)^{-1}, \tag{2.7}$$

leading to the often-quoted "WIMP Miracle" relation:

$$\boxed{\Omega_\chi h^2 \approx 0.1\,\frac{3 \times 10^{-26}\,\mathrm{cm}^3\mathrm{s}^{-1}}{\langle\sigma_{\chi\bar{\chi}}|v|\rangle}} \tag{2.8}$$

The miracle consists of the remarkable coincidence between the annihilation cross section giving the correct dark matter density and the typical cross section of a weak scale interaction, $\alpha^2/(100\,\mathrm{GeV})^2 \approx \mathrm{pb} \approx 3\times10^{-26}\,\mathrm{cm}^3\mathrm{s}^{-1}$. Moreover, being at the weak scale, WIMPs offer rich detection prospects. They can be searched for in laboratories through recoil off nuclei (N) via processes of type $\chi\, N \to \chi\, N$ (direct detection), in the sky by detecting their annihilation byproducts, $\chi\,\bar{\chi} \to \bar{\psi}\,\psi$ (indirect detection), and with colliders, for instance $\bar{p}p \to \bar{\chi}\chi\psi$ (p is the proton, and as before ψ represents any SM particle). We summarize these three possibilities in Figure (2.5). These considerations make WIMPs the front-runners in the zoo of DM candidates.

The standard thermal story discussed above is not free from caveats and at least three exceptional situation occur in the calculations of relic density. These are [128]:

- Resonances;
- Thresholds;
- Co-annihilations.

Resonant annihilation occurs when the cross section is near a pole, for instance when the mass of the dark matter candidate is nearly twice the mass of the s-channel propagator. In this case, either $M_\chi \gtrsim M_{propagator}/2$ and the cross section at freeze-out epoch ($T = T_{\rm FO}$) is much larger than the annihilation cross section now ($T \approx 0$) because the velocity effects in the early Universe put the cross section at its pole, which greatly enhances it. This situations makes indirect detection rates potentially tiny even if the relic density is good (unless a decay channel compensates for the lack of signal from annihilation as will be explained in Section (6.6)). Or $M_\chi \lesssim M_{propagator}/2$, in which case the cross section is maximal at $T = 0$, boosting indirect detection rates with respect to the standard scenario*.

The other way to alter the relation between the cross section at freeze-out epoch and at $T = 0$ is by means of thresholds, i.e., when new channels open up thanks to velocity effects in the early Universe. In this case $\langle\sigma_{\chi\bar{\chi}}|v|\rangle_{\rm FO} >$

*As long as the cross section is not velocity suppressed as in the case of Majorana DM.

$\langle\sigma_{\chi\bar{\chi}}|v|\rangle_0$.

Finally co-annihilation happens when there exist other species, $\chi_{1,\ldots,N}$, in the bath whose mass is close to that of the DM candidate at freeze-out, that is $M_{\chi_i} - M_\chi \approx T_{\rm FO}$. In this case, the annihilation cross section becomes [129]:

$$\langle\sigma_{\chi\bar{\chi}}|v|\rangle \to \langle\sigma_{eff}|v|\rangle = \frac{\Sigma_{i,j=1}^{N}\,\sigma_{ij}\exp\left(-\frac{\Delta M_i+\Delta M_j}{T}\right)}{\Sigma_{i=1}^{N}\,g_i\exp\left(-\frac{\Delta M_i}{T}\right)}\,, \tag{2.9}$$

where $\Delta M_i \equiv M_{\chi_i} - M_\chi$, g_i counts the number of degrees of freedom associated with χ_i and $\sigma_{ij} \equiv \sigma_{\chi_i\chi_j}$. The presence of co-annihilation usually leads to an enhanced annihilation cross section, but not always. Indeed, if the co-annihilating particles bring significant additional degrees of freedom for instance, then the effective cross section is smaller. This typically happens in models of universal extra-dimensions (UED) [130].

Other exceptions to the calculation of the relic density may happen when instead of changing the physics of the annihilation cross section one modifies the left-hand side of Equation (2.4), the Hubble expansion rate, see for instance [131, 132].

2.4 Dark matter searches

Dark matter can be searched for ‘directly’, through nuclear recoil in laboratory experiments or ‘indirectly’ through its annihilation byproducts. Additionally, colliders such as the LHCcan be used to constrain some properties of DM — see Figure (2.5) for an illustration in the particular case of WIMP dark matter. These strategies are in general complementary to each other. Next, we briefly summarize the different DM search strategies.

2.4.1 WIMP direct detection searches

Observations of rotation curves of galaxies suggest that our galaxy is surrounded by a DM halo that extends far beyond the radius of luminous matter.

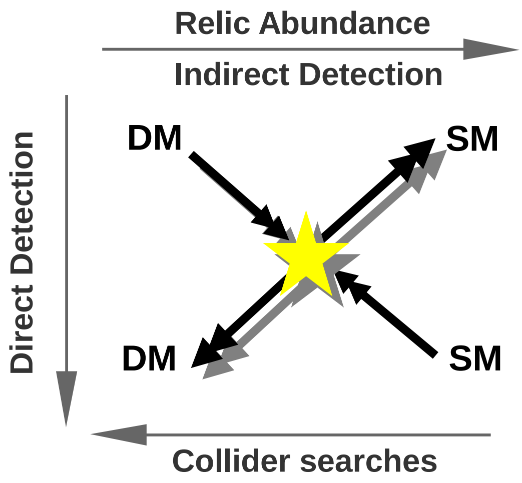

Figure 2.5: Schematic of WIMP interactions in the early Universe and now. The star represents a model-dependent physical interaction.

The local (i.e., at $\approx 8.5\,\text{kpc}$ from the Galactic center) density of dark matter is estimated (from galactic rotation curves and cosmological simulations among other considerations) to be [133]:

$$\rho_{DM}^{\text{local}} = (0.39 \pm 0.03)\frac{\text{GeV}}{\text{cm}^3}\,. \tag{2.10}$$

Since the sun (and us!) move through this halo, we experience a flux of dark matter particles moving with a velocity $v_0 \approx 220\,\text{km/s}$. WIMP dark matter can be searched for in underground detectors (low-background detectors) looking for nuclear recoils induced by the local dark matter scattering against the target material. It is easy to see that the recoil energy is $\mathcal{O}(\text{keV})$, from the naive estimate of the kinetic energy of DM particles $\frac{1}{2}\,M_{DM}\,v_0^2 \approx 27\,\text{keV}$ for $M_{DM} = 100\,\text{GeV}$. The experiments look for anomalous nuclear recoils in a low-background detector (this is satisfied by putting the detector deep underground). The rate scales as $R \propto N\rho_{DM}\sigma v_0$, with σ around $10^{-45}\,\text{cm}^2$ and N is the number of target nuclei. In general, the rate is of few events per year [134, 135] so detectors must have a large mass and long exposure time. A list of selected dark matter experiments, including their fiducial mass, and type of readout is given in Table (2.2).

A statistically significant positive signal of dark matter detection has been

Experiment	Location	Readout	Target mass [kg]	Target	Dates
DAMA/NaI	Gran Sasso	γ	87	NaI	1995–2002
DAMA/LIBRA	Gran Sasso	γ	233	NaI	2003–
ANAIS	Canfranc	γ	11	NaI	2000–2005
			100		2011–
KIMS	Yangyang	γ	35	CsI	2006–2007
			104		2008–
CDMS II	Soudan	ϕ, q	1	Si	2001–2008
			3	Ge	2001–2008
SuperCDMS	Soudan	ϕ, q	12	Ge	2010–2012
	SNOLAB				2013–2016
EDELWEISS I	Modane	ϕ, q	1	Ge	2000–2004
EDELWEISS II	Modane	ϕ, q	4	Ge	2005–
CRESST II	Gran Sasso	ϕ, γ	1	$CaWO_4$	2000–
SIMPLE	Rustrel	d	0.2	Freon	1999–
PICASSO	Sudbury	d	2	Freon	2001–
COUPP	Fermilab	d	2	Freon	2004–2009
			60		2010–
CoGeNT	Chicago	q	0.3	Ge	2005–
	Soudan	q	0.3	Ge	2008–
ZEPLIN III	Boulby	γ, q	7	LXe	2004–
LUX	Sanford	γ, q	100	LXe	2010–
XENON10	Gran Sasso	γ, q	5	LXe	2005–2007
XENON100	Gran Sasso	γ, q	50	LXe	2009–

Table 2.2: Some characteristics of selected dark matter experiments, including fiducial mass, and readout (scintillation light (γ), phonons (ϕ), ionization (q), or super-heated droplets (d)). Adapted from [145, 146].

claimed by the DAMA collaboration [136] for years. DAMA has reported a high statistical evidence for annual modulation of the event rate over 13 year cycles [136, 137]. These results have prompted many attempts to interpret the data in terms of dark matter interactions with nuclei. Assuming an elastic WIMP interactions off nuclei and for ‘standard’ astrophysical assumption on the local DM density and velocity distribution, the DAMA signal is in conflict with the null results reported by other experiments [138–140]. However astrophysical inputs are subject to large uncertainties (see e.g., [141–143]) and the detectors’ responses are not completely known, especially in the low mass region [144].

The latest results in direct detection experiments, particularly LUX [147] (the

first to reach the 'zeptobarn' world, or $10^{-45}\,\mathrm{cm}^2$!) and CDMSLite experiments [148], severely challenge a possible interpretation of DAMA in terms of recoil of WIMP DM off nuclei. It also seems to definitely rule out other anomalies seen in COGENT [149], CDMS-II [148, 150] and CRESST [151], although these have never been statistically significant anyway. Considering isospin-violating couplings no longer helps alleviating the tension between these experiments [152]. More recently, the excess seen in CRESST from 2009 to 2011 has not been confirmed in their latest analysis [153].
The status of WIMP direct detection results is summarized in Figure (2.6). By the year 2020, direct detection experiments are expected to have a sensitivity $\approx 10^{-48}\,\mathrm{cm}^2$ [154].

A final remark: direct detection experiments are reaching their limits due to the neutrino background as can be seen in Figure (2.6). An amusing relation between DM and neutrinos emerges: experiments designed to look for DM end up being used for neutrino physics (for a possible application, see [155] for instance). But, hopefully, DM will be found before that happens.

2.4.2 Indirect detection

Dark matter indirect detection experiments look for signatures of DM annihilation into photons (Fermi-LAT, EGRET), neutrinos (IceCUBE, ANTARES) and (anti-) matter (AMS, PAMELA). The expected DM signals depend on the astrophysical details related to the DM density distribution in the region of observation. Particle physics enters in the determination of the DM mass, annihilation cross section σv and the specific branching ratios of the various annihilation channels.

2.4.3 Dark matter at LHC

Since WIMPs are tied to the weak scale, they can be probed at colliders, including the LHC (see [158] and references therein). For colliders, dark matter is *missing* energy. The branching ratio of Higgs decays to invisible, for instance, provides a very strong constraint on DM models for masses below

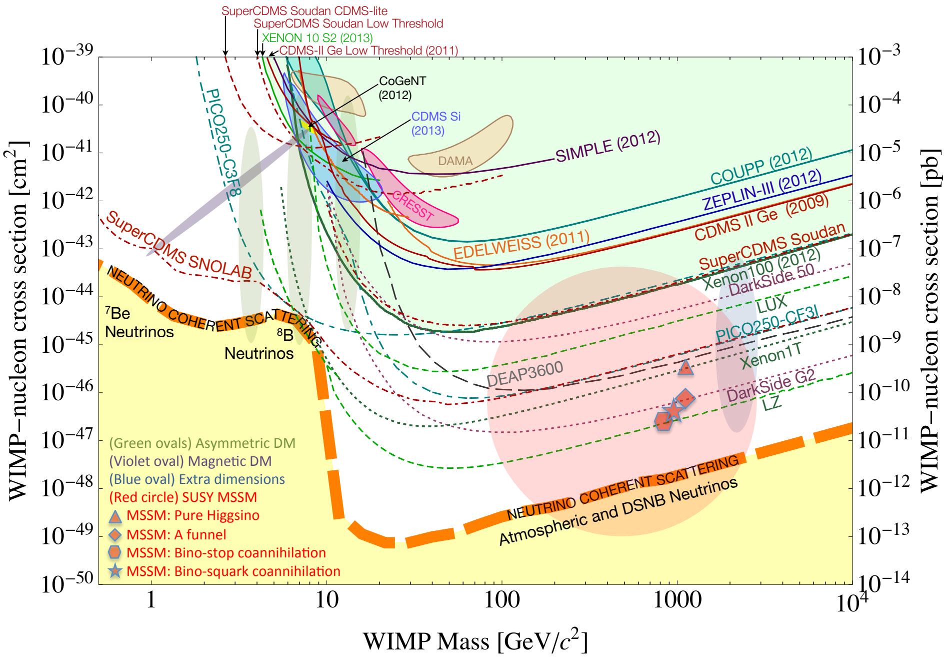

Figure 2.6: WIMP dark matter direct detection status, circa 2014, from [156] (based on figure from [157]).

$M_h/2$ and proceeding *via* the Higgs portal [159, 160]. Moreover, it is possible to relate the pair production rate of DM at colliders to the annihilation and scattering at indirect and direct detection experiments, making colliders a complementary probe in the search for the nature of DM [161].

Model independent analyses based on effective field theories (EFT)* or simplified models have been carried out with LEP [163], Tevatron [164] and LHC [159, 160, 165] data. In general, collider limits are very strong for spin-dependent interactions but are rather poor for spin-independent interactions where direct detection searches excel.

2.5 Dark matter and baryon asymmetry

The CMB data reveal that the dark matter content of the Universe is about five times that of the baryonic matter, $\Omega_{DM} \approx 5\,\Omega_B$ — see Table (2.1). Moreover, the visible matter density does not include anti-baryons i.e., the visible

*For an effective guide in constructing such operators, see [162].

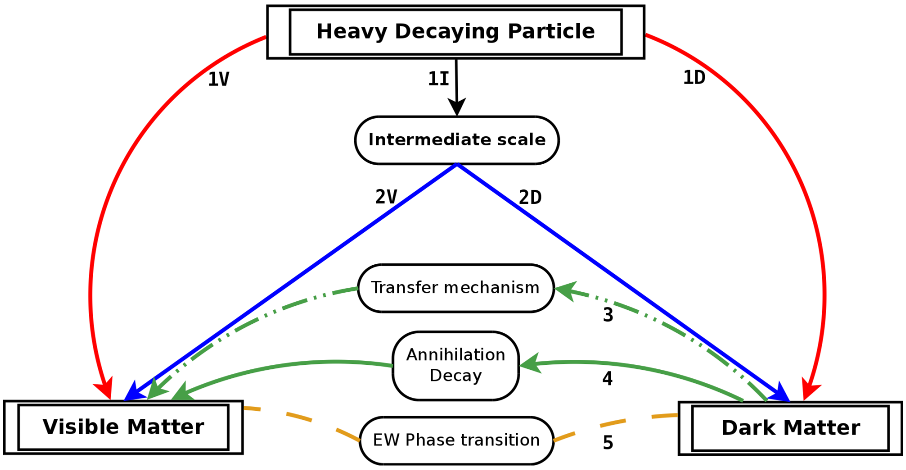

Figure 2.7: Schematic representing the different pathways to related dark matter to baryon asymmetry, for more details about the figure see [6].

Universe is asymmetric with an initial excess of baryons over anti-baryons parametrized by $\eta(b) = (n_b - n_{\bar{b}})/s \approx 10^{-10}$, where n denotes the number density and s the entropy density.

While the solutions to these two problems might well be unrelated to each other, it is nevertheless tempting to assume the new physics to be minimal and unifying enough so that it solves both of them with the same ingredients. Moreover if we discard simple numerical coincidence as an explanation to the intriguing vicinity of matter densities, we are left with the task to construct theories relating them or unifying their genesis. In Figure (2.7) we provide a depiction of the different possibilities invoked to relate DM to the baryon asymmetry of the Universe (BAU).

Indeed, numerous models have been proposed in the recent years to achieve this end. Broadly speaking, there are three approaches that are followed to relate dark matter to baryons:

- The WIMP paradigm is used as a framework to relate the abundances;
- There is a sector connecting DM and baryons in the early Universe. The connecting sector acts either as a parent sector, generating DM and baryons through decay for instance, or as a mediator mechanism trans-

ferring the asymmetry from the dark to the baryonic sector or vice versa. Asymmetric DM models (see below) used this approach extensively;

- The DM sector is an auxiliary to a successful baryogenesis scenario. The strength of the phase transition in electroweak baryogenesis may for instance be enhanced by the presence of DM.

The first two approaches are the most interesting and we will give two examples to show how they can be implemented.

2.5.1 WIMPy baryogenesis

It has been noted in Section (2.3) that thermal relics provide in a *miraculous* way the correct relic density of DM. Without any doubt, maintaining the success of the WIMP paradigm and extending it to relate DM to the baryon asymmetry is an attractive possibility. WIMPy baryogenesis [166] is among the most elegant theories tying the WIMP paradigm to baryogenesis. Other models preserving the WIMP miracle and attempting to relate DM to BAU can be found in [167–169], see [6] for a review.

In WIMPy baryogenesis, the baryon asymmetry arises from WIMP annihilation instead of the decay of some heavy state. Indeed, the annihilation of DM in the early Universe can satisfy the Sakharov conditions [170]* and leads to a net baryon asymmetry and the observed WIMP relic density.

The baryon asymmetry generated with the WIMP annihilation can be washed out by two kinds of processes: inverse annihilation of baryons to DM, and baryon to anti-baryon processes. Therefore the main requirement for any viable WIMPy baryogenesis scenario is that washout processes must freeze-out before WIMP freeze-out. Inverse annihilations are Boltzmann suppressed for $T < M_\chi$ but baryon to anti-baryon washout can be relevant also for $T \ll M_\chi$. One way

*A successful baryogenesis mechanism must satisfy the three Sakharov condition: B violation, $\mathcal{C}$ and $\mathcal{CP}$ violation and departure from thermal equilibrium. In this particular case the departure from equilibrium ensues from the non-relativistic decoupling of DM at freeze-out.

to suppress such a process is by introducing an exotic heavy anti-baryon X to which WIMPs annihilate through the process $\chi\chi \to B\,X$ where B is a SM baryon and X is an exotic anti-baryon. If X has mass $m_X > M_\chi$, for $T < M_\chi$ its abundance is Boltzmann suppressed and therefore the baryon to anti-baryon washout processes are suppressed. Therefore the condition:

$$M_\chi \lesssim M_X \lesssim 2M_\chi\,, \tag{2.11}$$

must be satisfied (the second inequality is due to kinematics). Baryon number violation is achieved by annihilating the DM to two sectors: baryons and exotic anti-baryons. It is important that the decays of the exotic particles do not erase the baryon asymmetry generated in the SM sector. For this end, an extra symmetry is required to decouple the exotic fields from the SM. After solving the Boltzmann equations, the comoving number density (yield) of baryons is given by:

$$Y_B \approx \frac{\epsilon}{2}[Y_\chi^{\rm washout} - Y_\chi]\,, \tag{2.12}$$

where $Y_{B,\chi} \equiv n_{B,\chi}/s$ are the observed baryon and DM yields, and ϵ is the baryon-anti-baryon asymmetry. It is required that $\epsilon < 1$. The observed baryon asymmetry is $Y_B \approx 9 \times 10^{-11}$ [77]. From Equation (2.12) and the relation that DM must satisfy at late time, we obtain:

$$Y_\chi \approx \frac{(5\,{\rm GeV})}{M_\chi}\,Y_B\,. \tag{2.13}$$

It follows that $Y_\chi^{washout} \gg Y_\chi$, namely it is crucial to freeze-out the washout processes *before* the WIMP ($\chi\chi$ annihilation) freeze-out temperature otherwise any generated asymmetry would be quickly erased. This is how the crucial out-of-equilibrium requirement of the Sakharov conditions is realized in WIMPy baryogenesis. Finally, the detection prospects are varied in this scenario and include direct detection (for models with annihilation to quarks), indirect detection (anti-deuteron) and collider signals. See [171, 172] for a general phenomenological study of this class of models.

2.5.2 Asymmetric dark matter models

Asymmetric dark matter (ADM) [173–180] (for reviews see [6, 181–183]) is a class of DM models often seen as an alternative to the WIMP paradigm. The rationale of ADM is based on the hypothesis that DM abundance is, similarly to baryons, only the surviving asymmetric part of the initial density and is of the same order as the baryon asymmetry, that is:

$$n_\chi - n_{\overline{\chi}} \approx n_b - n_{\overline{b}} \,. \tag{2.14}$$

The motivation comes from the fact that the observed DM and visible matter abundances are remarkably close to each other. These models usually lead to a relation between DM mass and proton mass: $M_\chi \approx 5\, m_p$ (where m_p is proton's mass) in contrast with WIMP dark matter models where the scale of reference is the weak scale. The relation between the DM mass and the proton mass is however not explained except in some models based on hidden sectors such as in mirror worlds [184–186], models with a dark QCD [187], or composite models.

ADM can be implemented in many ways leading to a wide theoretical and phenomenological landscape. While it is difficult to classify these models in a straightforward way, it is nevertheless enriching to highlight the key principles they usually rely on. Essentially, two main approaches are followed: (*i*) dark and visible matter asymmetries are generated at the same time. This is usually achieved with the decay of a heavy particle; (*ii*) the asymmetry is generated in the dark sector then is transferred (*via* sphaleron processes, higher dimension operators or renormalizable interactions) to the visible sector, or the other way around. It is also necessary to pass at some point by a thermalization phase either to get rid or to avoid the production of the symmetric part of DM (a less extreme cancellation of the asymmetric part leads to mixed scenarios between WIMP and ADM [188]).

One of the first models of ADM and a prototype of ADM theories is the one of

Ref. [179]. It is based on a mechanism originally proposed in [176] to unify in an elegant way the abundances of DM and baryons. In [179], a new symmetry is postulated, namely a $\mathbb{Z}_2$ parity, under which the SM particles are even and the new particles are odd, forming a dark or hidden sector. The lightest of the hidden particle is stable and is a DM candidate. A generalized $B-L$ number is unbroken and is shared between the SM and the dark sector, thus any excess of $B-L$ that is generated in one of the two sectors is compensated by the same excess in the other sector. After baryogenesis, the interactions between the visible and the dark sectors become negligible, and the $B-L$ excesses are separately conserved in the two sectors giving a relation between the visible and dark relic densities.

A simple model realizing the idea consists of a heavy particle P, a messenger particle X which carries a color charge, and the DM candidate χ, all odd under the $\mathbb{Z}_2$ while the SM is even. The mechanism proceeds through 3 stages. In the first stage P has $\mathcal{CP}$-violating out of equilibrium decays to SM fields and to a lighter messenger X generating an excess in both sectors but preserving the generalized $B-L$ globally. Then, it is assumed that below the baryogenesis temperature the two sector are decoupled and the two asymmetries are conserved such that we have:

$$n_{B-L}^{\rm SM} = -n_{B-L}^{X} \approx n_X - n_{\bar{X}} \, . \tag{2.15}$$

In the second stage the dark X messenger annihilate away its symmetric part with $\overline{X}$ through gauge interactions and we are left with its asymmetric part only. In the third and final stage, X decays to DM particles, χ, and we obtain:

$$n_\chi \propto n_{B-L}^{X} \, , \tag{2.16}$$

which gives a tight relation between the visible (baryonic) and DM number densities. To ensure that such a relation exists, it is important that X is long lived enough such that it decays after its symmetric part cancels out.

An interesting possibility is to consider X itself as the DM particle. This is not feasable here because of the charge assignment of X (colored particle). However, 'hylogenesis' [189] realizes this idea with a simple modification of the model. Note that the original asymmetry can be generated through the Affleck-Dine [190, 191] mechanism in a SUSY framework [192–195] or through leptogenesis as in [196].

2.6 Summary

Observations at different scales indicate that the bulk of the Universe's matter content must be in some as-yet-undetected form of dark matter. Although the nature of dark matter remains unknown, the case for its existence is quite compelling as we have seen. Inferences from what DM should *not* be like, allow us to gain some insights on its identity. This allowed theorists to propose well motivated candidates to solve the DM puzzle. Among them, axions and WIMPs are particularly attractive. Striving to find relations between DM and other problems of the SM such like the $\mathcal{CP}$ problem or baryogenesis is a driving force in DM model-building that usually leads to new candidates.

Dark matter is currently actively searched for by direct, indirect and collider experiments. There are reasons to be optimistic that such an intense and broad research program will shed light on the nature of dark matter. Specifically for WIMPs, the next few years are going to be decisive — for the better or for the worse. Much has been achieved since the 1930's when Zwicky first noticed the dark matter problem. But there still remains much to learn about it!

3

The lightness of being — massive neutrinos

I have done something very bad today by proposing a particle that cannot be detected;
it is something no theorist should ever do.
Wolfgang Pauli

Ever since W. Pauli first proposed their existence in 1930, neutrinos have fascinated theorists and experimentalists alike. After years of heroic experimental efforts, we have amassed considerable knowledge about these elusive particles. In particular we know that neutrinos oscillate, and that at least two of them are not massless. The mass splittings and oscillation parameters are now known with great accuracy, however it seems that we've barely scratched the surface of this physics — neutrinos still have a lot to reveal! Indeed, we still do not know whether neutrinos are Dirac or Majorana fermions, and many issues remain open regarding the nature of the associated mass-giving operator, for example,

- its underlying symmetries;
- its flavor structure;
- its dimensionality;
- its characteristic scale;
- its underlying mechanism or theory.

This leads to considerable theoretical freedom which makes model building a particularly hard task, a difficulty which to a large extent persists despite the tremendous experimental progress of the last fifteen years.

This chapter is organized as follows: after a short detour on preliminaries and notation in the next section, we will review the basics of neutrino mixings in Section (3.2). The status of neutrino oscillations is presented in Section (3.3). In Section (3.4) we will present the celebrated tri-bimaximal mixing *ansatz* before introducing the bi-large *ansatz* in Section (3.5) to account for the latest developments in the field. Then we review neutrino mass mechanisms (Section (3.6)): high and low scale seesaw models are reviewed in Section (3.6.1) and Section (3.6.2) respectively, and radiative neutrino mass models are presented in Section (3.6.3). Finally, we summarize the chapter in Section (3.7).

3.1 Preliminaries & notation

An adequate notation should be understood by at least two people,
one of whom may be the author.
Abdus Salam

We will now introduce the necessary definitions and formalism we will use in the following chapters*. In particular we will introduce the notion of Dirac and Majorana masses.

The proper orthochronous Lorentz group $SO^+(1,3)$, augmented with Parity ($\mathcal{P}$) and Time-reversal ($\mathcal{T}$) symmetries, is reducible to its double cover group $SL(2,\mathbb{C})$ (the set of complex 2×2 matrices with unit determinant). The irreducible representations (*irrep.*) of $SL(2,\mathbb{C})$ are labeled as (m,n), where m,n are non-negative half-integers. The spinorial representation is $(\frac{1}{2},0)$ or $(0,\frac{1}{2})$, and is also a fundamental representation of the Lorentz group. $(\frac{1}{2},0)$ representations act on two component objects called *left-handed Weyl spinors*. However the complex conjugate of these matrices is another inequivalent representation of $SL(2,\mathbb{C})$ (but equivalent in Lorentz, in pure analogy to $SO(3)/SU(2)$) called $(0,\frac{1}{2})$. Objects that are acted upon in this representation are now called *right-handed Weyl spinors*. These two representations are thus seen to be 2-dimensional. By taking the direct sum $(\frac{1}{2},0)\oplus(0,\frac{1}{2})$ of the two representations, we obtain a 4-dimensional (reducible) representation of the Lorentz group which acts upon 4-component objects called Dirac spinors.

Any Dirac spinor ψ can be decomposed into two independent components, i.e., chiralities, by means of the projection operators $P_{R/L}=(1\pm\gamma_5)/2$:

$$P_{R/L}\,:\,\psi\rightarrow\psi_{R/L}\equiv P_{R/L}\psi\,. \tag{3.1}$$

*This section is inspired from [197–200].

For convenience, we will use exclusively 4-spinors throughout. This formalism is rigorously equivalent to two-components spinors. In order to be able to write mass terms, we have to define the charge conjugation operation*:

$$\mathcal{C} \,:\, \psi \to \psi^c \equiv C(\psi^\dagger\gamma_0)^T = C\bar{\psi}^T \,. \qquad (3.2)$$

The appearance of the γ_0 matrix in Equation (3.2) is just a standard convention to make the bilinears manifestly Lorentz invariant†. The hermitian matrix C is defined by the relation $C^{-1}\gamma_i C = -\gamma_i^T$, where γ_i are the Dirac matrices. In both the Weyl and the Dirac bases only γ_2 is complex so that $C = \gamma_2\gamma_0$, up to an overall phase. We fix:

$$C = i\gamma_2\gamma_0 \,. \qquad (3.3)$$

In this case, C satisfies the following useful relations:

$$C^T = C^\dagger = C^{-1} = -C \,. \qquad (3.4)$$

Which implies in particular that:

$$(\psi^c)^c = \psi \,, \quad \bar{\psi^c} \equiv \psi^T C \,. \qquad (3.5)$$

Although $\mathcal{C}$ has nothing to do with Lorentz symmetries, under $\mathcal{C}$ transformation chiral fields see their chirality flipped. The transformation of a left handed field for instance reads:

$$\mathcal{C} \,:\, \psi_L \to (\psi_L)^c \equiv (\psi^c)_R. \qquad (3.6)$$

For fermions, the mass term must be a bilinear formed by the contraction of both chiralities: $\overline{\psi_R}\eta_L$, for any chiral spinors ψ_R and η_L. For a Dirac spinor ψ

*Note that charge conjugation and particle-anti-particle conjugation are identical for massive fermions but not for chiral fermions.

†The Dirac bilinears formed with $\psi^\dagger$ and ψ are not Lorentz invariant. One must use $\bar{\psi} = \psi^\dagger\gamma_0$ instead. This fact can be traced back to the $(+,-,-,-)$ signature of the flat space-time metric.

with the two chiralities, $\psi = \psi_L + \psi_R$, we have the following mass:

$$-\mathcal{L}_{Dirac} = M_\nu^{Dirac}\,\bar{\psi}\psi = M_\nu^{Dirac}\,\overline{\psi_L}\psi_R + \text{h.c.} \tag{3.7}$$

This is the *Dirac mass* term. In the presence of only one chirality, we can use Equation (3.6) and Equation (3.4) to construct the other one and form a *Majorana mass* term*:

$$-\mathcal{L}_{Maj} = \frac{1}{2}M_\nu^{Maj}\,(\overline{\psi_L^c}\psi_L + \text{h.c.}) = \frac{1}{2}M_\nu^{Maj}\,\psi_L^T C\psi_L + \text{h.c.} \equiv \frac{1}{2}M_\nu^{Maj}\,\widetilde{\psi_L}\psi_L + \text{h.c.} \tag{3.8}$$

In this case, ψ_L is necessarily invariant under any complex or pseudoreal transformation. In particular, it cannot carry an unbroken $U(1)$ charge (local and global alike) because the mass term would break it by two units. Notice that we have introduced the notation:

$$\boxed{\widetilde{\psi} = \psi^T C} \tag{3.9}$$

In general, M_ν^{Dirac} and M_ν^{Maj} are matrices whose dimension depends on the particle content of the model. While M_ν^{Dirac} is an arbitrary complex matrix, the Majorana mass matrix satisfies $M_\nu^{Maj} = M_\nu^{Maj\,T}$, i.e., it is a symmetric complex matrix.

To summarize, using a Dirac spinor we can construct two types of masses:

$$\begin{aligned} \text{Dirac} \quad &\rightarrow \quad \overline{\psi_R}\psi_L \\ \text{Majorana} \quad &\rightarrow \quad \widetilde{\psi_L}\psi_L\,(\widetilde{\psi_R}\psi_R) \end{aligned}$$

3.1.1 Majorana masses in the Standard Model

In the SM, the only particle eligible to have a Majorana type of mass is the electrically neutral neutrino. All the other fermions have Dirac-type masses through the Higgs mechanism (see for instance Equation (1.13)). However, writing a Majorana mass for neutrinos is not possible because of the $SU(2)_L \otimes$

*The factor $\frac{1}{2}$ is necessary in order to normalize the mass with respect to the Dirac equation.

$U(1)_Y$ gauge symmetry (at the renormalizable level). Indeed, such a term would require two lepton doublets and a Higgs doublet, schematically $\widetilde{L}LH$, and this contraction is not allowed by $SU(2)_L$. And even if it were, it would violate electric charge by two units because of the presence of charged leptons in L. Clearly, we need to go beyond the SM to provide Majorana masses to the neutrinos. For instance, adding a Higgs $SU(2)_L$ triplet Δ, with hypercharge $Y = 1$, endows the SM with terms of the form $\widetilde{L}\Delta L$, which lead to Majorana masses for neutrinos and full consistency with $SU(2)_L \otimes U(1)_Y$ at a minimal price. Note that any Majorana-type mass for neutrinos implies a violation of lepton number by two units. This is not a problem since lepton number is purely accidental in the SM (the same applies to baryon number) and imposing its conservation would be questionable anyway [201].

Of course, one can mimic the charged fermions and give a Dirac mass to the neutrinos. This would require the introduction of a new chiral fermion: the right-handed neutrino. This is a perfectly viable thing to do, though (i) given the smallness of neutrino masses, the Yukawa coupling would need to be extremely small, $\mathcal{O}(10^{-12})$ — not very appealing; (ii) an exact symmetry has to be imposed on the Lagrangian to forbid Majorana terms (for instance, lepton number symmetry).

We conclude that, either Dirac or Majorana, the fact that neutrinos are massive implies the existence of new physics beyond the SM. The rest of the chapter will expand more on this by giving the possible pathways of new physics, as hinted to by the problem of neutrino masses.
In all what follows we make the natural assumptions that neutrinos are Majorana particles, i.e., $M_\nu \equiv M_\nu^{Maj}$.

3.2 Neutrino mixings

With massive neutrinos, we are lead to reproduce the scenario of the quarks mixings — see Equation (1.10). Namely, we cannot redefine the fields without introducing mixings in the leptons sector. Therefore, we have the equivalent of the CKM matrix for the leptons: the lepton mixing matrix, sometimes called PMNS, for Pontecorvo-Maki-Nakagawa-Sakata matrix [202]:

$$\boxed{\mathcal{U}_{lep} \;=\; \mathcal{U}_L^{e\,\dagger}\,\mathcal{U}_L^{\nu}} \tag{3.10}$$

where $\mathcal{U}_L^e$ is the matrix that diagonalizes the charged leptons, Equation (1.9). In the case where charged leptons are diagonal, the mixing angles can be directly read off the neutrino mixing matrix. Contrary to quarks, the fact that the neutrino mass matrix is in general complex symmetric implies the existence of only one unitary matrix to diagonalize it, so that the neutrino masses are derived through:

$$\mathcal{U}_L^{\nu T}\, M_\nu\, \mathcal{U}_L^{\nu}, = D_\nu\,, \tag{3.11}$$

or $M_\nu = \mathcal{U}_L^{\nu *}\, D_\nu\, \mathcal{U}_L^{\nu\dagger}$, where $D_\nu \equiv \mathrm{diag}(m_1, m_2, m_3)$ is the diagonal neutrino mass matrix, and $\mathcal{U}_L^\nu$ is the neutrino mixing matrix:

$$\begin{pmatrix} \nu_e \\ \nu_\mu \\ \nu_\tau \end{pmatrix} = \mathcal{U}_L^\nu \begin{pmatrix} \nu_1 \\ \nu_2 \\ \nu_3 \end{pmatrix}. \tag{3.12}$$

Here, $\nu_{1,2,3}$ denote the neutrino mass eigenstates. In general two additional phases appear in D_ν on top of the Dirac phase, as opposed to only one in the quark sector. This is due to the Majorana nature of the neutrino mass term. After rotating away the unphysical phases, we have:

$$\begin{aligned} \mathcal{U}_L^\nu &= \begin{pmatrix} 1 & 0 & 0 \\ 0 & c_{23} & s_{23} \\ 0 & -s_{23} & c_{23} \end{pmatrix} \begin{pmatrix} c_{13} & 0 & e^{-i\delta} s_{13} \\ 0 & 1 & 0 \\ -e^{i\delta} s_{13} & 0 & c_{13} \end{pmatrix} \begin{pmatrix} c_{12} & s_{12} & 0 \\ -s_{12} & c_{12} & 0 \\ 0 & 0 & 1 \end{pmatrix} \mathcal{T} \\ &= \begin{pmatrix} c_{12}c_{13} & s_{12}c_{13} & s_{13}e^{-i\delta} \\ -s_{12}c_{23} - c_{12}s_{13}s_{23}e^{i\delta} & c_{12}c_{23} - s_{12}s_{13}s_{23}e^{i\delta} & c_{13}s_{23} \\ s_{12}s_{23} - c_{12}s_{13}c_{23}e^{i\delta} & -c_{12}s_{23} - s_{12}s_{13}c_{23}e^{i\delta} & c_{13}c_{23} \end{pmatrix} \mathcal{T}\,. \end{aligned} \tag{3.13}$$

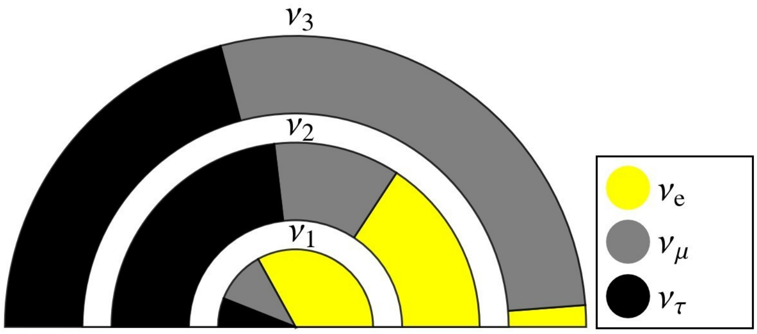

Figure 3.1: Flavor content of the neutrino mass eigenstates ν_1, ν_2 and ν_3. Angles taken from [203].

Here, δ is the Dirac $\mathcal{CP}$-violating phase and the matrix $\mathcal{T} \equiv \text{diag}(1, e^{i\beta}, e^{i\beta'})$ contains the Majorana phases. The three mixing angles are denoted by θ_{12}, θ_{23}, and θ_{13} ($s_{ij} = \sin\theta_{ij}$, $c_{ij} = \cos\theta_{ij}$).
In contrast with the quarks, Equation (1.12), the neutrino mixing angles are found to be quite large (see Table (3.1) for precise values and error estimates):

$$\theta_{12} \approx 34.6^\circ\,, \quad \theta_{23} \approx 49^\circ\,, \quad \theta_{13} \approx 9^\circ\,. \tag{3.14}$$

The composition of the neutrino mass eigenstates in terms of their interaction counterparts is depicted in Figure (3.1).
In summary there are nine physical parameters to describe neutrino masses and mixing: three masses, three angles and three phases. Before presenting the different proposed mechanisms to elucidate neutrino masses, we first review what the data tell us.

3.3 Experimental status

By now (2014), we have observed:

- Solar ν_e convert to ν_μ/ν_τ: Super-Kamiokande [204], SNO [205] and BOREXINO [206];
- Reactor $\bar{\nu}_e$ disappear at $L \approx 200\,\text{km}$: KamLAND [207];
- Atmospheric ν_μ and $\bar{\nu}_\mu$ disappear to ν_τ: Super-Kamiokande [208] and

MINOS [209];

- Accelerator ν_μ and $\bar{\nu}_\mu$ disappear at $L \approx 250\,\mathrm{km}$: T2K [210] and MINOS [209];
- Reactor ν_e disappear at $L \approx 1\,\mathrm{km}$: DOUBLE-CHOOZ[211], DAYA-BAY [212], RENO [213].

These observations confirm neutrino oscillations in vacuum and in matter at different scales and with different techniques. Table (3.1) summarizes the known neutrino properties, obtained from a global fit of the available experimental data [203] (other global fits are available in [214, 215]). We know from the data that at least two out of the three neutrinos are massive. That is because neutrino oscillation experiments are sensitive to the squared mass differences only; $\Delta m_{ij}^2 = m_i^2 - m_j^2$. Solar and atmospheric oscillations tell us that $\Delta m_{12}^2 \approx 7.5\,10^{-5}\,\mathrm{eV}^2$ and $|\Delta m_{31}^2| \approx 2.5\,10^{-3}\,\mathrm{eV}^2$ respectively. With these two mass splittings, the ordering (or *hierarchy*) of the masses cannot be determined. Depending on the sign of Δm_{13}^2 we distinguish:

$$\begin{aligned} \text{Normal ordering} \quad &\rightarrow \quad m_1 < m_2 < m_3\,, \\ \text{Inverted ordering} \quad &\rightarrow \quad m_3 < m_1 < m_2\,. \end{aligned}$$

The absolute mass of neutrinos is unknown. We only have upper limits on the neutrino masses or their sum, which only show that the neutrino masses are very small, $\mathcal{O}(\mathrm{eV})$ at most. Only two types of laboratory experiments are sensitive to the absolute scale of neutrinos: beta decay and neutrinoless double beta decay ($0\nu\beta\beta$). Tritium β decay sets the limit $m_\beta < 2.05\,\mathrm{eV}$ at 95% CL [216] while from $0\nu\beta\beta$ we have $m_{\beta\beta} \lesssim (0.2 - 0.4)\,\mathrm{eV}$ [217] at 90% CL (m_β and $m_{\beta\beta}$ are a combination of neutrino parameters). Additionally, the sum of (quasi-) stable neutrino masses is tightly constrained by cosmology:

$$\Sigma m_i < (0.23 \,-\, 1.08)\,\mathrm{eV}\,, \tag{3.15}$$

at 95% CL [77] (for more details about neutrinos in cosmology, see [218, 219]).

The current and future experimental programs are mostly devoted to resolve the following points:

- *Are neutrinos Majorana particles?* Neutrinoless double beta decay experiments (e.g., EXO and ZEN) are still testing the nature of neutrino masses. Detecting $0\nu\beta\beta$ would offer decisive evidence for the *Majorananess* of the neutrinos;

- *Is there leptonic $\mathcal{CP}$ violation?* Since $\theta_{13} \neq 0$, one expects $\mathcal{CP}$ violation in the leptonic sector. Measuring the $\mathcal{CP}$ phase is one of the main goals of experiments like MINOS, NOVA and LBNE;

- *What is the correct octant?* To know if the atmospheric neutrino angle in the first or second octant (cf. Table (3.1)) we need more precision in data from long baseline experiments;

- *What is the neutrino mass hierarchy?* Very long baseline experiments such as PINGU or a medium baseline reactor experiment like JUNO will strive to determine the hierarchy of neutrino masses. Also, Cosmology (PLANCK observations for instance) can provide information on the absolute scale of neutrino masses;

- *Are there sterile neutrinos?* By comparing the fits with and without the presence of light sterile neutrino states. Cosmology here is a powerful tool too (BICEP and PLANCK).

3.4 Tri-bimaximal mixing *ansatz*

In 2002, Harrison, Perkins and Scott remarked that the mixing of ν_μ and ν_τ at the atmospheric scale is almost bimaximal, while at the solar scale the mixing of ν_e with ν_μ is nearly trimaximal. This led them to suggest that the lepton mixing angles follow the tri-bimaximal (TBM) *ansatz* [220], defined by the

Parameter	Best Fit $\pm 1\sigma$		3σ interval	
	NH	IH	NH	IH
Δm^2_{21} $[10^{-5}\,\text{eV}^2]$	$7.60^{+0.19}_{-0.18}$		$[7.11, 8.18]$	
$\lvert\Delta m^2_{31}\rvert$ $[10^{-3}\,\text{eV}^2]$	$2.48^{+0.05}_{-0.07}$	$2.38^{+0.05}_{-0.06}$	$[2.30, 2.65]$	$[2.20, 2.54]$
$\sin^2\theta_{12} \times 10$	3.23 ± 0.16		$[2.78, 3.75]$	
$\sin^2\theta_{23} \times 10$	$5.67^{+0.32}_{-1.15}$	$5.73^{+0.25}_{-0.38}$	$[3.95, 6.42]$	$[4.05, 6.39]$
$\sin^2\theta_{13} \times 10^2$	$2.10^{+0.14}_{-0.09}$	$2.16^{+0.10}_{-0.12}$	$[1.79, 2.47]$	$[1.82, 2.50]$
δ/π	$1.48^{+0.43}_{-0.39}$	$1.48^{+0.28}_{-0.29}$	$[0, 2]$	

Table 3.1: Neutrino oscillation data circa 2014 [203]. It is also important to say that for normal hierarchy there is also another (local) minimum at $\sin^2\theta_{23} = 0.467$, in the first octant.

matrix*:

$$\mathcal{U}_{\text{TBM}} = \begin{pmatrix} 2/\sqrt{6} & 1/\sqrt{3} & 0 \\ -1/\sqrt{6} & 1/\sqrt{3} & 1/\sqrt{2} \\ 1/\sqrt{6} & -1/\sqrt{3} & 1/\sqrt{2} \end{pmatrix}. \tag{3.16}$$

Implying $\sin^2\theta_{12} = 1/3$, $\sin\theta_{13} = 0$ and $\sin^2\theta_{23} = 1/2$, as the data was suggesting until 2012 — charged leptons are assumed to be diagonal here. The *ansatz* became very popular and widely used by the neutrino *model-builders* community. Mixing parameters turn out to be simple numbers and such striking features point towards an underlying symmetry. Although the TBM *ansatz* requires the neutrino mass matrix to take a very special form in order to be diagonalized by Equation (3.16), models based on (mostly discrete) non-Abelian flavor symmetries were successful in reproducing it, notably the Ma-Babu-Valle model [223], and the Altarelli-Feruglio model [224].

TBM is a particular case of the $\mu - \tau$ symmetry, which is a matrix of the form

*The same matrix had been used by Wolfenstein back in the 70s [221]. Note also that the bimaximal *ansatz* [222] has also been widely used, although less than TBM.

(with the free parameters, x, y, z, w):

$$\mathcal{M}_\nu = \begin{pmatrix} x & y & y \\ y & z & w \\ y & w & z \end{pmatrix} . \tag{3.17}$$

Such a matrix predicts a maximal θ_{23} and vanishing θ_{13}. It can be easily obtained from discrete groups such as S_3, A_4 or D_4 (for a review, see for example [225–227]), and this explains to a large extent the successful predictions of TBM from flavor models based on discrete symmetries.

However the results published by the Double-Chooz [211], Daya-Bay [212], and RENO [213] collaborations, indicate that the reactor angle is relatively large so that corrections to the TBM pattern should be, in fact, quite large, casting doubt on its validity as a good first approximation reproducing the neutrino mixing pattern. To be more precise, on theoretical grounds a small deviation of order of the square of the Cabibbo angle was expected for the reactor angle, while recent observations indicate a much larger value of about the order of the Cabibbo angle. The TBM pattern may still be tenable if the underlying theory is capable of providing sufficiently large corrections to θ_{13} without affecting too much the solar angle, which is in principle possible albeit difficult to achieve.

To evade this problem, different *ansatz* have been considered like the 'bimaximal' mixing [228] or the 'tri-bimaximal-Cabibbo' mixing [229], see [230] for a review. However, most of these models assume a $\mu - \tau$-invariant structure in order to predict a maximal atmospheric mixing angle. In the next section we review a proposal of a new *ansatz*, where the reactor angle plays a central role.

3.5 Bi-large mixing *ansatz*

As we saw in the last section, the recent measurements of the neutrino mixing angles cast doubt on the validity of the so-far popular tri-bimaximal mixing *ansatz*. The bi-large (BL) *ansatz* is a different approach from TBM where we take the reactor mixing angle as the fundamental parameter, seeding the large solar and atmospheric mixing angles. The resulting parametrization does not reproduce the TBM pattern as a limiting case.

The main idea is that, since the reactor angle is the only small mixing parameter for the leptons, we can use it to seed both the solar and atmospheric mixing angles, as follows:

$$\begin{aligned} \sin\theta_{13} &= \lambda\,; \\ \sin\theta_{12} &= s\,\lambda\,; \\ \sin\theta_{23} &= a\,\lambda\,, \end{aligned} \tag{3.18}$$

where the small parameter λ is the reactor angle, while $s \approx a$ are free parameters of order a few. Solar and atmospheric mixings are expressed in terms of a linear dependence on the reactor angle. In the limit where $\lambda \to 0$ neutrinos are unmixed.

Using the general symmetric parametrization of the neutrino mixing matrix one can trivially obtain a simple approximate description by expanding only in the small parameter λ. For example, the Jarlskog invariant describing $\mathcal{CP}$ violation in neutrino oscillations is then given by:

$$J_{\mathcal{CP}} \approx a\ s\ \lambda^3\sqrt{1-a^2\lambda^2}\,\sqrt{1-s^2\lambda^2}\,\sin(\phi_{13}-\phi_{12}-\phi_{23}) \tag{3.19}$$

given explicitly in terms of the rephase-invariant Dirac combination. Likewise, the effective mass parameter describing the amplitude for neutrinoless double-beta decay is given in terms of the two Majorana $\mathcal{CP}$ phases.

From the data (Table (3.1)) we can directly read that $\sin\theta_{12} = \mathcal{O}(\sin\theta_{23})$. Now we go a step further and assume that $\sin\theta_{12} = \sin\theta_{23}$, which in our parametrization implies:

$$s = a. \tag{3.20}$$

Since both solar and atmospheric angles are large we call this case *BL mixing ansatz*.

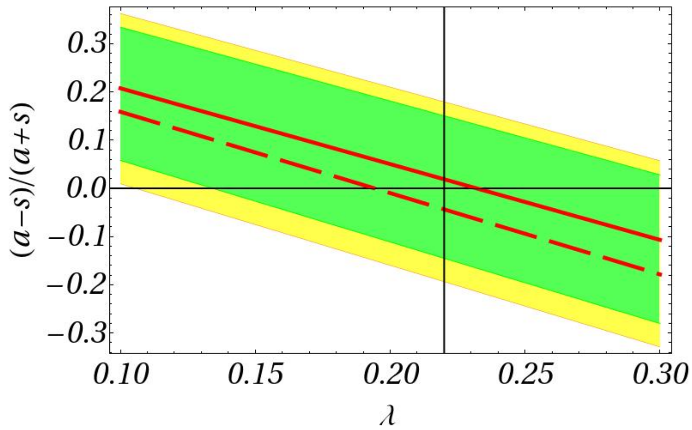

Figure 3.2: Deviation from the BL *ansatz* versus the expansion parameter λ at two and three sigma in the neutrino oscillation parameters. The solid and dashed lines indicate the best fits of Refs. [231] and [232], respectively. The strict BL *ansatz* holds when $\lambda \approx \lambda_C$ (vertical line).

Suppose now that we are given some model predicting *BL mixing* at leading order. Next-to-leading order operators in the Lagrangian in general induce deviations from the reference values in Equation (3.18) which may be reliably determined within a given model. Here we present a simple model-independent estimate of such corrections, obtained as follows. Typically it is expected that the corrections to the three mixing angles from next to leading order terms are of the same order, that is $\sin\theta_{ij} \to \sin\theta_{ij} \pm \epsilon$ where we have introduced a new parameter ϵ to characterize the magnitude of the correction. In this case our BL mixing gets corrections of the same order for the three mixing angles (given by ϵ) and which may either increase or decrease the starting BL values of the mixing angles. For definiteness let us consider an example where BL mixing is corrected as:

$$\begin{aligned} \sin\theta_{13} &= \lambda - \epsilon\,; \\ \sin\theta_{12} &= s\lambda - \epsilon\,; \\ \sin\theta_{23} &= a\lambda + \epsilon\,. \end{aligned} \tag{3.21}$$

where we take $s = a$ as in Equation (3.20). Since we have three free parameters, we can fix them using the best fit values.

In order to quantitatively clarify the role of the relation in Equation (3.20)

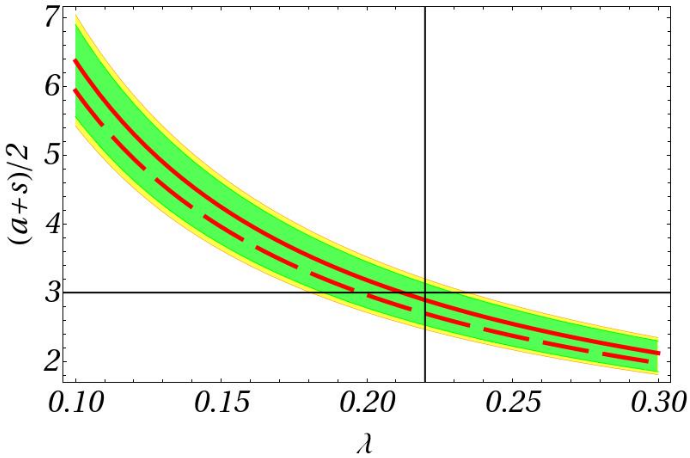

Figure 3.3: Average of solar and atmospheric angles versus the expansion parameter λ at two and three sigma in the neutrino oscillation parameters. The solid and dashed lines indicate the best fits of Refs. [231] and [232], respectively.

with respect to the reactor mixing angle, we consider here the most generic case given by Equation (3.21) where the three angles are given in terms of four parameters instead of three. Three of these parameters can be fixed from the three measured mixing angles, leaving one free parameter that we choose to be λ. In order to quantify the deviation from our exact BL mixing *ansatz* defined in Equation (3.20) we plot the combination $(a-s)/(a+s)$ as a function of the expansion parameter λ in Figure (3.2). The colored/shaded bands are calculated from the two and three sigma allowed ranges for the neutrino oscillation parameters obtained in the global fits. The solid and dashed lines indicate the best fits of [231] and [232], respectively. It is remarkable that the strict BL *ansatz* in Equation (3.20) holds when $\lambda \approx \lambda_C$ where $\lambda_C \approx 0.22$. This means that λ_C is the leading order value of $\sin\theta_{13}$. It has been shown that a similar relation can emerge in GUTs via charged lepton corrections [233].

In Figure (3.3) we show the average value of a and s, that is $(a+s)/2$, as a function of λ. The correlation is such that $(a+s)/2 \approx 3$ when $\lambda \approx \lambda_C$, the Cabibbo parameter. It follows that one possible form of our BL *ansatz*, which can be useful for model building, is:

$$\begin{aligned}\sin\theta_{13} &= \ \ \lambda\,;\\ \sin\theta_{12} &= 3\,\lambda\,;\\ \sin\theta_{23} &= 3\,\lambda\,.\end{aligned} \tag{3.22}$$

It is remarkable to see how such a simple form is nearly consistent with current global neutrino oscillation data. This appears to be an important numerological "coincidence" which may drastically change our theoretical approach for constructing neutrino mass models, by moving from a *geometrical* interpretation of the neutrino mixing angles to one in which these are no longer associated to Clebsch-Gordan coefficients of any symmetry, in sharp contrast to the previous (TBM) paradigm.

We conclude with a few words on model building. For the sake of illustration, we consider in the BL mixing *ansatz*, Equation (3.22), a normal and strongly hierarchical spectrum ($m_{\nu_1} = 0$) for neutrino masses and fix the squared mass differences at their best fit values, as given in [231]. We find that the resulting weak-basis neutrino mass matrix m_ν has the form:

$$m_\nu \approx \begin{pmatrix} 0.20 & 0.32 & 0.15 \\ & 0.75 & 0.70 \\ & & 1 \end{pmatrix} \approx \begin{pmatrix} \lambda_C & \lambda_C & \lambda_C \\ & 1 & 1 \\ & & 1 \end{pmatrix} \tag{3.23}$$

where in the last step the Cabibbo angle is used as the expansion parameter and we do not specify numerical coefficients of order one.
From the form obtained in Equation (3.23) one sees that the parameter λ_C appears only in the first row. On the other hand in the "atmospheric sector" there seems to be "democracy" in the choice of the neutrino mass entries. Altogether the above hints toward two general features regarding the neutrino mass generation mechanism:

- a Frogatt-Nielsen-like flavor symmetry [234] that could generate the required pattern given in Equation (3.23). This has been done in [235] for instance;

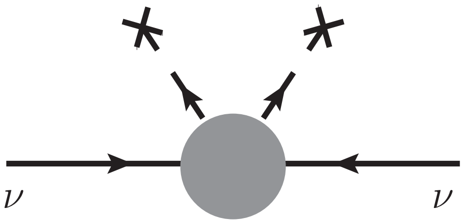

Figure 3.4: Depiction of Weinberg's dimension-5 $LLHH$ operator for generating Majorana neutrino masses. The *vev* insertions are from $SU(2)_L$ doublets.

- some gravity-like [236] "flavor-blind" mechanism operating within the "atmospheric sector". The problem in this case is that, for reasonable values of the coefficients of the dimension five operator, the induced neutrino masses are too small. However there may be other well-motivated "anarchy"-type schemes [237–240].

Still, a geometric interpretation of the mixing angles and derivation of the BL *ansatz* is still possible as was shown, for instance, in [241, 242]. Finally, interestingly enough the BL mixing can arise from F-theory (see for instance, Sec.(7), Eq.(7.13) of [243]).

3.6 Neutrino masses

In full generality, with Standard Model fields one can induce Majorana neutrino masses through the non-renormalizable dimension-5 operator:

$$\mathcal{O}_{\mathrm{dim}=5} = \frac{\lambda_{ij}}{\Lambda} \widetilde{L}_i H L_j \check{H} + \mathrm{h.c.}\,, \tag{3.24}$$

introduced by Weinberg [201]*. λ_{ij} is a dimensionless coupling and Λ denotes some unknown effective scale. Following the notation introduced in Equation (1.8), $\check{H} = i\tau_2 H$. Mechanisms inducing neutrino mass may be broadly divided on the basis of whether the associated messengers lie at the high energy scale (related say, to some unification scheme), or in contrast they involve new physics at the TeV scale, potentially accessible at the LHC.

*Higher order operators, e.g., of the type $LLHH(H^\dagger H)^m$ [244–248] are also possible, at the price of minimality.

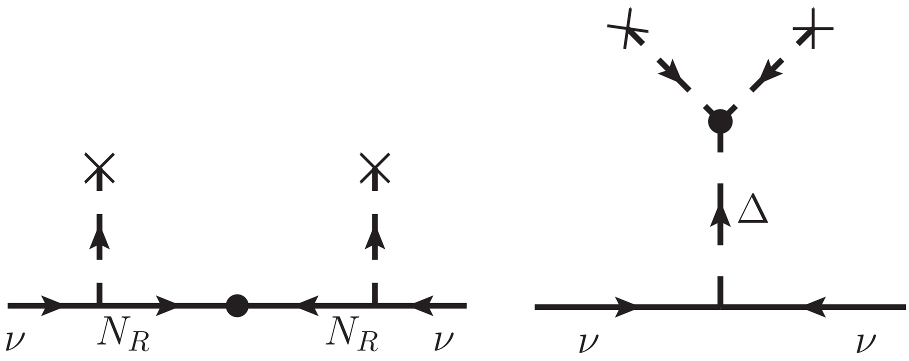

Figure 3.5: Neutrino mass generation in the type-I seesaw (left) and type-II seesaw (right). The small black disks show where lepton number violation takes place.

For simplicity here we tacitly assume neutrino masses to come from Weinberg's operator in Equation (3.24). This operator can arise in a rich variety of different pathways [249]. The seesaw mechanism, that we will review in the next section, is perhaps the most elegant and well motivated theory for neutrino masses. It can be realized at high (Section (3.6.1)) or low (Section (3.6.2)) scale. Neutrino masses can also have a radiative origin, with possible rich low scale phenomenology. We will review radiative models in Section (3.6.3).

3.6.1 The seesaw variations

In general, neutrino masses via tree level exchange of high scale messengers leads to neutrino masses of $\mathcal{O}(v_{SM}^2/M_{messenger})$. This suppression can be realized in three different ways:

- **Type I seesaw** requires at least two neutral iso-singlet fermions;
- **Type II seesaw** employs an $SU(2)_L$ scalar triplet;
- **Type III seesaw** requires at least two $SU(2)_L$ fermion triplets.

Seesaw Type-I

The seesaw mechanism [250–255], with a GUT-scale Majorana matrix $M_N \gg v_{SM}$, and the Dirac Yukawa matrix Y_D, is based on the Lagrangian:

$$-\mathcal{L} = Y_D \bar{L}\check{H} N + \frac{1}{2} M_N \widetilde{N_R} N_R + \text{h.c.}\,. \tag{3.25}$$

The mechanism generates small neutrino masses, as well as mixing of the neutrino flavors through the "seesaw relation":

$$M_\nu^{seesaw-I} = -m_D\, M_R^{-1}\, m_D^T\,, \tag{3.26}$$

where $m_D \equiv Y_D\, v_{SM}$ and M_R is the mass of the right handed neutrino N_R. This leads to the well-known type-I seesaw relation:

$$\boxed{m_\nu \approx m_D^2/M_{\text{messenger}}\,,} \tag{3.27}$$

where the messenger here is the right handed neutrino N_R. The mechanism is depicted in Figure (3.5) (left). In general, the 6×6 matrix U that diagonalizes the neutrino mass is unitarity and is given by:

$$U = \begin{pmatrix} \left(I - \frac{1}{2}m_D^*(M_R^*)^{-1}\, M_R^{-1}m_D^T\right) V_1 & m_D^*(M_R^*)^{-1}\, V_2 \\ -M_R^{-1}\, m_D^T\, V_1 & \left(I - \frac{1}{2}M_R^{-1}\, m_D^T\, m_D^*\, (M_R^*)^{-1}\right) V_2 \end{pmatrix} + O(\epsilon^3), \tag{3.28}$$

where V_1 and V_2 are the unitary matrices that diagonalize the light and heavy sub-block respectively. From Equation (3.28) one sees that the active 3×3 sub-block is no longer unitary and the deviation is of the order of $\epsilon^2 \approx (m_D/M_R)^2$. The expansion parameter ϵ is very small if the scale of new physics is at the GUT scale so the induced lepton flavor violation (LFV) processes are suppressed. In this case there are no detectable direct production signatures at colliders nor LFV processes. Equation (3.27) implies that:

$$\epsilon^2 \approx m_\nu/M_R\,, \tag{3.29}$$

is suppressed by the neutrino mass, hence negligible regardless of whether the messenger scale M_R lies at the TeV scale*. As a result there is a decoupling of the effects of the messengers at low energy, other than providing neutrino masses. This includes for example lepton flavor violation effects†. Regarding

*Weak universality tests as well as searches at LEP and previous colliders rule out lower messenger mass scales [216, 256].

†Although, if lepton number is approximately conserved [257], the strength of the charged and neutral current weak interactions may be large enough to allow the production of the

direct signatures at collider experiments these require TeV scale messengers which can be artificially implemented here by assuming the Dirac-type Yukawa couplings to be tiny. This makes messenger production at colliders hopeless for this scenario.

Seesaw Type-II

Instead of the right-handed neutrino, a $Y = 1$ scalar triplet Δ is considered in this case a messenger field [253, 259–262]. The relevant coupling is:

$$\mathcal{L} = Y_\Delta^{ij} \widetilde{L}_i \, \tau_2 \, \Delta \, L_j + \text{h.c.} \,, \tag{3.30}$$

leading to (see Figure (3.5) (right)):

$$M_\nu^{seesaw-II} = Y_\Delta \langle \Delta \rangle \,, \quad \text{with } \langle \Delta \rangle = \frac{\mu \, v_{SM}^2}{M_\Delta^2} \,, \tag{3.31}$$

The *vev* of Δ results from the scalar potential:

$$V = \mu H^T \tau_2 \Delta^* H + M_\Delta^2 \text{Tr}(\Delta^\dagger \Delta) + \text{h.c.} \tag{3.32}$$

Assuming Y_Δ of order one, in order to have light neutrino mass there are two possibilities: either M_Δ is large or μ is small. The first case is the standard type-II seesaw where all the parameters of the model are naturally of order one.

In contrast, if type-II seesaw schemes are chosen to lie at the TeV scale, then lepton flavor violation effects as well as same-sign di-lepton signatures at colliders remain [263]. Obviously supersymmetrized "low-scale" type-II seesaw have an even richer phenomenology [264, 265].

latter at the LHC [258].

Seesaw Type-III

Type III see-saw [266] employs at least two $SU(2)_L$ fermion triplets, with null hypercharge. The relevant terms in the Lagrangian are:

$$-\mathcal{L} = Y_D \widetilde{L}\,\tau_2\,T\,H + M_T \mathrm{Tr}(\widetilde{T}T) + \mathrm{h.c.}\,. \tag{3.33}$$

In a manner similar to type-I seesaw, we get neutrino masses for $M_{\mathrm{messenger}} \equiv M_T \gg v_{SM}$:

$$M_\nu^{seesaw-III} = -Y_D^T\, M_T^{-1}\, Y_D v_{SM}^2\,. \tag{3.34}$$

Type-III seesaw suffers the same drawbacks as type-I seesaw for LFV signatures. However, because Δ transforms under the $SU(2)_L \otimes U(1)_Y$ group, the mechanism can lead to new signals in collider experiments. The LHC phenomenology has been studied, for example in [267].

3.6.2 Low scale seesaw

The seesaw schemes presented in the previous section are *bona fide* high-scale seesaw in the sense that, to account for the observed neutrino masses with reasonable strength for the relevant neutrino Yukawa couplings, one needs very large scales for the messenger mass, hence inaccessible to collider experiments. Of course within such scenarios one may artificially take TeV scales for the messenger mass by assuming tiny Yukawas, so as to account for the smallness of neutrino mass*. However by doing so one erases a number of potential phenomenological implications. Within the framework of the standard model $SU(3)_c \otimes SU(2)_L \otimes U(1)_Y$ gauge structure, the models can be labeled by an integer, m, the number of singlets [253]†. For example, to account for current neutrino oscillation data, a type-I seesaw model with two right-handed neutrinos is sufficient ($m = 2$). Likewise for models with $m = 1$ in which another mechanism such as radiative corrections (see below) generates the remaining scale. Especially interesting are models with $m > 3$, where one can exploit the

*One can avoid this in schemes where *ad hoc* cancellations [268] or symmetries [269, 270] prevent seesaw-produced masses.

†It has long ago been realized that, carrying no anomalies, singlets can be added in an arbitrary number to any gauge theory.

extra freedom to realize symmetries, such as lepton number (L), so as to avoid seesaw-induced neutrino masses, naturally allowing for TeV-scale messengers. This is the idea behind the inverse [271] and linear seesaw schemes [272–274] described in the next section. We call such schemes as genuine *low scale seesaw* constructions.

Inverse seesaw

In its simplest realization the inverse seesaw extends the standard model by means of two sets of electroweak two-component singlet fermions N_{Ri} and S_{Lj} [271]. The lepton number of the two sets of fields N_R and S_L can be assigned as $L(N_R) = +1$ and $L(S_L) = +1$. One assumes that the fermion pairs are added sequentially, i.e., $i, j = 1, 2, 3$, though other variants are possible. After electroweak symmetry breaking the Lagrangian is given by:

$$\mathcal{L} = m_D \overline{\nu}_L N_R + M\, \overline{N}_R S_L + \mu\, \widetilde{S}_L S_L + \text{h.c.}\,, \tag{3.35}$$

where m_D and M are arbitrary 3×3 Dirac mass matrices and μ is a Majorana 3×3 matrix. We note that the lepton number is violated by the μ mass term here. The full neutrino mass matrix can be written as a 9×9 matrix instead of 6×6 as in the typical type-I seesaw and is given by (in the basis ν_L, N_R and S_L):

$$M_\nu = \begin{pmatrix} 0 & m_D^T & 0 \\ m_D & 0 & M^T \\ 0 & M & \mu \end{pmatrix} \tag{3.36}$$

The entry μ may be generated from the spontaneous breaking of lepton number through the vacuum expectation value of a gauge singlet scalar boson carrying $L = 2$ [257].

It is easy to see that in the limit where $\mu \to 0$ the exact $U(1)_L$ symmetry associated to total lepton number conservation holds, so the light neutrinos are strictly massless. However individual symmetries are broken hence flavor is violated, despite neutrinos being massless [275, 276]. For complex couplings, one can also show that $\mathcal{CP}$ is violated despite the fact that light neutrinos

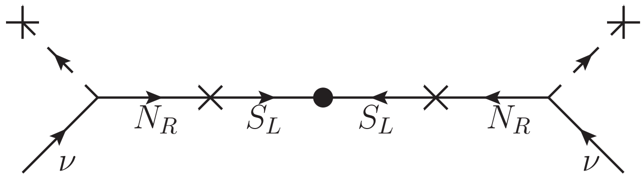

Figure 3.6: Neutrino mass generation in the type-I inverse seesaw.

are strictly degenerate [277, 278]. The fact that flavor and $\mathcal{CP}$ are violated in the massless limit implies that the attainable rates for the corresponding processes are unconstrained by the observed smallness of neutrino masses, and are potentially large.

This feature makes this scenario conceptually and phenomenologically interesting and is a consequence of the fact that the lepton number is conserved. However when $\mu \neq 0$ light neutrino masses are generated, see Figure (3.6). In particular in the limit where $\mu, m_D \lesssim M$ * the light neutrino 3×3 mass matrix is given by:

$$m_\nu^{inv.seesaw} \approx m_D \frac{1}{M} \mu \frac{1}{M^T} m_D^T \,. \tag{3.37}$$

It is clear from this formula that for "reasonable" Yukawa strength or m_D values, M of the order of TeV, and suitably small μ values one can account for the required light neutrino mass scale at the eV scale. There are two new physics scales, M and μ, the last of which is very small. Therefore it constitutes an extension of the standard model from below, rather than from above. For this reason, it has been called *inverse seesaw*: in contrast with the standard type-I seesaw mechanism, neutrino masses are suppressed by a small parameter, instead of the inverse of a large one. The smallness of the scale μ is *natural* in 't Hooft's sense, namely in the limit $\mu \to 0$, the symmetry is enhanced since lepton number is recovered†.

*On the other hand, the opposite limit $\mu \gg M$ is called double seesaw. In contrast to the inverse seesaw, the double seesaw brings no qualitative differences with respect to standard seesaw and will not be considered here.

†There are realizations where the low scale of μ is radiatively calculable. As examples see the supersymmetry framework given in [279], or the standard model extension suggested in [280].

In this case the seesaw expansion parameter $\epsilon \approx m_D/M$ also characterizes the strength of unitarity and universality violation and can be of order of percent or so [281, 282], leading to sizable lepton flavor violation rates, close to future experimental sensitivities. For example, with $m_D = 30$ GeV, $M = 300$ GeV and $\mu = 10$ eV we have that $\epsilon^2 \approx 10^{-2}$. The deviation from the unitary is typically of order ϵ^2. As mentioned above, typical expected lepton flavor violation rates in the inverse seesaw model can be potentially large (e.g., $\mu \to e\gamma$). Regarding direct production at colliders, although kinematically possible, the associated signatures are not easy to catch given the low rates as the right handed neutrinos are gauge singlets and due to the expected backgrounds (see for instance [283]).
One way out is by embedding the model within an extended gauge structure that can hold at TeV energies, such as an extra $U(1)$ coupled to $B - L$ which may arise from $SO(10)$ [274].

Linear type-I seesaw

This variant of low-scale seesaw was first studied in the context of $SU(2)_L \otimes SU(2)_R \otimes U(1)$ theories [272, 273] and subsequently demonstrated to arise naturally within the $SO(10)$ framework in the presence of gauge singlets [274]. The lepton number assignment is as follows: $L(\nu_{Li}) = +1$, $L(N_{Ri}) = +1$ and $L(S_{Li}) = +1$ so that, after electroweak symmetry breaking the Lagrangian is given by:

$$\mathcal{L} = m_D \overline{\nu}_L N_R + M_R \overline{N}_R S_L + M_L \nu_L \widetilde{S}_L + \text{h.c.}, \tag{3.38}$$

Notice that the lepton number is broken by the mass term proportional to M_L. This corresponds to the neutrino mass matrix in the basis ν_L, N_R and S_L given as:

$$M_\nu = \begin{pmatrix} 0 & m_D^T & M_L \\ m_D & 0 & M_R \\ M_L & M_R & 0 \end{pmatrix} \tag{3.39}$$

If $m_D \ll M_{L,R}$ then the effective light neutrino mass matrix is given by:

$$m_\nu^{lin.seesaw} = m_D\, M_L \frac{1}{M_R} + \text{Transpose}. \tag{3.40}$$

Model	Scalars	Fermions	LFV	LHC
Type-I		$(\mathbf{1},\mathbf{1},0)_{+1}$	✗	✗
Type-II	$(\mathbf{1},\mathbf{3},1)_{+2}$		✓	✓
Type-III		$(\mathbf{1},\mathbf{3},0)_{+1}$	✗	✓
Inverse		$(\mathbf{1},\mathbf{1},0)_{+1}$	✓	✗
Linear		$(\mathbf{1},\mathbf{1},0)_{+1}$	✓	✗

Table 3.2: Phenomenological implications of $SU(3)_c \otimes SU(2)_L \otimes U(1)_Y$ seesaw models together with their particle content. The subscript in the representations is lepton number. "✗" would change to "✓" in the presence of new gauge bosons or supersymmetry for instance.

Note that, in contrast with other seesaw varieties which lead to $m_\nu \propto m_D^2$, this relation is linear in the Dirac mass entry, hence the origin of the name "linear seesaw". Clearly neutrino masses will be suppressed by the small value of M_L irrespective of how low is the M_R scale characterizing the heavy messengers. For example, if one takes the SO(10) unification framework [274], natural in this context, one finds that the scale of M_L, i.e., v_L, is related to the scale of M_R, i.e., v_R, through:

$$v_L \approx \frac{v_R \, v_{SM}}{M_{\rm GUT}} \,, \tag{3.41}$$

where $M_{\rm GUT}$ is the unification scale of the order of $\mathcal{O}(10^{16}\,\text{GeV})$ and v_{SM} is the electroweak breaking scale of the order of $\mathcal{O}(100\,\text{GeV})$. Replacing the relation (3.41) in Equation (3.40) the new physics scale drops out and can be very light, of the order of TeV.

Neutrino mass messengers are naturally accessible at colliders, like the LHC, since the right handed neutrinos can be produced through the Z' "portal", as light as few TeV. The scenario has been shown to be fully consistent with the required smallness of neutrino mass as well as with the requirement of gauge coupling unification [274].

Similarly to the inverse type-I seesaw scheme, we also have here potentially large unitarity violation in the effective lepton mixing matrix governing the couplings of the light neutrinos. This gives rise to lepton flavor violation effects similar to the inverse seesaw case. Finally we note that, in general, a left-right symmetric linear seesaw construction also contains the lepton number violating Majorana mass term $\widetilde{S}_L S_L$ considered previously.

3.6.3 Radiative neutrino masses

In the previous sections we reviewed mechanisms ascribing the smallness of neutrino masses to the small coefficient in front of Weinberg's dimension-five operator. This was generated either through tree-level exchange of super-heavy messengers, with mass associated to high-scale symmetry breaking, or conversely, because of symmetry breaking at low scale. In what follows we turn to radiatively induced neutrino masses, a phenomenologically attractive way to account for neutrino masses. In such scenarios, the smallness of the neutrino mass follows from loop factor(s) suppression. From a purely phenomenological perspective, radiative models are quite interesting as they rely on new particles that typically lie around the TeV scale, hence accessible in principle to collider searches.

Unlike seesaw models, radiative mechanisms can go beyond the effective $\Delta L = 2$ dimension-five operator in Equation (3.24) and generate the neutrino masses at higher order. This leads to new operators and to further mass suppression. Such an approach has been reviewed in [284–288]. In what follows we will survey some representative underlying models up to the third loop level.

One-loop schemes

A general survey of one-loop neutrino mass operators leading to neutrino mass has been performed in [245]. Neutrino mass models in extensions of the SM with singlet right-handed neutrinos have been systematically analyzed in [289, 290] and for higher representations in [291]. Here we review the most representative model realizations.

▸ *Zee Model*

The Zee Model [292] extends the standard $SU(3)_c \otimes SU(2)_L \otimes U(1)_Y$ model with the following fields

$$h^+ \sim (\mathbf{1}, \mathbf{1}, +1)_{-2} \quad , \quad \phi_{1,2} \sim (\mathbf{1}, \mathbf{2}, +1/2)_0 \,, \tag{3.42}$$

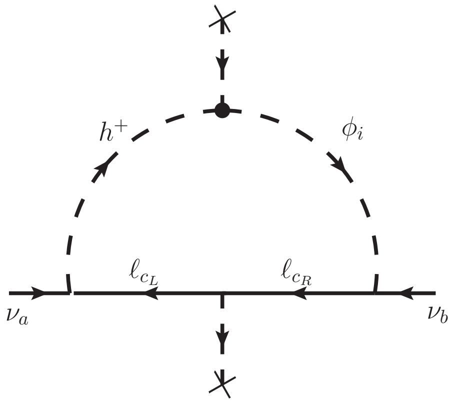

Figure 3.7: Neutrino mass generation in the Zee model.

where the subscript denotes lepton number. Given this particle content neutrino mass are one-loop calculable. The relevant terms are given by:

$$\mathcal{L} = y_i^{ab}\,\overline{L}_a\phi_i\ell_{bR} + f^{ab}\widetilde{L}_a\,i\tau_2\,L_b\,h^+ - \mu\,\phi_1^\dagger\,\check{\phi}_2\,h^+ + \text{h.c.}\,, \tag{3.43}$$

where a, b indicate the flavor indices, i.e., $a, b = e, \mu, \tau$ and τ_2 is the second Pauli matrix. Notice that the matrix f must be anti-symmetric in generation indices. The violation of lepton number, required to generate a Majorana mass term for neutrinos, resides in the coexistence of the two Higgs doublets in the μ term. The model has been extensively studied in the literature [293–316], particularly in the Zee-Wolfenstein limit where only ϕ_1 couples to leptons due to a $\mathbb{Z}_2$ symmetry [317].

This particular simplification forbids tree-level Higgs-mediated flavor-changing neutral currents (FCNC), although it is now disfavored by neutrino oscillation data [305, 318]. However the general Zee model is still valid phenomenologically [302] and is in testable with FCNC experiments. For instance the exchange of the Higgs bosons leads to tree level decays of the form $\ell_i \to \ell_j\ell_k\bar{\ell}_k$, in particular $\tau \to \mu\mu\bar{\mu}, \mu e\bar{e}$ (see for instance [319]). Collider phenomenology has been studied in [320, 321].
Recently, a variant of the Zee model have been considered in [322] by imposing a family-dependent $\mathbb{Z}_4$ symmetry acting on the leptons, thereby reducing the number of effective free parameters to four. The model predicts inverse

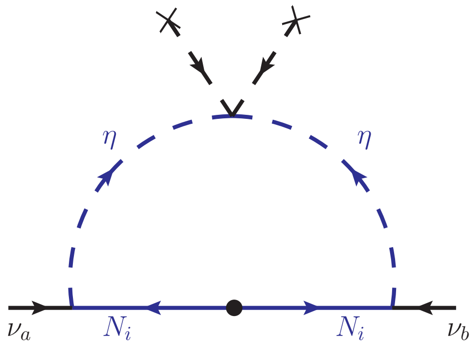

Figure 3.8: Neutrino mass generation in the radiative seesaw model. The blue color represents the potential dark matter candidates.

hierarchy spectrum in addition to correlations among the mixing angles.

▸ *Radiative seesaw: The scotogenic model*

Another one-loop scenario was suggested by Ma [323]. Besides the standard model fields, three right-handed Majorana fermions N_i ($i = 1, 2, 3$) and a Higgs doublet are added to the $SU(3)_c \otimes SU(2)_L \otimes U(1)_Y$ model,

$$N_i \sim (\mathbf{1}, \mathbf{1}, 0)_{+1} \quad , \quad \eta \sim (\mathbf{1}, \mathbf{2}, +1/2)_0 \,. \tag{3.44}$$

In addition, a parity symmetry acting only on the new fields is postulated. This $\mathbb{Z}_2$ is imposed in order to forbid Dirac neutrino mass terms. The relevant interactions of this model are given by:

$$\mathcal{L} = y_{ab}\, \overline{L}_a\, \check{\eta} N_b - \frac{M_{N_i}}{2} \widetilde{N}_i N_i + \text{h.c.} \tag{3.45}$$

In the scalar potential a quartic scalar term of the form $(H^\dagger \eta)^2$ is allowed. The one-loop radiative diagram is shown in Figure (3.8) and generates calculable $\mathcal{M}_\nu$ if $\langle \eta \rangle = 0$, which follows from the assumed symmetry. The neutrino masses are given by:

$$(M_\nu)_{ab} = \sum_i \frac{y_{ai} y_{bi}\, M_{N_i}}{16\pi^2} \left[\frac{m_R^2}{m_R^2 - M_{N_i}^2} \ln \frac{m_R^2}{M_{N_i}^2} - \frac{m_I^2}{m_I^2 - M_{N_i}^2} \ln \frac{m_I^2}{M_i^2} \right], \tag{3.46}$$

where m_R (m_I) is the mass of the real (imaginary) part of the neutral component of η.

Thanks to its simplicity and rich array of predictions, the model has become very popular and an extensive literature has been devoted to its phenomenological consequences. As is generally the case with multi-Higgs standard model extensions, the induced lepton flavor violation effects such as $\mu \to e\gamma$ provide a way to probe the model parameters. In particular the lepton flavor violation phenomenology has been studied in [324–329]. The effect of corrections induced by renormalization group running have also been considered [330], showing that highly symmetric patterns such as the bimaximal lepton mixing structure can still be valid at high-energy but modified by the running to correctly account for the parameters required by the neutrino oscillation measurements [231]. Collider signatures have also been investigated in [331–334].

A remarkable feature of this model is the natural inclusion of a WIMP dark matter candidate. Indeed, the same parity that makes the neutrino mass calculable, also stabilizes N_i and the neutral component of η. The lightest $\mathbb{Z}_2$-odd particle, either a boson or a fermion, can play the role of WIMP cold dark matter candidate [324, 326, 329, 335, 335–339].

Two-loop schemes

As a prototype two-loop scheme we consider the model proposed by Zee [340] and Babu [341] (which first appeared in [259]), that leads to neutrino masses at two-loop level by extending the standard model with two complex singly and doubly [342] charged $\mathrm{SU}(2)_L$ singlet scalars,

$$h^+ \sim (\mathbf{1}, \mathbf{1}, +1)_{-2} \quad , \quad k^{++} \sim (\mathbf{1}, \mathbf{1}, +2)_{-2} \,. \tag{3.47}$$

The relevant terms in the Lagrangian are therefore:

$$\mathcal{L} = f_{ab}\, \widetilde{L_a}\, i\tau_2\, L_b h^+ + g_{ab} \widetilde{\ell_{aR}}\, \ell_{bR} k^{++} - \mu\, h^- h^- k^{++} + \text{h.c.} \tag{3.48}$$

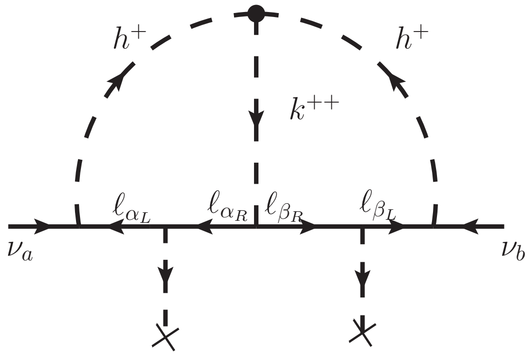

Figure 3.9: Neutrino mass generation in the Zee-Babu model.

The trilinear μ term in the scalar potential* provides lepton number violation and leads to a calculable Majorana neutrino mass generated at the second loop order, as shown in Figure (3.9) and given by:

$$(M_\nu)_{ab} \approx \mu \frac{1}{(16\pi)^2} \frac{1}{M} \frac{16\pi^2}{3} f_{ac} m_c g^*_{cd} m_d f_{bd} \,, \tag{3.49}$$

where $M = \max(M_{k^{++}}, M_{h^+})$ and m_a are charged lepton masses [344]. As in the Zee model, the matrix f is anti-symmetric. Therefore the determinant of m_ν vanishes and, as a result, one of the light neutrinos must be massless.

The Zee-Babu model is constrained by a variety of lepton flavor violation processes among which the tree-level lepton flavor violation $\ell_i \to \ell_j \ell_k \bar{\ell}_l$ decays induced by k^{++} exchange and the radiative decays $\ell_i \to \ell_j \gamma$ mediated by the charged scalars h^+ and k^{++}. Weak universality is also violated since the h^+ exchange induces new contributions for muon decay [344–347]. Both lepton flavor violation and weak universality tests constrain the model parameters. Combining lepton flavor violation and universality constraints [345] pushes the mass of h^+ and k^{++} above the TeV scale, for both inverted and normal hierarchies, making it a challenge to probe the model at the LHC. The collider phenomenology of the model has been considered in [344, 345, 348].

*This term can arise spontaneously through the *vev* of an extra gauge singlet scalar boson [343].

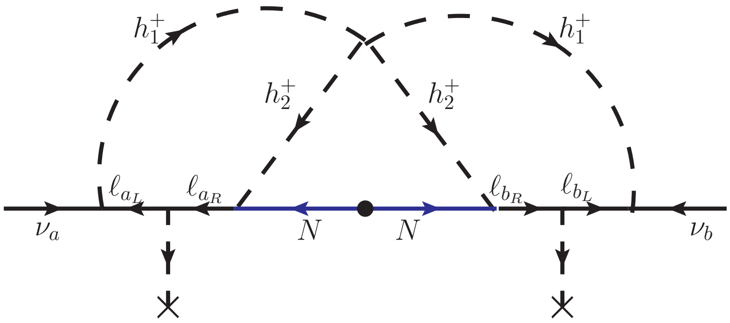

Figure 3.10: Neutrino mass generation in the KNT model.

Three-loop schemes

Of the possible three-loop schemes we will focus on the one suggested by Krauss-Nasri-Trodden (KNT) [349]. These authors considered an extension of the standard model with two charged scalar singlets h_1 and h_2 and one right-handed neutrino N,

$$h_{1,2}^+ \sim (\mathbf{1},\mathbf{1},+1)_{-2} \quad , \quad N \sim (\mathbf{1},\mathbf{1},0)_{+1}\,. \tag{3.50}$$

As usual in radiative neutrino mass models that include gauge singlet Majorana fermions, an additional $\mathbb{Z}_2$ symmetry is imposed, under which the SM fields as well as h_1 transform trivially, while N and h_2 are odd. The most general renormalizable terms that may be added to the SM fermion Lagrangian are:

$$\mathcal{L} = f_{ab}\widetilde{L}_a\, i\tau_2 L_b\, h_1^+ + g_a N h_2^+ \ell_{a_R} - \frac{1}{2} M_N \widetilde{N} N + \text{h.c.} \tag{3.51}$$

Note that the scalar potential contains a term of the form $(h_1 h_2^*)^2$, which makes possible the diagram of Figure (3.10) possible. Hence neutrinos acquire Majorana masses induced only at the 3-loop level. Such strong suppression allows for sizable couplings of the TeV scale singlet messenger states.

In addition to neutrino masses, the model also includes a WIMP dark matter candidate. Indeed for the choice of parameters $M_{h_2} > M_N$, N is stable and can be thermally produced in the early universe, leading naturally to the correct dark matter abundance.

A very similar model with the same loop topology has been proposed in [350], replacing the neutral gauge singlets by new colored fields and the charged leptons by quarks and in [351] the triplet variant of the model has been introduced. These variations makes the model potentially testable at hadron colliders. Other three loop mass models have also been considered more recently, for instance in [351–354]. A systematic study generalizing the KNT model was presented in [355].

	Model	Scalars	Fermions	LFV	DM	LHC
1-Loop	Zee	$(\mathbf{1},\mathbf{1},+1)_{-2}$, $(\mathbf{1},\mathbf{2},+1/2)_0$		✓	✗	✓
	Ma	$(\mathbf{1},\mathbf{2},+1/2)_0$	$(\mathbf{1},\mathbf{1},0)_{+1}$	✓	✓	✓
2-Loops	Zee-Babu	$(\mathbf{1},\mathbf{1},+1)_{-2}$, $(\mathbf{1},\mathbf{1},+2)_{-2}$		✓	✗	✓
3-Loops	KNT	$(\mathbf{1},\mathbf{1},+1)_{-2}$	$(\mathbf{1},\mathbf{1},0)_{+1}$	✓	✓	✗

Table 3.3: Phenomenological implications of radiative $SU(3)_c \otimes SU(2)_L \otimes U(1)_Y$ neutrino mass models discussed in this thesis. Representations are labeled as in the rest of the paper.

3.7 Summary and outlook

We have given a brief overview of neutrino physics, from the experimental status and theoretical models. Both high and low-scale approach to neutrino mass generation were reviewed. The different mass mechanisms and their phenomenological impacts are summarized in Table (3.2) for seesaw models and Table (3.3) for radiative mechanisms. We stressed the phenomenological interest of low scale models, in particular radiative models.

In conclusion if the messengers responsible for the light neutrino masses lie at a very high scale, like in type-I seesaw, it will be very difficult if not impossible to have any detectable signal within the non-supersymmetric SM seesaw framework. In contrast, within the low scale approach to neutrino mass we can have very interesting phenomenological implications. They can give rise to signatures at high energy collider experiments, as well as lepton flavor violation rates close to the sensitivity of planned experiments. In short, these scenarios may help reconstructing the neutrino mass from a variety of potentially over-constrained set of observables.

Additionally, we pointed out that some of the neutrino mass schemes naturally include a WIMP dark matter candidate. We will comment more on this latter point in the next chapter.

4

Intermezzo — the dark side of neutrinos

In the previous chapters we reviewed the status of neutrinos and dark matter; two compelling cases for new physics. Both neutrinos and dark matter enigmas stem from genuine experimental data. And, as we have seen, for both of them there are numerous ideas and insights as to how to amend the SM to accommodate them. Certainly, a unified description of dark matter and neutrinos is tempting and appealing. Hence the question:

Do dark matter and neutrinos share the same origin?

The first answer to the question was contemplated already in the 1970's. The audacious proposal was to identify SM neutrinos with dark matter [356]. Unfortunately, this does not work. The proposal is ruled out for two reasons:

abundance and temperature. Indeed, while being the second most abundant particles species after the photons*, neutrinos fail to accommodate the observed abundance of dark matter. The cosmological density of light neutrinos is [356]:

$$\Omega_\nu h^2 \approx \frac{\Sigma_i m_{\nu_i}}{93.2\,\mathrm{eV}}\,. \tag{4.1}$$

Applying the bound in Equation (3.15), we see that neutrinos cannot contribute for more than $\approx 2\%$ to the content of the Universe. In addition to being sub-abundant, neutrinos decouple while relativistic, when the temperature is $\mathcal{O}(\mathrm{MeV})$, and are thus hot relics. Thus neutrinos are not suitable DM candidates.

In light of the available data and theoretical ideas summarized in the previous chapters, we can distinguish —broadly speaking— two main approaches that are followed in order to positively answer the question above:

(i) Dark matter is identified with one of the new particles needed in order to give mass to neutrinos;

(ii) Dark matter is associated to the symmetries of the neutrino sector.

Approach I: mass mechanism

In Section (3.6) we distinguished between tree-level 'seesaw' mechanisms and radiative mechanisms to generate neutrino masses. These two possibilities are conceptually different and consequently the approach (i) is realized differently in one or the other. In seesaw schemes we can have for instance sterile neutrino keV warm dark matter or MeV dark matter [280], while in the radiative schemes we can have (either fermionic or bosonic) WIMPs. We briefly review the proposal of the sterile neutrino as a DM candidate and that of the WIMP in the radiative seesaw model:

*$n_\nu = \frac{3}{11}\, n_\gamma = \frac{6\zeta(3)}{11\pi^2} T^3_{\mathrm{CMB}}$, per flavour.

▸ Sterile neutrinos

Sterile neutrinos are neutrinos that are singlets under $SU(3)_c \otimes SU(2)_L \otimes U(1)_Y$. They have been invoked to generate masses for light neutrinos, see Section (3.6.1), or explain certain neutrino-experiment anomalies such as LSND. Since sterile neutrinos mix with light neutrinos, they can be produced via oscillations [357]. With this mechanism, their relic density is estimated to be:

$$\Omega_N \approx 0.2 \left(\frac{\sin^2\theta}{3\times 10^{-9}}\right)\left(\frac{M_N}{3\,\mathrm{keV}}\right)^{1.8} . \tag{4.2}$$

Here, θ is the mixing angle between the sterile neutrino N (of mass M_N) and the active ones. We see that a viable sterile neutrino DM requires keV masses and a very small mixing angle. With this mass, the sterile neutrino is a warm DM candidate. We note that the original oscillation mechanism is in conflict with Lyman-α bounds [358] at present. To remedy this, we can either amend the original mechanism (for instance by including lepton asymmetry [359]), or invoke a new contribution from a different mechanism (for instance, non-thermal production from inflaton decay [360]).

Recently, the detection of an unidentified emission line at energy $\approx 3.5\,\mathrm{keV}$ [13, 361] sparkled strong interest in sterile neutrino DM. It is remarkable that this line falls in the bulk of the allowed range of sterile neutrino DM, but further data and scrutiny are needed to assess the validity of this signal. A review on sterile neutrino as dark matter candidates can be found in [362]. Sterile neutrinos offer an economical solutions to the dark matter problem as well as an attractive link with neutrinos, however, they are not theoretically very appealing because they rely on a tuning of the parameters that does not seem natural.

▸ WIMPs in neutrino loops

We saw in Section (3.6.3) that neutrino masses can be generated radiatively. In particular, the 'scotogenic' model, presented in Equation (3.44) and Figure (3.8) has the remarkable feature of naturally including a WIMP dark matter candidate. Indeed, the parity symmetry introduced to forbid the seesaw contribution, stabilizes the lightest $\mathbb{Z}_2$-odd particle by the same token. The stable particle can be either a boson or a fermion, and can play the role of WIMP cold dark matter candidate thanks to its interactions with the Higgs or the neutrinos [324, 326, 329, 335, 335–339].

The most interesting possibility is to consider the singlet fermion as DM because it has interactions that are limited to the neutrino sector. Indeed, N_1 * couples to the SM only via the Yukawa interaction with the lepton doublet and therefore it is a leptophilic DM. Annihilation proceeds via the t-channel $N_1 N_1 \to \nu\nu$ with η exchange. However, there is a severe discrepancy between the magnitude of Yukawa couplings required by the dark matter relic abundance and the one needed to get neutrino masses and suppress lepton flavor violating processes. This is solved by assuming two things: (*i*) the $\mathcal{CP}$-odd and $\mathcal{CP}$-even parts of the scalar doublet (η) have to be degenerate to a high degree — the coupling responsible for this degeneracy has to be tiny, $\mathcal{O}(10^{-11})$; (*ii*) N_1 and N_2 have to be almost degenerate in mass in order to use their co-annihilation to obtain the correct relic abundance and agreement with lepton flavor violation limits. These unfortunate prescriptions render the N_1 candidate of the scotogenic model less attractive than what seems at first glance.

There is also the interesting possibility of the dark matter being warm in this setup [325, 363]. Various extensions of the model have also been considered, for e.g., [364, 365]. The scotogenic model is the simplest radiative mechanism for neutrinos that includes WIMPs, but it is by no means unique. In fact, we already pointed out that the three-loop mechanism introduced in Equation (3.50) offers as well a DM candidate. For a review on models with one–loop radiative neutrino masses and viable dark matter candidates we refer the reader to the complete classification given in [366, 367].

*We assume the hierarchy $N_1 < N_2 < N_3$.

The two models that we reviewed offer strong conceptual links between dark matter and neutrinos. However, they both rely on tunings of their parameters in order to work. More complex models are of course possible, but in that case the eventual correlations between the dark sector and neutrino physics are lost, buried in the high number of parameters. So we can see sterile neutrinos and the radiative seesaw as archetypes of models relating dark matter to neutrinos through the neutrino mass mechanism. We conclude that although this approach is theoretically viable and appealing, in practice the unpleasant tuning of the parameters renders it less attractive.

Approach II: lepton symmetries

The second approach links neutrinos to DM through the symmetries of the neutrino sector, i.e., the mixing patterns and/or lepton number. As noted in Section (2.1), one of the key requirements of any viable dark matter candidate is stability. From a particle physics point of view this is understood by having a symmetry that stabilizes the DM. On the other hand, neutrino masses are tightly linked to the accidental lepton number symmetry and its breakdown. Furthermore, the data suggest some underlying symmetry controlling leptons mixing patterns, see Section (3.4).

The lepton number offers an attractive portal to link DM and neutrinos. An interesting possibility is to apply an axion-like scheme to neutrinos. Namely, to promote the symmetry of neutrinos —lepton number— to a dynamical symmetry and identify its Nambu-Goldstone boson with a physical state playing the role of dark matter. This is the majoron. In Chapter (7) we will consider majoron DM in an inflationary scenario. Another approach using lepton number can be motivated by a gauged $U(1)_{B-L}$ symmetry, see for instance [368].

Finally, the link between neutrinos and dark matter through the leptons mixing patterns is an attractive possibility that will be the focus of the next two chapters, Chapter (5) and Chapter (6).

5

Discrete dark matter

Remember that all models are wrong;
the practical question is how wrong do they have to be to not be useful.
G. E. P. Box

Among the most important requirements a DM candidate has to satisfy are neutrality, stability over cosmological time scales, and agreement with the observed relic density, see Section (2.1) for more details. From a model building point of view, the conditions listed in Section (2.1) are not difficult to arrange, except for: (*i*) stability, that is in general assumed in an *ad-hoc* fashion; (*ii*) agreement with relic density, that depends on the details of the production mechanism.

From a particle physics viewpoint, the stability suggests the existence of a symmetry that forbids the couplings that would otherwise induce decay. Typically, the most common way to stabilize the DM particle is to invoke a $\mathbb{Z}_2$ parity and impose it by hand, an example of which is R parity in supersymmetry.
It would certainly be more appealing to motivate such a symmetry from a top-down perspective. This is what motivated attempts such gauged as $U(1)_{B-L}$ [369], discrete gauged symmetries [370–372], or accidental symmetries [373–375]. For a review on the possible origins of dark matter stability, see [376].

A new mechanism of stabilizing the DM has been proposed in [377] in which DM stability originates from the flavor structure of the SM. Indeed the same discrete flavor symmetry which explains the pattern of neutrino mixing can also stabilize the dark matter*. This opens an attractive link between neutrino physics and DM; two sectors that show a clear need for physics beyond the SM. Note that since the publication of [1, 377], other flavor models with DM candidates have been proposed, for e.g., [338, 378–384], and more recently [385] where the mechanism has been applied to asymmetric DM (Section (2.5.2)).

The model proposed in [377] is based on an A_4 symmetry extending the Higgs sector of the SM with three scalar doublets. After electroweak symmetry breaking two of the scalars of the model acquire vacuum expectation values which spontaneously break A_4 leaving a residual $\mathbb{Z}_2$. The lightest $\mathbb{Z}_2$ neutral odd scalar is then automatically stable and will be our DM candidate.
On the other hand, the fermion sector is extended by four right handed neutrinos which are singlets of $SU(3)_c \otimes SU(2)_L \otimes U(1)_Y$. Light neutrino masses are generated via a type I seesaw mechanism, obey an inverted hierarchy with $m_{\nu 3} = 0$ and vanishing reactor neutrino angle. For pioneer studies on the use of A_4 in neutrino physics see [223, 224].

*Models based on non-Abelian discrete symmetries but with a decaying dark matter candidate can be found for example in [378].

We study the regions in parameter space of the model where the correct dark matter relic density is reproduced and the various experimental and theoretical constraints are fulfilled. We then consider the prospects for direct dark matter detection in underground experiments. Indirect dark matter searches through astrophysical observations are not currently probing the model apart from some small regions of the parameter space where the dark matter annihilation cross section is enhanced via a Breit-Wigner resonance.

The objective of this chapter is to show to which extent DM and neutrinos can be related within a flavor model. This chapter is a significantly extended and updated presentation of the results obtained in [1]. The discovery of the Higgs and its tremendous consequences on Higgs portal DM models, WIMP in particular, are reflected in this revised version. Also PLANCK and direct detection experiments such as LUX, which significantly reduced the experimentally allowed regions of WIMP dark matter, were included for completeness. The main result of this updated analysis is that the model in its minimal realization cannot account for the entire abundance of dark matter. It is still enlightening nevertheless to present the DM phenomenology of the model because its conceptual and physical results are quite general. In other words, while the model is clearly wrong in its original form, it is still useful.

The chapter is organized as follows: in Section (5.1) we introduce the model, followed by its neutrino phenomenology in Section (5.2). A closer look to the origin of the stabilizing symmetry is given in Section (5.3). After a short interlude on Inert doublet models (Section (5.4)), we proceed with the DM phenomenological study by: (*i*) deriving the mass spectrum of the model (Section (5.5)); (*ii*) imposing the various experimental and theoretical constraints on the model (Section (5.6.1)), followed by a calculation of the relic density (Section (5.6.2)) and an evaluation of the impact of direct (Section (5.6.3)) and indirect (Section (5.6.4)) detection experiments on the model (Section (5.6)). Finally, in Section (5.7) we impose the limits derived from LHC and we conclude the chapter in Section (5.9).

	$\{I\}$	$\{T\}$	$\{T^2\}$	$\{S\}$
1	1	1	1	1
1′	1	ω	ω^2	1
1″	1	ω^2	ω	1
3	3	0	0	-1

$$\begin{aligned}(ab)_{\mathbf{1}} &= a_1b_1 + a_2b_2 + a_3b_3\\ (ab)_{\mathbf{1'}} &= a_1b_1 + \omega a_2b_2 + \omega^2 a_3b_3\\ (ab)_{\mathbf{1''}} &= a_1b_1 + \omega^2 a_2b_2 + \omega a_3b_3\\ (ab)_{\mathbf{3_1}} &= (a_2b_3, a_3b_1, a_1b_2)^T\\ (ab)_{\mathbf{3_2}} &= (a_3b_2, a_1b_3, a_2b_1)^T\end{aligned}$$

Figure 5.1: A_4 basics – Character table of the group (left), and rules for contractions of two triplets $a = (a_1, a_2, a_3)^T$ and $b = (b_1, b_2, b_3)^T$ (right). We use the (complex) basis where the generator S is diagonal. See Appendix (A.1) for more details.

5.1 Simple discrete dark matter model

We now provide a concrete realization of the discrete dark matter (DDM) mechanism based on the A_4 flavor symmetry in a type-I seesaw [250–255] framework introduced in Section (3.6.1). The matter fields are assigned to irreducible representations of the group of even permutations of four objects, $\Delta(12) \equiv A_4$. Geometrically, A_4 is isomorphic to the symmetry group of the tetrahedron (see Figure (A.1)). It has twelve elements and four irreducible representations: three singlet representations **1**, **1′** and **1″**, and one triplet representation **3**. The basic properties of A_4 are summarized in Figure (5.1). with $\omega^3 = 1$. We refer the reader to Appendix (A.1) for more details about the mathematical properties of this group. The Higgs sector consists of three Higgs doublets $\eta \equiv (\eta_1, \eta_2, \eta_3)^T$ transforming as a triplet, namely $\eta \sim \mathbf{3}$ and an iso-doublet H that is singlet of A_4. The model has in total four Higgs doublets, implying the existence of four $\mathcal{CP}$ even neutral scalars, three physical $\mathcal{CP}$-odd scalars* (three of the scalars are 'eaten' to give mass to the $W^\pm$ and Z gauge bosons). In the fermion sector, we have four right-handed neutrinos; three transforming as an A_4 triplet, $N_T \equiv (N_1, N_2, N_3)^T \sim \mathbf{3}$, and one singlet N_4. For simplicity, quarks are trivially left blind to A_4 (although see [379, 387] for a variation of the model including quarks). The lepton and Higgs assignments

*Although the imaginary part of the neutral component of Higgs doublets, A, is generally referred to as pseudo-scalar, this is not rigorously correct. In the absence of fermions $\mathcal{C}$ and $\mathcal{P}$ are separately conserved and $\mathcal{P}(A) = +1$. However $\mathcal{C}(A) = -1$ with or without fermions, therefore we find it preferable throughout the text to refer to A as $\mathcal{CP}$-odd scalar instead of pseudo-scalar [386].

are summarized in Table (5.1). The resulting Yukawa Lagrangian for leptons reads as

$$\begin{aligned}\mathcal{L}_Y &= y_e L_e l^c_e \hat{H} + y_\mu L_\mu l^c_\mu \hat{H} + y_\tau L_\tau l^c_\tau \hat{H} \\ &+ y^\nu_1 L_e\, N_T \eta + y^\nu_2 L_\mu [N_T \eta]_{\mathbf{1}''} + y^\nu_3 L_\tau [N_T \eta]_{\mathbf{1}'} \\ &+ y^\nu_4 L_e N_4 \hat{H} - \frac{M_1}{2} \widetilde{N_T} N_T - \frac{M_2}{2} \widetilde{N_4} N_4 + \text{h.c.}\end{aligned} \tag{5.1}$$

with $\tilde{N} \equiv N^T C$. The field $\hat{H}$ is the only one that couples to charged leptons and to quarks.

The scalar potential is:

$$\begin{aligned}V &= \mu^2_\eta \eta^\dagger \eta + \mu^2_{\hat{H}} \hat{H}^\dagger \hat{H} + \lambda_1 (\hat{H}^\dagger \hat{H})^2 + \lambda_2 [\eta^\dagger \eta]^2_{\mathbf{1}} + \lambda_3 [\eta^\dagger \eta]_{\mathbf{1}'} [\eta^\dagger \eta]_{\mathbf{1}''} \\ &+ \lambda_4 [\eta^\dagger \eta^\dagger]_{\mathbf{1}'} [\eta\eta]_{\mathbf{1}''} + \lambda_{4'} [\eta^\dagger \eta^\dagger]_{\mathbf{1}''} [\eta\eta]_{\mathbf{1}'} + \lambda_5 [\eta^\dagger \eta^\dagger]_{\mathbf{1}} [\eta\eta]_{\mathbf{1}} \\ &+ \lambda_6 ([\eta^\dagger \eta]_{\mathbf{3_1}} [\eta^\dagger \eta]_{\mathbf{3_1}} + \text{h.c.}) + \lambda_7 [\eta^\dagger \eta]_{\mathbf{3_1}} [\eta^\dagger \eta]_{\mathbf{3_2}} + \lambda_8 [\eta^\dagger \eta^\dagger]_{\mathbf{3_1}} [\eta\eta]_{\mathbf{3_2}} \\ &+ \lambda_9 [\eta^\dagger \eta]_{\mathbf{1}'} \hat{H}^\dagger \hat{H} + \lambda_{10} [\eta^\dagger \hat{H}]_{\mathbf{3_1}} [\hat{H}^\dagger \eta]_{\mathbf{3_1}} + \lambda_{11} ([\eta^\dagger \eta^\dagger]_{\mathbf{1}} \hat{H} \hat{H} + \text{h.c.}) \\ &+ \lambda_{12} ([\eta^\dagger \eta^\dagger]_{\mathbf{3_1}} [\eta \hat{H}]_{\mathbf{3_1}} + \text{h.c.}) + \lambda_{13} ([\eta^\dagger \eta^\dagger]_{\mathbf{3_2}} [\eta \hat{H}]_{\mathbf{3_1}} + \text{h.c.}) \\ &+ \lambda_{14} ([\eta^\dagger \eta]_{\mathbf{3_1}} \eta^\dagger \hat{H} + \text{h.c.}) + \lambda_{15} ([\eta^\dagger \eta]_{\mathbf{3_2}} \eta^\dagger \hat{H} + \text{h.c.})\,,\end{aligned} \tag{5.2}$$

where $[...]_{\mathbf{3_{1,2}}}$ ($[...]_{\mathbf{1},\mathbf{1}',\mathbf{1}''}$) is the product of two triplets contracted into a triplet (singlet) representation of A_4, following the rules stated in Figure (5.1). For the sake of simplicity, we assume $\mathcal{CP}$ conservation so that all the couplings and *vevs* are real, and consequently we can distinguish between scalars and $\mathcal{CP}$-odd scalars. For convenience we also assume $\lambda_4 = \lambda'_4$ in order to have manifest $\mathcal{CP}$ conservation in our chosen A_4 basis*.

The minimization of the scalar potential leads to the following *vev* alignment:

$$\left\langle \hat{H}^0 \right\rangle = v_H \neq 0, \quad \left\langle \eta^0_1 \right\rangle = v_\eta \neq 0, \quad \left\langle \eta^0_{2,3} \right\rangle = 0\,. \tag{5.3}$$

This particular *vev* alignment breaks the group A_4 to its subgroup $\mathbb{Z}_2$. In

*To see this, consider for instance the coupling $(\omega\lambda_4 + \omega^2 \lambda'_4)(\eta^\dagger_1 \eta_2)^2$ + h.c. arising from the terms proportional to λ_4 and λ'_4 in Equation (5.2). Since $\omega + \omega^2 = -1$ this coupling is real if $\lambda_4 = \lambda'_4$.

Group	L_e	L_μ	L_τ	l_e^c	l_μ^c	l_τ^c	N_T	N_4	$\hat{H}$	η
$SU(2)_L$	2	2	2	1	1	1	1	1	2	2
A_4	1	$1'$	$1''$	1	$1''$	$1'$	3	1	1	3

Table 5.1: Summary of the particle content of the model.

the next sections we show how this remnant symmetry emerges from A_4 and stabilizes some fields of the model. To fix the notation, after electroweak symmetry breaking and the minimization of the potential we write:

$$\hat{H} = \begin{pmatrix} H'^{+} \\ (v_H + H' + iA')/\sqrt{2} \end{pmatrix}; \tag{5.4}$$

$$\eta_1 = \begin{pmatrix} H_1'^{+} \\ (v_\eta + H_1' + iA_1')/\sqrt{2} \end{pmatrix}; \tag{5.5}$$

$$\eta_2 = \begin{pmatrix} H_2'^{+} \\ (H_2' + iA_2')/\sqrt{2} \end{pmatrix}; \quad \eta_3 = \begin{pmatrix} H_3'^{+} \\ (H_3' + iA_3')/\sqrt{2} \end{pmatrix}. \tag{5.6}$$

5.2 Neutrino phenomenology

Before anything, the model presented in the previous section is neutrino flavor model. It is thus mandatory before moving the DM phenomenology, to start with neutrino phenomenology. The model contains four heavy right-handed neutrinos. It is a special case of the general type-I seesaw mechanism (see Section (3.6.1)). After electroweak symmetry breaking, it is characterized by the following Dirac and Majorana mass matrices:

$$m_D = \begin{pmatrix} x_1 & 0 & 0 & x_4 \\ x_2 & 0 & 0 & 0 \\ x_3 & 0 & 0 & 0 \end{pmatrix}, \quad M_R = \begin{pmatrix} M_1 & 0 & 0 & 0 \\ 0 & M_1 & 0 & 0 \\ 0 & 0 & M_1 & 0 \\ 0 & 0 & 0 & M_2 \end{pmatrix}. \tag{5.7}$$

where x_1, x_2, x_3 and x_4 are respectively proportional to y_1^ν, y_2^ν, y_3^ν and y_4^ν of Equation (5.1) and are of the order of the electroweak scale, while $M_{1,2}$ are assumed to be close to the unification scale. Light neutrinos get Majorana masses by means of the type-I seesaw relation so that the light neutrinos mass matrix is of the form:

$$m_\nu = -m_{D_{3\times 4}} M_{R_{4\times 4}}^{-1} m_{D_{3\times 4}}^T \equiv \begin{pmatrix} y^2 & ab & ac \\ ab & b^2 & bc \\ ac & bc & c^2 \end{pmatrix}. \quad (5.8)$$

Such a matrix texture has a null eigenvalue $m_3 = 0$ corresponding to the eigenvector $(0,\, -b/c,\, 1)^{T*}$ implying a vanishing reactor mixing angle $\theta_{13} = 0$ and inverse hierarchy. The atmospheric angle; the solar angle; and the two squared mass differences can be fitted. The model implies a neutrinoless double beta decay effective mass parameter in the range 0.03 to 0.05 eV at 3σ, within reach of upcoming experiments.

Now that Daya-Bay has discovered that θ_{13} is actually quite large, an amendment is necessary. However, this will not affect the DM phenomenology or the general principle of discrete dark matter. In the next chapter we will present a model that is compatible with large θ_{13} based on [2], see also [388, 389] for other variations.

5.3 Origin of dark matter stability

The group A_4 has two generators, S and T, which satisfy the relations $S^2 = T^3 = (ST)^3 = I$ (see Appendix (A.1) for the mathematical properties of A_4). In the three dimensional real basis, S is given by

$$S = \begin{pmatrix} 1 & 0 & 0 \\ 0 & -1 & 0 \\ 0 & 0 & -1 \end{pmatrix}. \quad (5.9)$$

*Note that if we were to stick to the minimal type-I seesaw scheme with just three $SU(2)_L$ singlet states, one would find a projective nature of the effective tree-level light neutrino mass matrix with two zero eigenvalues, hence phenomenologically inconsistent. That is why we adopted the scheme with 4 singlets instead.

In this basis, S is manifestly the generator of a $\mathbb{Z}_2$ symmetry that is a subgroup of A_4. Indeed, for a generic triplet irreducible representation of A_4, $\Psi = (a_1,\ a_2,\ a_3)^T$, we have:

$$S\Psi = \begin{pmatrix} 1 & 0 & 0 \\ 0 & -1 & 0 \\ 0 & 0 & -1 \end{pmatrix} \begin{pmatrix} a_1 \\ a_2 \\ a_3 \end{pmatrix} = \begin{pmatrix} a_1 \\ -a_2 \\ -a_3 \end{pmatrix}. \qquad (5.10)$$

So that the second and third component of A_4 triplets are odd under a $\mathbb{Z}_2$ subgroup. The particular alignment found in Equation (5.3), $\langle \eta \rangle \sim (1, 0, 0)$, breaks spontaneously A_4 to $\mathbb{Z}_2$ because $(1, 0, 0)$ is invariant under the S generator; $S \langle \eta \rangle = \langle \eta \rangle$. Consequently, the $\mathbb{Z}_2$ residual symmetry is defined as

$$\begin{array}{lllllll} N_1 & \to & +N_1\,, & \quad & \eta_1 & \to & +\eta_1, \\ N_2 & \to & -N_2\,, & \quad & \eta_2 & \to & -\eta_2, \\ N_3 & \to & -N_3\,, & \quad & \eta_3 & \to & -\eta_3, \end{array} \qquad (5.11)$$

and the rest of the matter fields are $\mathbb{Z}_2$-even, because the singlet representation transforms trivially under S. We summarize in Table (5.2) the transformation of the fields of the model under the remnant parity symmetry.

One of the key requirements a DM candidate must fulfill is stability over cosmological scales. However, the existence of a $\mathbb{Z}_2$ symmetry in the Lagrangian, while stabilizing the neutral fields it acts on, does not guarantee *per se* the existence of a viable WIMP DM candidate. Indeed, one needs to make sure that:

(*i*) the mass of the lightest $\mathbb{Z}_2$-odd particle lies around the electroweak scale;

(*ii*) there exists a “portal” to efficiently thermally produce the DM candidate in the early Universe;

(*iii*) the protecting symmetry is stable under radiative corrections;

(*iv*) the WIMP candidate can account for the observed dark matter density and successfully evades current experimental bounds.

	L_e	L_μ	L_τ	l_e^c	l_μ^c	l_τ^c	N_T	N_4	H	η
$\mathbb{Z}_2$	$+$	$+$	$+$	$+$	$+$	$+$	$(+,-,-)$	$+$	$+$	$(+,-,-)$

Table 5.2: Transformation of the fields under the remnant $\mathbb{Z}_2$ symmetry.

The first point is satisfied in the following way: since there are no couplings with charged fermions nor quarks because of the A_4 symmetry, the only Yukawa interactions of the lightest neutral component of $\eta_{2,3}$ are with the heavy singlet right-handed neutrinos $N_{2,3}$. In other words, the "dark sector" is composed of $N_{2,3}$ and $\eta_{2,3}$, the lightest of which is the DM candidate. The right handed neutrinos are constrained by neutrino physics to lie at the seesaw scale, $\approx 10^{12}$ GeV, and $\eta_{2,3}$, being $SU(2)_L$ doublets have naturally masses around the electroweak scale (in fact, they are *forced* by A_4 and SM gauge group to be close to the electroweak scale. See next section, Equation (5.40)). Notice that we want a link with the electroweak scale because we interpret "Weakly" in WIMP as related to the SM weak interaction — see Equation (2.8). Indeed, this is where the so-called 'WIMP miracle' makes sense*. The second requirement is then readily satisfied, $\eta_{2,3}$ has quartic couplings with the Higgses. Such couplings constitute a production portal for the DM. Finally, the $\mathbb{Z}_2$ symmetry is exact because it comes from an exact symmetry of the Lagrangian, A_4, i.e., it is not accidental.

Thus the lightest neutral component of $\eta_{2,3}$, stabilized by the remnant parity symmetry, constitutes our (bosonic) DM candidate. To assess the last point (iv) of the WIMP DM requirements, we need to undertake a dedicated DM phenomenological study. For the sake of definiteness, we consider the DM to be the $\mathcal{CP}$-even state H_2.

We now turn to the explicit description of the mass spectrum of the scalars in the model. The particular mixing patterns and masses of the scalars reveal the underlying symmetries of the potential and the interactions between the

*Although, in full generality, a generic WIMP where production in the early Universe proceeds via physics that is unrelated to the weak scale is possible and is commonly used in the literature.

different fields of the model, in particular they show how A_4 constrains the DM properties. But before that, we remind the reader of some general features of the simplest extension of the SM with a Higgs: the Inert Higgs Doublet model (IDM). This will help us to highlight the features that are particular to the model we have under scrutiny.

5.4 Interlude: Inert Doublet Model(s)

The model presented in Section (5.1) consists of two "active" Higgs fields *ie* taking part in electroweak symmetry breaking, H and η_1, augmented with two inert higgses, η_2 and η_3. Two Higgs models (2HDM) are perhaps the simplest alternative to the Standard Model. They constitute a minimal extension that offers a wide array of new phenomena: $\mathcal{CP}$ non-conservation, flavor violating processes (FCNC), new charged scalar particles, etc. Their historical importance resides mostly in the fact that they are essential to low-energy supersymmetry, though they appear in other models that allow a broader parameter range. Multi-Higgs models are now more important than ever after LHC confirmed the existence of (most likely fundamental) scalars in nature. For a recent review on 2HDM, see [390].

If we call multi-Higgs models with N active higgses and M inert ones: $(N + M)$IDM, then the model of Section (5.1) is of type $(2 + 2)$. Models of type $(2 + M)$IDM would be similar to 2HDM as long as the active higgses are concerned but offer in addition to that a DM candidate and new phenomenological signatures thanks, for instance, to the presence of new inert charged particles in the spectrum. $(N + M)$IDM differ in their DM phenomenology in a number of ways, for instance:

- the number of DM production portals and direct detection channels increases with N;
- the number of possible co-annihilation channels depends on M (e.g., there are 2 possible co-annihilation diagrams for $M = 1$ and 5 for $M = 2$);
- the facility with which the DM candidate could evade experimental

bounds (LEP, LHC, direct and indirect detection experiments) depends also on the interplay between N and M. Clearly, now that LHC confirms the existence of the Higgs boson and finds spectacular agreement with SM predictions, the case $N > 1$ is more favored for phenomenological studies as it provides more freedom. The particularly minimal case with $N = 2$ is, perhaps, the most attractive for phenomenology since it's just a step further from the SM.

The simplest $(N + M)$IDM model is the $(1 + 1)$IDM, or IDM for short. Given its historic importance, rich phenomenology and extensive use in DM studies it is particularly enlightening to compare DM models based on multi-Higgs extension of the SM with IDM. In this section we remind the reader of its basic features. The Inert Doublet Model consists of the extension of the SM by a Higgs doublet, H_1, that is odd under a $\mathbb{Z}_2$ symmetry. It has been originally introduced three decades ago in [391] in order to study electroweak symmetry breaking patterns. It has been later advocated to address the naturalness problem [392]. The model was later on extended with right-handed neutrinos to radiatively generate neutrino masses, in the so-called "scotogenic" model [323], presented in Equation (3.44) and Section (4). It has become an "archetype" [393] of WIMP dark matter offering a simple and phenomenologically rich model. Although the recent data from direct detection experiments combined with LHC bounds strongly constrain the parameter space of the model, it is nevertheless an interesting case of study and it is generally illuminating to compare properties of scalar DM with IDM.

Because of the $\mathbb{Z}_2$, the Yukawa sector of the SM is unchanged. However, the scalar potential becomes:

$$\begin{aligned} V \;=\; & -\mu^2(H^\dagger H + \mu_1^2 H_1^\dagger H_1 + \lambda_1 (H^\dagger H)^2 + \lambda_2 (H_1^\dagger H_1)^2 \\ & + \lambda_3 (H^\dagger H)(H_1^\dagger H_1) + \lambda_4 (H^\dagger H_1)(H_1^\dagger H) \\ & + \lambda_5 ((H^\dagger H_1)^2 + \text{h.c.}), \end{aligned} \tag{5.12}$$

where H is the Higgs doublet of the SM. The minimization of the potential results in the usual SM relation:

$$\langle H \rangle = \frac{v_{SM}}{\sqrt{2}} \equiv \mu^2 \sqrt{2} \lambda_1 \,, \tag{5.13}$$

with $v_{SM} = 246\,\mathrm{GeV}$. In order to preserve the $\mathbb{Z}_2$ symmetry, H_1 is forbidden from taking *vev*, $\langle H_1 \rangle = 0$, i.e., $\mu_1^2 > -v_S M^2$. After electroweak symmetry breaking we can write:

$$H = \begin{pmatrix} 0 \\ (v_{SM} + h)/\sqrt{2} \end{pmatrix} \quad , \quad H_1 = \begin{pmatrix} H_1^+ \\ (H_1 + iA_1)/\sqrt{2} \end{pmatrix}, \tag{5.14}$$

with h being the SM Higgs boson. Notice that we use the letter h to refer exclusively to the SM Higgs as observed by ATLAS [25] and CMS [26] at the LHC. The spectrum of the model is then given by:

$$M_h^2 = 2\lambda_1 v_{SM} \equiv 2\mu^2 \,; \tag{5.15}$$

$$M_{H^1}^2 = \mu_2^2 + \lambda_L v_{SM}^2 \,; \tag{5.16}$$

$$M_{A^1}^2 = \mu_2^2 + \lambda_S v_{SM}^2 \,; \tag{5.17}$$

$$M_{H_1^+}^2 = \mu_2^2 + \lambda_3 v_{SM}^2/2 \,. \tag{5.18}$$

We used the usual definition: $\lambda_{L,S} = \lambda_3 + \lambda_4 \pm \lambda_5$. We understand better the utility of these definitions if we point out that λ_L (λ_S) is the coupling of a pair of H_1 (A_1) particles to the Higgs; the Higgs portal couplings.

Because of the requirement of preservation of $\mathbb{Z}_2$ symmetry ($\langle H_1 \rangle = 0$), the μ_1 parameter is not constrained by any tadpole equation, contrary to μ (Equation (5.13)). The mass scale of the fields of the doublet H_1 is then essentially free* and *a priori* unrelated to the electroweak scale, even if $\lambda_{3,4,5}$ are constrained by perturbativity considerations. This is generally common to multi-Higgs models based on unbroken symmetries: to preserve the symmetry, the quadratic ("μ") terms of the Higgs fields charged under this symmetry, are forced to be positive and contribute to the mass spectrum in an unconstrained fashion.

*They are free *in principle*. As commented in Section (2.2), unitarity constrains the mass of a WIMP to be $\lesssim 130\,\mathrm{TeV}$ [120].

The DM is the lightest particle between H_1 and A_1 depending on the sign of λ_5. The phenomenology of this DM candidate can be summarized as follows:

Low masses: $M_{DM} < M_W$

Production in the early Universe is achieved through Higgs portals.Gauge bosons portals are inefficient (Z) or inoperative (W^+, because of LEP bounds on charged scalars) so that the Higgs is the only production portal. There's a possibility of co-annihilation allowed by LEP in the mass range $[45, 80]$ GeV [394]. Now that the mass of the Higgs boson is fixed, there's little room left to control the abundance of DM. Moreover, the branching ratio of invisible Higgs decays constrains the low mass region ($M_{DM} < M_h/2 \approx 60$ GeV) so well that the model is essentially ruled out in the relevant range [395]. This is generally the problem of models of type $(1 + M)$. An available regions remains open though, albeit fine-tuned, when we approach the kinematic threshold $M_{DM} \approx M_h/2$.

High masses: $M_{DM} \gtrsim M_W$

For large masses the annihilations to gauge bosons (and the 2 Higgs final states from the quartic coupling, when the channels are opened) are so efficient that any DM abundance is rapidly diluted away. Although, three-body decays and cancellations among diagrams push this lower limit a little bit further than M_W, to $\approx$ 120 GeV [396]. The abundance remains negligible until the DM mass reaches $\approx$ 600 GeV [393] and the gauge interactions reach a critical value. Indeed, in this case the cross section into gauge bosons scales as α_W/M_{DM}^2 and gives the correct relic density for $M_{DM} \approx 600$ GeV. Of course, the higgs portal couplings should be switched off ($\lambda_{L,S} \approx 0$) in order to preserve the correct relic density. Unfortunately, there's no WIMP DM experiment that is sensitive to this parameter space.

To conclude this section, some of the general lessons that can be extracted from the IDM are:

- Because of the $\mathbb{Z}_2$ symmetry, there's no tadpole equation constraining the quadratic term (μ) of the inert Higgs. As a result the mass scale of dark matter and its coannihilation partners is free;
- Production and annihilation proceed via a single Higgs portal and are strongly constrained by LHC and direct detection experiments in the low mass region;
- There is a viable region at $M_{DM} \approx 600\,\text{GeV}$.

We now go back to our model to explicitly derive the masses of the scalars before proceeding to the phenomenological analysis of the model.

5.5 The hidden tetrahedron

This section deals with hidden manifestations of A_4 as revealed by the mass spectrum. As in the case of IDM, the expressions of the masses already say a lot about the ensuing DM phenomenology. The neutral scalars mass matrix in the basis $H' - H_1' - A' - A_1' - H_2' - H_3' - A_2' - A_3'$ is found to reproduce the following structure:

$$M^2_{neutrals} = \begin{pmatrix} M^2_{HH_1} & 0 & 0 & 0 \\ 0 & M^2_{GA_1} & 0 & 0 \\ 0 & 0 & M^2_{H_2H_3} & 0 \\ 0 & 0 & 0 & M^2_{A_2A_3} \end{pmatrix} , \tag{5.19}$$

whereas the charged scalars mass matrix in the basis $H_1'^+ - H_1'^+ - H_2'^+ - H_3'^+$ is of the form:

$$M^2_{charged} = \begin{pmatrix} M^2_{G^+H_1^+} & 0 \\ 0 & M^2_{H_2^+H_3^+} \end{pmatrix} , \tag{5.20}$$

where $M^2_{HH_1}, M^2_{GA_1}, M^2_{H_2H_3}, M^2_{A_2A_3}, M^2_{G^+H_1^+}, M^2_{H_2^+H_3^+}$ are 2×2 symmetric matrices. M_{GA_1} and $M_{G^+H_1^+}$ have vanishing eigenvalues corresponding respectively to the neutral and charged Goldstone bosons being eaten by the Z and $W^\pm$ gauge bosons.

What is important to notice here is that Equation (5.20) and Equation (5.19) are block-diagonal matrices. The fact that the $\mathcal{CP}$-odd scalars (A') do not mix with the scalars (H') follows from the conservation of $\mathcal{CP}$, however the absence of mixing between $\eta_{2,3}$ and the two Higgs scalars that take *vev*; H and H_1 is a direct consequence of the remnant $\mathbb{Z}_2$ symmetry, Table (5.2).

From this point on, we will leave off the primes on particles' names to denote the mass eigenstates in order to distinguish the physical states from the non-physical ones. The $\mathbb{Z}_2$-odd sector contains two real $\mathcal{CP}$ even scalars; H_2 and H_3, two real $\mathcal{CP}$ odd scalars; A_2 and A_3, and four charged scalars; $H_2^\pm$ and $H_3^\pm$. The $\mathbb{Z}_2$ even scalars consist of two real $\mathcal{CP}$ even scalars; H and H_1, that we generically call 'higgses', a $\mathcal{CP}$-odd scalar A_1 and two charged scalars; $H_0^\pm$. The masses of the $W^\pm$ and Z gauge bosons impose the relation:

$$v_H^2 + v_\eta^2 = v_{SM}^2 \,, \tag{5.21}$$

where $v_{SM} = 246\,\text{GeV}$. We call $\tan\beta$ the ratio of the two *vevs* and following the convention used in 2HDM, we define it as:

$$\tan\beta \;=\; v_H/v_\eta \,. \tag{5.22}$$

The passage from gauge eigenstates to mass eigenstates proceeds via the following rotation matrices:

$$\begin{aligned} U_{12} &= \begin{pmatrix} \cos\beta & -\sin\beta \\ \sin\beta & \cos\beta \end{pmatrix} \;; \quad U_{23} = \begin{pmatrix} -1/\sqrt{2} & 1/\sqrt{2} \\ 1/\sqrt{2} & 1/\sqrt{2} \end{pmatrix} \;; \\ U_{HH_1} &= \begin{pmatrix} -\sin\alpha & \cos\alpha \\ \cos\alpha & \sin\alpha \end{pmatrix} \,. \end{aligned} \tag{5.23}$$

U_{23} diagonalizes the mass-squared matrices in the $\mathbb{Z}_2$ odd sector, i.e., $M^2_{H_2H_3}$, $M^2_{A_2A_3}$, and $M^2_{H_2^+H_3^+}$. The mixing angle is maximal, equal to $\pi/4$. The rotation that diagonalizes the neutral scalars H and H_1 is controlled by the angle α. Without loss of generality, α is considered to vary from $[-\pi/2, \pi/2]$. The angle β (commonly referred to by its tangent, $\tan\beta$) is perhaps the most important parameter in 2HDM analyses. It characterizes the rotation which diagonalizes the mass-squared matrices of the charged scalars and of the $\mathcal{CP}$-odd scalars in the $\mathbb{Z}_2$ even sector. The angles α and β both contribute in the characterization of the SM Higgs boson. Indeed, using the rotation matrix U_{HH_1}, the physical scalars are:

$$H = -\sin\alpha\, H' + \cos\alpha\, H'_1\,; \tag{5.24}$$

$$H_1 = \cos\alpha\, H' + \sin\alpha\, H'_1\,. \tag{5.25}$$

Therefore the SM Higgs boson, h, defined by its couplings to vector bosons is:

$$h = \cos\beta\, H' + \sin\beta\, H'_1 \tag{5.26}$$

$$= \sin(\beta-\alpha)\, H + \cos(\beta-\alpha)\, H_1\,. \tag{5.27}$$

The results of LHC show no departure from an SM Higgs boson, therefore $\sin(\beta-\alpha)$ has to be close to unity. How close depends on the specificity of the model. The particular case $\sin(\beta-\alpha)=1$ constitutes the so-called decoupling limit, when H behaves *exactly* like the SM h. We will come back to this point when we implement the LHC bounds for the DM analysis, Section (5.7).

Before giving the expressions of the scalars' masses, we find it useful and simplifying to define the following combinations of the couplings of the potential, Equation (5.2),

$$L = \lambda_9 + \lambda_{10} + 2\lambda_{11}\,; \tag{5.28}$$

$$Q = \lambda_{12} + \lambda_{13} + \lambda_{14} + \lambda_{15}\,; \tag{5.29}$$

$$P = \lambda_2 + \lambda_3 + 2\lambda_4 + \lambda_5\,; \tag{5.30}$$

$$R_1 = -3\lambda_3 - 6\lambda_4 + 2\lambda_6 + \lambda_7 + \lambda_8\,; \tag{5.31}$$

$$R_2 = -3\lambda_3 - 2\lambda_4 - 2\lambda_6 + \lambda_7 + \lambda_8 - 4\lambda_5\,; \tag{5.32}$$

$$R_3 = -3\lambda_3 - 4\lambda_4 - 2\lambda_5 + \lambda_8\,. \tag{5.33}$$

With these variables, the nontrivial matrix $M^2_{HH_1}$ is given by:

$$M^2_{HH_1} = \begin{pmatrix} 2v_H\,\lambda_1 & L\,v_H v_\eta \\ L\,v_H v_\eta & 2P\,v_H^2 \end{pmatrix} . \tag{5.34}$$

And therefore:

$$\tan 2\alpha = \frac{2\,L\,v_H v_\eta}{2v_H\,\lambda_1 - 2P\,v_H^2} . \tag{5.35}$$

Finally, the mass spectrum of the $\mathbb{Z}_2$-odd states, i.e., the Higgses, reads as:

$$\begin{aligned} M^2_H &= \lambda_1 {v_H}^2 + P{v_\eta}^2 \\ &\quad - \sqrt{{v_\eta}^2 {v_H}^2 (L^2 - 4P\lambda_1) + (P{v_\eta}^2 + \lambda_1 {v_H}^2)^2}\,; \end{aligned} \tag{5.36}$$

$$\begin{aligned} M^2_{H_1} &= \lambda_1 {v_H}^2 + P{v_\eta}^2 \\ &\quad + \sqrt{{v_\eta}^2 {v_H}^2 (L^2 - 4P\lambda_1) + (P{v_\eta}^2 + \lambda_1 {v_H}^2)^2}\,; \end{aligned} \tag{5.37}$$

$$M^2_{H_1^+} = -\frac{1}{2}\,(\lambda_{10} + 2\lambda_{11})\,v_{SM}^2\,; \tag{5.38}$$

$$M^2_{A_1} = -2\,v_{SM}^2\,\lambda_{11}\,, \tag{5.39}$$

and for the “dark sector” we have:

$$M^2_{H_2} = (-3Qv_H + R_1 v_\eta)v_\eta/2\,; \tag{5.40}$$

$$M^2_{H_3} = M^2_{H_2} + 3\,Q\,v_H\,v_\eta\,; \tag{5.41}$$

$$M^2_{A_2} = (-4\lambda_{11}{v_H}^2 + Qv_\eta v_H + R_2{v_\eta}^2)/2\,; \tag{5.42}$$

$$M^2_{A_3} = M^2_{A_2} + Q\,v_H\,v_\eta\,; \tag{5.43}$$

$$M^2_{H_2^+} = ((\lambda_{10} + 2\lambda_{11}){v_H}^2 - Qv_\eta v_H + R_3{v_\eta}^2)/2\,; \tag{5.44}$$

$$M^2_{H_3^+} = M^2_{H_2^+} + Q\,v_H\,v_\eta\,. \tag{5.45}$$

We notice the following from this mass spectrum:

- The masses of inert particles are not free. Contrary to IDM (see Equation (5.15)), here the quadratic mass term does not appear;
- The splitting between $\mathcal{CP}$-even scalars and $\mathcal{CP}$-odd scalars, $M^2_{H_{2,3}} - M^2_{A_{2,3}}$, depends on the couplings $Q, \lambda_6, \lambda_{11}$ and λ_5 *. These are analogous to λ_5

*In general, the splitting scalar-$\mathcal{CP}$-odd scalar of the inert doublet H_2 originates from of IDM in Equation (5.15) and likewise putting them to zero enhances the symmetry of the potential with an extra $U(1)$. They are particularly important for direct detection (a quasi-null splitting is ruled out for instance) and co-annihilation;

- The splitting between the first inert doublet particles and those of the second inert doublet is fixed and is proportional to $Q\, v_H v_\eta$: $M^2_{H_3} - M^2_{H_2} = 3(M^2_{A_3} - M^2_{A_2}) = 3(M^2_{H^+_3} - M^2_{H^+_2}) = 3\, Q\, v_H v_\eta$.

All these features are manifestations of A_4 symmetry and can be of particular interest in collider searches. Finding any one of these relations hints to an underlying symmetry. They also have important consequences on the dark matter phenomenology, as we will see next.

5.6 Dark matter phenomenology

We now have everything we need to tackle the phenomenological study of the DM candidate of the model, H_2. We remind the reader that the free parameters of the model are the 15 λ_i couplings appearing in the scalar potential, Equation (5.2), and the ratio of the vacuum expectation values $\tan\beta$. The μ parameters are related to the couplings and *vevs* via the minimization equations and the couplings appearing in the leptonic Yukawa Lagrangian, Equation (5.1), are not relevant for the dark matter phenomenology given the high scale of the right-handed neutrinos masses.

The expressions of the mass spectrum, Equation (5.36), and redefinition of the couplings expressed in Equation (5.28) allow us, without loss of generality, to trade the free parameters of the model with the following set:

$$\{M_{H_2} \equiv M_{DM}, M_H, M_{H^+_1}, M_{A_1}, M_{A_2}, M_{H^+_2}, Q, L, P,\ \lambda_{3,6,8},\ \tan\beta\}. \tag{5.46}$$

H is set to be the lightest active Higgs of the model and is the would-be SM Higgs boson. Q, L, P have been defined in Equation (5.28). However, not all

terms of the form: $H_2 H_2 H^\dagger H_1^\dagger$ + h.c., where $\langle H \rangle \neq 0$ and $\langle H_1 \rangle \neq 0$. $(H_2 H^\dagger)^2$ + h.c. is a particular case corresponding to $H_1 \equiv H$ as in the IDM model, Equation (5.12).

these parameters are relevant for determining the DM properties. For instance, $M_{H_1^+}$ is important only in cases of co-annihilation $H_2 - H_2^+$ which are accessible for $M_{H_2} \gtrsim 100\,\text{GeV}$ only, because of LEP bounds. As for the IDM, such a range of masses for DM is not viable in this model because for $M_{DM} \gtrsim M_W$ the gauge bosons interactions become so efficient that they dilute all the relic abundance. The couplings $\lambda_{3,6,8}$ play a minor role in all the parameter space of the model. M_{A_2} and $M_{H_2^+}$ are important only when they are close to M_{H_2}, ie. in the co-annihilation regime. However, from what we know about IDM, we expect the bulk of the viable parameter space of the model to lie at low masses ($\approx M_W$). Therefore co-annihilations will be very limited. At the end, from the previous set of free parameters, the most relevant ones for DM phenomenology are:

$$\{M_{H_2} \equiv M_{DM},\ Q,\ L,\ P,\ \tan\beta\} \tag{5.47}$$

Here, P is just a handy way to parametrize the mixing angle α between the active higgses, see Equation (5.35). Q and L control the Higgs portals. It is easier to see this analytically if we impose some tuning in the free couplings $\lambda_{3,6,8}$ *. In this case, the couplings of the vertices $v_{SM}\,\lambda_H\, H_2^2 H$ and $v_{SM}\,\lambda_{H_1}\, H_2^2 H_1$ take the simple form:

$$\lambda_H \approx \frac{3}{4} Q\, \cos(\alpha+\beta) + \frac{1}{2} L\, \sin(\alpha-\beta)\,; \tag{5.48}$$

$$\lambda_{H_1} \approx \frac{3}{4} Q\, \sin(\alpha+\beta) + \frac{1}{2} L\, \cos(\alpha-\beta)\,. \tag{5.49}$$

Q is also responsible for the splitting between the first and second generation of inert higgses (Equation (5.40)): $\Delta_{H_3 H_2} = 3\,\Delta_{A_3 A_2} = 3\,\Delta_{H_2^+ H_3^+} = 3\,Q\,v_H v_\eta$, with $\Delta_{AB} = M_A^2 - M_B^2$.

Before moving to the calculation of the relic abundance we list in the next section the phenomenological constraints that we have to impose on the model.

*namely $-\lambda_3 + 2\,\lambda_6 + \lambda_8 = -\lambda_2 + 2\,\lambda_4 - 2\,\lambda_5 - \lambda_7$.

5.6.1 Phenomenological constraints on the model

In order to find the viable regions in parameter space where to perform our study of dark matter, we must impose various theoretical and experimental constraints on the model. We remark that flavor physics ($\mu \to e\gamma, b \to s\gamma$, etc.) does not constrain the scalar sector because only one Higgs couples to fermions, i.e., we have a type-I 2HDM so that FCNC are naturally absent. Moreover lepton flavor violating processes are suppressed by the large right-handed neutrino scale.

In order to illustrate the phenomenological interplays and characteristics of the model, we leave the discussion of the (severe) LHC constraints for a separate section (Section (5.7)). In addition to positivity requirement of mass eigenstates, which is automatically encoded in the parameter set we chose as input variables, we impose the following constraints on the model:

- Positive definiteness of the Hessian
  For the alignment $\langle \eta \rangle = (\frac{v_\eta}{\sqrt{2}}, 0, 0)$ and $\langle H \rangle = \frac{v_H}{\sqrt{2}}$ to be the minimum of the potential, the Hessian matrix must have a positive definite determinant. This requirement translates as the following inequalities:

$$L^2 - 4\,P\,\lambda_1 \quad < \quad 0\,; \tag{5.50}$$

$$R_1^2 - 9\,Q^2\,\tan^2\beta \quad > \quad 0\,. \tag{5.51}$$

- Perturbativity
  The requirement of perturbativity imposes the following generic bound on the Yukawa couplings of the model:

$$|\lambda_i| < 4\pi\,, \qquad i = 1, .., 15\,. \tag{5.52}$$

  This leads to an upper bound on the masses of the scalars, including the inert doublets, of the order of the "naturalness" scale $\approx 1.2\,\mathrm{TeV}$ (the exact upper limit is determined by the perturbativity constraint applied to each mass expression specifically). This is a particular feature of the model, as noticed in the end of Section (5.5). The DM candidate is therefore tightly linked to the electroweak scale.

A well motivated WIMP dark matter particle, as the acronym suggests, has to be related to the weak scale and this is enforced by A_4 in this instance. The reason for this is that albeit the inert higgses do not develop *vev*, they belong to a multiplet, namely A_4 triplet, in which the first component does take a *vev*. The flavor symmetry imposes the same quadratic mass term for all the components of the multiplet who will therefore inherit the constraints obtained by the minimization of the potential. As we noticed before, in the case of the IDM such a bound is absent for the inert Higgs because its mass receives a direct contribution from the quadratic mass term — see Equation (5.15) and subsequent discussion.

- Vacuum stability

  We require that the potential in Equation (5.2) is bounded from below, which means that the vacuum is stable (at tree level). These conditions are obtained by studying the behavior of the potential along specific field directions, for instance $|H_1| \to \infty$ and all the other directions set to 0. The sufficient conditions ensuring stability read:

$$0 < \lambda_1 ; \tag{5.53}$$

$$0 < \lambda_2 + \lambda_3 + 2\lambda_4 + \lambda_5 ; \tag{5.54}$$

$$0 < \lambda_1 + 3P + 3(\lambda_9 + M_1) + 3(2\lambda_2 - \lambda_3 + \lambda_8 + M_2) - 6Q' . \tag{5.55}$$

$$\tag{5.56}$$

Here, we have defined:

$$M_1 = \mathrm{Min}(\lambda_{10} - 2|\lambda_{11}|, 0) ; \tag{5.57}$$

$$M_2 = \mathrm{Min}(\lambda_7 - 2|\lambda_4 - \lambda_5 - \lambda_6|, 0) ; \tag{5.58}$$

$$Q' = |\lambda_{12}| + |\lambda_{13}| + |\lambda_{14}| + |\lambda_{15}| . \tag{5.59}$$

- Electroweak precision tests

  The oblique parameters S, T, U provide stringent constraints on theories beyond the Standard Model [397]. In general, S and U parameters receive negligible contributions from the scalars of the model [392, 398], hence we focus on the T parameter. We compute the effect on T induced by the scalars following [399] and we impose the bounds from electroweak measurements [400],

$$-0.08 \leqslant T \leqslant 0.14 \tag{5.60}$$

  The expression of T involves the differences of all the bosons masses of the model. For every point of the calculation, we explicitly verify that we can choose the mass spectrum of the model, by modifying $M_{H_1^+}$, in such a way that this constraint is always respected. We refer to Appendix (B) for more detail about the derivation of the expression of T in this model.

- LEP bounds

  Searches for charginos at LEP put the generic lower bound on charged particles: $M_{H^+} \gtrsim 70 - 90\,\text{GeV}$. The non-deviation of the Z and $W^\pm$ widths from SM predictions imposes the following constraints on the neutral members of $SU(2)_L$ doublets: $M_A + M_H > M_Z$, as well as the charged state $M_{H^+} + M_{H,A} > M_W$ and $2M_{H^\pm} > M_Z$. LEP II searches for neutralinos and charginos, adapted to the IDM, allow for a small window $M_A - M_H \gtrsim 8\,\text{GeV}$ for $45\,\text{GeV} \lesssim M_{H_2} \lesssim 80\,\text{GeV}$ [394]. This window applies directly to the $\mathbb{Z}_2$-odd scalar sector of our model and is of particular interest for DM phenomenology as the small splitting between H_2 and A_2 implies strong co-annihilation effects. We take this into account in the scan. Note that in the degenerate case, $M_A = M_H$, the diagram relevant for direct detection involving Z exchange is greatly enhanced and excludes such a case immediately. A small splitting of $\mathcal{O}(100)\,\text{keV}$ is enough to avoid this catastrophic end.

  To be conservative we fix the lower bound of the masses of the charged scalars of our model to 100 GeV, lowering this bound might still be consistent with LEP data [401] though it leads to no substantial differences

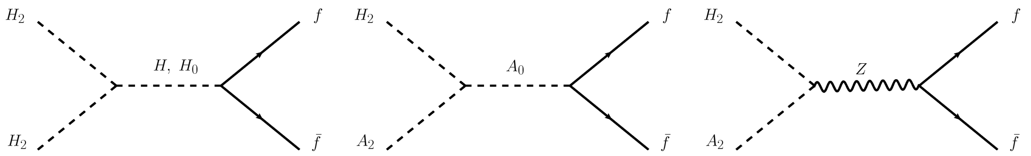

Figure 5.2: Left: Tree level Feynman diagrams for the H_2 annihilation into fermions. Center and right: diagrams for H_2 co-annihilation with the pseudscalar A_2 into fermions.

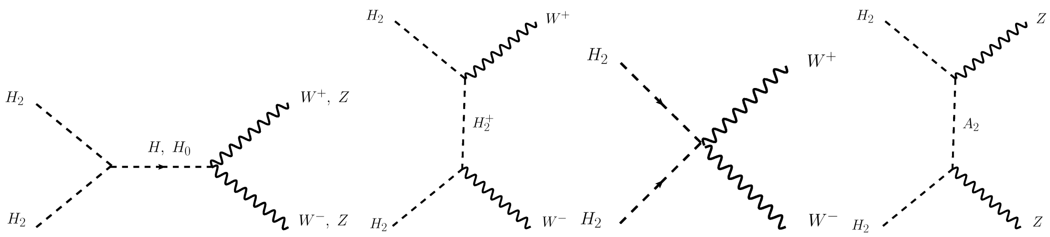

Figure 5.3: Tree level Feynman diagrams for the H_2 annihilation into $W^\pm$ and $Z\,Z$.

in the ensuing phenomenology.

5.6.2 Relic density

The phenomenologically viable points in the parameter space of the model have to satisfy all the constraints listed in the previous section. After having assured that, the points have to pass the specifically DM-related tests: relic abundance and (in)direct detection limits. We start with the relic density requirement and leave the WIMP experimental exclusion limits for the next section. As we said before, LHC limits are not yet implemented here so the mass of the lightest Higgs is left free to vary. This would allow us to present the DM phenomenology of the model in full generality, for a generic portal, before applying the LHC cuts in a subsequent section (Section (5.7)).

The thermal relic abundance of H_2 is controlled by its annihilation cross section into SM particles. In Figure (5.2) and Figure (5.3) we show the Feynman diagrams for the most relevant processes. In order to study the viable regions of the model we perform a random linear sampling over the input parameters as chosen in Equation (5.46) within their allowed ranges and compute the dark matter relic abundance using the `micrOMEGAs` package [402, 403]. At each iteration, we keep only the points which satisfy the constraints listed

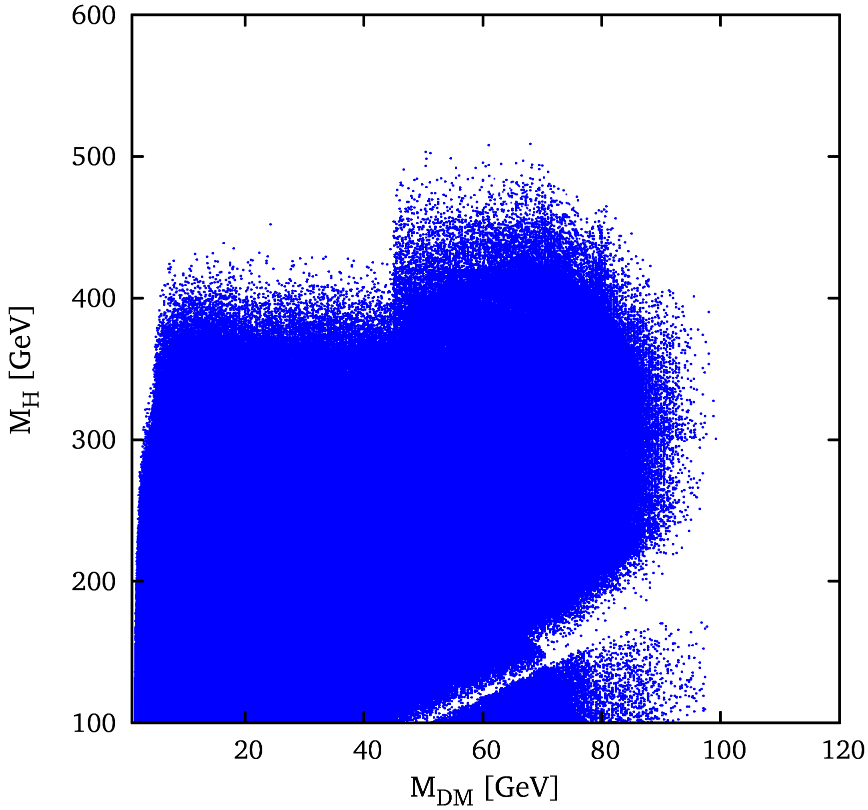

Figure 5.4: Regions in the plane DM mass (M_{DM}) - lightest Higgs boson M_H allowed by collider constraints and leading to a DM relic abundance compatible with combined PLANCK and WMAP measurements.

in the previous section (Section (5.6.1)). Finally, we apply the relic density constraints which with the combined WMAP and PLANCK measurements translate as [77]:

$$0.09 \leqslant \Omega_{DM} h^2 \leqslant 0.13. \tag{5.61}$$

The range is a bit more enlarged than the precise 3σ statistical significance range $[0.018, 0.128]$. The best fit being at $\Omega_{DM} h^2 = 0.1199 \pm 0.0027$, see Table (2.1). In Figure (5.4) we show the regions with a correct relic abundance in the plane DM mass (M_{DM}) *versus* the lightest Higgs boson mass M_H. We distinguish five distinct regions:

- $M_{DM} < 45\,\mathrm{GeV}$

  For dark matter masses well below the $W^{\pm}$ threshold, dark matter annihilations into fermions are driven by the s-channel exchange of the Higgs scalars of the model with interactions of the type $H_2H_2 \to H^* \to f\bar{f}$, where f is an SM fermion. The relevant diagrams are shown in Figure (5.2). The gauge bosons interactions play no role here.

- $45\,\mathrm{GeV} < M_{DM} < M_W$
  For $M_H \lesssim 400\,\mathrm{GeV}$ the annihilation cross sections are large enough to obtain the correct relic density for all DM masses up to the the $W^\pm$ threshold. At larger Higgs boson masses, annihilations into light fermions are suppressed so that the relic abundance is typically too large unless efficient co-annihilations with the $\mathcal{CP}$-odd scalars $A_{2,3}$ or with $H^\pm_{2,3}$ occur. These processes are shown in Figure (5.2) for A_2. Note that the possibility to co-annihilate with the charged scalar is ruled out since LEP data requires $M_{H_2^\pm} \gtrsim 100\,\mathrm{GeV}$. However, as commented in the LEP constraints, there exists a narrow window in the $M_{A_2} - M_{H_2}$ plane with $M_{H_2} < 100\,\mathrm{GeV}$ that is still allowed by LEP II. The allowed region is defined roughly by the condition $M_{A_2} - M_{H_2} \lesssim 8\,\mathrm{GeV}$ and $45\,\mathrm{GeV} \lesssim M_{H_2} \lesssim 80\,\mathrm{GeV}$. This is the origin of the increase in the region of allowed M_H above 400 GeV.

- $M_{DM} \approx M_H/2$
  The absence of points on the strip corresponding to the line $M_{DM} \approx M_H/2$ is associated to the presence of the H resonance, which would enhance the DM annihilation cross section giving a too small dark matter abundance.

- $M_W < M_{DM} \lesssim 120\,\mathrm{GeV}$
  For dark matter masses larger than M_W, the annihilation cross section into gauge bosons is typically too large so that H_2 can only be a subdominant component of the dark matter budget of the Universe. However, for certain combinations of masses and parameters, the annihilations into gauge bosons may be suppressed by a cancellation between the Feynman diagrams (Figure (5.3)), leading to an acceptable relic density. Indeed, this happens for some points in Figure (5.4)*. Ref. [404] shows

*For the Inert Doublet model, these cancellations have been noted in [394] and have been that these processes allow for dark matter masses up to 160 GeV, just below the threshold for annihilations into top pairs. In our scan, the viable region of the parameter space extends only up to $M_{DM} \approx 100\,\text{GeV}$. Solutions at higher masses cannot be excluded, though their scrutiny is rather involved due to the large number of parameters of the model.

- $M_{DM} \approx 600\,\text{GeV}$
  We now turn to the region $M_{DM} \approx 600\,\text{GeV}$. As noted in [373], a scalar dark matter candidate annihilating into massive vector bosons inherits the correct relic abundance for this value of the mass if all other annihilation processes are absent. At first glance, it might seem that this scenario could be realized in our model by tuning the couplings in order to suppress the dark matter annihilation, i.e., the couplings with the higgses λ_H and λ_{H_1} (Equation (5.48)). This is indeed possible but the value of Q would have to be necessarily vanishing. This in turn would introduce a strong degeneracy in the spectrum, namely $M_{DM} = M_{A_{2,3}} = M_{H^+_{2,3}}$ (see Equation (5.40)), and opens efficient co-annihilation interactions that would essentially nullify the relic density obtained from the gauge bosons interactions only. Contrary to IDM, the masses and the couplings controlling the portals and co-annihilations are not independent from each other. We conclude that the region around 600 GeV is not accessible in our setup because of the constraints imposed by the A_4 symmetry.

In the next two sections we study the prospects for direct and indirect dark matter detection.

5.6.3 Direct detection

The scalar dark matter candidate we are considering couples to quarks via Higgs boson exchange, leading therefore to pure spin independent (SI) interactions with the nucleons. In Figure (5.5) we show the SI scattering cross section off proton for the models with a correct dark matter abundance. We note that a large region of the parameter space is ruled out by the constrained imposed

studied in detail in [404].

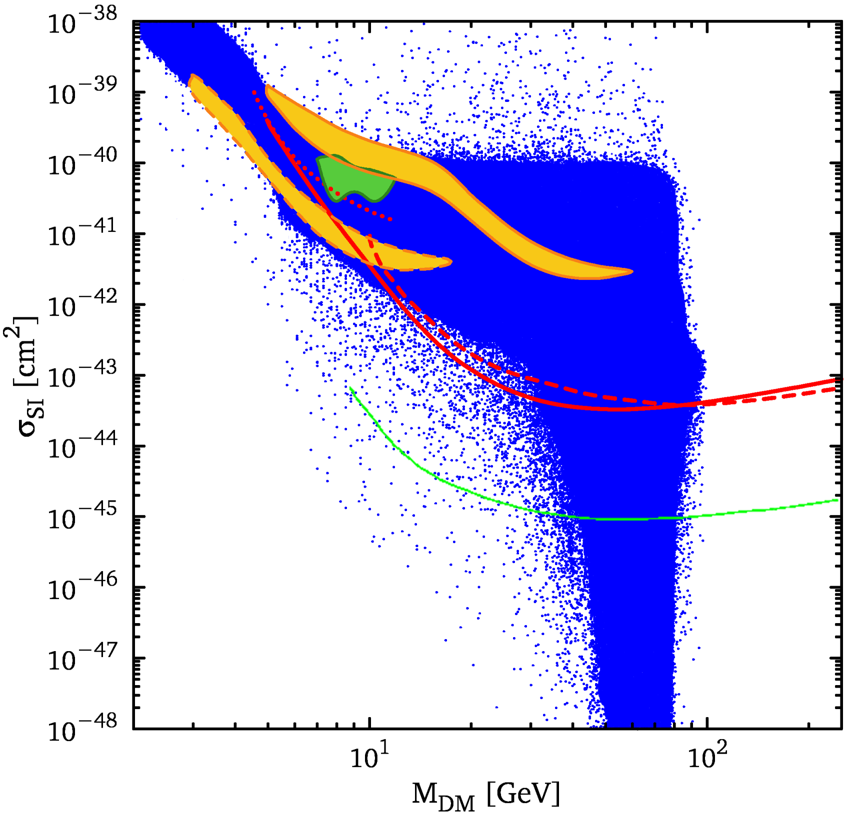

Figure 5.5: Spin-independent DM scattering cross section off-protons as a function of the dark matter mass. The orange regions delimited by the dashed (solid) line show the DAMA/LIBRA annual modulation regions including (neglecting) the channeling effect [405]. The green region corresponds to the COGENT data [138]. Dashed and dotted red lines correspond to the upper bound from CDMS (respectively from [150] and [406]). XENON100 bounds [407] are shown as a solid red line. For completeness, we added the limit from LUX [147] (solid green line), which are the strongest to date.

by current dark matter direct detection experiments.

We find that the model albeit being based on two extended Higgs sectors is strongly constrained by direct detection experiments. We witness here the limits of the WIMP "miracle". The null results of various and varied probes of DM recoils off nuclei severely limit the available parameter space of WIMPs. In our specific setup, the bulk of the points passing direct detection tests is due almost entirely to the co-annihilation region between 45 GeV $< M_{DM} <$ 80 GeV. Including the constraints from the discovery of the Higgs boson at the LHC will further reduce the parameter space of the model. Before implementing

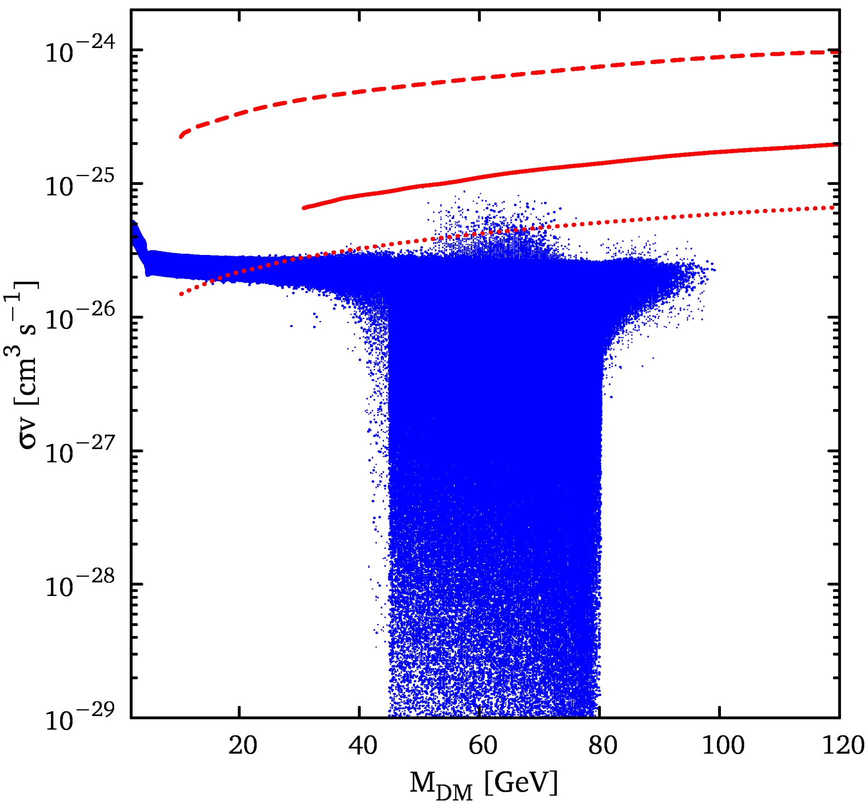

Figure 5.6: annihilation cross section times velocity as a function of the dark matter mass. The solid and dashed red lines show respectively the upper bound inferred by Fermi-LAT observations of the Draco dwarf galaxy [408] and Fermi-LAT measurements of the isotropic diffuse gamma-ray emission [409]. Projected 5 years sensitivity from measurements of the isotropic diffuse gamma-ray emission are shown as a dotted red line [410].

them though, we consider the impact of indirect detection experiments.

5.6.4 Dark matter indirect detection

In Figure (5.6) we show $\langle \sigma v \rangle$ at small velocity, relevant for DM annihilations inside our galaxy, as a function of M_{DM}. For $M_{DM} \lesssim 40\,\mathrm{GeV}$, $\langle \sigma v \rangle$ remains close to the thermal value at freeze-out, $\approx 3 \times 10^{-26}\,\mathrm{cm}^3\mathrm{s}^{-1}$, as expected for the s-wave DM annihilation into light fermions. At larger DM masses, the presence of co-annihilations allows for much smaller values of $\langle \sigma v \rangle$. That is because the relic density is accounted for by processes of the type $H_2 A_2 \to f \bar{f}$ in the early Universe (close to freeze-out) which are no longer active now because A_2 decayed already.

The solutions at $\langle \sigma v \rangle \approx 10^{-25}\,\mathrm{cm^3 s^{-1}}$ correspond to DM masses just below the Higgs resonance. In this case the annihilation cross section at small velocities is boosted with respects to its values at the DM freeze-out. This behavior of $\langle \sigma v \rangle$ close to a narrow Breit-Wigner resonance has been recently widely exploited in order to boost the annihilation signal so to explain the cosmic-rays anomalies reported by the PAMELA collaboration [411–414].

In order to sketch the prospects for indirect DM detection we show in Figure (5.6) the constraints on $\langle \sigma v \rangle$ imposed by the Fermi-LAT observations of the Draco dwarf spheroidal galaxy [408] and the Fermi-LAT measurements of the isotropic diffuse gamma-ray emission [409]. We caution that these upper bounds have been computed assuming DM annihilations into $b\bar{b}$, therefore they would directly apply only for parameter choices in our model where this annihilation channel dominates. Still, this happens in large part of the parameter space, and in particular at low dark matter masses, where the Fermi-LAT constraints are close to the predictions of the model. For a comparison of these bounds with those obtained for different annihilation channels we refer the reader to the original references. Further constraints for different targets of observations are obtained in Ref. [415–419]

One sees from Figure (5.6) that current bounds are not yet able to significantly constrain the model. However, the Fermi-LAT sensitivity is expected to improve considerably with larger statistics and for different targets of observations, see e.g., [410, 418–420]). For example, in Figure (5.6) we show the forecasted 5 years Fermi-LAT sensitivities from the isotropic diffuse gamma-ray emission [410]. Fermi-LAT measurements should be able to test the model for low dark matter masses.

We now pass to implementation of the LHC results.

5.7 The return of the ring: LHC limits

The wealth of data that followed the discovery of the Higgs, and the spectacular agreement with SM predictions in all the probed regions puts strong constraints on multi-Higgs models. It is time to include these results in the analysis of the model. It may seem, at first sight at least, that the model offers a lot of freedom given its quite extended scalar sector. If so, then all what the Higgs discovery does is fixing the mass of M_H in the previous analysis. However, we will see that this is not the case.

In general, the Higgs data constrain DM models in two ways:

- *Through the identification of the SM Higgs boson:* the identification of the SM Higgs is mandatory to make sure that the model can reproduce the LHC data. As shown in Equation (5.26), the lightest Higgs of the model (H) couples to vector bosons with a strength normalized to the SM value equal to $\sin(\beta - \alpha)$. This coupling is usually denoted as C_V. For what is known as type-II 2HDM, like the Higgs sector of the MSSM, C_V is required to be very close to unity meaning that the heavy Higgs is almost entirely decoupled [395]. In type-I 2HDM such the model we are considering, a single Higgs couples to both up and down types quarks, thus the normalized couplings of the Higgs-like particle to up- and down-quarks satisfy $C_U \equiv C_D = \cos\alpha/\sin\beta$ (Using Equation (5.23)). Type-I 2HDM allows for non-negligible departures from unity [395]. We summarized the couplings of the higgses of the model in Table (5.3).

  Global fits of LHC data constrain the plane $C_D - C_V$. Roughly speaking, although the two couplings are correlated, C_D is found to be in the range 0.5 to 1.4 at 95% CL, whereas C_V has to be larger than 0.65 at the same CL. More precisely, we consider in this analysis the region derived in the global fit [395] for type I 2HDM in the plane $\beta - \cos(\beta - \alpha)$ at 95% CL. The models lying within this region ensure us that the light Higgs H

behaves like the SM Higgs and the heavy one successfully eludes direct detection. Note that the only sector that is constrained by the identification of the Higgs is the active one. LHC exclusions for the SM Higgs do not apply to the neutral members of the inert doublets because they do not couple to fermions, and they do not decay to gauge bosons thanks to the stabilizing symmetry. The constraints derived on β and α have a direct consequence on DM phenomenology in that they play a major role in the couplings of DM with its portals: H and H_1, as can be seen in Equation (5.48).

On the other hand, the extra charged scalars ($H^{\pm}_{1,2,3}$) could affect radiative Higgs decays, in particular $\mu_{\gamma\gamma}$; the parameter that quantifies the SM Higgs deviations in the diphoton channel (the 'signal strength' of the channel). In particular a light ($H^{\pm}_{2,3}$) can enhance the signal by entering in radiative decays of the Higgs (triangle-loops for instance). Now that ATLAS and CMS show no or statistically insignificant enhancement for $\mu_{\gamma\gamma}$, we consider that the SM prediction is valid and do not aim at reproducing any excess in this analysis. In fact, this assumption has been implicitly done when we considered the C_V and C_D bounds. A deviation in the diphoton channel would introduce a new coefficient, C_γ, that affects the global fit.

Higgs	C_V	C_U	C_D	C_L
H	$\sin(\beta-\alpha)$	$\cos\alpha/\sin\beta$	$\cos\alpha/\sin\beta$	$\cos\alpha/\sin\beta$
H_1	$\cos(\beta-\alpha)$	$\sin\alpha/\sin\beta$	$\sin\alpha/\sin\beta$	$\sin\alpha/\sin\beta$
A_1	0	$\cot\beta$	$-\cot\beta$	$-\cot\beta$

Table 5.3: Summary of tree level couplings of the higgses of the model to gauge bosons C_V, up- and down-quarks (C_U and C_D respectively) and leptons (C_L). The couplings are normalized to their SM values.

- *Through the limit on unseen Higgs decays:* The characterization of the branching ratio of the Higgs to invisible products, i.e., to particles eluding detection, constitutes one of the main consequences of its discovery for DM searches. ATLAS [421] (CMS [422]) gives the following upper limits on such decays: $BR(h \to inv.) < 37\%\,(58\%)$. Global fits for a Higgs boson with SM couplings and additional invisible decay modes reduce the bound to a more stringent [395]:

$$BR(h \to inv.) < 29\%\,, \tag{5.62}$$

at 95% CL. In our model, the SM Higgs can decay to any pair of H_2, H_3, A_2 or A_3 as long as their masses are below $M_H/2 \approx 62\,\text{GeV}$:

$$BR(h \to inv.) = \frac{\Sigma\Gamma(h \to XX)}{\Gamma_h^{SM} + \Sigma\Gamma(h \to XX)}\,; \tag{5.63}$$

$$\Gamma(h \to XX) = \frac{\lambda_H v_{SM}^2}{32\pi M_h}\sqrt{1 - \frac{4M_X^2}{M_h^2}}\,, \tag{5.64}$$

with $X = H_2, H_3, A_2, A_3$, and Γ_h^{SM} is the width of the Higgs as predicted by the SM. Of course, $BR(h \to inv.)$ ceases to be constraining as soon as the DM mass is larger than $M_h/2$.

In addition to Higgs data, the LHC can constrain DM models through events with large missing transverse energy where pairs of dark matter particles are produced in association with hard SM radiation. These searches are typically called "mono-X" channels, where X can be a jet; a photon; a W or Z boson; or even a Higgs.

Results

We distinguish two distinct regions:

- $M_{DM} < M_h/2$
  For low masses, getting a good relic density implies sizable couplings with the portals. If we identify the SM Higgs with H, then this would imply the usual drawback: significant branching ratio of $h \to 2\text{DM}$ and tension with direct detection limits. However, we can couple the DM preferentially to the second Higgs, H_1, and pass the $Br(h \to inv.)$ test

in a fairly easy way. However, the strength of the coupling to H_1 depends on the actual value of α and the latter is correlated with β for the correct identification of the SM Higgs.

- $M_{DM} > M_h/2$
  In this region, $Br(h \to inv.)$ plays no role. However we have to make sure that α and β can account for the SM Higgs. For $M_{DM} \gtrsim 62\,\text{GeV}$ the gauge bosons interactions are already open due the non-negligible kinetic energy of DM at freeze-out epoch. Since these processes are efficient, we want to suppress the scalar portals in this region if we want to reproduce the observed relic density and avoid a strong dilution of the DM density. Qualitatively, using the simplified expression of couplings with the portals, Equation (5.48), this amounts at setting the parameters Q and L to zero. But $L \approx 0$ implies $\alpha = \pm\pi/2$, see Equation (5.35). So we expect the region compatible with relic density to be on the curve $\sin\beta$ in the plane $\beta - \cos(\beta - \alpha)$. That means that the Higgs identification requirement is incompatible with the relic density constraint. A more precise treatment of these considerations using the precise (lengthy) expression confirms our conclusion. However, in order to make sure there's no subtle cancellation that is taking place somewhere, we implemented a numerical scan using latest version of `micrOMEGAs` [423]. The results are displayed in Figure (5.7) in the plane $\beta - \cos(\beta - \alpha)$. The figure shows a scatter plot of models passing all the constraints discussed in Section (5.6.1) plus the $Br(h \to inv.)$ limit. The points that have the correct relic abundance are shown in blue (diamond shape) and those which provide sub-dominant contributions are in green. They all lie on the curve corresponding to $\alpha = \pm\pi/2$ as expected.

We conclude that after taking into account the latest results of LHC, the model presented in this chapter is not able to provide a viable DM candidate. This is due to the fact that the flavor symmetry tightly constrains the scalar potential, and thus the DM sector: by relating the inert sector of the model to the active one, we are able to constrain the DM with LHC in a way that goes beyond the $Br(h \to inv.)$ observable. The result is seen as positive because it shows

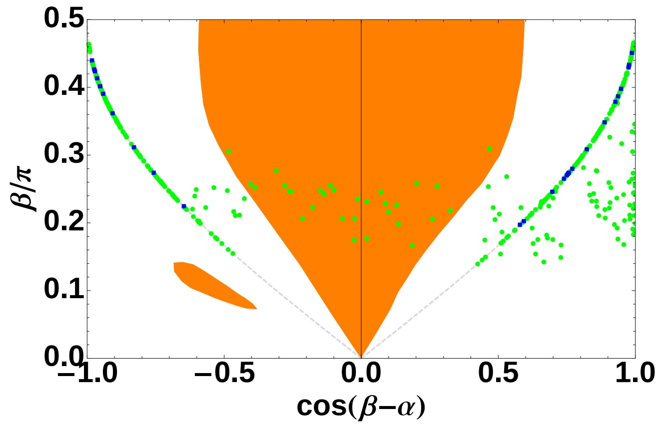

Figure 5.7: LHC Limits: The orange (solid) regions correspond to 95% CL bounds obtained in the global fit [395] for type I 2HDM. Dashed line correspond to $\alpha = \pm\pi/2$. Blue (Diamond) points satisfy the constraints listed in Section (5.6.1) plus relic density and $BR(h \to inv.)$. Green points have $\Omega h^2 \ll 0.1$.

that the link neutrino–dark matter through the flavor symmetry is not only conceptual but it actually does have strong impact on the viability of the DM candidate of the model. Of course, even though the simple(est) "discrete dark matter" model presented here is ruled out, the idea *per se*, is still viable and less minimal models could accommodate all the existing constraints including LHC-related ones.

Can we save the model?

From Figure (5.7), we see that the only viable point seems to be the particular limit $\cos(\beta - \alpha) = \beta = 0$. In this case the group A_4 is not broken, because $\tan(\beta) = 0$. The neutrino phenomenology and motivation are of course lost and the group serves merely as an imposed $\mathbb{Z}_2$-like symmetry on the potential, with the difference that is much more constraining than a simple parity. For the sake of illustration, let us see what happens in the case $\cos(\beta - \alpha) = \beta = 0$ in more details (assuming the Higgs H_1 is decoupled from the theory). In this case the mass spectrum is highly degenerate due to the unbroken A_4 symmetry.

It reads:

$$M_h^2 = 2\,\lambda_1\,v_{SM}^2\,; \tag{5.65}$$

$$M_{A_i}^2 = \mu_\eta^2 + \frac{1}{2}\,(\lambda_9 + \lambda_{10} - 2\lambda_{11})\,v_{SM}^2\,; \tag{5.66}$$

$$M_{H_i}^2 = \mu_\eta^2 + \frac{1}{2}\,(\lambda_9 + \lambda_{10} + 2\lambda_{11})\,v_{SM}^2\,; \tag{5.67}$$

$$M_{H_i^\pm}^2 = \mu_\eta^2 + \frac{1}{2}\,\lambda_9\,v_{SM}^2\,, \tag{5.68}$$

with $i = 1, 2, 3$. Such expressions for the masses are reminiscent of the IDM. Indeed the spectrum is very similar to the one derived in Equation (5.15) except that we have three copies of the inert Higgs here. The Higgs portal couplings become:

$$\lambda_h = +\frac{1}{2}\,L\,; \tag{5.69}$$

$$\lambda_{H_1} = -\frac{3}{4}\,Q\,, \tag{5.70}$$

and $L \equiv \lambda_9 + \lambda_{10} + 2\lambda_{11}$ plays the role of λ_L in IDM. We see that in this case, the masses are essentially decoupled from the couplings and we recover the same phenomenological features of IDM, including the high mass region at $\approx 600\,\mathrm{GeV}$.

Of course, imposing a flavor symmetry without breaking has no sense. It would be more interesting to contemplate the possibility of changing the particle content of the model instead. It turns out, it is not difficult to imagine modifications of the models that preserve the original motivation of the mechanism and the neutrino phenomenology. Indeed, it is enough to add another A_4 triplet of $SU(2)_L$ scalar doublets η_2, analogue to η, that will couple to the right handed neutrinos just like η in the original model. Of course, to preserve a remnant $\mathbb{Z}_2$, η_2 should take *vev* in the $(1, 0, 0)$ direction. Granted the alignments $\langle\eta\rangle = (0, 0, 0)$ * and $\langle\eta_2\rangle = (v_\eta, 0, 0)$ are indeed solutions of

*The alignment $\langle\eta\rangle = (1, 0, 0)$ is possible too! In this case the active Higgs sector is comprised of three higgses and a dedicated LHC global fit is required in order to assess its viability, though such an extended Higgs sector may give enough freedom for the DM to be the vacuum of the theory, we have then a variant of the model that has a less constrained Higgs sector. In particular, the relevant DM couplings will be decoupled from its mass and from the mixing of the 2HDM sector in contrast with the model considered here, but just like the IDM. That is because the alignment $\langle \eta \rangle = (0, 0, 0)$ keeps the quadratic 'μ' term free to contribute to the masses. Note that in this case, the components of η need not be $SU(2)_L$ doublets: η can well be composed of scalar iso-singlets. The singlet DM parameter space is usually bigger than its inert higgs counterpart because of the absence of gauge bosons interactions. For instance, a good relic density can be found for masses well beyond the M_W threshold since the DM has no gauge couplings.

5.8 Completion of the model

So far, the quark sector has not been studied and it was assumed that quarks are generically singlets of A_4 in order to preclude catastrophic DM decays. However, it is possible to extend such a model to the quarks by embedding it into the grand unified group $SU(5)$. It is beyond our scope to give a complete grand unified model and we merely sketch here a way to embed the model into a GUT group.

We consider the following matter assignment:

	T_1	T_2	T_3	F_1	F_2	F_3	N_T	N_4
$SU(5)$	$\mathbf{10}$	$\mathbf{10}$	$\mathbf{10}$	$\bar{\mathbf{5}}$	$\bar{\mathbf{5}}$	$\bar{\mathbf{5}}$	$\mathbf{1}$	$\mathbf{1}$
A_4	$\mathbf{1}$	$\mathbf{1'}$	$\mathbf{1''}$	$\mathbf{1}$	$\mathbf{1''}$	$\mathbf{1'}$	$\mathbf{3}$	$\mathbf{1}$

where we have assumed three copies of ten-multiplets and three of five-multiplets of $SU(5)$ to describe the three flavors. On the other hand, the assignments of the scalars read:

$SU(5)$	$\mathbf{5_H}$	$\bar{\mathbf{5}}_\mathbf{H}$	$\mathbf{5}_\eta$	$\mathbf{45_H}$
A_4	$\mathbf{1}$	$\mathbf{1}$	$\mathbf{3}$	$\mathbf{1}$

viable.

Then the Lagrangians for the up- and down-quarks and neutrinos are given by:

$$
\begin{aligned}
\mathcal{L}_d &= y_1^{l,d} T_1 F_1 \bar{5}_H + y_2^{l,d} T_2 F_2 \bar{5}_H + y_3^{l,d} T_3 F_3 \bar{5}_H \\
&\quad + y_1'^{l,d} T_1 F_1 45_H + y_2'^{l,d} T_2 F_2 45_H + y_3'^{l,d} T_3 F_3 45_H \,, &(5.71)\\
\mathcal{L}_u &= y_1^u T_1 T_1 5_H + y_2^u T_2 T_3 5_H + y_1'^u T_1 T_1 45_H + y_2'^u T_2 T_3 45_H \,, &(5.72)\\
\mathcal{L}_\nu &= y_1^\nu T_1 N_4 5_H + y_2^\nu T_2 N_4 5_H + y_3^\nu T_3 N_4 5_H + y_1^\nu T_1 N_T 5_\eta \\
&\quad + M_1\, N_T N_T + M_2\, N_4 N_4. &(5.73)
\end{aligned}
$$

The charged lepton and down quark mass matrix are diagonal with eigenvalues:

$$
\begin{aligned}
m_e &= y_1^{l,d} \langle 5_H \rangle - 3 y_1'^{l,d} \langle 45_H \rangle \,; \\
m_\mu &= y_2^{l,d} \langle 5_H \rangle - 3 y_2'^{l,d} \langle 45_H \rangle \,; \\
m_\tau &= y_3^{l,d} \langle 5_H \rangle - 3 y_3'^{l,d} \langle 45_H \rangle \,; \\
m_d &= y_1^{l,d} \langle 5_H \rangle + y_1'^{l,d} \langle 45_H \rangle \,; \\
m_s &= y_2^{l,d} \langle 5_H \rangle + y_2'^{l,d} \langle 45_H \rangle \,; \\
m_b &= y_3^{l,d} \langle 5_H \rangle + y_3'^{l,d} \langle 45_H \rangle \,.
\end{aligned}
$$

The three charged lepton masses as well as the three down-quark masses can be easily reproduced. The up-quark mass matrix is:

$$
M^u = \begin{pmatrix} m_u & 0 & 0 \\ 0 & 0 & m_c \\ 0 & m_t & 0 \end{pmatrix}, \quad M^u\, M^{u\dagger} = \begin{pmatrix} m_u^2 & 0 & 0 \\ 0 & m_c^2 & 0 \\ 0 & 0 & m_t^2 \end{pmatrix}, \tag{5.74}
$$

where:

$$
\begin{aligned}
m_u &= y_1^u \langle 5_H \rangle \,; \\
m_c &= y_2^u \langle 5_H \rangle - y_2'^u \langle 45_H \rangle \,; \\
m_t &= y_2^u \langle 5_H \rangle + y_2'^u \langle 45_H \rangle \,.
\end{aligned} \tag{5.75}
$$

Given the structure of the up- and down-quark mass matrices, the quark mixing matrix is diagonal. While this may be regarded as a good first approximation, since quark mixing angles are small, clearly another ingredient is needed such as, possibly, radiative corrections or extra vector-like quark states. A full fit of the quark sector observables within a unified extension incorporating the flavor symmetry is beyond the scope of this study, however we see that such an extension is possible.

5.9 Conclusions and discussion

We have studied a model where the stability of the dark matter particle arises from a flavor symmetry. The A_4 non-Abelian discrete group accounts both for the observed pattern of neutrino mixing as well as for DM stability. We have analyzed the constraints that follow from theoretical bounds, electroweak precision tests and collider searches. We have also analyzed the prospects for direct and indirect dark matter detection and found that, although the former already excludes a large region in parameter space, we cannot constrain the mass of the DM candidate. In contrast, indirect DM detection is not yet sensitive enough to probe our predictions.

All of the above relies mainly on the properties of the scalar sector responsible for the breaking of the gauge and flavor symmetry. A basic idea of our approach is to link the origin of dark matter to the origin of neutrino mass and the understanding of the pattern of neutrino mixing, two of the most outstanding challenges in particle physics today. For the neutrinos, one finds an inverted neutrino mass hierarchy, hence a neutrinoless double beta decay rate accessible to upcoming searches, while $\theta_{13} = 0$.

In this updated DM analysis we have included the latest constraints on the model, in particular the Higgs bounds. We find that the tight constraints imposed by the flavor symmetry A_4 on the properties of the WIMP candidates cannot fit the LHC results. That is mostly due to the fact that the mass of the dark matter and its production portals couplings and relevant co-annihilations splittings are not independent from each other because of A_4. We have also discussed possible modifications of the model to solve this problem.

The simplicity of this A_4-based discrete dark matter while making the DM phenomenology and interplay with the flavor symmetry transparent, has the drawback of providing rather poor neutrino physics predictions and does not include the quark sector. In the next chapter we will present a predictive discrete dark matter scenario, incorporating quarks and providing a 3-Higgs doublet model sector allowing for more freedom for the dark matter candidate.

6

Discrete dark matter meets θ_{13}

We have to be economical in principles rather than in structures.
Abdus Salam

In its minimal realization, the DDM scenario presented in Chapter (5) links the DM to neutrino phenomenology through the stability issue. While such a link tightly constrains the phenomenology of the DM candidate, because of the flavor symmetry it does not provide a strong neutrino phenomenology. That is because: (i) the lepton doublets transform as singlets under the flavor group; (ii) the right-handed neutrinos transform as A_4 triplets $N \sim \mathbf{3}$, the contraction rules imply that the DM, $\eta \sim \mathbf{3}$, couples only to higgses and heavy right-handed neutrinos $\bar{L}_i \, N \, \tilde{\eta}$.

What if leptons are assigned to a triplet representation instead? This does not work because it implies that the would-be DM candidate would decay too fast to light leptons, through the contraction of the triplet representations. This problem has been considered by Ref. [424] using a T' flavor symmetry. While the suggested model has the merit of incorporating quarks non-trivially, it requires an "external" $\mathbb{Z}_2$ asymmetry in order to stabilize dark matter. In fact, the problem of putting both the would-be DM candidate and the leptons in nontrivial representations of the same group seemed so problematic that it led Ref. [425] to claim that a successful realization of the DDM scenario requires the lepton doublets to be in three inequivalent singlet representations of the flavor group.

In addition to all these theoretical, and perhaps aesthetic considerations, simple schemes of this type lead to $\theta_{13} = 0$ as a first-order prediction. This is at variance with recent reactor results [212, 213, 426, 427] which find that θ_{13} is actually quite large.

The aim of this chapter is to address these point specifically. Following the same motivation and philosophy of the A_4-based discrete dark matter model, we will construct a model that is able to connect the two sectors in a deeper way and account for the recently discovered values of the mixing angles. The explicit example we will present in this chapter is based on a unique symmetry group; $\Delta(54)$, in which: (i) left-handed leptons are assigned to nontrivial representations; (ii) there exist a viable stable dark matter particle; and (iii) the quarks are included in a nontrivial way. In contrast to the simplest "flavor-blind" inert dark matter scheme (Section (5.4)), the model predicts correlations among the neutrino oscillation parameters, consistent with the recent reactor angle measurements [212, 213, 426, 427].

The chapter is organized as follows: in the next section, Section (6.1), we will list the requirements a group has to satisfy to have a non-trivial embedding

$$\begin{aligned} \mathbf{2_k} \times \mathbf{2_k} &= \mathbf{1}_+ + \mathbf{1}_- + \mathbf{2_k} \\ \mathbf{2_1} \times \mathbf{2_2} &= \mathbf{2_3} + \mathbf{2_4} \quad \text{(and cyclic permutations)} \\ \mathbf{2_k} \times \mathbf{1}_\pm &= \mathbf{2_k} \end{aligned}$$

Figure 6.1: $\Delta(54)$ basics — rules for doublet contractions. See Appendix (A.2) for more details.

of dark matter, and introduce the $\Delta(54)$ discrete group. Then we construct a mode based on this group in Section (6.2), and study its neutrino phenomenology in Section (6.3). The quark sector is described in Section (6.4). The dark matter candidate is introduced in the following section, Section (6.5). Motivated by the 'gravity breaks all global symmetries' conjecture, we attempt to quantify the effect of non-renormalizable, Planck-suppressed, operators on the stability of WIMP dark matter in Section (6.6). Finally, we conclude in Section (6.7).

6.1 Beyond A_4 discrete dark matter

It is clear that A_4 is too small to address all the points discussed in the introduction, so we have to consider a larger group. More precisely, we search for a group G that contains at least two irreducible representations of dimension larger than one, namely r_a and r_b with $\dim(r_{a,b}) > 1$. We also require that all the components of r_a transform trivially under an Abelian subgroup of $G \supset Z_N$ (with $N = 2, 3$) while at least one component of r_b is charged with respect to Z_N. The stability of the lightest component of r_b is guaranteed by Z_N giving a potential DM candidate.

The simplest group we have found with this feature is $\Delta(54)$ [428], that is isomorphic to $(Z_3 \times Z_3) \rtimes S_3$. $\Delta(54)$ is part of the $\Delta(6N^2)$ series, it comes after $\Delta(24) \equiv S_3$ and $\Delta(6N^2) \equiv S_4$. In addition to two irreducible triplet representations, $\Delta(54)$ contains four different doublets $\mathbf{2_{1,2,3,4}}$ and two irreducible singlet representations, $\mathbf{1}_\pm$. The product rules for the doublets are (k runs from 1 to 4) shown in Figure (6.1). More details about $\Delta(54)$ can be found in

Appendix (A.2). Of the four doublets, $\mathbf{2_1}$ is the only *irrep* that is left invariant under the subgroup $P \equiv (Z_3 \times Z_3)$. The other doublets transform nontrivially. That is because the generators of P on each doublet *irrep*, a and $a' \equiv a$ are given by [429, 430]:

$$a_{\mathbf{2_1}} = \begin{pmatrix} 1 & 0 \\ 0 & 1 \end{pmatrix}; \tag{6.1}$$

$$a_{\mathbf{2_2}} = \begin{pmatrix} \omega^2 & 0 \\ 0 & \omega \end{pmatrix}; \tag{6.2}$$

$$a_{\mathbf{2_{3,4}}} = \begin{pmatrix} \omega & 0 \\ 0 & \omega^2 \end{pmatrix}. \tag{6.3}$$

Here $\omega^3 = 1$. We can see that by taking $r_a = \mathbf{2_1}$ and $r_b = \mathbf{2_3}$ that $\Delta(54)$ is a perfect choice for our purpose. In the next section, we construct a model based on this group.

6.2 The model

Let us now turn to the explicit model, described in Table (6.1), where $L_D \equiv (L_\mu, L_\tau)$ and $l_D \equiv (\mu_R, \tau_R)$. We have five $SU(2)_L$ doublets of Higgs scalars, four of them paired as $\Delta(54)$ doublets: H is a singlet of $\Delta(54)$, while $\eta = (\eta_1, \eta_2) \sim \mathbf{2_3}$ and $\chi = (\chi_1, \chi_2) \sim \mathbf{2_1}$ are the doublets. In order to preserve a remnant P symmetry, the doublet η is not allowed to take a *vev.* This is equivalent to the prescription $\langle \eta_{2,3} \rangle = 0$ in the model based on A_4 (Section (5.3)). Such a prescription is not necessary for H, χ_1 and χ_2 since these are all invariant under P. We also need to introduce an $SU_L(2)$ Higgs triplet scalar field $\Delta \sim \mathbf{2_1}$ whose *vev* will induce neutrino masses through the type-II seesaw mechanism [253, 259–262] presented in Section (3.6.1).

Regarding dark matter, note that the lightest P-charged particle in $\eta_{1,2}$ can play the role of inert DM, as it has no direct couplings to matter. The link between dark matter and neutrino phenomenology arises from the fact that the DM stabilizing symmetry is a remnant of the underlying flavor symmetry

Group	L_e	L_D	e_R	l_D	H	χ	η	Δ
$SU(2)_L$	$\mathbf{2}$	$\mathbf{2}$	$\mathbf{1}$	$\mathbf{1}$	$\mathbf{2}$	$\mathbf{2}$	$\mathbf{2}$	$\mathbf{3}$
$\Delta(54)$	$\mathbf{1}_+$	$\mathbf{2_1}$	$\mathbf{1}_+$	$\mathbf{2_1}$	$\mathbf{1}_+$	$\mathbf{2_1}$	$\mathbf{2_3}$	$\mathbf{2_1}$

Table 6.1: Summary of the quantum numbers of the model.

which accounts for the observed pattern of oscillations.

The lepton part of the Yukawa Lagrangian is given by $\mathcal{L}_Y = \mathcal{L}_\ell + \mathcal{L}_\nu$, where:

$$\begin{aligned} \mathcal{L}_\ell &= y_1 \bar{L}_e e_R H + y_2 \bar{L}_e l_D \chi + y_3 \bar{L}_D e_R \chi \\ &\quad + y_4 \bar{L}_D l_D H + y_5 \bar{L}_D l_D \chi\,; \end{aligned} \tag{6.4}$$

$$\mathcal{L}_\nu = y_b \bar{L}_D \bar{L}_D \Delta + y_a \bar{L}_D \bar{L}_e \Delta\,. \tag{6.5}$$

After electroweak symmetry breaking $\mathcal{L}_\ell$ gives the following charged lepton mass matrix:

$$M_\ell = \begin{pmatrix} a & br & b \\ cr & d & e \\ c & e & dr \end{pmatrix}, \tag{6.6}$$

where $a = y_1 \langle H \rangle$, $b = y_2 \langle \chi_1 \rangle$, $c = y_3 \langle \chi_1 \rangle$, $d = y_5 \langle \chi_1 \rangle$, $e = y_4 \langle H \rangle$, and

$$r = \frac{\langle \chi_2 \rangle}{\langle \chi_1 \rangle}\,. \tag{6.7}$$

Note that all these parameters are in general complex. On the other hand, $\mathcal{L}_\nu$ is responsible for generating the neutrino mass matrix. Choosing the solution $\langle \Delta \rangle \sim (1,1)$ and $\langle \chi_1 \rangle \neq \langle \chi_2 \rangle$, one finds that:

$$M_\nu \propto \begin{pmatrix} 0 & \delta & \delta \\ \delta & \alpha & 0 \\ \delta & 0 & \alpha \end{pmatrix}, \tag{6.8}$$

where the complex parameters δ and α are defined as $\delta = y_a \langle \Delta \rangle$, $\alpha = y_b \langle \Delta \rangle$. Such a *vev* alignment is consistent with the minimization of the scalar potential.

Our model corresponds to a "flavored" realization of the *inert dark matter*

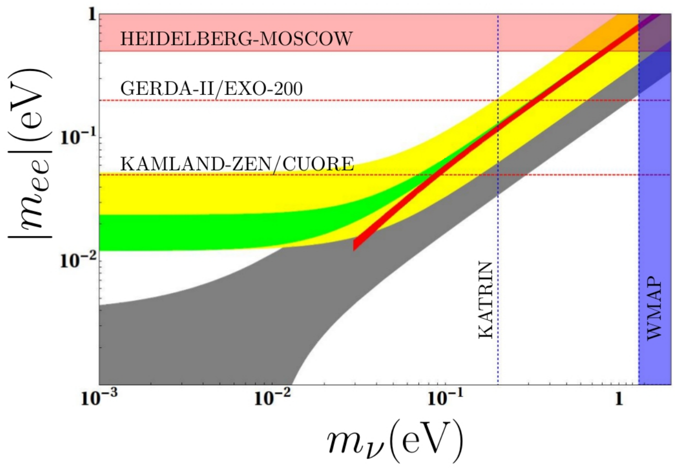

Figure 6.2: Effective neutrinoless double beta decay parameter m_{ee} versus the lightest neutrino mass. The thick upper and lower branches correspond the "flavor-generic" inverse (yellow) and normal (gray) hierarchy neutrino spectra, respectively. The model predictions are indicated by the green and red (darker-shaded) regions, respectively. They were obtained by taking the 3σ band on the mass squared differences. Only these sub-bands are allowed by the $\Delta(54)$ model. For comparison we give the current limit and future sensitivities on m_{ee} [431, 432] and m_ν [433, 434], respectively.

scenario [391, 392], Section (5.4). As such, it has nontrivial consequences for neutrino phenomenology, which we now study in detail.

6.3 Neutrino phenomenology

As seen in Equation (6.8) the neutrino mass matrix depends only on two parameters, δ and α, which can be expressed as a function of the measured squared mass differences as follows:

$$m^\nu_{1,3} = \frac{\alpha \mp \sqrt{8\delta^2 + \alpha^2}}{2} \qquad m^\nu_2 = \alpha. \tag{6.9}$$

The number of predictions can be readily obtained from parameter counting considerations. Indeed, restricting to the lepton sector we have 7 parameters in total if $\mathcal{CP}$ is conserved, a; b; c; d; e; α; δ, plus the ratio r nearly fixed from the quark sector (see below). This is to be compared with the measured observables, namely 3 charged lepton masses, plus the solar and atmospheric mass splittings. To sum up, we have $2 = 7 - 5$ predictions, as illustrated in Figure (6.2), Figure (6.3) and Figure (6.4). The parameters of the neutrino mass matrix are fixed by the neutrino squared mass differences (within the 2σ range). The two free parameters are in the charged lepton sector and are taken to be random variables in the scans.

As for the first prediction, notice that the masses in Equation (6.9) obey a neutrino mass sum rule of the form $m_1^\nu + m_2^\nu = m_3^\nu$ which has implications for neutrinoless double beta decay [435], as seen in Figure (6.2). We now turn to the second prediction. For simplicity, we consider in what follows only real parameters and we fix the intrinsic neutrino $\mathcal{CP}$–signs [436] as $\eta = diag(-, +, +)$, where η is defined so that the $\mathcal{CP}$ conservation condition in the charged current weak interaction reads $U^\star = U\eta$, with U being the lepton mixing matrix. It is easy to check that in this case only a normal hierarchy spectrum is allowed. In contrast, a different permutation of the eigenvalues corresponding to the η matrix, namely $(1, 2, 3) \to (1, 3, 2)$ in Equation (6.9), gives only inverse hierarchy spectrum.

Although in our scheme neutrino mixing parameters in the lepton mixing matrix are not strictly predicted, there are correlations between the reactor and the atmospheric angle, as illustrated in Figure (6.3)* and Figure (6.4) for the cases of normal and inverse mass hierarchies, respectively. While the solar angle is clearly unconstrained and can take all the values within in the experimental limits, correlations exist with the reactor mixing angle, indicated by the curved yellow bands in Figure (6.3) and Figure (6.4). These correspond to 2σ regions of θ_{23} as determined in Ref. [437]. The horizontal lines give the best global fit value and the recent best fit values obtained in Daya-Bay and RENO reactors [212, 213, 426, 427] (see also results from T2K [438]). One sees that for the IH case the agreement between model prediction and angle determinations is not as good as in the NH case.

*There is also a second band allowed in this case which is, however, experimentally ruled out by the measurements of θ_{12} and θ_{13}.

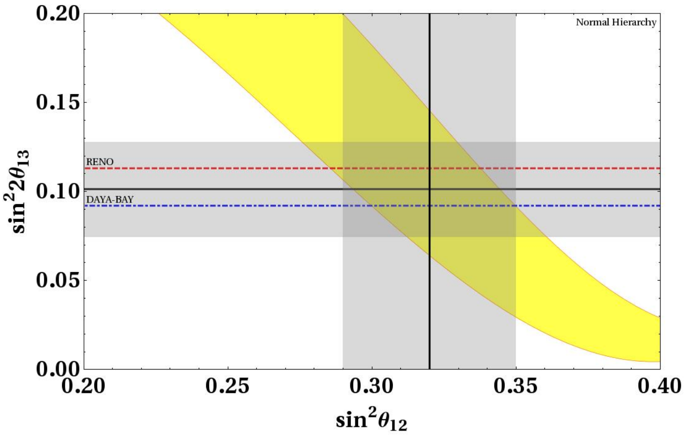

Figure 6.3: The shaded (yellow) curved band gives the predicted correlation between solar and reactor angles when θ_{23} is varied within 2σ for the normal hierarchy spectrum. The solid (black) line gives the global best fit values for θ_{12} and θ_{13}, along with the corresponding two-sigma bands, from Ref. [437]. The dashed lines correspond to the central values of the recently published reactor measurements [212, 213, 426, 427].

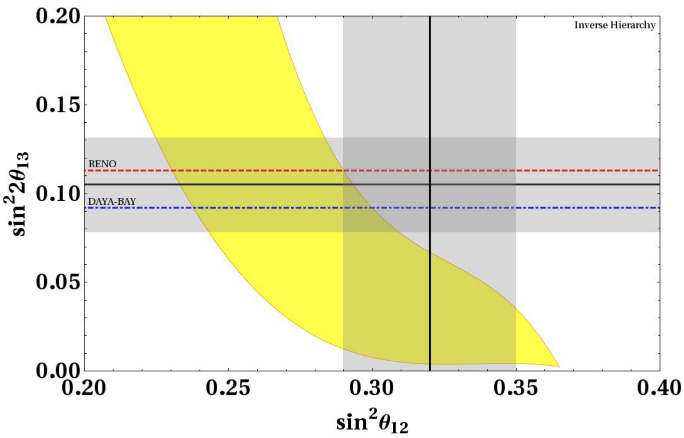

Figure 6.4: Same as above for the inverse hierarchy case.

We now turn our attention to the mixing angles. In previous models of discrete dark matter, including the original one discussed in Chapter (5) [1, 377, 379, 383] quarks were singlets of the flavor symmetry. That is because A_4 was too small a group to accommodate both DM stability and CKM predictions. Consequently the generation of quark mixing was difficult [387]. This problem has been recently considered in [424] using T' flavor symmetry.

Group	$Q_{1,2}$	Q_3	(u_R, c_R)	t_R	d_R	s_R	b_R
$SU(2)_L$	$\mathbf{2}$	$\mathbf{2}$	$\mathbf{1}$	$\mathbf{1}$	$\mathbf{1}$	$\mathbf{1}$	$\mathbf{1}$
$\Delta(54)$	$\mathbf{2_1}$	$\mathbf{1}_+$	$\mathbf{2_1}$	$\mathbf{1}_+$	$\mathbf{1}_-$	$\mathbf{1}_+$	$\mathbf{1}_+$

Table 6.2: Gauge and flavor representation assignments for quarks.

6.4 The quark sector

A nice feature of our current model is that with $\Delta(54)$, given the specific number and characteristics of the doublet *irrep*, we can assign quarks to the nontrivial doublet *irrep* even though the DM is also a doublet of $\Delta(54)$. This opens new possibilities to fit the CKM mixing parameters. Indeed, as shown in Table (6.2) quarks transforming nontrivially under the flavor symmetry can be consistently added in our picture. The resulting up- and down-type quark mass matrices in our model are given by:

$$M_d = \begin{pmatrix} ra_d & rb_d & rd_d \\ -a_d & b_d & d_d \\ 0 & c_d & e_d \end{pmatrix}, \quad M_u = \begin{pmatrix} ra_u & b_u & d_u \\ b_u & a_u & rd_u \\ c_u & rc_u & e_u \end{pmatrix}. \tag{6.10}$$

Note that the Higgs fields H and χ are common to the lepton and the quark sectors and in particular the parameter r. Assuming for simplicity real couplings we have 11 free parameters characterizing this sector, 10 Yukawa couplings plus the ratio of the the isodoublet *vevs*, r, introduced earlier in the neutrino sector (Equation (6.7)). We have verified that we can make a fit of all quark masses and mixings provided r lies in the range of about $0.1 < r < 0.2$. We do not extend further the discussion on the quark interactions which can be easily obtained from Table (6.2).

6.5 The dark matter candidate

The (scalar) Dark Matter candidate of the model is the lightest neutral components of η. It is stabilized by the P symmetry that is left intact after the breaking of $\Delta(54)$. For definiteness, let us say that the DM is η_1.

The active Higgs sector is composed of three scalars whereas the dark sector is constituted by two $SU(2)_L$ doublets. η_1 has quartic couplings with the higgses of the model, such as $\eta^\dagger\eta H^\dagger H$ and $\eta^\dagger\eta\chi^\dagger\chi$. These weak-strength couplings provide a Higgs portal DM production mechanism, and ensure an adequate cosmological relic abundance. The general phenomenology of such a candidate is very similar to the one we have studied in the previous chapter and we do not find it useful to redo the study here. The only difference resides in the fact that the active sector is a 3HDM instead of a 2HDM. While this does not add anything conceptually relevant for DM phenomenology, it might help evade the strict LHC limits and constraints that apply to 2HDM as we have seen in the case of the A_4-based discrete dark matter model. Direct and indirect detection prospects are similar to those of a generic WIMPs as provided by multi-Higgs extensions of the SM.

6.6 The 'Gravity breaks them all' issue

Dealing with global symmetries usually raises the question: *"What about gravity?"*. That is because it has been conjectured and argued for years that non-perturbative gravitational effects break all global symmetries (continuous and discrete alike) [439, 440]. The original motivation was based on black hole physics arguments, but since then perturbative string theory has confirmed this conjecture in various cases [440]. Such gravitational effects have already been considered in a number of scenarios and models invoked to solve fundamental theoretical problems, such as axions [441–443] and majorons [236, 444–447].

Here we turn our attention to the implications of such a claim on WIMP dark matter phenomenology. WIMPs are generally *assumed* to be stable particles. This is achieved in most models by imposing in an *ad hoc* way a global symmetry (usually a $\mathbb{Z}_2$) that forbids the decay of the DM candidate to lighter states. More theoretically motivated models such as those based on the discrete DM mechanism achieve the stability in a dynamic way as a result of the breaking of a flavor symmetry group, as discussed in this thesis. However, if the flavor group is global or is not itself originating from a local group, then the conjecture "Gravity breaks global symmetries" holds. It is our goal here to quantify the effect of this claim on WIMP dark matter candidates.

In full generality, unless the symmetry responsible for the DM stability is local, or comes from a local symmetry (a 'gauged' $\mathbb{Z}_2$ for instance), it is expected to be broken at short distances by gravitational effects leading to a decaying WIMP DM. From the phenomenological point of view absolute stability is not a necessary condition for DM candidates. Instead, what is required is a lifetime larger than the current age of the Universe $H^{-1} \approx 10^{17}\,\mathrm{s}$, where H is the Hubble constant. Cosmic and gamma rays analysis constrain the lifetime of a DM candidate even further to be $\tau_{\rm DM} > 10^{26}\,\mathrm{s}$ [90–93]. An important question to be addressed is then *what are the requirements on the gravity-induced decay lifetimes in order to preserve the validity of the DM candidate?*

Prototype model

In order to illustrate the discussion, let us consider a very simple prototype scheme, exhibiting generic WIMP dark matter features over a broad phenomenological range [448, 449]. The SM is extended by S_i ($i = 1 \ldots N$) real gauge-singlets under an imposed parity symmetry to which the SM particles are blind. Note that the stabilizing symmetry need not be a $\mathbb{Z}_2$; any global (discrete or continuous) symmetry that forbids the decay of the lightest S_i is a valid choice. This scenario provides a production and thermalization mechanism via Higgs boson exchange. For small enough the mass splittings [128], co-annihilations between the LSP (lightest singlet particle), which is the DM candidate S_1, and the remaining $S_{i>1}$ are potentially important, as discussed in Section (2.3). In a conventional WIMP dark matter scenario our LSP would be stable and the scalar potential would read as (summation over indexes is understood):

$$\mathcal{V}_{\rm sym} \;=\; -\mu_h^2 H^\dagger H + \mu_{ij}^2 S_i S_j + \lambda_{ij} S_i S_j H^\dagger H + \lambda'_{ijkl} S_i S_j S_k S_l \,. \quad (6.11)$$

For the sake of simplicity, we consider the case $N = 2$ and $\mu_{ii}^2 > 0$. The latter precludes spontaneous breaking of the $\mathbb{Z}_2$ symmetry, and the associated domain walls.

We now assume that the global symmetry responsible for the stability of dark matter is violated due to the presence of gravitational effects. To this end, we add to $\mathcal{V}_{\rm sym}$ (Equation (6.11)) an effective potential that breaks explicitly the stabilizing symmetry through non–renormalizable terms suppressed by powers of the Planck mass $M_{pl} \approx 10^{19}$ GeV:

$$\mathcal{V}_{\rm non-sym} = \sum_{n>4} \frac{\kappa_n}{M_{pl}^{n-4}} \hat{\mathcal{O}}_n \,, \tag{6.12}$$

where $\hat{\mathcal{O}}_n$ are operators of dimension n that explicitly break the stabilizing symmetry and κ_n are in general complex parameters. This potential clearly leads to the decay of S_1. Note that we can always arrange the model such that there is an accidental symmetry stabilizing the DM at the level of renormalizable operators, leaving the Planck-mass suppressed dimension five and higher operators responsible of the decay.

In order to illustrate the interplay between decay and annihilation we consider the following dimension five operators

$$\hat{\mathcal{O}}_5^{ffh} = Y_f \bar{F}_L H f_R S_1,$$

where F_L is an isodoublet SM fermion, f_R the corresponding right-handed isosinglet partner and Y_f its Yukawa coupling. Lacking deeper motivation we model the gravitational effects by parametrizing them as a scaling factor times the corresponding Yukawa coupling. These operators lead to a decay lifetime $\tau_{\rm DM} = \hbar/\Gamma^{ff}$ where:

$$\Gamma^{ff}(M_{\rm DM}) = \sum_f \frac{N_c}{8\pi^2} \left(\frac{\kappa_5 Y_f v}{M_{pl}}\right)^2 M_{\rm DM} \left(1 - \frac{4m_f^2}{M_{\rm DM}^2}\right)^{\frac{3}{2}} \,, \tag{6.13}$$

is the dark matter decay width into a fermions of mass m_f, v is the vacuum expectation value of the Higgs boson and N_c is the color number (3 for quarks and 1 for leptons).

WIMP dark matter annihilation

The dark matter phenomenology in our prototype model is essentially determined by 5 parameters *: M_{S_1}, M_{S_2}, λ_{11}, λ_{12} and λ_{22}. The strength of co-annihilations is controlled by λ_{12}. In the no co-annihilations limit ($\lambda_{12} \to 0$), λ_{11} is responsible for DM abundance as well as direct (σ_{SI}) and indirect detection (σ_A) cross sections. The coupling λ_{22} is the Higgs coupling of S_2 (the next-to-LSP) to the Higgs scalar and has direct impact on the relic abundance of S_1 in regions of the parameter space where the mass splitting is small and both annihilations and co-annihilations are inefficient to reproduce a good relic abundance. In this case the latter could arise partly from the early decays of $S_2 \to S_1$.

We present in Figure (6.5) the attainable values of the thermal average of the annihilation cross–section times velocity at present time, σ_A, compatible with DM relic abundance when the couplings are varied within the limits of perturbativity, and the Higgs mass is fixed to 126 GeV [25, 26]. The results were obtained using the MicrOMEGAS code [403, 450]. In the presence of pure annihilations, σ_A reproduces the thermal value $\langle\sigma v\rangle_{\text{f.o.}} \approx 3 \times 10^{-26}\,\text{cm}^3/\text{s}$. Deviations from the thermal value exist in regions where the cross section is velocity-dependent as in the case of the Breit–Wigner enhancement at the threshold of the Higgs pole [411]. The expected indirect detection signal in this case is at the edge of FERMI's [451] sensitivity. Substantial deviations occur at $m_H/2$ and at the Higgs boson mass m_H and are associated with the Higgs boson pole and contact interaction term, respectively.

In regions where $\langle\sigma v\rangle_{\text{f.o.}}$ is dominated by co-annihilation ($S_1S_2 \to \text{SM} + \text{SM}$ and/or $S_2S_2 \to \text{SM} + \text{SM}$) processes, the annihilation cross–section is suppressed well below the expected thermal value. Such "inhibited annihilation" regions can arise in various ways. Co-annihilation is just a possible mechanism, common to many dark matter models, such as the minimal supersymmetric standard model or two-Higgs-doublet dark matter models as in Chapter (5),

*Choosing, for simplicity, a null mixing between S_1 and S_2.

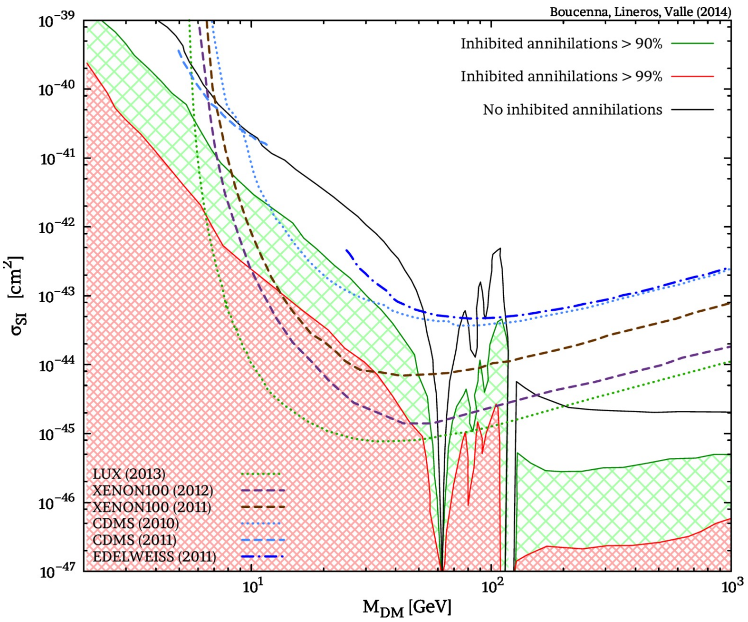

Figure 6.5: Annihilation cross section σ_A compatible with DM relic abundance versus DM mass. The line shown in black corresponds to the simplest case of unsuppressed annihilation. The case of where annihilations at freeze–out are inhibited (see text) above 90 and 99 % is illustrated by the green and red shaded regions, respectively. The thermal cross section $\langle \sigma v \rangle = 3 \times 10^{-26} \mathrm{cm}^2/\mathrm{s}$ and FERMI's constraints for annihilation into $b\bar{b}$ are also shown.

whose generic features are mimicked by our illustrative prototype model.

Inhibition mechanisms are often required in order to obtain (or to extend) an allowed region in the parameters space of the considered model [129, 452]. The general drawback, however, is that the WIMP's indirect detection signal becomes much fainter.

Effect of Planck-induced dark matter decays

As mentioned above, the dark matter stabilizing global symmetry is likely to be broken due to the presence of gravitational effects [439, 440]. We will see now that the mere fact of considering the global symmetry leading to dark matter stability as an approximate one, leads to new observational signals which allow for potentially detectable WIMP-like decaying dark matter signals even when annihilations are suppressed.

In Figure (6.6), display the expected gamma–ray fluxes arising from dark matter annihilation and decay, assuming that the signal comes only from the pro-

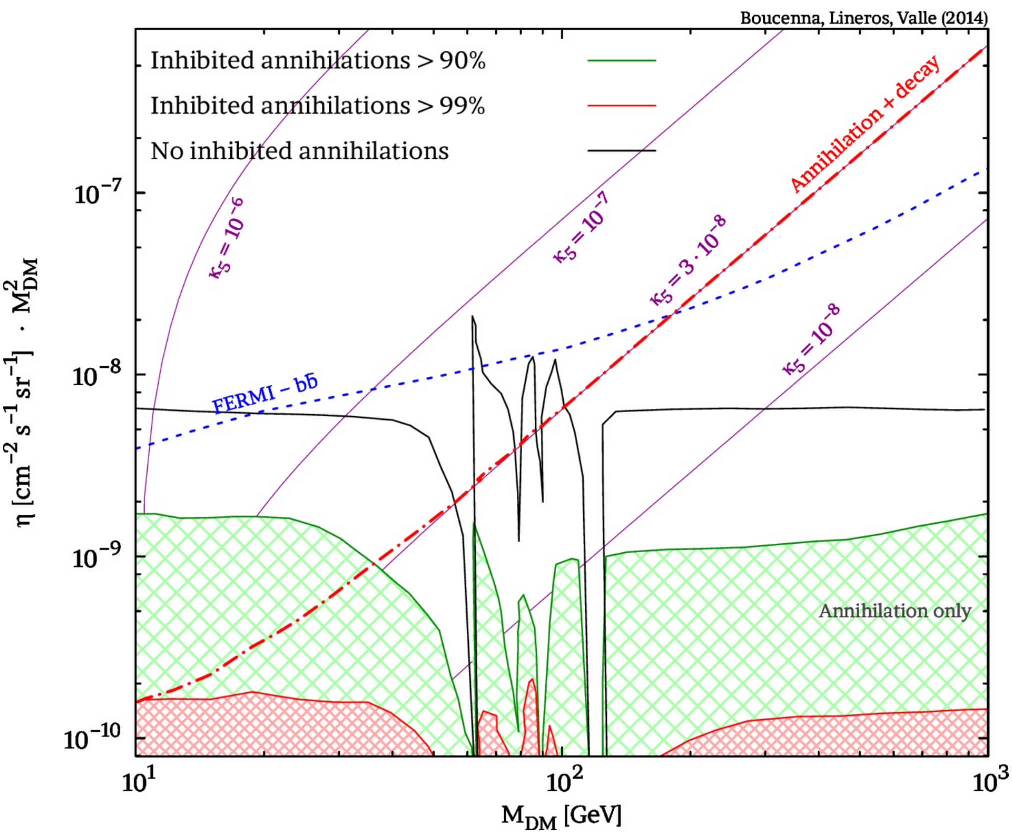

Figure 6.6: The flux associated with dark matter decay versus DM mass (see text for details). We give estimates for the annihilation flux for the cases of 90%, 99%, and no suppression (solid green, red, and black lines respectively). Purple lines correspond to decay signal induced by the operator $\hat{\mathcal{O}}_5^{bbh}$ for fixed κ_5 values. A combined signal annihilation and decay is in red doted–dashed line assuming $\kappa_5 = 3 \times 10^{-8}$ and 99% inhibited annihilation. The bound from FERMI-LAT on annihilation into $b\bar{b}$ [451] is also shown.

duction of $b\bar{b}$ through the operator $\hat{\mathcal{O}}_5^{bbh}$. We compare with the constraints from FERMI-LAT on annihilation into $b\bar{b}$ [451]. In order to compare the decay and annihilation signals we define the flux:

$$\eta(M_{\rm DM}) = \begin{cases} \dfrac{1}{4\pi}\dfrac{\sigma_A J_{\Delta\Omega}^{\rm ann}}{2M_{\rm DM}^2} & \text{for annihilations} \\ \\ \dfrac{1}{4\pi}\dfrac{J_{\Delta\Omega}^{\rm dec}}{2\tau_{\rm DM} M_{\rm DM}} & \text{for decays} \end{cases} , \qquad (6.14)$$

where $J_{\Delta\Omega}$ is the angular averaged line of sight integral of the DM density (squared) for decaying (annihilating) WIMP. In order to estimate the fluxes we use the $J_{\Delta\Omega}$ given in Ref. [92]. The observable gamma–rays flux is directly related to the flux as:

$$\Phi_\gamma(E, M_{\rm DM}) = \eta(M_{\rm DM}) \times \frac{dn_\gamma}{dE}(E)\,, \tag{6.15}$$

where dn_γ/dE is the photon spectrum per single annihilation (or decay) event. This quantity allows us to compare on the same footing both annihilation and decay signals withFERMI-LATconstraints. In our particular case, we compare the signal related to the production of $b\bar{b}$ pairs.

We notice that fluxes coming only from decays rise with the dark matter mass starting at restively low masses for large enough κ_5 values, and quickly exceed theFERMI-LATsensitivity. For instance, for a 50 GeV DM mass, we would require κ_5 to be smaller than $\approx 10^{-7}$ in order to fulfill the observational constraints.

In contrast, inhibited annihilations (same regions as in Figure (6.5)) lead to signals that are faint and well below observational sensitivities of indirect dark matter searches.

6.7 Conclusions and discussion

We have described how the spontaneous breaking of a $\Delta(54)$ flavor symmetry can stabilize the dark matter by means of a residual unbroken symmetry and provide rich neutrino phenomenology at the same time. In our scheme left-handed leptons as well as quarks transform non-trivially under the flavor group, with neutrino masses arising from a type-II seesaw mechanism. We have found lower bounds for neutrinoless double beta decay, even in the case of normal hierarchy, as seen in Figure (6.2). In addition, we have correlations between solar and reactor angles consistent with the recent DAYA-BAY and RENO reactor measurements, see Figure (6.3) and Figure (6.4), interesting in their own right. Moreover, the model has a conceptual link between DM and neutrino physics. The dark matter candidate is a WIMP similar to the one analyzed in Chapter (5), but with the difference that here the higgs sector is 3-HDM instead of 2-HDM which, in principle, gives more freedom to accommodate LHC limits.

Since we are dealing with global symmetries, we took seriously the conjecture "gravity breaks global symmetries". We have also considered the effect of explicit gravitational breaking of the global symmetry protecting WIMP dark matter stability. Using a generic toy model and an effective parametrization of Planck–scale effects, we find that the WIMP paradigm is safe as long as dimension 5 operators are absent. Indeed, higher dimensional operators lead to very long DM lifetimes and faint signals, rendering their effect invisible. Assuming that these breaking effects are small enough to yield sufficiently long dark matter decay lifetimes, there appears a genuine new signal in regions that were previously dark.
Finally, an unambiguous detection of a mixed decay and annihilation signal may offer a very interesting window into Planck scale physics, offering an unexpected phenomenological ramification of the WIMP paradigm.

7

Neutrinos and the inflationary Universe

Un chant mystérieux tombe des astres d'or.
Arthur Rimbaud

Much has been said since the announcement of the discovery of primordial gravitational waves by BICEP2 collaboration earlier this year. From excitement to confusion, for many cosmologists the reported results passed from being 5σ major discovery to being a good map of dust. Recently PLANCK published on the Arxiv their findings on dust emission at intermediate and high Galactic latitudes [453]. These include parts of the sky being observed by the BICEP2 experiment. Although they cannot be conclusive yet, they find that in the region explored by BICEP2 there is more dust than what the collaboration had previously assumed in their analysis. This certainly downgrades the significance of the results reported by BICEP2 and casts doubt on their validity. Still, a genuine signal of gravitational waves is possible and only a joint analysis between the two teams may definitely settle the issue. The two collaborations are currently working on a joint assessment of the primordial waves detection claim [454]. We will assume that the BICEP2 measurements are correct. Although the model we will present can account for PLANCK's favored small values for the spectral index as well as for the large value found by BICEP2.

Apart from the intrinsic significance of the (eventual) discovery made by BICEP2, the measurement of nonzero r implies important constraints on inflationary models of the Universe [455–457]. This caused tremendous interest in the community, see for instance [458–463] and references therein.

Previously, we have considered the symmetries suggested by the mixing patterns. Here, we will consider the lepton number symmetry. That is, the defining symmetry of neutrinos. We consider the simplest type-I seesaw scenario [250–255] of neutrino mass generation, introduced in Section (3.6.1), and we promote lepton number to a spontaneously broken symmetry [255, 464]. As we will see, this model incorporates inflation quite naturally.

In order to consistently formulate the spontaneous violation of lepton number within the $SU(3)_c \otimes SU(2)_L \otimes U(1)_Y$ model, one requires the presence of a lepton-number-carrying complex scalar singlet, σ, coupled to the singlet "right-handed" neutrinos N. The real part of σ drives inflation through a Higgs potential [462, 465–468] while the imaginary part, which is the associated Nambu-Goldstone boson, is assumed to pick up a mass due to the presence of small explicit soft lepton number violation terms in the scalar potential, whose origin we need not specify at this stage. For suitable masses such a majoron can account for the dark matter [445], consistent with the CMB observations [469].

We show how, for reasonable parameter choices, this simple scheme for neutrino masses provides an acceptable inflationary scenario. The model has also the potential to account for baryogenesis through leptogenesis. A previous attempt relating inflation to neutrinos can be found in [470] where a supersymmetric model was suggested in which the right-handed sneutrino drives chaotic inflation.

The chapter is organized as follows: the majoron is introduced in Section (7.1), followed by its related inflationary potential in Section (7.2). Then present three inflationary scenario available in the model: 'higgs' inflation in Section (7.3), quartic inflation in Section (7.4), and the non-minimally coupled scalar to gravity in Section (7.5). We conclude the chapter in Section (7.6).

7.1 Introducing the majoron

The majoron (J) is the pseudo-Nambu-Goldstone (pNGB) associated to lepton number symmetry. In the simplest model [255, 464], lepton number is spontaneously broken by the *vev* of a singlet complex scalar σ through its coupling to right-handed neutrinos, Equation (3.25) becomes:

$$-\mathcal{L} = Y_D \bar{L}\check{H}N + \frac{1}{2}\, Y_N\, \sigma\, \widetilde{N}N + \text{h.c.} \tag{7.1}$$

Where, the symmetric matrix Y_N characterizes the coupling of σ to the right-handed neutrinos. After symmetry breaking, we can write:

$$\sigma = \frac{1}{\sqrt{2}}(\langle\sigma\rangle + \rho + iJ)\,. \tag{7.2}$$

The term $Y_N\,\langle\sigma\rangle$ is identified with M_N in Equation (3.25). We have the usual seesaw Lagrangian (Section (3.6.1)) plus two particles: the $\mathcal{CP}$-even scalar ρ mixing with the Higgs and the $\mathcal{CP}$-odd scalar J, the majoron, that is the Nambu-Goldstone boson. More formally, after symmetry breaking characterized by the lepton number violation scale $v_{\text{L}} = \langle\sigma\rangle$ [255, 464], and the electroweak scale v_{SM} the resulting seesaw scheme is characterized by singlet and doublet neutrino mass terms, described by:

$$\mathcal{M}_\nu = \begin{pmatrix} 0 & Y_D v_{\rm SM} \\ {Y_D}^T v_{\rm SM} & Y_N v_{\rm L} \end{pmatrix}, \tag{7.3}$$

in the basis (ν_L, N). The Yukawa coupling matrix Y_D generates the Dirac neutrino mass term, while Y_N gives the right-handed Majorana mass term. While the former is in principle arbitrary, the matrix Y_N characterizing the coupling of σ to the right-handed neutrinos is symmetric and can be taken diagonal and with real positive entries without loss of generality. The effective light neutrino mass, obtained by perturbative diagonalization of Equation (7.3) is of the form:

$$m_\nu \approx Y_D {Y_N}^{-1} {Y_D}^T \frac{{v_{\rm SM}}^2}{v_{\rm L}} . \tag{7.4}$$

Assuming Y_D of $\mathcal{O}(1)$, one needs $v_{\rm L} \gtrsim 10^{14}\,$GeV,

$$Y_N \approx \frac{10^{14}\ \text{GeV}}{v_{\rm L}} . \tag{7.5}$$

As a Goldstone boson, the majoron is strictly massless. However soft explicit lepton number violation may arise from a variety of sources, including quantum gravity effects [444, 471] leading to a massive majoron. A massive majoron can always decay to two neutrinos:

$$\Gamma_{J\to\nu\nu} = \frac{m_J}{32\pi} \frac{\Sigma(m_\nu)^2}{2\left<\sigma\right>^2} , \tag{7.6}$$

where m_J is the mass of the majoron and the sum runs over the light neutrino masses. Though generally sub-leading, there's also the possibility of decaying to two photons through charged fermions loops. However, the latter is model-dependent. For instance, $J \to \gamma\gamma$ is boosted in models where the majoron arises from non-singlets of $SU(2)_L \otimes U(1)_Y$ since it would be accompanied with new charged fermions. $\nu\nu$ and $\gamma\gamma$ are the two main channels of (indirect) detection of majoron DM. For suitable masses the majoron can account for the dark matter [445], consistent with the CMB observations [469, 472]. The existence of this two–neutrino decay mode modifies the power spectrum of the cosmic microwave background temperature anisotropies [469]. One can deter-

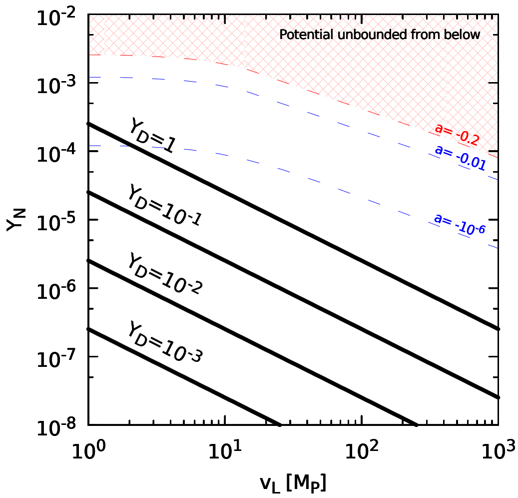

Figure 7.1: Majoron inflation: Y_N vs. v_L for various Y_D. Dashed lines show some values of the coefficient a of the Coleman-Weinberg term in the potential. Solid black lines are upper bounds on Y_N for the corresponding Dirac neutrino Yukawa coupling Y_D.

mine the majoron lifetime and mass values required by the CMB observations in order for the majoron dark matter picture of the Universe to be consistent. It has been shown that the majoron provides an acceptable decaying dark matter scenario for suitably chosen mass values [472] which depend on whether or not the majorons are thermal or not. If the majoron production cannot be thermal, as it may be the case in the first inflationary scenario we considered, due to the smallness of the Y_N and λ_{mix} couplings, one can still consider non-thermal mechanisms such as freeze-in [124, 473] or scalar field oscillations [122, 474]. Moreover, in such non-thermal case, the mass of the majoron is not constrained to be of $\mathcal{O}(\mathrm{keV})$ and can lie in a large range depending on the details of the mechanism under consideration.

It is interesting to note that the model includes leptogenesis [475] as a baryogenesis scenario: After spontaneous lepton number violation occurs at the scale v_L, the type I seesaw mechanism is generated and the Universe reheats at the same time. The presence of right-handed neutrinos with direct couplings to the inflaton field is an important ingredient for leptogenesis [476]. See [477] for an analysis of leptogenesis in the presence of majorons.

Solutions above the *vev* ($\rho > v_{\rm L}$)

$v_L(M_P)$	$\log_{10}(\lambda)$	n_s	r	$\alpha\,(10^{-4})$	$V^{1/4}\,(10^{16}\,\text{GeV})$	$\rho_0\,(M_P)$	$\rho_e\,(M_P)$
1.	-12.8521	0.951168	0.260263	-7.96468	2.30678	22.2218	3.14626
5.	-13.0093	0.954908	0.237136	-7.05625	2.25373	24.2634	6.61037
10	-13.2351	0.958581	0.211972	-6.37463	2.1914	28.1285	11.5137
20.	-13.599	0.962148	0.184081	-5.89025	2.11546	37.1396	21.4642
50.	-14.2262	0.964453	0.159253	-5.80242	2.04021	66.1458	48.6058
100	-14.7789	0.965456	0.147557	-5.72255	2.00167	115.805	98.5958
500.	-16.1392	0.966211	0.137189	-5.66368	1.96554	515.506	498.588
1000.	-16.7367	0.9663	0.135828	-5.6565	1.96065	1015.47	998.587

Solutions below the *vev* ($\rho < v_{\rm L}$)

$v_L(M_P)$	$\log_{10}(\lambda)$	n_s	r	$\alpha\,(10^{-4})$	$V^{1/4}\,(10^{16}\,\text{GeV})$	$\rho_0\,(M_P)$	$\rho_e\,(M_P)$
8.	-13.9086	0.87488	0.000385304	-0.150585	0.452484	0.111018	6.70982
9.	-13.5255	0.900769	0.00148882	-0.460638	0.6344	0.27599	7.69622
10.	-13.3033	0.918822	0.00377031	-0.949789	0.800289	0.541141	8.68529
15.	-13.1004	0.95579	0.0279442	-3.49461	1.32046	3.17548	13.6523
20.	-13.2562	0.964198	0.0518562	-4.54129	1.54118	7.05055	18.6357
30.	-13.5959	0.967596	0.0798131	-5.09597	1.71661	16.0451	28.6191
50.	-14.0675	0.96807	0.102141	-5.30133	1.8258	35.3404	48.6058
500.	-16.1213	0.966555	0.131662	-5.63496	1.94544	484.653	501.416
1000.	-16.7278	0.966472	0.133065	-5.64214	1.9506	984.613	1001.42

Table 7.1: Higgs inflation scenario (no radiative corrections): The values of parameters for number of e-folds $N = 60$. Solutions above *vev* favor the BICEP2 claims whereas solutions below *vev* are compatible with PLANCK sensitivity and hint.

7.2 The inflationary potential

We now turn to the dynamical justification of this scenario*, starting from the scalar potential. The tree level Higgs potential associated with the singlet and doublet scalar multiplets σ and H is a simple extension of that which characterizes the standard model,

$$V_{\rm tree} = \lambda\left(\sigma^\dagger\sigma - \frac{v_{\rm L^2}}{2}\right)^2 + \lambda_{\rm mix}(\sigma^\dagger\sigma)(H^\dagger H) + V_H\,, \tag{7.7}$$

where V_H is the SM potential. As will become clear later, inflation and neutrino masses require that $\langle\sigma\rangle \gg \langle H\rangle$. We also consider $\lambda_{\rm mix}$ to be negligible in order to use the small decay width approximation [468]. The inflaton is identified with the real part of σ:

$$\rho \equiv \sqrt{2}\,\Re[\sigma]\,, \tag{7.8}$$

*For simplicity, we take a one-generation neutrino seesaw scheme with 0.1 eV mass scale in the analysis of our proposed inflationary scenario.

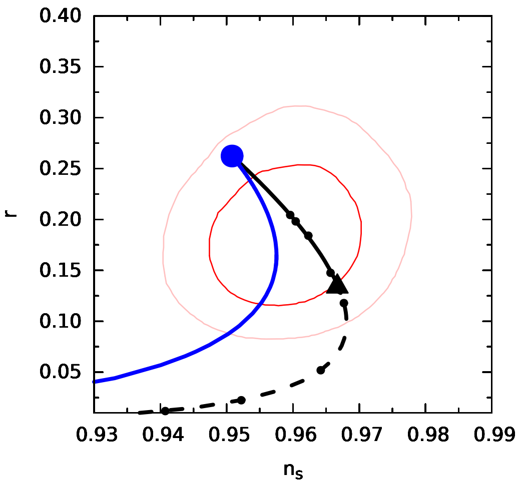

Figure 7.2: Majoron Inflation: The tensor-to-scalar ratio r is shown versus the spectral index n_s. Black line is the majoron inflation scenario with $v_{\rm L} > M_P$. The small black points on each branch, from left to right, indicate the values $v_{\rm L}/M_P = 12, 14, 20$ and 100. The dashed branch corresponds to $\sigma < v_{\rm L}$ and the solid one to $\sigma > v_{\rm L}$. The point and the triangle are the quartic and quadratic inflation predictions, respectively. The blue (gray) line is for $v_{\rm L} \ll M_P$. The contours are the 68% and 95% CL allowed region, combining PLANCK, WP, highL and BICEP2, given in [479] and N is taken to be 60.

and we parametrize the effective potential in the leading-log approximation, with the renormalization scale fixed at $v_{\rm L}$, as [478]:

$$V = \lambda \left[\frac{1}{4} \left(\rho^2 - v_{\rm L}^2 \right)^2 + a \log \left[\frac{\rho}{v_{\rm L}} \right] \rho^4 + V_0 \right] , \tag{7.9}$$

where $a = \frac{\beta_\lambda}{16\pi^2\lambda}$ and the coefficient β_λ is given as:

$$\begin{aligned} \beta_\lambda &= 20\lambda^2 + 2\lambda \left(\sum_i (Y_N^i)^2 \right) - \sum_i (Y_N^i)^4 \\ &\approx -\sum_i (Y_N^i)^4 \, . \end{aligned} \tag{7.10}$$

The last approximation $\lambda \ll Y_N$ will be justified later. An analysis of the potential reveals that $a \gtrsim -0.2$ ensures a consistent local minimum.

The slow-roll paradigm

Here we consider the radiatively corrected ρ^4 potential. Inflation takes places as the inflaton slowly rolls down to the potential minimum either from above ($\sigma > v_{\rm L}$) or from below ($\sigma < v_{\rm L}$). The inflationary slow-roll parameters are given by:

$$\begin{aligned}
\epsilon(\rho) &= \frac{1}{2} M_P^2 \left(\frac{V'}{V}\right)^2 ; \\
\eta(\rho) &= M_P^2 \left(\frac{V''}{V}\right) ; \\
\zeta^2(\rho) &= M_P^4 \left(\frac{V' V'''}{V^2}\right) ,
\end{aligned} \tag{7.11}$$

where prime denotes a derivative with respect to ρ and $M_P = 2.4 \times 10^{18}$ is the (reduced) Planck mass. The slow-roll approximation is valid as long as the conditions $\epsilon, |\eta|, \zeta^2 \ll 1$ hold. In this case, the scalar spectral index n_s, the tensor-to-scalar ratio r, and the running of the spectral index α are given by:

$$\begin{aligned}
n_s &\approx 1 - 6\epsilon + 2 ; \\
r &\approx 16\epsilon ; \\
\alpha &\equiv \frac{dn_s}{d\ln k} \approx 16\epsilon\eta - 24\epsilon^2 - 2\zeta^2 .
\end{aligned} \tag{7.12}$$

The amplitude of the curvature perturbation $\Delta_{\mathcal{R}}$ is:

$$\Delta_{\mathcal{R}}^2 = \left.\frac{V}{24\,\pi^2\,,M_P^4\,\epsilon}\right|_{k_0} , \tag{7.13}$$

and is taken as $\Delta_{\mathcal{R}}^2 = 2.215 \times 10^{-9}$ to fit PLANCK CMB anisotropy measurements [480], with the pivot scale chosen at $k_0 = 0.05\,{\rm Mpc}^{-1}$. Finally, the number of e-folds realized during inflation is:

$$N = \frac{1}{\sqrt{2} M_P} \int_{\rho_e}^{\rho_0} \frac{d\rho}{\sqrt{\epsilon(\rho)}} \quad , \tag{7.14}$$

where ρ_0 is the field value that corresponds to k_0 and ρ_e denotes the value of ρ at the end of inflation, i.e., when $\epsilon(\rho_e) \approx 1$.

At this stage we have four parameters (Y_D, a, $v_{\rm L}$ and λ) for five observables (m_ν, r, n_s, α and $\Delta_{\mathcal{R}}^2$). Once we calculate ρ_e and ρ_0, λ is fixed from the

constrain on $\Delta^2_{\mathcal{R}}$ and we find that $\lambda \approx 10^{-17} - 10^{-12}$ in the parameter space of the model, which justifies the approximation made in Equation (7.10). We are then left with a (i.e., Y_N), Y_D and $v_{\rm L}$ and neutrino masses further constrain the relation between Y_N and Y_D. The predicted values of r, n_s and α are therefore predicted for fixed values of a and $v_{\rm BL}$.
We will consider two limits: $v_{\rm L} > M_P$, the so-called Higgs inflation as well as $v_{\rm L} \ll M_P$ when the scalar potential considered in Equation (7.9) reduces to the radiatively corrected quartic inflation [481].

7.3 Higgs inflation

This scenario requires trans-Planckian *vevs*. The seesaw relation, Equation (3.26) imposes $Y_N \ll 1$ in order to suppress the right handed neutrino mass. For instance for $v_{\rm L} = 10^3\,{\rm M_P}$, one gets $Y_N \approx 10^{-6}$, a value similar to the electron Yukawa coupling. The Coleman-Weinberg radiative corrections are negligible in this case and we consider only the tree level potential. Black lines in Figure (7.2) show the predicted values of r and n_s obtained by varying $v_{\rm L}$ and taking the number of e-foldings $N = 60$. The allowed 68% and 95% CL contours are indicated. The dashed line is when the inflaton rolls from "below" ($\rho < v_{\rm BL}$) while the solid one is for the opposite case. Both branches converge toward quadratic (indicated by a triangle) inflation in the limit $\rho \to \infty$, (n_s, r)=(0.967, 0.132). We show various values of $v_{\rm L}$ as small circles. The small *vev* limit, depicted by a big circle corresponds to the textbook quartic inflation potential, (n_s, r)=(0.951, 0.262). The running of the spectral index, α, is depicted in Figure (7.3). In Figure (7.1) we show the connection between inflation and neutrino masses, in the plane Y_N vs. $v_{\rm L}$. The black lines are upper bounds on Y_N for a given Dirac coupling Y_D. We also show some values of a corresponding to each Y_N and $v_{\rm L}$ for completeness. The numerical results for this case are displayed in Table (7.1).

7.4 Quartic inflation

The sub-Planckian inflationary scenario $v_{\rm L} \ll M_P$, in principle physically more attractive, is well approximated by the quartic potential. In this case, Y_N

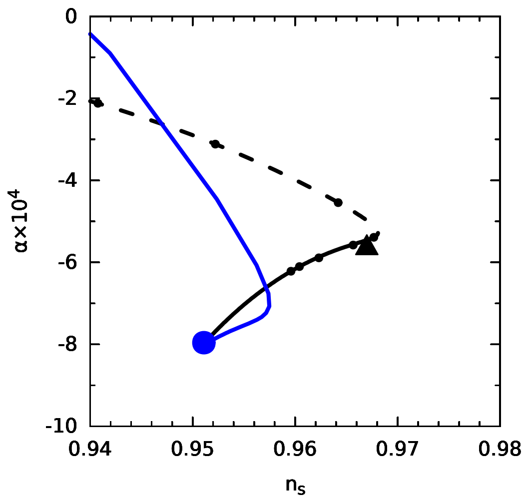

Figure 7.3: Majoron inflation: α vs. n_s for various $v_{\rm BL}$ values. See caption of Figure (7.2) for more details.

can be large so that the radiative corrections to the ρ^4 potential should be taken into account. The quantum corrections allow us to depart from the fixed textbook prediction of quartic inflation to lie closer to the BICEP2 region. Figure (7.2) and Figure (7.3) show the effect of the coupling of the inflaton to right handed neutrinos on the inflationary observables. The blue line, departing from the quartic inflation prediction is obtained by varying a, and consequently Y_N in the range [-0.2, 0] corresponding to a variation of Y_N around $\approx 10^{-3}$. If $v_{\rm L}$ is taken to lie around $10^{14}\,$GeV then $Y_N \approx 10^{-2}$ reproduces the correct neutrino mass scale. We display in Table (7.2) the numerical results for this case.

7.5 Non-minimal coupling to gravity

For completeness we add the case of non-minimal coupling to gravity, originally not covered in [3]. We consider a class of models [482, 483] which invokes a quartic potential for the inflaton field with an additional non-minimal coupling of the inflaton field to gravity [484, 485].

Perhaps the simplest scenario of this kind is the so-called 'Higgs inflation' [486], where the SM Higgs drives inflation. This is achieved by coupling the Higgs

Small solutions ($0.01 \lesssim r \lesssim 0.02$)

a	$\lvert Y_N \rvert$	$\log_{10}(\lvert\lambda\rvert)$	n_s	r	$\alpha\,(10^{-4})$	$V^{1/4}\,(10^{16}\,\text{GeV})$	$\rho_0\,(M_P)$	$\rho_e\,(M_P)$
-0.01307	0.00135604	-11.7856	0.890248	0.0100493	7.9222	1.02256	15.1923	2.49121
-0.01305	0.00142537	-11.6983	0.899145	0.0137211	7.32328	1.10535	15.5053	2.49559
-0.01304	0.00145721	-11.6596	0.903321	0.0158434	6.92563	1.14582	15.6575	2.49774
-0.01303	0.00148709	-11.624	0.907307	0.0181559	6.47185	1.18552	15.8065	2.49987
-0.01302	0.00151498	-11.5914	0.911098	0.0206547	5.97014	1.22435	15.9522	2.50198

Large solutions ($0.1 \lesssim r \lesssim 0.2$)

a	$\lvert Y_N \rvert$	$\log_{10}(\lvert\lambda\rvert)$	n_s	r	$\alpha\,(10^{-4})$	$V^{1/4}\,(10^{16}\,\text{GeV})$	$\rho_0\,(M_P)$	$\rho_e\,(M_P)$
-0.01279	0.00172752	-11.3556	0.952953	0.101404	-4.68889	1.82249	18.3706	2.54494
-0.01265	0.00167379	-11.4057	0.957019	0.141706	-6.48511	1.98152	19.1795	2.56674
-0.01261	0.00165322	-11.4258	0.957343	0.150727	-6.71294	2.01234	19.3554	2.57247
-0.01256	0.00162674	-11.4521	0.957507	0.160678	-6.9129	2.04476	19.5497	2.57934
-0.0125	0.00159495	-11.4843	0.957484	0.170937	-7.07347	2.07664	19.7519	2.5872
-0.0124	0.00154397	-11.5373	0.957174	0.184759	-7.2355	2.1174	20.0299	2.59943
-0.0123	0.00149676	-11.5877	0.956735	0.195481	-7.33264	2.14748	20.2527	2.61069
-0.0122	0.00145363	-11.635	0.956276	0.20395	-7.39978	2.17037	20.4349	2.62107
-0.0121	0.00141436	-11.679	0.95584	0.210759	-7.45154	2.18826	20.5865	2.63068
-0.0119	0.00134587	-11.7579	0.955081	0.220938	-7.53147	2.21422	20.8243	2.64788
-0.0116	0.00126256	-11.8579	0.954217	0.230944	-7.62064	2.23887	21.0753	2.66959

Table 7.2: Radiatively corrected quartic potential: The values of parameters for number of e-folds $N = 60$.

field in a non-minimal way to gravity, i.e., the Ricci scalar, leading to a typical prediction $(n_s, r) = (0.968, 0.003)$ for $N = 60$ e-folds. Note that these predictions are obtained thanks to very large non-minimal couplings and depend on the exact top quark mass [487]. In non-minimal quartic inflation, the inflationary predictions vary from those in quartic inflation (Section (7.4)) depending on the strength of the non-minimal coupling [482–485].

The action of non-minimal ρ^4 inflation is given by (in the Jordan frame):

$$S_J^{\text{tree}} = \int d^4x\sqrt{-g}\left[-\left(\frac{1+\xi\rho^2}{2}\right)\mathcal{R} + \frac{1}{2}(\partial\rho)^2 - \frac{\lambda}{4!}\rho^4\right], \tag{7.15}$$

where ρ is a gauge singlet scalar field defined in Equation (7.8) and λ is its self-coupling. In the Einstein frame the action becomes:

$$S_E = \int d^4x\sqrt{-g_E}\left[-\frac{1}{2}\mathcal{R}_E + \frac{1}{2}(\partial\phi)^2 - V_E(\phi(\rho))\right], \tag{7.16}$$

where the canonically normalized scalar field is written in terms of the original

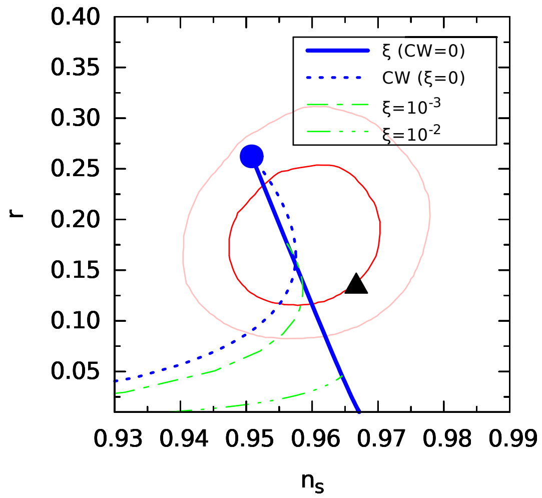

Figure 7.4: Majoron inflation: r vs. n_s for inflation with non-minimal coupling to gravity for various couplings ξ. Solid (blue) curve is in the presence of the non-minimal coupling only, i.e., no Coleman-Weinberg corrections. Long (green) dashed lines are for scenario including both radiative corrections and non-minimal coupling. For the sake of comparison we also plot the prediction of Coleman-Weinberg corrections alone (dotted (blue) line) as in Figure (7.2). The lepton number breaking scale is much smaller than M_P, $v_{\mathrm{L}} = 10^{-7} M_P$.

scalar as:

$$\left(\frac{d\phi}{d\rho}\right)^{-2} = \frac{(1+\xi\rho^2)^2}{1+(6\xi+1)\xi\rho^2}\,, \tag{7.17}$$

and the inflation potential in the Einstein frame is:

$$V_E(\phi(\rho)) = \frac{\frac{1}{4!}\lambda(t)\rho^4}{(1+\xi\,\rho^2)^2}\,. \tag{7.18}$$

The inflationary slow-roll parameters in terms of the original scalar field (ρ) are now expressed as:

$$\begin{aligned} \epsilon(\rho) &= \frac{1}{2}\left(\frac{V_E'}{V_E\phi'}\right)^2; \\ \eta(\rho) &= \frac{V_E''}{V_E(\phi')^2} - \frac{V_E'\phi''}{V_E(\phi')^3}; \\ \zeta(\rho) &= \left(\frac{V_E'}{V_E\phi'}\right)\left(\frac{V_E'''}{V_E(\phi')^3} - 3\frac{V_E''\phi''}{V_E(\phi')^4} + 3\frac{V_E'(\phi'')^2}{V_E(\phi')^5} - \frac{V_E'\phi'''}{V_E(\phi')^4}\right), \end{aligned} \tag{7.19}$$

$N = 60$

ξ	n_s	r	$\alpha\,(10^{-4})$	$V^{1/4}(10^{16}\,\text{GeV})$	$\rho_0\,(M_P)$	$\rho_e\,(M_P)$
0.0005	0.954036	0.21082	-6.44459	2.81719	22.0865	2.82279
0.0006	0.954534	0.202853	-6.69298	2.81496	22.085	2.82167
0.0013	0.957192	0.160428	-8.65762	2.7995	22.0695	2.81387
0.0020	0.958936	0.132724	-9.67817	2.78431	22.0481	2.80615
0.0060	0.963119	0.0672979	-8.2811	2.70236	21.8755	2.76359
0.0100	0.964558	0.0455816	-6.30856	2.62769	21.6723	2.7234
0.0500	0.966936	0.0125961	-1.98213	2.12149	19.6921	2.4099
0.1000	0.967342	0.00784365	-1.25435	1.77579	17.7835	2.14612

$N = 50$

ξ	n_s	r	$\alpha\,(10^{-4})$	$V^{1/4}(10^{16}\,\text{GeV})$	$\rho_0\,(M_P)$	$\rho_e\,(M_P)$
0.0005	0.944498	0.260543	-9.01182	2.81719	20.1955	2.82279
0.0006	0.945033	0.251993	-9.22631	2.81496	20.1942	2.82167
0.0013	0.94798	0.204923	-11.6336	2.7995	20.1814	2.81387
0.0020	0.950005	0.17271	-13.3355	2.78431	20.1635	2.80615
0.0060	0.955183	0.0915609	-12.7058	2.70236	20.0143	2.76359
0.0100	0.957073	0.062932	-10.0515	2.62769	19.8344	2.7234
0.0500	0.960319	0.0177504	-3.31781	2.12149	18.0409	2.4099
0.1000	0.960887	0.011078	-2.11173	1.77579	16.2979	2.14612

Table 7.3: Non-minimally coupled singlet field (ρ) to gravity, with $N = 50$ and $N = 60$ efolds.

where a prime denotes a derivative with respect to ρ. The number of e-folds is then given by:

$$N = \frac{1}{\sqrt{2}} \int_{\rho_e}^{\rho_0} \frac{d\rho}{\sqrt{\epsilon(\rho)}} \left(\frac{d\phi}{d\rho}\right) . \tag{7.20}$$

The inflationary predictions for n_s, r, and α are obtained after fixing N and ξ. In Figure (7.4) we show the predicted values of this scenario in the plane (n_s, r) for the number of e-folds $N = 60$. We have varied the non-minimal coupling strength ξ with and without the Coleman-Weinberg corrections. We display in Table (7.3) some numerical benchmarks for this inflationary scenario.

7.6 Conclusions

We have discussed the possibility that neutrino masses, inflation and dark matter may have a common origin. We have illustrated this with the simplest type-I seesaw model with spontaneous breaking of global lepton number. The resulting inflationary scenario is consistent with the recent CMB B-mode observation by the BICEP2 experiment. We have analysed three possible scenarios: higgs inflation, Coleman-Weinberg corrected quartic inflation and inflation through non-minimal coupling to gravity. In all the cases, the model can also account for smaller spectral indices accessible to PLANCK.

On the other hand, the scheme may also account for majoron dark matter and possibly also leptogenesis induced through the out-of-equilibrium decays of the right-handed neutrinos, for reasonable parameter values. If supersymmetry is invoked, then one has a majoron version of the supersymmetric type-I seesaw, in which lepton flavor violation processes may be within the reach of future experiments.

8

Conclusions and outlook

It was the time of lightness, it was the time of darkness...

The Standard Model picture of the Nature suffers from two important flaws. On the one hand, massive neutrinos hint toward a new mechanism at work beyond the Standard Model, and on the other, the universe is dominated by an enigmatic form of matter that outnumbers the baryonic matter 5-to-1, implying the existence of new particles and perhaps new forces as well. The early universe is the place where these two mysteries meet.

This thesis revolved around the following questions: *Are neutrinos and dark matter related to each other? Do they share the same origin? Is there a unified, predictive, description of dark matter and neutrinos?*

To answer these questions, a survey of the literature was done. The physics of dark matter was briefly reviewed in Chapter (2) where we also touched upon its link with the baryon asymmetry of the universe. Neutrino mass mechanisms, both high and low scale, tree-level and radiative, were reviewed in Chapter (3). The status and general categorization of the approaches followed to link dark matter and neutrinos were summarized in Chapter (4).

Instead of focusing on a link between DM and neutrinos through the neutrino mass mechanism, we found it more interesting and perhaps deeper to consider a relation originating from the symmetries of the leptons instead. In Chapter (5), we have studied in detail the DM phenomenology of a model where the stability of the WIMP dark matter candidate arises from a flavor symmetry. The A_4 non-Abelian discrete group accounts both for the observed pattern of neutrino mixing as well as for DM stability. In Chapter (6), we constructed and analyzed a more predictive model encompassing the most recent development in neutrino physics and including the CKM in a nontrivial way.

Following the path of leptonic symmetries, and specifically the lepton number, we enlarged the description of neutrinos and dark matter to include a simple and predictive inflationary scenario. We showed that the type-I seesaw mechanism not only includes an elegant dark matter candidate but also can drive inflation.

During the thesis, numerous attempts have been considered to answer the questions above in the framework of the $SU(3)_c \otimes SU(2)_L \otimes U(1)_Y$ gauge group, extended by continuous or discrete (flavor) symmetries. Most of them have failed to offer a 'natural' relation. Some less than others. This may be due to two reasons. Either neutrinos and dark matter have fundamentaly nothing to do with each other and our minimalist bias is misleading, or the local structure of the theory must be enlarged to allow for new kinds of interactions and (predictive) links that are not possible within the SM framework. The idea that neutrinos and dark matter may originate from the same physics is too attractive to be abandoned so hastily. Therefore we contemplate extensions of the SM gauge group that naturally include both DM and neutrinos. As a first step toward such a description, we proposed a new (radiative) neutrino mass model based on the $SU(3)_c \otimes SU(3)_L \otimes U(1)_X$ local group [9, 10]. Under this group, the left-handed leptons are triplets written as:

$$\psi_L^\ell = \begin{pmatrix} \ell^- \\ -\nu_\ell \\ N_\ell^c \end{pmatrix}_L ,$$

such that right-handed neutrinos and light neutrinos belong to the same gauge multiplet. As a consequence, interactions mediated by gauge bosons connect them. This attractive fact allowed us to generate calculable neutrino masses radiatively through gauge boson exchange. It would certainly be most interesting to consider a natural embedding of dark matter in such a setup. Perhaps, we can get a nice interplay between dark matter and neutrinos in this case with some testable correlations. But that remains to be seen ...

A

Group Theory

Here we review the mathematics of the non-Abelian discrete groups used in the models presented in this work, A_4 and $\Delta(54)$. For more details about the mathematics of non-Abelian discrete groups for particle physicists, we refer the reader to [429] and [488].

A.1 A_4 group

All finite groups are completely characterized by means of a set of elements called generators of the group and a set of relations, so that all the elements of the group are given as product of the generators. The group A_4 consists of the even permutations of four objects and then contains $4!/2 = 12$ elements. The generators are S and T with the relations $S^2 = T^3 = (ST)^3 = \mathcal{I}$, then the elements are $1, S, T, ST, TS, T^2, ST^2, STS, TST, T^2S, TST^2, T^2ST$. A_4 is isomorphic to the symmetry group of the tetrahedron, Figure (A.1). A_4 has four irreducible representations (see Table (A.1)), three singlets $1,\ 1'$ and $1''$

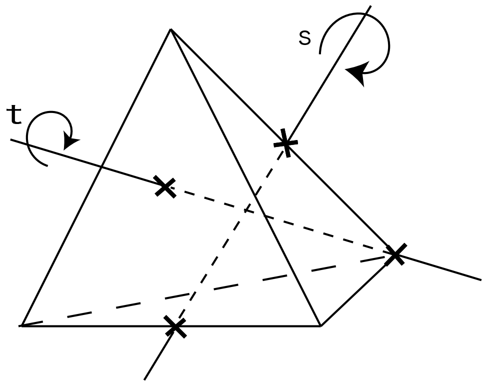

Figure A.1: The A_4 symmetry of tetrahedron.

and one triplet. The one-dimensional unitary representations are obtained by:

$$\begin{array}{lll} 1 & S=1 & T=1 \\ 1' & S=1 & T=\omega \\ 1'' & S=1 & T=\omega^2 \end{array} \tag{A.1}$$

where $\omega^3 = 1$. The product rule for the singlets are:

$$\begin{aligned} &1\times 1 = 1'\times 1'' = 1 \\ &1'\times 1' = 1'' \\ &1''\times 1'' = 1' \end{aligned} \tag{A.2}$$

In the basis where S is real diagonal,

$$S = \begin{pmatrix} 1 & 0 & 0 \\ 0 & -1 & 0 \\ 0 & 0 & -1 \end{pmatrix}; \quad T = \begin{pmatrix} 0 & 1 & 0 \\ 0 & 0 & 1 \\ 1 & 0 & 0 \end{pmatrix}; \tag{A.3}$$

one has the following triplet multiplication rules,

$$\begin{aligned} (ab)_1 &= a_1b_1 + a_2b_2 + a_3b_3\,; \\ (ab)_{1'} &= a_1b_1 + \omega a_2b_2 + \omega^2 a_3b_3\,; \\ (ab)_{1''} &= a_1b_1 + \omega^2 a_2b_2 + \omega a_3b_3\,; \\ (ab)_{3_1} &= (a_2b_3, a_3b_1, a_1b_2)\,; \\ (ab)_{3_2} &= (a_3b_2, a_1b_3, a_2b_1)\,, \end{aligned} \tag{A.4}$$

	$C_1 = \{I\}$	$C_2 = \{T\}$	$C_3 = \{T^2\}$	$C_4 = \{S\}$
1	1	1	1	1
$1'$	1	ω	ω^2	1
$1''$	1	ω^2	ω	1
3	3	0	0	-1

Table A.1: Character table of A_4 where C_i are the different classes and $\omega^3 \equiv 1$.

where $a = (a_1, a_2, a_3)$ and $b = (b_1, b_2, b_3)$.

A.2 $\Delta(54)$ group

In the $\Delta(6N^2)$ family, the first member $\Delta(6)$ is equivalent to S_3, $\Delta(24)$ is isomorphic to the S_4 group. Then comes $\Delta(54)$.

Since in the model of Chapter (6) we use only doublet and singlet representations, we leave aside the triplet representations in what follows.

There are four doublets and the generators, a, a', b and c, are represented by

$$a = a' = \begin{pmatrix} 1 & 0 \\ 0 & 1 \end{pmatrix}, \qquad b = \begin{pmatrix} \omega & 0 \\ 0 & \omega^2 \end{pmatrix}, \qquad c = \begin{pmatrix} 0 & 1 \\ 1 & 0 \end{pmatrix}, \qquad \text{on } \mathbf{2}_1, \tag{A.5}$$

$$a = a' = \begin{pmatrix} \omega^2 & 0 \\ 0 & \omega \end{pmatrix}, \qquad b = \begin{pmatrix} \omega & 0 \\ 0 & \omega^2 \end{pmatrix}, \qquad c = \begin{pmatrix} 0 & 1 \\ 1 & 0 \end{pmatrix}, \qquad \text{on } \mathbf{2}_2, \tag{A.6}$$

$$a = a' = \begin{pmatrix} \omega & 0 \\ 0 & \omega^2 \end{pmatrix}, \qquad b = \begin{pmatrix} \omega & 0 \\ 0 & \omega^2 \end{pmatrix}, \qquad c = \begin{pmatrix} 0 & 1 \\ 1 & 0 \end{pmatrix}, \qquad \text{on } \mathbf{2}_3, \tag{A.7}$$

	χ_{1_+}	χ_{1_-}	$\chi_{3_{1(k)}}$	$\chi_{3_{2(k)}}$	χ_{2_1}	χ_{2_2}	χ_{2_3}	χ_{2_4}
C_1	1	1	3	3	2	2	2	2
$C_1^{(1)}$	1	1	$3\omega^k$	$3\omega^{2k}$	2	2	2	2
$C_1^{(2)}$	1	1	$3\omega^{2k}$	$3\omega^k$	2	2	2	2
$C_6^{(0)}$	1	1	0	0	2	-1	-1	-1
$C_6^{(1,0)}$	1	1	0	0	-1	-1	-1	2
$C_6^{(1,1)}$	1	1	0	0	-1	2	-1	-1
$C_6^{(1,2)}$	1	1	0	0	-1	-1	2	-1
$C_9^{(0)}$	1	-1	1	-1	0	0	0	0
$C_9^{(1)}$	1	-1	ω^{2k}	$-\omega^{2k}$	0	0	0	0
$C_9^{(2)}$	1	-1	ω^k	$-\omega^k$	0	0	0	0

Table A.2: Characters of $\Delta(54)$ ($k = 0, 1, 2$).

$$a = a' = \begin{pmatrix} \omega & 0 \\ 0 & \omega^2 \end{pmatrix}, \qquad b = \begin{pmatrix} 1 & 0 \\ 0 & 1 \end{pmatrix}, \qquad c = \begin{pmatrix} 0 & 1 \\ 1 & 0 \end{pmatrix}, \qquad \text{on } \mathbf{2}_4. \tag{A.8}$$

Then, characters χ_2 for $\mathbf{2}_{1,2,3,4}$ are shown in Table (A.2).

The tensor products between doublets are obtained as

$$\begin{pmatrix} x_1 \\ x_2 \end{pmatrix}_{\mathbf{2}_k} \otimes \begin{pmatrix} y_1 \\ y_2 \end{pmatrix}_{\mathbf{2}_k} = \left(x_1y_2 + x_2y_1\right)_{\mathbf{1}_+} \oplus \left(x_1y_2 - x_2y_1\right)_{\mathbf{1}_-} \oplus \begin{pmatrix} x_2y_2 \\ x_1y_1 \end{pmatrix}_{\mathbf{2}_k}, \tag{A.9}$$

for $k = 1, 2, 3, 4$,

$$\begin{pmatrix} x_1 \\ x_2 \end{pmatrix}_{\mathbf{2}_1} \otimes \begin{pmatrix} y_1 \\ y_2 \end{pmatrix}_{\mathbf{2}_2} = \begin{pmatrix} x_2y_2 \\ x_1y_1 \end{pmatrix}_{\mathbf{2}_3} \oplus \begin{pmatrix} x_2y_1 \\ x_1y_2 \end{pmatrix}_{\mathbf{2}_4}, \tag{A.10}$$

$$\begin{pmatrix} x_1 \\ x_2 \end{pmatrix}_{\mathbf{2}_1} \otimes \begin{pmatrix} y_1 \\ y_2 \end{pmatrix}_{\mathbf{2}_3} = \begin{pmatrix} x_2y_2 \\ x_1y_1 \end{pmatrix}_{\mathbf{2}_2} \oplus \begin{pmatrix} x_2y_1 \\ x_1y_2 \end{pmatrix}_{\mathbf{2}_4}, \tag{A.11}$$

$$\begin{pmatrix} x_1 \\ x_2 \end{pmatrix}_{\mathbf{2}_1} \otimes \begin{pmatrix} y_1 \\ y_2 \end{pmatrix}_{\mathbf{2}_4} = \begin{pmatrix} x_1 y_2 \\ x_2 y_1 \end{pmatrix}_{\mathbf{2}_2} \oplus \begin{pmatrix} x_1 y_1 \\ x_2 y_2 \end{pmatrix}_{\mathbf{2}_3}, \tag{A.12}$$

$$\begin{pmatrix} x_1 \\ x_2 \end{pmatrix}_{\mathbf{2}_2} \otimes \begin{pmatrix} y_1 \\ y_2 \end{pmatrix}_{\mathbf{2}_3} = \begin{pmatrix} x_2 y_2 \\ x_1 y_1 \end{pmatrix}_{\mathbf{2}_1} \oplus \begin{pmatrix} x_1 y_2 \\ x_2 y_1 \end{pmatrix}_{\mathbf{2}_4}, \tag{A.13}$$

$$\begin{pmatrix} x_1 \\ x_2 \end{pmatrix}_{\mathbf{2}_2} \otimes \begin{pmatrix} y_1 \\ y_2 \end{pmatrix}_{\mathbf{2}_4} = \begin{pmatrix} x_1 y_1 \\ x_2 y_2 \end{pmatrix}_{\mathbf{2}_1} \oplus \begin{pmatrix} x_1 y_2 \\ x_2 y_1 \end{pmatrix}_{\mathbf{2}_3}, \tag{A.14}$$

$$\begin{pmatrix} x_1 \\ x_2 \end{pmatrix}_{\mathbf{2}_3} \otimes \begin{pmatrix} y_1 \\ y_2 \end{pmatrix}_{\mathbf{2}_4} = \begin{pmatrix} x_1 y_2 \\ x_2 y_1 \end{pmatrix}_{\mathbf{2}_1} \oplus \begin{pmatrix} x_1 y_1 \\ x_2 y_2 \end{pmatrix}_{\mathbf{2}_2}. \tag{A.15}$$

Furthermore, the tensor products of the non-trivial singlet $\mathbf{1}_-$ with other representations are obtained as

$$\mathbf{2}_k \otimes \mathbf{1}_- = \mathbf{2}_k. \tag{A.16}$$

B

Oblique parameters for discrete dark matter

We give more details about the derivation of T parameters for the Discrete Dark Matter model of Chapter (5). Following the notation of [399], the T oblique parameter for the Standard Model extended by n Higgs doublets with hypercharge 1/2 is

$$\begin{aligned}
\Delta\rho = \alpha T \quad = \quad & \frac{g^2}{64\pi^2 m_W^2} \left\{ \sum_{a=2}^{n} \sum_{b=2}^{2n} \left| \left(U^\dagger V\right)_{ab} \right|^2 F\left(m_a^2, \mu_b^2\right) \right. \\
& - \sum_{b=2}^{2n-1} \sum_{b'=b+1}^{2n} \left[\mathrm{Im} \left(V^\dagger V\right)_{bb'} \right]^2 F\left(\mu_b^2, \mu_{b'}^2\right) \\
& -2 \sum_{a=2}^{n-1} \sum_{a'=a+1}^{n} \left| \left(U^\dagger U\right)_{aa'} \right|^2 F\left(m_a^2, m_{a'}^2\right) \\
& +3 \sum_{b=2}^{2n} \left[\mathrm{Im} \left(V^\dagger V\right)_{1b} \right]^2 \left[F\left(m_Z^2, \mu_b^2\right) - F\left(m_W^2, \mu_b^2\right) \right] \\
& \left. -3 \left[F\left(m_Z^2, m_h^2\right) - F\left(m_W^2, m_h^2\right) \right] \right\}, \qquad \text{(B.1)}
\end{aligned}$$

where m_a, m_a denote the masses of the charged scalars and μ_b, μ_b are the masses of the neutral ones, α is the fine-structure constant and the function F is defined as $(x, y > 0)$

$$F(x,y) \equiv \begin{cases} \dfrac{x+y}{2} - \dfrac{xy}{x-y} \ln \dfrac{x}{y} & \Leftarrow \; x \neq y, \\ 0 & \Leftarrow \; x = y. \end{cases} \qquad \text{(B.2)}$$

We evaluate the U and V matrices for our model as:

$$U = \begin{pmatrix} U_{12} & 0 \\ 0 & U_{23} \end{pmatrix}; \quad V = \begin{pmatrix} iU_{12} & U_{HH_1} & 0 & 0 \\ 0 & 0 & U_{23} & iU_{23} \end{pmatrix}. \qquad \text{(B.3)}$$

The matrices U_{12}, U_{23} and U_{H_1} and the mixing matrices introduced in Equation (5.23).

References

[1] S. Boucenna, M. Hirsch, S. Morisi, E. Peinado, M. Taoso, *et al.*, "Phenomenology of Dark Matter from A_4 Flavor Symmetry," *JHEP* **1105** (2011) 037, arXiv:1101.2874 [hep-ph].

[2] S. Boucenna, S. Morisi, E. Peinado, Y. Shimizu, and J. Valle, "Predictive discrete dark matter model and neutrino oscillations," *Phys.Rev.* **D86** (2012) 073008, arXiv:1204.4733 [hep-ph].

[3] S. M. Boucenna, S. Morisi, Q. Shafi, and J. W. F. Valle, "Inflation and majoron dark matter in the seesaw mechanism," arXiv:1404.3198 [hep-ph].

[4] S. Boucenna, S. Morisi, M. Tortola, and J. Valle, "Bi-large neutrino mixing and the Cabibbo angle," *Phys.Rev.* **D86** (2012) 051301, arXiv:1206.2555 [hep-ph].

[5] S. M. Boucenna, S. Morisi, and J. W. F. Valle, "The low-scale approach to neutrino masses," arXiv:1404.3751 [hep-ph].

[6] S. M. Boucenna and S. Morisi, "Theories relating baryon asymmetry and dark matter: A mini review," *Front.Phys.* **1** (2014) 33, arXiv:1310.1904 [hep-ph].

[7] S. Boucenna, R. Lineros, and J. Valle, "Planck-scale effects on WIMP dark matter," *Front.Phys.* **1** (2013) 34, arXiv:1204.2576 [hep-ph].

[8] S. Boucenna and S. Profumo, "Direct and Indirect Singlet Scalar Dark Matter Detection in the Lepton-Specific two-Higgs-doublet Model," *Phys.Rev.* **D84** (2011) 055011, arXiv:1106.3368 [hep-ph].

[9] S. M. Boucenna, S. Morisi, and J. W. F. Valle, "Radiative neutrino mass in 331 scheme," *Phys.Rev.* **D90** (2014) 013005, arXiv:1405.2332 [hep-ph].

[10] S. M. Boucenna, R. M. Fonseca, F. Gonzalez-Canales, and J. W. F. Valle, "Small neutrino masses and gauge coupling unification," arXiv:1411.0566 [hep-ph].

[11] **DAMA Collaboration** Collaboration, R. Bernabei *et al.*, "First results from DAMA/LIBRA and the combined results with DAMA/NaI," *Eur.Phys.J.* **C56** (2008) 333–355, arXiv:0804.2741 [astro-ph].

[12] D. Hooper and L. Goodenough, "Dark Matter Annihilation in The Galactic Center As Seen by the Fermi Gamma Ray Space Telescope," *Phys.Lett.* **B697** (2011) 412–428, arXiv:1010.2752 [hep-ph].

[13] E. Bulbul, M. Markevitch, A. Foster, R. K. Smith, M. Loewenstein, *et al.*, "Detection of An Unidentified Emission Line in the Stacked X-ray spectrum of Galaxy Clusters," *Astrophys.J.* **789** (2014) 13, arXiv:1402.2301 [astro-ph.CO].

[14] S. Weinberg, "A Model of Leptons," *Phys.Rev.Lett.* **19** (1967) 1264–1266.

[15] A. Salam, "Weak and Electromagnetic Interactions," *Conf.Proc.* **C680519** (1968) 367–377.

[16] S. Glashow, "Partial Symmetries of Weak Interactions," *Nucl.Phys.* **22** (1961) 579–588.

[17] D. J. Gross and F. Wilczek, "Ultraviolet Behavior of Nonabelian Gauge Theories," *Phys.Rev.Lett.* **30** (1973) 1343–1346.

[18] H. D. Politzer, "Reliable Perturbative Results for Strong Interactions?," *Phys.Rev.Lett.* **30** (1973) 1346–1349.

[19] S. Weinberg, "Nonabelian Gauge Theories of the Strong Interactions," *Phys.Rev.Lett.* **31** (1973) 494–497.

[20] M. Gell-Mann, "Quarks," *Acta Phys.Austriaca Suppl.* **9** (1972) 733–761.

[21] H. Fritzsch, M. Gell-Mann, and H. Leutwyler, "Advantages of the Color Octet Gluon Picture," *Phys.Lett.* **B47** (1973) 365–368.

[22] P. W. Higgs, "Broken symmetries, massless particles and gauge fields," *Phys.Lett.* **12** (1964) 132–133.

[23] F. Englert and R. Brout, "Broken Symmetry and the Mass of Gauge Vector Mesons," *Phys.Rev.Lett.* **13** (1964) 321–323.

[24] G. Guralnik, C. Hagen, and T. Kibble, "Global Conservation Laws and Massless Particles," *Phys.Rev.Lett.* **13** (1964) 585–587.

[25] **ATLAS Collaboration** Collaboration, G. Aad *et al.*, "Observation of a new particle in the search for the Standard Model Higgs boson with the ATLAS detector at the LHC," *Phys.Lett.* **B716** (2012) 1–29, arXiv:1207.7214 [hep-ex].

[26] **CMS Collaboration** Collaboration, S. Chatrchyan *et al.*, "Observation of a new boson at a mass of 125 GeV with the CMS experiment at the LHC," *Phys.Lett.* **B716** (2012) 30–61, arXiv:1207.7235 [hep-ex].

[27] B. Richter, "The Rise of colliding beams, in "The Rise of the Standard Model", Ed. Lillian Hoddeson et al., Cambridge University Press," 1997.

[28] T. Wyatt, "High-energy colliders and the rise of the standard model," *Nature* **448** (2007) 274–280.

[29] C.-N. Yang and R. L. Mills, "Conservation of Isotopic Spin and Isotopic Gauge Invariance," *Phys.Rev.* **96** (1954) 191–195.

[30] A. Salam and J. C. Ward, "Electromagnetic and weak interactions," *Phys.Lett.* **13** (1964) 168–171.

[31] C. Rovelli, "Why Gauge?," *Found.Phys.* **44** (2014) 91–104, arXiv:1308.5599 [hep-th].

[32] A. Pais, "Inward bound of matter and forces in the physical world, Oxford University Press," 1986.

[33] L. H. Hoddeson, L. Brown, M. Riordan, and M. Dresden, "The Rise of the standard model: Particle physics in the 1960s and 1970s. Proceedings, Conference, Stanford, USA, June 24-27, 1992,".

[34] S. Weinberg, "The Making of the standard model," *Eur.Phys.J.* **C34** (2004) 5–13, arXiv:hep-ph/0401010 [hep-ph].

[35] T. Cheng and L. Li, "Gauge theory of elementary particle physics," 1984.

[36] J. Donoghue, E. Golowich, and B. R. Holstein, "Dynamics of the standard model," *Camb.Monogr.Part.Phys.Nucl.Phys.Cosmol.* **2** (1992) 1–540.

[37] G. 't Hooft and M. Veltman, "Regularization and Renormalization of Gauge Fields," *Nucl.Phys.* **B44** (1972) 189–213.

[38] T. Kibble, "Topology of Cosmic Domains and Strings," *J.Phys.* **A9** (1976) 1387–1398.

[39] M. Zubkov, "The Observability of Z(6) symmetry in the standard model," *Phys.Lett.* **B649** (2007) 91–94, arXiv:hep-ph/0609029 [hep-ph].

[40] J. A. Bryan, S. M. Carroll, and T. Pyne, "A Texture bestiary," *Phys.Rev.* **D50** (1994) 2806–2818, arXiv:hep-ph/9312254 [hep-ph].

[41] B. Bakker, A. Veselov, and M. Zubkov, "An Additional symmetry in the Weinberg: Salam model," *Yad.Fiz.* **68** (2005) 1045–1053, arXiv:hep-lat/0402004 [hep-lat].

[42] B. Bakker, A. Veselov, and M. Zubkov, "Standard model with the additional Z(6) symmetry on the lattice," *Phys.Lett.* **B620** (2005) 156–163, arXiv:hep-lat/0502006 [hep-lat].

[43] Y. Nambu, "Quasiparticles and Gauge Invariance in the Theory of Superconductivity," *Phys.Rev.* **117** (1960) 648–663.

[44] J. Goldstone, "Field Theories with Superconductor Solutions," *Nuovo Cim.* **19** (1961) 154–164.

[45] J. Goldstone, A. Salam, and S. Weinberg, "Broken Symmetries," *Phys.Rev.* **127** (1962) 965–970.

[46] M. Kobayashi and T. Maskawa, "CP Violation in the Renormalizable Theory of Weak Interaction," *Prog.Theor.Phys.* **49** (1973) 652–657.

[47] N. Cabibbo, "Unitary Symmetry and Leptonic Decays," *Phys.Rev.Lett.* **10** (1963) 531–533.

[48] **Belle Collaboration** Collaboration, K. Abe *et al.*, "Observation of large CP violation in the neutral B meson system," *Phys.Rev.Lett.* **87** (2001) 091802, arXiv:hep-ex/0107061 [hep-ex].

[49] **BaBar Collaboration** Collaboration, B. Aubert *et al.*, "Observation of CP violation in the B^0 meson system," *Phys.Rev.Lett.* **87** (2001) 091801, arXiv:hep-ex/0107013 [hep-ex].

[50] L.-L. Chau and W.-Y. Keung, "Comments on the Parametrization of the Kobayashi-Maskawa Matrix," *Phys.Rev.Lett.* **53** (1984) 1802.

[51] D. G. Charlton, "LEP, SLC and the standard model," *eConf* **C020805** (2002) TW05, arXiv:hep-ex/0211003 [hep-ex].

[52] B. Richter, "High Energy Colliding Beams; What Is Their Future?," arXiv:1409.1196 [hep-ex].

[53] J. C. Pati and A. Salam, "Lepton Number as the Fourth Color," *Phys.Rev.* **D10** (1974) 275–289.

[54] H. Georgi and S. Glashow, "Unity of All Elementary Particle Forces," *Phys.Rev.Lett.* **32** (1974) 438–441.

[55] H. Fritzsch and P. Minkowski, "Unified Interactions of Leptons and Hadrons," *Annals Phys.* **93** (1975) 193–266.

[56] J. R. Ellis, S. Kelley, and D. V. Nanopoulos, "Probing the desert using gauge coupling unification," *Phys.Lett.* **B260** (1991) 131–137.

[57] P. Fayet, "Supersymmetry and Weak, Electromagnetic and Strong Interactions," *Phys.Lett.* **B64** (1976) 159.

[58] P. Fayet, "Spontaneously Broken Supersymmetric Theories of Weak, Electromagnetic and Strong Interactions," *Phys.Lett.* **B69** (1977) 489.

[59] G. R. Farrar and P. Fayet, "Phenomenology of the Production, Decay, and Detection of New Hadronic States Associated with Supersymmetry," *Phys.Lett.* **B76** (1978) 575–579.

[60] P. Fayet, "Relations Between the Masses of the Superpartners of Leptons and Quarks, the Goldstino Couplings and the Neutral Currents," *Phys.Lett.* **B84** (1979) 416.

[61] N. Arkani-Hamed, A. G. Cohen, and H. Georgi, "Electroweak symmetry breaking from dimensional deconstruction," *Phys.Lett.* **B513** (2001) 232–240, arXiv:hep-ph/0105239 [hep-ph].

[62] L. Randall and R. Sundrum, "A Large mass hierarchy from a small extra dimension," *Phys.Rev.Lett.* **83** (1999) 3370–3373, arXiv:hep-ph/9905221 [hep-ph].

[63] F. Zwicky, "Die Rotverschiebung von extragalaktischen Nebeln," *Helv.Phys.Acta* **6** (1933) 110–127.

[64] V. C. Rubin and J. Ford, W. Kent, "Rotation of the Andromeda Nebula from a Spectroscopic Survey of Emission Regions," *Astrophys.J.* **159** (1970) 379–403.

[65] E. W. Kolb and M. S. Turner, "The Early Universe," *Front.Phys.* **69** (1990) 1–547.

[66] G. Jungman, M. Kamionkowski, and K. Griest, "Supersymmetric dark matter," *Phys.Rept.* **267** (1996) 195–373, arXiv:hep-ph/9506380 [hep-ph].

[67] D. Hooper, "TASI 2008 Lectures on Dark Matter," arXiv:0901.4090 [hep-ph].

[68] S. Profumo, "TASI 2012 Lectures on Astrophysical Probes of Dark Matter," arXiv:1301.0952 [hep-ph].

[69] A. Borriello and P. Salucci, "The Dark matter distribution in disk galaxies," *Mon.Not.Roy.Astron.Soc.* **323** (2001) 285, arXiv:astro-ph/0001082 [astro-ph].

[70] H. Hoekstra, H. Yee, and M. Gladders, "Current status of weak gravitational lensing," *New Astron.Rev.* **46** (2002) 767–781, arXiv:astro-ph/0205205 [astro-ph].

[71] R. B. Metcalf, L. A. Moustakas, A. J. Bunker, and I. R. Parry, "Spectroscopic gravitational lensing and limits on the dark matter substructure in Q2237+0305," *Astrophys.J.* **607** (2004) 43–59, arXiv:astro-ph/0309738 [astro-ph].

[72] L. A. Moustakas and R. B. Metcalf, "Detecting dark matter substructure spectroscopically in strong gravitational lenses," *Mon.Not.Roy.Astron.Soc.* **339** (2003) 607, arXiv:astro-ph/0206176 [astro-ph].

[73] J. A. Tyson, G. P. Kochanski, and I. P. Dell'Antonio, "Detailed mass map of CL0024+1654 from strong lensing," *Astrophys.J.* **498** (1998) L107, arXiv:astro-ph/9801193 [astro-ph].

[74] H. Dahle, "A compilation of weak gravitational lensing studies of clusters of galaxies," arXiv:astro-ph/0701598 [astro-ph].

[75] B. Paczynski, "Gravitational microlensing by the galactic halo," *Astrophys.J.* **304** (1986) 1–5.

[76] D. Clowe, M. Bradac, A. H. Gonzalez, M. Markevitch, S. W. Randall, *et al.*, "A direct empirical proof of the existence of dark matter," *Astrophys.J.* **648** (2006) L109–L113, arXiv:astro-ph/0608407 [astro-ph].

[77] **Planck Collaboration** Collaboration, P. Ade *et al.*, "Planck 2013 results. XVI. Cosmological parameters," *Astron.Astrophys.* (2014) , arXiv:1303.5076 [astro-ph.CO].

[78] N. A. Bahcall, J. P. Ostriker, S. Perlmutter, and P. J. Steinhardt, "The Cosmic triangle: Assessing the state of the universe," *Science* **284** (1999) 1481–1488, arXiv:astro-ph/9906463 [astro-ph].

[79] M. Taoso, G. Bertone, and A. Masiero, "Dark Matter Candidates: A Ten-Point Test," *JCAP* **0803** (2008) 022, arXiv:0711.4996 [astro-ph].

[80] A. De Rujula, S. Glashow, and U. Sarid, "CHARGED DARK MATTER," *Nucl.Phys.* **B333** (1990) 173.

[81] S. Dimopoulos, D. Eichler, R. Esmailzadeh, and G. D. Starkman, "Getting a Charge Out of Dark Matter," *Phys.Rev.* **D41** (1990) 2388.

[82] G. D. Starkman, A. Gould, R. Esmailzadeh, and S. Dimopoulos, "Opening the Window on Strongly Interacting Dark Matter," *Phys.Rev.* **D41** (1990) 3594.

[83] S. Davidson, S. Hannestad, and G. Raffelt, "Updated bounds on millicharged particles," *JHEP* **0005** (2000) 003, arXiv:hep-ph/0001179 [hep-ph].

[84] C. El Aisati, T. Hambye, and T. Scarn, "Can a millicharged dark matter particle emit an observable γ-ray line?," *JHEP* **1408** (2014) 133, arXiv:1403.1280 [hep-ph].

[85] **SDSS Collaboration** Collaboration, M. Tegmark *et al.*, "The 3-D power spectrum of galaxies from the SDSS," *Astrophys.J.* **606** (2004) 702–740, arXiv:astro-ph/0310725 [astro-ph].

[86] P. Peebles, "Large scale background temperature and mass fluctuations due to scale invariant primeval perturbations," *Astrophys.J.* **263** (1982) L1–L5.

[87] G. R. Blumenthal, S. Faber, J. R. Primack, and M. J. Rees, "Formation of Galaxies and Large Scale Structure with Cold Dark Matter," *Nature* **311** (1984) 517–525.

[88] J. Sommer-Larsen and A. Dolgov, "Formation of disk galaxies: warm dark matter and the angular momentum problem," *Astrophys.J.* **551** (2001) 608–623, arXiv:astro-ph/9912166 [astro-ph].

[89] P. Bode, J. P. Ostriker, and N. Turok, "Halo formation in warm dark matter models," *Astrophys.J.* **556** (2001) 93–107, arXiv:astro-ph/0010389 [astro-ph].

[90] A. Ibarra, D. Tran, and C. Weniger, "Decaying Dark Matter in Light of the PAMELA and Fermi LAT Data," *JCAP* **1001** (2010) 009, arXiv:0906.1571 [hep-ph].

[91] A. Ibarra and D. Tran, "Decaying Dark Matter and the PAMELA Anomaly," *JCAP* **0902** (2009) 021, arXiv:0811.1555 [hep-ph].

[92] X. Huang, G. Vertongen, and C. Weniger, "Probing Dark Matter Decay and Annihilation with Fermi LAT Observations of Nearby Galaxy Clusters," *JCAP* **1201** (2012) 042, arXiv:1110.1529 [hep-ph].

[93] A. Esmaili, A. Ibarra, and O. L. Peres, "Probing the stability of superheavy dark matter particles with high-energy neutrinos," *JCAP* **1211** (2012) 034, arXiv:1205.5281 [hep-ph].

[94] K. A. Olive, G. Steigman, and T. P. Walker, "Primordial nucleosynthesis: Theory and observations," *Phys.Rept.* **333** (2000) 389–407, arXiv:astro-ph/9905320 [astro-ph].

[95] D. N. Spergel and P. J. Steinhardt, "Observational evidence for selfinteracting cold dark matter," *Phys.Rev.Lett.* **84** (2000) 3760–3763, arXiv:astro-ph/9909386 [astro-ph].

[96] O. Y. Gnedin and J. P. Ostriker, "Destruction of the galactic globular cluster system," *Astrophys.J.* **474** (1997) 223, arXiv:astro-ph/9603042 [astro-ph].

[97] M. Milgrom, "A Modification of the Newtonian dynamics as a possible alternative to the hidden mass hypothesis," *Astrophys.J.* **270** (1983) 365–370.

[98] J. D. Bekenstein, "Relativistic gravitation theory for the MOND paradigm," *Phys.Rev.* **D70** (2004) 083509, arXiv:astro-ph/0403694 [astro-ph].

[99] C. Skordis, D. Mota, P. Ferreira, and C. Boehm, "Large Scale Structure in Bekenstein's theory of relativistic Modified Newtonian Dynamics," *Phys.Rev.Lett.* **96** (2006) 011301, arXiv:astro-ph/0505519 [astro-ph].

[100] L. Roszkowski, "Particle dark matter: A Theorist's perspective," *Pramana* **62** (2004) 389–401, arXiv:hep-ph/0404052 [hep-ph].

[101] R. Peccei and H. R. Quinn, "CP Conservation in the Presence of Instantons," *Phys.Rev.Lett.* **38** (1977) 1440–1443.

[102] R. Peccei and H. R. Quinn, "Constraints Imposed by CP Conservation in the Presence of Instantons," *Phys.Rev.* **D16** (1977) 1791–1797.

[103] S. Weinberg, "A New Light Boson?," *Phys.Rev.Lett.* **40** (1978) 223–226.

[104] F. Wilczek, "Problem of Strong p and t Invariance in the Presence of Instantons," *Phys.Rev.Lett.* **40** (1978) 279–282.

[105] J. Preskill, M. B. Wise, and F. Wilczek, "Cosmology of the Invisible Axion," *Phys.Lett.* **B120** (1983) 127–132.

[106] H.-Y. Cheng, "The Strong CP Problem Revisited," *Phys.Rept.* **158** (1988) 1.

[107] J. E. Kim, "Light Pseudoscalars, Particle Physics and Cosmology," *Phys.Rept.* **150** (1987) 1–177.

[108] M. S. Turner, "Windows on the Axion," *Phys.Rept.* **197** (1990) 67–97.

[109] L. D. Duffy and K. van Bibber, "Axions as Dark Matter Particles," *New J.Phys.* **11** (2009) 105008, arXiv:0904.3346 [hep-ph].

[110] S. P. Martin, "A Supersymmetry primer," *Adv.Ser.Direct.High Energy Phys.* **21** (2010) 1–153, arXiv:hep-ph/9709356 [hep-ph].

[111] H. Pagels and J. R. Primack, "Supersymmetry, Cosmology and New TeV Physics," *Phys.Rev.Lett.* **48** (1982) 223.

[112] A. Ibarra and D. Tran, "Antimatter Signatures of Gravitino Dark Matter Decay," *JCAP* **0807** (2008) 002, arXiv:0804.4596 [astro-ph].

[113] A. Ibarra and D. Tran, "Gamma Ray Spectrum from Gravitino Dark Matter Decay," *Phys.Rev.Lett.* **100** (2008) 061301, arXiv:0709.4593 [astro-ph].

[114] L. Covi, M. Grefe, A. Ibarra, and D. Tran, "Unstable Gravitino Dark Matter and Neutrino Flux," *JCAP* **0901** (2009) 029, arXiv:0809.5030 [hep-ph].

[115] D. Gorbunov, A. Khmelnitsky, and V. Rubakov, "Is gravitino still a warm dark matter candidate?," *JHEP* **0812** (2008) 055, arXiv:0805.2836 [hep-ph].

[116] M. Fujii, M. Ibe, and T. Yanagida, "Upper bound on gluino mass from thermal leptogenesis," *Phys.Lett.* **B579** (2004) 6–12, arXiv:hep-ph/0310142 [hep-ph].

[117] M. Bolz, W. Buchmuller, and M. Plumacher, "Baryon asymmetry and dark matter," *Phys.Lett.* **B443** (1998) 209–213, arXiv:hep-ph/9809381 [hep-ph].

[118] G. Steigman and M. S. Turner, "Cosmological Constraints on the Properties of Weakly Interacting Massive Particles," *Nucl.Phys.* **B253** (1985) 375.

[119] G. Bertone, D. Hooper, and J. Silk, "Particle dark matter: Evidence, candidates and constraints," *Phys.Rept.* **405** (2005) 279–390, arXiv:hep-ph/0404175 [hep-ph].

[120] K. Griest and M. Kamionkowski, "Unitarity Limits on the Mass and Radius of Dark Matter Particles," *Phys.Rev.Lett.* **64** (1990) 615.

[121] K. Schmitz, "The B-L Phase Transition: Implications for Cosmology and Neutrinos, (PhD thesis)," arXiv:1307.3887.

[122] M. S. Turner, "Coherent Scalar Field Oscillations in an Expanding Universe," *Phys.Rev.* **D28** (1983) 1243.

[123] H. Baer, K.-Y. Choi, J. E. Kim, and L. Roszkowski, "Non-thermal dark matter: supersymmetric axions and other candidates," arXiv:1407.0017 [hep-ph].

[124] X. Chu, T. Hambye, and M. H. Tytgat, "The Four Basic Ways of Creating Dark Matter Through a Portal," *JCAP* **1205** (2012) 034, arXiv:1112.0493 [hep-ph].

[125] M. Srednicki, R. Watkins, and K. A. Olive, "Calculations of Relic Densities in the Early Universe," *Nucl.Phys.* **B310** (1988) 693.

[126] P. Gondolo and G. Gelmini, "Cosmic abundances of stable particles: Improved analysis," *Nucl.Phys.* **B360** (1991) 145–179.

[127] B. Patt and F. Wilczek, "Higgs-field portal into hidden sectors," arXiv:hep-ph/0605188 [hep-ph].

[128] K. Griest and D. Seckel, "Three exceptions in the calculation of relic abundances," *Phys.Rev.* **D43** (1991) 3191–3203.

[129] J. Edsjo and P. Gondolo, "Neutralino relic density including coannihilations," *Phys.Rev.* **D56** (1997) 1879–1894, arXiv:hep-ph/9704361 [hep-ph].

[130] D. Hooper and S. Profumo, "Dark matter and collider phenomenology of universal extra dimensions," *Phys.Rept.* **453** (2007) 29–115, arXiv:hep-ph/0701197 [hep-ph].

[131] P. Salati, "Quintessence and the relic density of neutralinos," *Phys.Lett.* **B571** (2003) 121–131, arXiv:astro-ph/0207396 [astro-ph].

[132] S. Profumo and P. Ullio, "SUSY dark matter and quintessence," *JCAP* **0311** (2003) 006, arXiv:hep-ph/0309220 [hep-ph].

[133] R. Catena and P. Ullio, "A novel determination of the local dark matter density," *JCAP* **1008** (2010) 004, arXiv:0907.0018 [astro-ph.CO].

[134] J. Lewin and P. Smith, "Review of mathematics, numerical factors, and corrections for dark matter experiments based on elastic nuclear recoil," *Astropart.Phys.* **6** (1996) 87–112.

[135] S. R. Golwala, "Exclusion limits on the WIMP nucleon elastic scattering cross-section from the Cryogenic Dark Matter Search," (PhD thesis) 2000.

[136] **DAMA Collaboration** Collaboration, R. Bernabei *et al.*, "Search for WIMP annual modulation signature: Results from DAMA / NaI-3 and DAMA / NaI-4 and the global combined analysis," *Phys.Lett.* **B480** (2000) 23–31.

[137] **DAMA Collaboration, LIBRA Collaboration** Collaboration, R. Bernabei *et al.*, "New results from DAMA/LIBRA," *Eur.Phys.J.* **C67** (2010) 39–49, arXiv:1002.1028 [astro-ph.GA].

[138] C. Savage, G. Gelmini, P. Gondolo, and K. Freese, "XENON10/100 dark matter constraints in comparison with CoGeNT and DAMA: examining the Leff dependence," *Phys.Rev.* **D83** (2011) 055002, arXiv:1006.0972 [astro-ph.CO].

[139] J. Kopp, T. Schwetz, and J. Zupan, "Global interpretation of direct Dark Matter searches after CDMS-II results," *JCAP* **1002** (2010) 014, arXiv:0912.4264 [hep-ph].

[140] S. Andreas, C. Arina, T. Hambye, F.-S. Ling, and M. H. Tytgat, "A light scalar WIMP through the Higgs portal and CoGeNT," *Phys.Rev.* **D82** (2010) 043522, arXiv:1003.2595 [hep-ph].

[141] P. Belli, R. Bernabei, A. Bottino, F. Donato, N. Fornengo, *et al.*, "Extending the DAMA annual modulation region by inclusion of the uncertainties in the astrophysical velocities," *Phys.Rev.* **D61** (2000) 023512, arXiv:hep-ph/9903501 [hep-ph].

[142] A. M. Green, "Dependence of direct detection signals on the WIMP velocity distribution," *JCAP* **1010** (2010) 034, arXiv:1009.0916 [astro-ph.CO].

[143] P. J. Fox, J. Liu, and N. Weiner, "Integrating Out Astrophysical Uncertainties," *Phys.Rev.* **D83** (2011) 103514, arXiv:1011.1915 [hep-ph].

[144] N. Bozorgnia, G. B. Gelmini, and P. Gondolo, "Channeling in solid Xe, Ar and Ne direct dark matter detectors," *Nucl.Instrum.Meth.* **A654** (2011) 162–169, arXiv:1011.6006 [astro-ph.CO].

[145] R. Gaitskell, "Direct detection of dark matter," *Ann.Rev.Nucl.Part.Sci.* **54** (2004) 315–359.

[146] R. Schnee, "Introduction to dark matter experiments," arXiv:1101.5205 [astro-ph.CO].

[147] **LUX Collaboration** Collaboration, D. Akerib *et al.*, "First results from the LUX dark matter experiment at the Sanford Underground Research Facility," *Phys.Rev.Lett.* **112** (2014) 091303, arXiv:1310.8214 [astro-ph.CO].

[148] **CDMS Collaboration** Collaboration, R. Agnese *et al.*, "Silicon Detector Dark Matter Results from the Final Exposure of CDMS II," *Phys.Rev.Lett.* **111** (2013) 251301, arXiv:1304.4279 [hep-ex].

[149] **CoGeNT collaboration** Collaboration, C. Aalseth *et al.*, "Results from a Search for Light-Mass Dark Matter with a P-type Point Contact Germanium Detector," *Phys.Rev.Lett.* **106** (2011) 131301, arXiv:1002.4703 [astro-ph.CO].

[150] **CDMS-II Collaboration** Collaboration, Z. Ahmed *et al.*, "Dark Matter Search Results from the CDMS II Experiment," *Science* **327** (2010) 1619–1621, arXiv:0912.3592 [astro-ph.CO].

[151] G. Angloher, M. Bauer, I. Bavykina, A. Bento, C. Bucci, *et al.*, "Results from 730 kg days of the CRESST-II Dark Matter Search," *Eur.Phys.J.* **C72** (2012) 1971, arXiv:1109.0702 [astro-ph.CO].

[152] E. Del Nobile, G. B. Gelmini, P. Gondolo, and J.-H. Huh, "Update on Light WIMP Limits: LUX, lite and Light," *JCAP* **1403** (2014) 014, arXiv:1311.4247 [hep-ph].

[153] **CRESST-II Collaboration** Collaboration, G. Angloher *et al.*, "Results on low mass WIMPs using an upgraded CRESST-II detector," arXiv:1407.3146 [astro-ph.CO].

[154] P. Cushman, C. Galbiati, D. McKinsey, H. Robertson, T. Tait, *et al.*, "Working Group Report: WIMP Dark Matter Direct Detection," arXiv:1310.8327 [hep-ex].

[155] P. Coloma, P. Huber, and J. M. Link, "Combining dark matter detectors and electron-capture sources to hunt for new physics in the neutrino sector," arXiv:1406.4914 [hep-ph].

[156] R. Gaitskell and D. M. (LUX Collaboration), "First results from the LUX dark matter search at SURF,". http://luxdarkmatter.org/talks/20131030_LUX_First_Results.pdf.

[157] J. Billard, L. Strigari, and E. Figueroa-Feliciano, "Implication of neutrino backgrounds on the reach of next generation dark matter direct detection experiments," *Phys.Rev.* **D89** (2014) 023524, arXiv:1307.5458 [hep-ph].

[158] A. Askew, S. Chauhan, B. Penning, W. Shepherd, and M. Tripathi, "Searching for Dark Matter at Hadron Colliders," *Int.J.Mod.Phys.* **A29** (2014) 1430041, arXiv:1406.5662 [hep-ph].

[159] A. Djouadi, O. Lebedev, Y. Mambrini, and J. Quevillon, "Implications of LHC searches for Higgs–portal dark matter," *Phys.Lett.* **B709** (2012) 65–69, arXiv:1112.3299 [hep-ph].

[160] G. Belanger, B. Dumont, U. Ellwanger, J. Gunion, and S. Kraml, "Status of invisible Higgs decays," *Phys.Lett.* **B723** (2013) 340–347, arXiv:1302.5694 [hep-ph].

[161] J. Goodman, M. Ibe, A. Rajaraman, W. Shepherd, T. M. Tait, *et al.*, "Constraints on Light Majorana dark Matter from Colliders," *Phys.Lett.* **B695** (2011) 185–188, arXiv:1005.1286 [hep-ph].

[162] E. Masso, "An Effective Guide to Beyond the Standard Model Physics," arXiv:1406.6376 [hep-ph].

[163] P. J. Fox, R. Harnik, J. Kopp, and Y. Tsai, "LEP Shines Light on Dark Matter," *Phys.Rev.* **D84** (2011) 014028, arXiv:1103.0240 [hep-ph].

[164] Y. Bai, P. J. Fox, and R. Harnik, "The Tevatron at the Frontier of Dark Matter Direct Detection," *JHEP* **1012** (2010) 048, arXiv:1005.3797 [hep-ph].

[165] P. J. Fox, R. Harnik, J. Kopp, and Y. Tsai, "Missing Energy Signatures of Dark Matter at the LHC," *Phys.Rev.* **D85** (2012) 056011, arXiv:1109.4398 [hep-ph].

[166] Y. Cui, L. Randall, and B. Shuve, "A WIMPy Baryogenesis Miracle," *JHEP* **1204** (2012) 075, arXiv:1112.2704 [hep-ph].

[167] S. Davidson and M. Elmer, "Similar Dark Matter and Baryon abundances with TeV-scale Leptogenesis," *JHEP* **1210** (2012) 148, arXiv:1208.0551 [hep-ph].

[168] J. McDonald, "Baryomorphosis: Relating the Baryon Asymmetry to the 'WIMP Miracle'," *Phys.Rev.* **D83** (2011) 083509, arXiv:1009.3227 [hep-ph].

[169] Y. Cui and R. Sundrum, "Baryogenesis for weakly interacting massive particles," *Phys.Rev.* **D87** no. 11, (2013) 116013, arXiv:1212.2973 [hep-ph].

[170] A. Sakharov, "Violation of CP Invariance, c Asymmetry, and Baryon Asymmetry of the Universe," *Pisma Zh.Eksp.Teor.Fiz.* **5** (1967) 32–35.

[171] N. Bernal, F.-X. Josse-Michaux, and L. Ubaldi, "Phenomenology of WIMPy baryogenesis models," *JCAP* **1301** (2013) 034, arXiv:1210.0094 [hep-ph].

[172] N. Bernal, S. Colucci, F.-X. Josse-Michaux, J. Racker, and L. Ubaldi, "On baryogenesis from dark matter annihilation," *JCAP* **1310** (2013) 035, arXiv:1307.6878.

[173] S. Nussinov, "TECHNOCOSMOLOGY: COULD A TECHNIBARYON EXCESS PROVIDE A 'NATURAL' MISSING MASS CANDIDATE?," *Phys.Lett.* **B165** (1985) 55.

[174] S. M. Barr, R. S. Chivukula, and E. Farhi, "Electroweak Fermion Number Violation and the Production of Stable Particles in the Early Universe," *Phys.Lett.* **B241** (1990) 387–391.

[175] S. M. Barr, "Baryogenesis, sphalerons and the cogeneration of dark matter," *Phys.Rev.* **D44** (1991) 3062–3066.

[176] V. A. Kuzmin, "A Simultaneous solution to baryogenesis and dark matter problems," *Phys.Part.Nucl.* **29** (1998) 257–265, arXiv:hep-ph/9701269 [hep-ph].

[177] D. Hooper, J. March-Russell, and S. M. West, "Asymmetric sneutrino dark matter and the Omega(b) / Omega(DM) puzzle," *Phys.Lett.* **B605** (2005) 228–236, arXiv:hep-ph/0410114 [hep-ph].

[178] G. R. Farrar and G. Zaharijas, "Dark matter and the baryon asymmetry of the universe," arXiv:hep-ph/0406281 [hep-ph].

[179] R. Kitano and I. Low, "Dark matter from baryon asymmetry," *Phys.Rev.* **D71** (2005) 023510, arXiv:hep-ph/0411133 [hep-ph].

[180] D. E. Kaplan, M. A. Luty, and K. M. Zurek, "Asymmetric Dark Matter," *Phys.Rev.* **D79** (2009) 115016, arXiv:0901.4117 [hep-ph].

[181] F. Sannino, "Conformal Dynamics for TeV Physics and Cosmology," *Acta Phys.Polon.* **B40** (2009) 3533–3743, arXiv:0911.0931 [hep-ph].

[182] K. Petraki and R. R. Volkas, "Review of asymmetric dark matter," *Int.J.Mod.Phys.* **A28** (2013) 1330028, arXiv:1305.4939 [hep-ph].

[183] K. M. Zurek, "Asymmetric Dark Matter: Theories, Signatures, and Constraints," *Phys.Rept.* **537** (2014) 91–121, arXiv:1308.0338 [hep-ph].

[184] R. Foot and R. Volkas, "Explaining Omega(Baryon) approximately 0.2 Omega(Dark) through the synthesis of ordinary matter from mirror matter: A More general analysis," *Phys.Rev.* **D69** (2004) 123510, arXiv:hep-ph/0402267 [hep-ph].

[185] H. Hodges, "Mirror baryons as the dark matter," *Phys.Rev.* **D47** (1993) 456–459.

[186] R. Mohapatra and V. Teplitz, "Mirror dark matter," arXiv:astro-ph/0004046 [astro-ph].

[187] Y. Bai and P. Schwaller, "The Scale of Dark QCD," *Phys.Rev.* **D89** (2014) 063522, arXiv:1306.4676 [hep-ph].

[188] M. L. Graesser, I. M. Shoemaker, and L. Vecchi, "Asymmetric WIMP dark matter," *JHEP* **1110** (2011) 110, arXiv:1103.2771 [hep-ph].

[189] H. Davoudiasl, D. E. Morrissey, K. Sigurdson, and S. Tulin, "Hylogenesis: A Unified Origin for Baryonic Visible Matter and Antibaryonic Dark Matter," *Phys.Rev.Lett.* **105** (2010) 211304, arXiv:1008.2399 [hep-ph].

[190] I. Affleck and M. Dine, "A New Mechanism for Baryogenesis," *Nucl.Phys.* **B249** (1985) 361.

[191] R. Allahverdi and A. Mazumdar, "A mini review on Affleck-Dine baryogenesis," *New J.Phys.* **14** (2012) 125013.

[192] N. F. Bell, K. Petraki, I. M. Shoemaker, and R. R. Volkas, "Pangenesis in a Baryon-Symmetric Universe: Dark and Visible Matter via the Affleck-Dine Mechanism," *Phys.Rev.* **D84** (2011) 123505, arXiv:1105.3730 [hep-ph].

[193] C. Cheung and K. M. Zurek, "Affleck-Dine Cogenesis," *Phys.Rev.* **D84** (2011) 035007, arXiv:1105.4612 [hep-ph].

[194] B. von Harling, K. Petraki, and R. R. Volkas, "Affleck-Dine dynamics and the dark sector of pangenesis," *JCAP* **1205** (2012) 021, arXiv:1201.2200 [hep-ph].

[195] L. Roszkowski and O. Seto, "Axino dark matter from Q-balls in Affleck-Dine baryogenesis and the Omega(b) - Omega(DM) coincidence problem," *Phys.Rev.Lett.* **98** (2007) 161304, arXiv:hep-ph/0608013 [hep-ph].

[196] N. Cosme, L. Lopez Honorez, and M. H. Tytgat, "Leptogenesis and dark matter related?," *Phys.Rev.* **D72** (2005) 043505, arXiv:hep-ph/0506320 [hep-ph].

[197] E. K. Akhmedov, "Neutrino physics," arXiv:hep-ph/0001264 [hep-ph].

[198] W. Grimus, "Neutrino physics - Theory," *Lect.Notes Phys.* **629** (2004) 169–214, arXiv:hep-ph/0307149 [hep-ph].

[199] W. Grimus, "Neutrino Physics - Models for Neutrino Masses and Lepton Mixing," *PoS* **P2GC** (2006) 001, arXiv:hep-ph/0612311 [hep-ph].

[200] A. Zee, "Quantum field theory in a nutshell,".

[201] S. Weinberg, "Baryon and Lepton Nonconserving Processes," *Phys.Rev.Lett.* **43** (1979) 1566–1570.

[202] Z. Maki, M. Nakagawa, and S. Sakata, "Remarks on the unified model of elementary particles," *Prog.Theor.Phys.* **28** (1962) 870–880.

[203] D. Forero, M. Tortola, and J. Valle, "Neutrino oscillations refitted," *Phys.Rev.D (in press)* (2014) , arXiv:1405.7540 [hep-ph].

[204] **Super-Kamiokande Collaboration** Collaboration, S. Fukuda *et al.*, "Solar B-8 and hep neutrino measurements from 1258 days of Super-Kamiokande data," *Phys.Rev.Lett.* **86** (2001) 5651–5655, arXiv:hep-ex/0103032 [hep-ex].

[205] **SNO Collaboration** Collaboration, Q. Ahmad *et al.*, "Direct evidence for neutrino flavor transformation from neutral current interactions in the Sudbury Neutrino Observatory," *Phys.Rev.Lett.* **89** (2002) 011301, arXiv:nucl-ex/0204008 [nucl-ex].

[206] **Borexino Collaboration** Collaboration, C. Arpesella *et al.*, "Direct Measurement of the Be-7 Solar Neutrino Flux with 192 Days of Borexino Data," *Phys.Rev.Lett.* **101** (2008) 091302, arXiv:0805.3843 [astro-ph].

[207] **KamLAND Collaboration** Collaboration, K. Eguchi *et al.*, "First results from KamLAND: Evidence for reactor anti-neutrino disappearance," *Phys.Rev.Lett.* **90** (2003) 021802, arXiv:hep-ex/0212021 [hep-ex].

[208] **Super-Kamiokande Collaboration** Collaboration, S. Fukuda *et al.*, "Tau neutrinos favored over sterile neutrinos in atmospheric muon-neutrino oscillations," *Phys.Rev.Lett.* **85** (2000) 3999–4003, arXiv:hep-ex/0009001 [hep-ex].

[209] **MINOS Collaboration** Collaboration, D. Michael *et al.*, "Observation of muon neutrino disappearance with the MINOS detectors and the NuMI neutrino beam," *Phys.Rev.Lett.* **97** (2006) 191801, arXiv:hep-ex/0607088 [hep-ex].

[210] **T2K Collaboration** Collaboration, K. Abe *et al.*, "First Muon-Neutrino Disappearance Study with an Off-Axis Beam," *Phys.Rev.* **D85** (2012) 031103, arXiv:1201.1386 [hep-ex].

[211] **DOUBLE-CHOOZ Collaboration** Collaboration, Y. Abe *et al.*, "Indication for the disappearance of reactor electron antineutrinos in the Double Chooz experiment," *Phys.Rev.Lett.* **108** (2012) 131801, arXiv:1112.6353 [hep-ex].

[212] **DAYA-BAY Collaboration** Collaboration, F. An *et al.*, "Observation of electron-antineutrino disappearance at Daya Bay," *Phys.Rev.Lett.* **108** (2012) 171803, arXiv:1203.1669 [hep-ex].

[213] **RENO collaboration** Collaboration, J. Ahn *et al.*, "Observation of Reactor Electron Antineutrino Disappearance in the RENO Experiment," *Phys.Rev.Lett.* **108** (2012) 191802, arXiv:1204.0626 [hep-ex].

[214] F. Capozzi, G. Fogli, E. Lisi, A. Marrone, D. Montanino, *et al.*, "Status of three-neutrino oscillation parameters, circa 2013," *Phys.Rev.* **D89** (2014) 093018, arXiv:1312.2878 [hep-ph].

[215] M. Gonzalez-Garcia, M. Maltoni, and T. Schwetz, "Updated fit to three neutrino mixing: status of leptonic CP violation," arXiv:1409.5439 [hep-ph].

[216] **Particle Data Group** Collaboration, J. Beringer *et al.*, "Review of Particle Physics (RPP)," *Phys.Rev.* **D86** (2012) 010001.

[217] **EXO Collaboration** Collaboration, M. Auger *et al.*, "Search for Neutrinoless Double-Beta Decay in ^{136}Xe with EXO-200," *Phys.Rev.Lett.* **109** (2012) 032505, arXiv:1205.5608 [hep-ex].

[218] J. Lesgourgues and S. Pastor, "Neutrino cosmology and Planck," *New J.Phys.* **16** (2014) 065002, arXiv:1404.1740 [hep-ph].

[219] J. Lesgourgues, G. Mangano, G. Miele, and S. Pastor, "Neutrino Cosmology," Cambridge University Press, 2013.

[220] P. Harrison, D. Perkins, and W. Scott, "Tri-bimaximal mixing and the neutrino oscillation data," *Phys.Lett.* **B530** (2002) 167, arXiv:hep-ph/0202074 [hep-ph].

[221] L. Wolfenstein, "Oscillations Among Three Neutrino Types and CP Violation," *Phys.Rev.* **D18** (1978) 958–960.

[222] V. D. Barger, S. Pakvasa, T. J. Weiler, and K. Whisnant, "Bimaximal mixing of three neutrinos," *Phys.Lett.* **B437** (1998) 107–116, arXiv:hep-ph/9806387 [hep-ph].

[223] K. Babu, E. Ma, and J. Valle, "Underlying A(4) symmetry for the neutrino mass matrix and the quark mixing matrix," *Phys.Lett.* **B552** (2003) 207–213, arXiv:hep-ph/0206292 [hep-ph].

[224] G. Altarelli and F. Feruglio, "Tri-bimaximal neutrino mixing from discrete symmetry in extra dimensions," *Nucl.Phys.* **B720** (2005) 64–88, arXiv:hep-ph/0504165 [hep-ph].

[225] G. Altarelli, F. Feruglio, and L. Merlo, "Tri-Bimaximal Neutrino Mixing and Discrete Flavour Symmetries," *Fortsch.Phys.* **61** (2013) 507–534, arXiv:1205.5133 [hep-ph].

[226] S. F. King and C. Luhn, "Neutrino Mass and Mixing with Discrete Symmetry," *Rept.Prog.Phys.* **76** (2013) 056201, arXiv:1301.1340 [hep-ph].

[227] S. F. King, A. Merle, S. Morisi, Y. Shimizu, and M. Tanimoto, "Neutrino Mass and Mixing: from Theory to Experiment," *New J.Phys.* **16** (2014) 045018, arXiv:1402.4271 [hep-ph].

[228] G. Altarelli, F. Feruglio, and L. Merlo, "Revisiting Bimaximal Neutrino Mixing in a Model with S(4) Discrete Symmetry," *JHEP* **0905** (2009) 020, arXiv:0903.1940 [hep-ph].

[229] S. King, "Tri-bimaximal-Cabibbo Mixing," *Phys.Lett.* **B718** (2012) 136–142, arXiv:1205.0506 [hep-ph].

[230] C. H. Albright, A. Dueck, and W. Rodejohann, "Possible Alternatives to Tri-bimaximal Mixing," *Eur.Phys.J.* **C70** (2010) 1099–1110, arXiv:1004.2798 [hep-ph].

[231] D. Forero, M. Tortola, and J. Valle, "Global status of neutrino oscillation parameters after Neutrino-2012," *Phys.Rev.* **D86** (2012) 073012, arXiv:1205.4018 [hep-ph].

[232] G. Fogli, E. Lisi, A. Marrone, D. Montanino, A. Palazzo, *et al.*, "Global analysis of neutrino masses, mixings and phases: entering the era of leptonic CP violation searches," *Phys.Rev.* **D86** (2012) 013012, arXiv:1205.5254 [hep-ph].

[233] S. Antusch, C. Gross, V. Maurer, and C. Sluka, "$\theta_{13}^{PMNS} = \theta_C/\sqrt{2}$ from GUTs," *Nucl.Phys.* **B866** (2013) 255–269, arXiv:1205.1051 [hep-ph].

[234] C. Froggatt and H. B. Nielsen, "Hierarchy of Quark Masses, Cabibbo Angles and CP Violation," *Nucl.Phys.* **B147** (1979) 277.

[235] G.-J. Ding, S. Morisi, and J. Valle, "Bilarge neutrino mixing and Abelian flavor symmetry," *Phys.Rev.* **D87** no. 5, (2013) 053013, arXiv:1211.6506 [hep-ph].

[236] A. de Gouvea and J. Valle, "Minimalistic neutrino mass model," *Phys.Lett.* **B501** (2001) 115–127, arXiv:hep-ph/0010299 [hep-ph].

[237] L. J. Hall, H. Murayama, and N. Weiner, "Neutrino mass anarchy," *Phys.Rev.Lett.* **84** (2000) 2572–2575, arXiv:hep-ph/9911341 [hep-ph].

[238] A. de Gouvea and H. Murayama, "Neutrino Mixing Anarchy: Alive and Kicking," arXiv:1204.1249 [hep-ph].

[239] G. Altarelli, F. Feruglio, and I. Masina, "Models of neutrino masses: Anarchy versus hierarchy," *JHEP* **0301** (2003) 035, arXiv:hep-ph/0210342 [hep-ph].

[240] G. Altarelli, F. Feruglio, I. Masina, and L. Merlo, "Repressing Anarchy in Neutrino Mass Textures," *JHEP* **1211** (2012) 139, arXiv:1207.0587 [hep-ph].

[241] S. F. King, C. Luhn, and A. J. Stuart, "A Grand Delta(96) x SU(5) Flavour Model," *Nucl.Phys.* **B867** (2013) 203–235, arXiv:1207.5741 [hep-ph].

[242] R. M. Fonseca and W. Grimus, "Classification of lepton mixing matrices from finite residual symmetries," *JHEP* **1409** (2014) 033, arXiv:1405.3678 [hep-ph].

[243] V. Bouchard, J. J. Heckman, J. Seo, and C. Vafa, "F-theory and Neutrinos: Kaluza-Klein Dilution of Flavor Hierarchy," *JHEP* **1001** (2010) 061, arXiv:0904.1419 [hep-ph].

[244] F. Bonnet, M. Hirsch, T. Ota, and W. Winter, "Systematic decomposition of the neutrinoless double beta decay operator," *JHEP* **1303** (2013) 055, arXiv:1212.3045 [hep-ph].

[245] F. Bonnet, M. Hirsch, T. Ota, and W. Winter, "Systematic study of the d=5 Weinberg operator at one-loop order," *JHEP* **1207** (2012) 153, arXiv:1204.5862 [hep-ph].

[246] A. de Gouvea and J. Jenkins, "A Survey of Lepton Number Violation Via Effective Operators," *Phys.Rev.* **D77** (2008) 013008, arXiv:0708.1344 [hep-ph].

[247] F. Bonnet, D. Hernandez, T. Ota, and W. Winter, "Neutrino masses from higher than d=5 effective operators," *JHEP* **0910** (2009) 076, arXiv:0907.3143 [hep-ph].

[248] M. B. Krauss, D. Meloni, W. Porod, and W. Winter, "Neutrino Mass from a d=7 Effective Operator in an SU(5) SUSY-GUT Framework," *JHEP* **1305** (2013) 121, arXiv:1301.4221 [hep-ph].

[249] E. Ma, "Pathways to naturally small neutrino masses," *Phys.Rev.Lett.* **81** (1998) 1171–1174, arXiv:hep-ph/9805219 [hep-ph].

[250] P. Minkowski, "$\mu \to e\gamma$ at a Rate of One Out of 1-Billion Muon Decays?," *Phys.Lett.* **B67** (1977) 421.

[251] T. Yanagida, "HORIZONTAL SYMMETRY AND MASSES OF NEUTRINOS," *Conf.Proc.* **C7902131** (1979) 95–99.

[252] M. Gell-Mann, P. Ramond, and R. Slansky, "Complex Spinors and Unified Theories," *Conf.Proc.* **C790927** (1979) 315–321, arXiv:1306.4669 [hep-th].

[253] J. Schechter and J. Valle, "Neutrino Masses in SU(2) x U(1) Theories," *Phys.Rev.* **D22** (1980) 2227.

[254] R. N. Mohapatra and G. Senjanovic, "Neutrino Mass and Spontaneous Parity Violation," *Phys.Rev.Lett.* **44** (1980) 912.

[255] J. Schechter and J. Valle, "Neutrino Decay and Spontaneous Violation of Lepton Number," *Phys.Rev.* **D25** (1982) 774.

[256] **DELPHI Collaboration** Collaboration, P. Abreu *et al.*, "Search for neutral heavy leptons produced in Z decays," *Z.Phys.* **C74** (1997) 57–71.

[257] M. Gonzalez-Garcia and J. Valle, "Fast Decaying Neutrinos and Observable Flavor Violation in a New Class of Majoron Models," *Phys.Lett.* **B216** (1989) 360.

[258] A. Ibarra, E. Molinaro, and S. Petcov, "Low Energy Signatures of the TeV Scale See-Saw Mechanism," *Phys.Rev.* **D84** (2011) 013005, arXiv:1103.6217 [hep-ph].

[259] T. Cheng and L.-F. Li, "Neutrino Masses, Mixings and Oscillations in SU(2) x U(1) Models of Electroweak Interactions," *Phys.Rev.* **D22** (1980) 2860.

[260] M. Magg and C. Wetterich, "Neutrino Mass Problem and Gauge Hierarchy," *Phys.Lett.* **B94** (1980) 61.

[261] C. Wetterich, "Neutrino Masses and the Scale of B-L Violation," *Nucl.Phys.* **B187** (1981) 343.

[262] R. N. Mohapatra and G. Senjanovic, "Neutrino Masses and Mixings in Gauge Models with Spontaneous Parity Violation," *Phys.Rev.* **D23** (1981) 165.

[263] P. Fileviez Perez, T. Han, and T. Li, "Testability of Type I Seesaw at the CERN LHC: Revealing the Existence of the B-L Symmetry," *Phys.Rev.* **D80** (2009) 073015, arXiv:0907.4186 [hep-ph].

[264] D. Aristizabal Sierra, M. Hirsch, J. Valle, and A. Villanova del Moral, "Reconstructing neutrino properties from collider experiments in a Higgs triplet neutrino mass model," *Phys.Rev.* **D68** (2003) 033006, arXiv:hep-ph/0304141 [hep-ph].

[265] J. Esteves, J. Romao, A. Villanova del Moral, M. Hirsch, J. Valle, *et al.*, "Flavour violation at the LHC: type-I versus type-II seesaw in minimal supergravity," *JHEP* **0905** (2009) 003, arXiv:0903.1408 [hep-ph].

[266] R. Foot, H. Lew, X. He, and G. C. Joshi, "Seesaw Neutrino Masses Induced by a Triplet of Leptons," *Z.Phys.* **C44** (1989) 441.

[267] R. Franceschini, T. Hambye, and A. Strumia, "Type-III see-saw at LHC," *Phys.Rev.* **D78** (2008) 033002, arXiv:0805.1613 [hep-ph].

[268] J. Kersten and A. Y. Smirnov, "Right-Handed Neutrinos at CERN LHC and the Mechanism of Neutrino Mass Generation," *Phys.Rev.* **D76** (2007) 073005, arXiv:0705.3221 [hep-ph].

[269] P.-H. Gu, M. Hirsch, U. Sarkar, and J. Valle, "Neutrino masses, leptogenesis and dark matter in hybrid seesaw," *Phys.Rev.* **D79** (2009) 033010, arXiv:0811.0953 [hep-ph].

[270] P. S. B. Dev, A. Pilaftsis, and U.-k. Yang, "New Production Mechanism for Heavy Neutrinos at the LHC," *Phys.Rev.Lett.* **112** (2014) 081801, arXiv:1308.2209 [hep-ph].

[271] R. Mohapatra and J. Valle, "Neutrino Mass and Baryon Number Nonconservation in Superstring Models," *Phys.Rev.* **D34** (1986) 1642.

[272] E. K. Akhmedov, M. Lindner, E. Schnapka, and J. Valle, "Left-right symmetry breaking in NJL approach," *Phys.Lett.* **B368** (1996) 270–280, arXiv:hep-ph/9507275 [hep-ph].

[273] E. K. Akhmedov, M. Lindner, E. Schnapka, and J. Valle, "Dynamical left-right symmetry breaking," *Phys.Rev.* **D53** (1996) 2752–2780, arXiv:hep-ph/9509255 [hep-ph].

[274] M. Malinsky, J. Romao, and J. Valle, "Novel supersymmetric SO(10) seesaw mechanism," *Phys.Rev.Lett.* **95** (2005) 161801, arXiv:hep-ph/0506296 [hep-ph].

[275] J. Bernabeu, A. Santamaria, J. Vidal, A. Mendez, and J. Valle, "Lepton Flavor Nonconservation at High-Energies in a Superstring Inspired Standard Model," *Phys.Lett.* **B187** (1987) 303.

[276] M. Gonzalez-Garcia and J. Valle, "Enhanced lepton flavor violation with massless neutrinos: A Study of muon and tau decays," *Mod.Phys.Lett.* **A7** (1992) 477–488.

[277] G. Branco, M. Rebelo, and J. Valle, "Leptonic CP Violation With Massless Neutrinos," *Phys.Lett.* **B225** (1989) 385.

[278] N. Rius and J. Valle, "Leptonic CP Violating Asymmetries in Z^0 Decays," *Phys.Lett.* **B246** (1990) 249–255.

[279] F. Bazzocchi, D. Cerdeno, C. Munoz, and J. Valle, "Calculable inverse-seesaw neutrino masses in supersymmetry," *Phys.Rev.* **D81** (2010) 051701, arXiv:0907.1262 [hep-ph].

[280] F. Bazzocchi, "Minimal Dynamical Inverse See Saw," *Phys.Rev.* **D83** (2011) 093009, arXiv:1011.6299 [hep-ph].

[281] H. Hettmansperger, M. Lindner, and W. Rodejohann, "Phenomenological Consequences of sub-leading Terms in See-Saw Formulas," *JHEP* **1104** (2011) 123, arXiv:1102.3432 [hep-ph].

[282] D. Forero, S. Morisi, M. Tortola, and J. Valle, "Lepton flavor violation and non-unitary lepton mixing in low-scale type-I seesaw," *JHEP* **1109** (2011) 142, arXiv:1107.6009 [hep-ph].

[283] A. Das and N. Okada, "Inverse seesaw neutrino signatures at the LHC and ILC," *Phys.Rev.* **D88** no. 11, (2013) 113001, arXiv:1207.3734 [hep-ph].

[284] K. Babu and C. N. Leung, "Classification of effective neutrino mass operators," *Nucl.Phys.* **B619** (2001) 667–689, arXiv:hep-ph/0106054 [hep-ph].

[285] A. de Gouvea and J. Jenkins, "A Survey of Lepton Number Violation Via Effective Operators," *Phys.Rev.* **D77** (2008) 013008, arXiv:0708.1344 [hep-ph].

[286] P. W. Angel, N. L. Rodd, and R. R. Volkas, "Origin of neutrino masses at the LHC: $\Delta L = 2$ effective operators and their ultraviolet completions," *Phys.Rev.* **D87** no. 7, (2013) 073007, arXiv:1212.6111 [hep-ph].

[287] Y. Farzan, S. Pascoli, and M. A. Schmidt, "Recipes and Ingredients for Neutrino Mass at Loop Level," *JHEP* **1303** (2013) 107, arXiv:1208.2732 [hep-ph].

[288] S. S. Law and K. L. McDonald, "The simplest models of radiative neutrino mass," *Int.J.Mod.Phys.* **A29** (2014) 1450064, arXiv:1303.6384 [hep-ph].

[289] A. Pilaftsis, "Radiatively induced neutrino masses and large Higgs neutrino couplings in the standard model with Majorana fields," *Z.Phys.* **C55** (1992) 275–282, arXiv:hep-ph/9901206 [hep-ph].

[290] P. B. Dev and A. Pilaftsis, "Minimal Radiative Neutrino Mass Mechanism for Inverse Seesaw Models," *Phys.Rev.* **D86** (2012) 113001, arXiv:1209.4051 [hep-ph].

[291] P. Fileviez Perez and M. B. Wise, "On the Origin of Neutrino Masses," *Phys.Rev.* **D80** (2009) 053006, arXiv:0906.2950 [hep-ph].

[292] A. Zee, "A Theory of Lepton Number Violation, Neutrino Majorana Mass, and Oscillation," *Phys.Lett.* **B93** (1980) 389.

[293] D. Aristizabal Sierra and D. Restrepo, "Leptonic Charged Higgs Decays in the Zee Model," *JHEP* **0608** (2006) 036, `arXiv:hep-ph/0604012 [hep-ph]`.

[294] A. Y. Smirnov and M. Tanimoto, "Is Zee model the model of neutrino masses?," *Phys.Rev.* **D55** (1997) 1665–1671, `arXiv:hep-ph/9604370 [hep-ph]`.

[295] C. Jarlskog, M. Matsuda, S. Skadhauge, and M. Tanimoto, "Zee mass matrix and bimaximal neutrino mixing," *Phys.Lett.* **B449** (1999) 240, `arXiv:hep-ph/9812282 [hep-ph]`.

[296] P. H. Frampton and S. L. Glashow, "Can the Zee ansatz for neutrino masses be correct?," *Phys.Lett.* **B461** (1999) 95–98, `arXiv:hep-ph/9906375 [hep-ph]`.

[297] A. S. Joshipura and S. D. Rindani, "Neutrino anomalies in an extended Zee model," *Phys.Lett.* **B464** (1999) 239–243, `arXiv:hep-ph/9907390 [hep-ph]`.

[298] G. McLaughlin and J. Ng, "Singlet interacting neutrinos in the extended Zee model and solar neutrino transformation," *Phys.Lett.* **B464** (1999) 232–238, `arXiv:hep-ph/9907449 [hep-ph]`.

[299] K.-m. Cheung and O. C. Kong, "Zee neutrino mass model in SUSY framework," *Phys.Rev.* **D61** (2000) 113012, `arXiv:hep-ph/9912238 [hep-ph]`.

[300] D. Chang and A. Zee, "Radiatively induced neutrino Majorana masses and oscillation," *Phys.Rev.* **D61** (2000) 071303, `arXiv:hep-ph/9912380 [hep-ph]`.

[301] D. A. Dicus, H.-J. He, and J. N. Ng, "Neutrino - lepton masses, Zee scalars and muon g-2," *Phys.Rev.Lett.* **87** (2001) 111803, `arXiv:hep-ph/0103126 [hep-ph]`.

[302] K. Balaji, W. Grimus, and T. Schwetz, "The Solar LMA neutrino oscillation solution in the Zee model," *Phys.Lett.* **B508** (2001) 301–310, `arXiv:hep-ph/0104035 [hep-ph]`.

[303] E. Mitsuda and K. Sasaki, "Zee model and phenomenology of lepton sector," *Phys.Lett.* **B516** (2001) 47–53.

[304] A. Ghosal, Y. Koide, and H. Fusaoka, "Lepton flavor violating Z decays in the Zee model," *Phys.Rev.* **D64** (2001) 053012, arXiv:hep-ph/0104104 [hep-ph].

[305] Y. Koide, "Can the Zee model explain the observed neutrino data?," *Phys.Rev.* **D64** (2001) 077301, arXiv:hep-ph/0104226 [hep-ph].

[306] B. Brahmachari and S. Choubey, "Viability of bimaximal solution of the Zee mass matrix," *Phys.Lett.* **B531** (2002) 99–104, arXiv:hep-ph/0111133 [hep-ph].

[307] T. Kitabayashi and M. Yasue, "Large solar neutrino mixing in an extended Zee model," *Int.J.Mod.Phys.* **A17** (2002) 2519–2534, arXiv:hep-ph/0112287 [hep-ph].

[308] Y. Koide, "Prospect of the Zee model," *Nucl.Phys.Proc.Suppl.* **111** (2002) 294–296, arXiv:hep-ph/0201250 [hep-ph].

[309] M.-Y. Cheng and K.-m. Cheung, "Zee model and neutrinoless double beta decay," arXiv:hep-ph/0203051 [hep-ph].

[310] X. G. He and A. Zee, "Some simple mixing and mass matrices for neutrinos," *Phys.Lett.* **B560** (2003) 87–90, arXiv:hep-ph/0301092 [hep-ph].

[311] K. Hasegawa, C. Lim, and K. Ogure, "Escape from washing out of baryon number in a two zero texture general Zee model compatible with the LMA-MSW solution," *Phys.Rev.* **D68** (2003) 053006, arXiv:hep-ph/0303252 [hep-ph].

[312] S. Kanemura, T. Ota, and K. Tsumura, "Lepton flavor violation in Higgs boson decays under the rare tau decay results," *Phys.Rev.* **D73** (2006) 016006, arXiv:hep-ph/0505191 [hep-ph].

[313] B. Brahmachari and S. Choubey, "Modified Zee mass matrix with zero-sum condition," *Phys.Lett.* **B642** (2006) 495–502, arXiv:hep-ph/0608089 [hep-ph].

[314] N. Sahu and U. Sarkar, "Extended Zee model for Neutrino Mass, Leptogenesis and Sterile Neutrino like Dark Matter," *Phys.Rev.* **D78** (2008) 115013, arXiv:0804.2072 [hep-ph].

[315] T. Fukuyama, H. Sugiyama, and K. Tsumura, "Phenomenology in the Zee Model with the A_4 Symmetry," *Phys.Rev.* **D83** (2011) 056016, arXiv:1012.4886 [hep-ph].

[316] F. del Aguila, A. Aparici, S. Bhattacharya, A. Santamaria, and J. Wudka, "Effective Lagrangian approach to neutrinoless double beta decay and neutrino masses," *JHEP* **1206** (2012) 146, arXiv:1204.5986 [hep-ph].

[317] L. Wolfenstein, "A Theoretical Pattern for Neutrino Oscillations," *Nucl.Phys.* **B175** (1980) 93.

[318] P. H. Frampton, M. C. Oh, and T. Yoshikawa, "Zee model confronts SNO data," *Phys.Rev.* **D65** (2002) 073014, arXiv:hep-ph/0110300 [hep-ph].

[319] X.-G. He, "Is the Zee model neutrino mass matrix ruled out?," *Eur.Phys.J.* **C34** (2004) 371–376, arXiv:hep-ph/0307172 [hep-ph].

[320] S. Kanemura, T. Kasai, G.-L. Lin, Y. Okada, J.-J. Tseng, *et al.*, "Phenomenology of Higgs bosons in the Zee model," *Phys.Rev.* **D64** (2001) 053007, arXiv:hep-ph/0011357 [hep-ph].

[321] K. A. Assamagan, A. Deandrea, and P.-A. Delsart, "Search for the lepton flavor violating decay $A0, H0 \rightarrow \tau \pm \mu^{\pm}$ at hadron colliders," *Phys.Rev.* **D67** (2003) 035001, arXiv:hep-ph/0207302 [hep-ph].

[322] K. Babu and J. Julio, "Predictive Model of Radiative Neutrino Masses," *Phys.Rev.* **D89** no. 5, (2014) 053004, arXiv:1310.0303 [hep-ph].

[323] E. Ma, "Verifiable radiative seesaw mechanism of neutrino mass and dark matter," *Phys.Rev.* **D73** (2006) 077301, arXiv:hep-ph/0601225 [hep-ph].

[324] J. Kubo, E. Ma, and D. Suematsu, "Cold Dark Matter, Radiative Neutrino Mass, $\mu \rightarrow e\gamma$, and Neutrinoless Double Beta Decay," *Phys.Lett.* **B642** (2006) 18–23, arXiv:hep-ph/0604114 [hep-ph].

[325] D. Aristizabal Sierra, J. Kubo, D. Restrepo, D. Suematsu, and O. Zapata, "Radiative seesaw: Warm dark matter, collider and lepton flavour violating signals," *Phys.Rev.* **D79** (2009) 013011, arXiv:0808.3340 [hep-ph].

[326] D. Suematsu, T. Toma, and T. Yoshida, "Reconciliation of CDM abundance and $\mu \rightarrow e\gamma$ in a radiative seesaw model," *Phys.Rev.* **D79** (2009) 093004, arXiv:0903.0287 [hep-ph].

[327] A. Adulpravitchai, M. Lindner, and A. Merle, "Confronting Flavour Symmetries and extended Scalar Sectors with Lepton Flavour Violation Bounds," *Phys.Rev.* **D80** (2009) 055031, arXiv:0907.2147 [hep-ph].

[328] T. Toma and A. Vicente, "Lepton Flavor Violation in the Scotogenic Model," *JHEP* **1401** (2014) 160, arXiv:1312.2840.

[329] D. Schmidt, T. Schwetz, and T. Toma, "Direct Detection of Leptophilic Dark Matter in a Model with Radiative Neutrino Masses," *Phys.Rev.* **D85** (2012) 073009, arXiv:1201.0906 [hep-ph].

[330] R. Bouchand and A. Merle, "Running of Radiative Neutrino Masses: The Scotogenic Model," *JHEP* **1207** (2012) 084, arXiv:1205.0008 [hep-ph].

[331] M. Aoki and S. Kanemura, "Probing the Majorana nature of TeV-scale radiative seesaw models at collider experiments," *Phys.Lett.* **B689** (2010) 28–35, arXiv:1001.0092 [hep-ph].

[332] M. Aoki, S. Kanemura, and H. Yokoya, "Reconstruction of Inert Doublet Scalars at the International Linear Collider," *Phys.Lett.* **B725** (2013) 302–309, arXiv:1303.6191 [hep-ph].

[333] S.-Y. Ho and J. Tandean, "Probing Scotogenic Effects in e+e- Colliders," *Phys.Rev.* **D89** (2014) 114025, arXiv:1312.0931 [hep-ph].

[334] S.-Y. Ho and J. Tandean, "Probing Scotogenic Effects in Higgs Boson Decays," *Phys.Rev.* **D87** no. 9, (2013) 095015, arXiv:1303.5700 [hep-ph].

[335] Y. Kajiyama, J. Kubo, and H. Okada, "D(6) Family Symmetry and Cold Dark Matter at LHC," *Phys.Rev.* **D75** (2007) 033001, arXiv:hep-ph/0610072 [hep-ph].

[336] D. Suematsu, T. Toma, and T. Yoshida, "Enhancement of the annihilation of dark matter in a radiative seesaw model," *Phys.Rev.* **D82** (2010) 013012, arXiv:1002.3225 [hep-ph].

[337] Y. Kajiyama, H. Okada, and T. Toma, "Direct and Indirect Detection of Dark Matter in D_6 Flavor Symmetric Model," *Eur.Phys.J.* **C71** (2011) 1688, arXiv:1104.0367 [hep-ph].

[338] Y. Kajiyama, H. Okada, and T. Toma, "A Light Scalar Dark Matter for CoGeNT and DAMA in D_6 Flavor Symmetric Model," arXiv:1109.2722 [hep-ph].

[339] M. Klasen, C. E. Yaguna, J. D. Ruiz-Alvarez, D. Restrepo, and O. Zapata, "Scalar dark matter and fermion coannihilations in the radiative seesaw model," *JCAP* **1304** (2013) 044, arXiv:1302.5298 [hep-ph].

[340] A. Zee, "Quantum Numbers of Majorana Neutrino Masses," *Nucl.Phys.* **B264** (1986) 99.

[341] K. Babu, "Model of 'Calculable' Majorana Neutrino Masses," *Phys.Lett.* **B203** (1988) 132.

[342] J. Schechter and J. Valle, "Neutrinoless Double beta Decay in SU(2) x U(1) Theories," *Phys.Rev.* **D25** (1982) 2951.

[343] J. Peltoniemi and J. Valle, "Massive neutrinos and electroweak baryogenesis," *Phys.Lett.* **B304** (1993) 147–151, `arXiv:hep-ph/9301231 [hep-ph]`.

[344] M. Nebot, J. F. Oliver, D. Palao, and A. Santamaria, "Prospects for the Zee-Babu Model at the CERN LHC and low energy experiments," *Phys.Rev.* **D77** (2008) 093013, `arXiv:0711.0483 [hep-ph]`.

[345] D. Schmidt, T. Schwetz, and H. Zhang, "Status of the Zee-Babu model for neutrino mass and possible tests at a like-sign linear collider," `arXiv:1402.2251 [hep-ph]`.

[346] K. Babu and C. Macesanu, "Two loop neutrino mass generation and its experimental consequences," *Phys.Rev.* **D67** (2003) 073010, `arXiv:hep-ph/0212058 [hep-ph]`.

[347] D. Aristizabal Sierra and M. Hirsch, "Experimental tests for the Babu-Zee two-loop model of Majorana neutrino masses," *JHEP* **0612** (2006) 052, `arXiv:hep-ph/0609307 [hep-ph]`.

[348] J. Herrero-Garcia, M. Nebot, N. Rius, and A. Santamaria, "The Zee-Babu Model revisited in the light of new data," `arXiv:1402.4491 [hep-ph]`.

[349] L. M. Krauss, S. Nasri, and M. Trodden, "A Model for neutrino masses and dark matter," *Phys.Rev.* **D67** (2003) 085002, `arXiv:hep-ph/0210389 [hep-ph]`.

[350] J. N. Ng and A. de la Puente, "Top Quark as a Dark Portal and Neutrino Mass Generation," *Phys.Lett.* **B727** (2013) 204–210, `arXiv:1307.2606`.

[351] A. Ahriche, C.-S. Chen, K. L. McDonald, and S. Nasri, "A Three-Loop Model of Neutrino Mass with Dark Matter," *Phys.Rev.* **D90** (2014) 015024, `arXiv:1404.2696 [hep-ph]`.

[352] M. Aoki, S. Kanemura, and O. Seto, "Neutrino mass, Dark Matter and Baryon Asymmetry via TeV-Scale Physics without Fine-Tuning," *Phys.Rev.Lett.* **102** (2009) 051805, arXiv:0807.0361 [hep-ph].

[353] M. Aoki, S. Kanemura, and O. Seto, "A Model of TeV Scale Physics for Neutrino Mass, Dark Matter and Baryon Asymmetry and its Phenomenology," *Phys.Rev.* **D80** (2009) 033007, arXiv:0904.3829 [hep-ph].

[354] M. Gustafsson, J. M. No, and M. A. Rivera, "Predictive Model for Radiatively Induced Neutrino Masses and Mixings with Dark Matter," *Phys.Rev.Lett.* **110** no. 21, (2013) 211802, arXiv:1212.4806 [hep-ph].

[355] C.-S. Chen, K. L. McDonald, and S. Nasri, "A Class of Three-Loop Models with Neutrino Mass and Dark Matter," arXiv:1404.6033 [hep-ph].

[356] R. Cowsik and J. McClelland, "An Upper Limit on the Neutrino Rest Mass," *Phys.Rev.Lett.* **29** (1972) 669–670.

[357] S. Dodelson and L. M. Widrow, "Sterile-neutrinos as dark matter," *Phys.Rev.Lett.* **72** (1994) 17–20, arXiv:hep-ph/9303287 [hep-ph].

[358] V. K. Narayanan, D. N. Spergel, R. Dave, and C.-P. Ma, "Constraints on the mass of warm dark matter particles and the shape of the linear power spectrum from the Lyα forest," *Astrophys.J.* **543** (2000) L103–L106, arXiv:astro-ph/0005095 [astro-ph].

[359] X.-D. Shi and G. M. Fuller, "A New dark matter candidate: Nonthermal sterile neutrinos," *Phys.Rev.Lett.* **82** (1999) 2832–2835, arXiv:astro-ph/9810076 [astro-ph].

[360] M. Shaposhnikov and I. Tkachev, "The nuMSM, inflation, and dark matter," *Phys.Lett.* **B639** (2006) 414–417, arXiv:hep-ph/0604236 [hep-ph].

[361] A. Boyarsky, O. Ruchayskiy, D. Iakubovskyi, and J. Franse, "An unidentified line in X-ray spectra of the Andromeda galaxy and Perseus galaxy cluster," arXiv:1402.4119 [astro-ph.CO].

[362] A. Kusenko, "Sterile neutrinos: The Dark side of the light fermions," *Phys.Rept.* **481** (2009) 1–28, arXiv:0906.2968 [hep-ph].

[363] P.-K. Hu, "Radiative Seesaw Model with Non-zero θ_{13} and Warm Dark Matter Scenario," arXiv:1208.2613 [hep-ph].

[364] M. Hirsch, R. Lineros, S. Morisi, J. Palacio, N. Rojas, *et al.*, "WIMP dark matter as radiative neutrino mass messenger," *JHEP* **1310** (2013) 149, arXiv:1307.8134 [hep-ph].

[365] V. Brdar, I. Picek, and B. Radovcic, "Radiative Neutrino Mass with Scotogenic Scalar Triplet," *Phys.Lett.* **B728** (2014) 198–201, arXiv:1310.3183 [hep-ph].

[366] D. Restrepo, O. Zapata, and C. E. Yaguna, "Models with radiative neutrino masses and viable dark matter candidates," *JHEP* **1311** (2013) 011, arXiv:1308.3655 [hep-ph].

[367] S. S. Law and K. L. McDonald, "A Class of Inert N-tuplet Models with Radiative Neutrino Mass and Dark Matter," *JHEP* **1309** (2013) 092, arXiv:1305.6467 [hep-ph].

[368] N. Okada and O. Seto, "Higgs portal dark matter in the minimal gauged $U(1)_{B-L}$ model," *Phys.Rev.* **D82** (2010) 023507, arXiv:1002.2525 [hep-ph].

[369] M. Ibe, S. Matsumoto, and T. T. Yanagida, "The GeV-scale dark matter with B-L asymmetry," *Phys.Lett.* **B708** (2012) 112–118, arXiv:1110.5452 [hep-ph].

[370] B. Batell, "Dark Discrete Gauge Symmetries," *Phys.Rev.* **D83** (2011) 035006, arXiv:1007.0045 [hep-ph].

[371] K. Hamaguchi, Y. Nomura, and T. Yanagida, "Superheavy dark matter with discrete gauge symmetries," *Phys.Rev.* **D58** (1998) 103503, arXiv:hep-ph/9805346 [hep-ph].

[372] K. Hamaguchi, Y. Nomura, and T. Yanagida, "Longlived superheavy dark matter with discrete gauge symmetries," *Phys.Rev.* **D59** (1999) 063507, arXiv:hep-ph/9809426 [hep-ph].

[373] M. Cirelli, N. Fornengo, and A. Strumia, "Minimal dark matter," *Nucl.Phys.* **B753** (2006) 178–194, arXiv:hep-ph/0512090 [hep-ph].

[374] L. Lavoura, S. Morisi, and J. Valle, "Accidental Stability of Dark Matter," *JHEP* **1302** (2013) 118, arXiv:1205.3442 [hep-ph].

[375] O. Cata and A. Ibarra, "Dark Matter Stability without New Symmetries," *Phys.Rev.* **D90** (2014) 063509, arXiv:1404.0432 [hep-ph].

[376] T. Hambye, "On the stability of particle dark matter," *PoS* **IDM2010** (2011) 098, arXiv:1012.4587 [hep-ph].

[377] M. Hirsch, S. Morisi, E. Peinado, and J. Valle, "Discrete dark matter," *Phys.Rev.* **D82** (2010) 116003, arXiv:1007.0871 [hep-ph].

[378] Y. Kajiyama and H. Okada, "T(13) Flavor Symmetry and Decaying Dark Matter," *Nucl.Phys.* **B848** (2011) 303–313, arXiv:1011.5753 [hep-ph].

[379] D. Meloni, S. Morisi, and E. Peinado, "Stability of dark matter from the D4xZ2 flavor group," *Phys.Lett.* **B703** (2011) 281–287, arXiv:1104.0178 [hep-ph].

[380] Y. Kajiyama, K. Kannike, and M. Raidal, "Symmetryless Dark Matter," *Phys.Rev.* **D85** (2012) 033008, arXiv:1111.1270 [hep-ph].

[381] Y. Daikoku, H. Okada, and T. Toma, "Two Component Dark Matters in $S_4 \times Z_2$ Flavor Symmetric Extra $U(1)$ Model," *Prog.Theor.Phys.* **126** (2011) 855–883, arXiv:1106.4717 [hep-ph].

[382] N. Haba, Y. Kajiyama, S. Matsumoto, H. Okada, and K. Yoshioka, "Universally Leptophilic Dark Matter From Non-Abelian Discrete Symmetry," *Phys.Lett.* **B695** (2011) 476–481, arXiv:1008.4777 [hep-ph].

[383] D. Meloni, S. Morisi, and E. Peinado, "Neutrino phenomenology and stable dark matter with A4," *Phys.Lett.* **B697** (2011) 339–342, arXiv:1011.1371 [hep-ph].

[384] A. Adulpravitchai, B. Batell, and J. Pradler, "Non-Abelian Discrete Dark Matter," *Phys.Lett.* **B700** (2011) 207–216, arXiv:1103.3053 [hep-ph].

[385] F. Bishara and J. Zupan, "Continuous Flavor Symmetries and the Stability of Asymmetric Dark Matter," arXiv:1408.3852 [hep-ph].

[386] J. F. Gunion, H. E. Haber, G. L. Kane, and S. Dawson, "The Higgs Hunter's Guide," *Front.Phys.* **80** (2000) 1–448.

[387] R. de Adelhart Toorop, F. Bazzocchi, and S. Morisi, "Quark mixing in the discrete dark matter model," *Nucl.Phys.* **B856** (2012) 670–681, arXiv:1104.5676 [hep-ph].

[388] Y. Hamada, T. Kobayashi, A. Ogasahara, Y. Omura, F. Takayama, *et al.*, "Revisiting Discrete Dark Matter Model: $\theta_{13} \neq 0$ and ν_R Dark Matter," arXiv:1405.3592 [hep-ph].

[389] Y. Ahn and S. K. Kang, "Non-zero θ_{13} and CP violation in a model with A_4 flavor symmetry," *Phys.Rev.* **D86** (2012) 093003, arXiv:1203.4185 [hep-ph].

[390] G. Branco, P. Ferreira, L. Lavoura, M. Rebelo, M. Sher, *et al.*, "Theory and phenomenology of two-Higgs-doublet models," *Phys.Rept.* **516** (2012) 1–102, arXiv:1106.0034 [hep-ph].

[391] N. G. Deshpande and E. Ma, "Pattern of Symmetry Breaking with Two Higgs Doublets," *Phys.Rev.* **D18** (1978) 2574.

[392] R. Barbieri, L. J. Hall, and V. S. Rychkov, "Improved naturalness with a heavy Higgs: An Alternative road to LHC physics," *Phys.Rev.* **D74** (2006) 015007, arXiv:hep-ph/0603188 [hep-ph].

[393] L. Lopez Honorez, E. Nezri, J. F. Oliver, and M. H. Tytgat, "The Inert Doublet Model: An Archetype for Dark Matter," *JCAP* **0702** (2007) 028, arXiv:hep-ph/0612275 [hep-ph].

[394] E. Lundstrom, M. Gustafsson, and J. Edsjo, "The Inert Doublet Model and LEP II Limits," *Phys.Rev.* **D79** (2009) 035013, arXiv:0810.3924 [hep-ph].

[395] G. Belanger, B. Dumont, U. Ellwanger, J. Gunion, and S. Kraml, "Global fit to Higgs signal strengths and couplings and implications for extended Higgs sectors," *Phys.Rev.* **D88** (2013) 075008, arXiv:1306.2941 [hep-ph].

[396] C. E. Yaguna, "Large contributions to dark matter annihilation from three-body final states," *Phys.Rev.* **D81** (2010) 075024, arXiv:1003.2730 [hep-ph].

[397] M. E. Peskin and T. Takeuchi, "Estimation of oblique electroweak corrections," *Phys.Rev.* **D46** (1992) 381–409.

[398] W. Grimus, L. Lavoura, O. Ogreid, and P. Osland, "The Oblique parameters in multi-Higgs-doublet models," *Nucl.Phys.* **B801** (2008) 81–96, arXiv:0802.4353 [hep-ph].

[399] W. Grimus, L. Lavoura, O. Ogreid, and P. Osland, "A Precision constraint on multi-Higgs-doublet models," *J.Phys.* **G35** (2008) 075001, arXiv:0711.4022 [hep-ph].

[400] **Particle Data Group** Collaboration, K. Nakamura *et al.*, "Review of particle physics," *J.Phys.* **G37** (2010) 075021.

[401] A. Pierce and J. Thaler, "Natural Dark Matter from an Unnatural Higgs Boson and New Colored Particles at the TeV Scale," *JHEP* **0708** (2007) 026, arXiv:hep-ph/0703056 [HEP-PH].

[402] G. Belanger, F. Boudjema, P. Brun, A. Pukhov, S. Rosier-Lees, *et al.*, "Indirect search for dark matter with micrOMEGAs2.4," *Comput.Phys.Commun.* **182** (2011) 842–856, arXiv:1004.1092 [hep-ph].

[403] G. Belanger, F. Boudjema, A. Pukhov, and A. Semenov, "Dark matter direct detection rate in a generic model with micrOMEGAs 2.2," *Comput.Phys.Commun.* **180** (2009) 747–767, arXiv:0803.2360 [hep-ph].

[404] L. Lopez Honorez and C. E. Yaguna, "A new viable region of the inert doublet model," *JCAP* **1101** (2011) 002, arXiv:1011.1411 [hep-ph].

[405] N. Fornengo, S. Scopel, and A. Bottino, "Discussing direct search of dark matter particles in the Minimal Supersymmetric extension of the Standard Model with light neutralinos," *Phys.Rev.* **D83** (2011) 015001, arXiv:1011.4743 [hep-ph].

[406] **CDMS-II Collaboration** Collaboration, Z. Ahmed *et al.*, "Results from a Low-Energy Analysis of the CDMS II Germanium Data," *Phys.Rev.Lett.* **106** (2011) 131302, arXiv:1011.2482 [astro-ph.CO].

[407] **XENON100 Collaboration** Collaboration, E. Aprile *et al.*, "First Dark Matter Results from the XENON100 Experiment," *Phys.Rev.Lett.* **105** (2010) 131302, arXiv:1005.0380 [astro-ph.CO].

[408] **Fermi-LAT Collaboration** Collaboration, A. Abdo *et al.*, "Observations of Milky Way Dwarf Spheroidal galaxies with the Fermi-LAT detector and constraints on Dark Matter models," *Astrophys.J.* **712** (2010) 147–158, arXiv:1001.4531 [astro-ph.CO].

[409] **Fermi-LAT Collaboration** Collaboration, A. Abdo *et al.*, "Constraints on Cosmological Dark Matter Annihilation from the Fermi-LAT Isotropic Diffuse Gamma-Ray Measurement," *JCAP* **1004** (2010) 014, arXiv:1002.4415 [astro-ph.CO].

[410] K. N. Abazajian, S. Blanchet, and J. P. Harding, "Current and Future Constraints on Dark Matter from Prompt and Inverse-Compton Photon Emission in the Isotropic Diffuse Gamma-ray Background," *Phys.Rev.* **D85** (2012) 043509, arXiv:1011.5090 [hep-ph].

[411] M. Ibe, H. Murayama, and T. Yanagida, "Breit-Wigner Enhancement of Dark Matter Annihilation," *Phys.Rev.* **D79** (2009) 095009, arXiv:0812.0072 [hep-ph].

[412] W.-L. Guo and Y.-L. Wu, "Enhancement of Dark Matter Annihilation via Breit-Wigner Resonance," *Phys.Rev.* **D79** (2009) 055012, arXiv:0901.1450 [hep-ph].

[413] D. Feldman, Z. Liu, and P. Nath, "PAMELA Positron Excess as a Signal from the Hidden Sector," *Phys.Rev.* **D79** (2009) 063509, arXiv:0810.5762 [hep-ph].

[414] M. Ibe, Y. Nakayama, H. Murayama, and T. T. Yanagida, "Nambu-Goldstone Dark Matter and Cosmic Ray Electron and Positron Excess," *JHEP* **0904** (2009) 087, arXiv:0902.2914 [hep-ph].

[415] M. Ackermann, M. Ajello, A. Allafort, L. Baldini, J. Ballet, *et al.*, "Constraints on Dark Matter Annihilation in Clusters of Galaxies with the Fermi Large Area Telescope," *JCAP* **1005** (2010) 025, arXiv:1002.2239 [astro-ph.CO].

[416] M. Papucci and A. Strumia, "Robust implications on Dark Matter from the first FERMI sky gamma map," *JCAP* **1003** (2010) 014, arXiv:0912.0742 [hep-ph].

[417] M. Cirelli, P. Panci, and P. D. Serpico, "Diffuse gamma ray constraints on annihilating or decaying Dark Matter after Fermi," *Nucl.Phys.* **B840** (2010) 284–303, arXiv:0912.0663 [astro-ph.CO].

[418] **Fermi-LAT collaboration** Collaboration, G. Zaharijas, A. Cuoco, Z. Yang, and J. Conrad, "Constraints on the Galactic Halo Dark Matter from Fermi-LAT Diffuse Measurements," *PoS* **IDM2010** (2011) 111, arXiv:1012.0588 [astro-ph.HE].

[419] **Fermi-LAT Collaboration** Collaboration, B. Anderson, "Fermi-LAT constraints on diffuse Dark Matter annihilation from the Galactic Halo," *PoS* **IDM2010** (2011) 113, arXiv:1012.0863 [hep-ph].

[420] A. Cuoco, A. Sellerholm, J. Conrad, and S. Hannestad, "Anisotropies in the Diffuse Gamma-Ray Background from Dark Matter with Fermi LAT: a closer look," *Mon.Not.Roy.Astron.Soc.* **414** (2011) 2040–2054, arXiv:1005.0843 [astro-ph.HE].

[421] **ATLAS Collaboration** Collaboration, "Constraints on New Phenomena via Higgs Coupling Measurements with the ATLAS Detector,".

[422] **CMS Collaboration** Collaboration, S. Chatrchyan *et al.*, "Search for invisible decays of Higgs bosons in the vector boson fusion and associated ZH production modes," *Eur.Phys.J.* **C74** (2014) 2980, arXiv:1404.1344 [hep-ex].

[423] G. Belanger, F. Boudjema, A. Pukhov, and A. Semenov, "micrOMEGAs4.1: two dark matter candidates," arXiv:1407.6129 [hep-ph].

[424] D. A. Eby and P. H. Frampton, "Dark Matter from Binary Tetrahedral Flavor Symmetry," *Phys.Lett.* **B713** (2012) 249–254, arXiv:1111.4938 [hep-ph].

[425] L. Lavoura, "On a possible relationship between lepton mixing and the stability of dark matter," *J.Phys.* **G39** (2012) 025202, arXiv:1109.6854 [hep-ph].

[426] **Daya Bay Collaboration** Collaboration, F. An *et al.*, "Spectral measurement of electron antineutrino oscillation amplitude and frequency at Daya Bay," *Phys.Rev.Lett.* **112** (2014) 061801, arXiv:1310.6732 [hep-ex].

[427] **Double Chooz Collaboration** Collaboration, Y. Abe *et al.*, "Improved measurements of the neutrino mixing angle θ_{13} with the Double Chooz detector," arXiv:1406.7763 [hep-ex].

[428] C. Luhn, S. Nasri, and P. Ramond, "The Flavor group $\Delta(3N^2)$," *J.Math.Phys.* **48** (2007) 073501, arXiv:hep-th/0701188 [hep-th].

[429] H. Ishimori, T. Kobayashi, H. Ohki, Y. Shimizu, H. Okada, *et al.*, "Non-Abelian Discrete Symmetries in Particle Physics," *Prog.Theor.Phys.Suppl.* **183** (2010) 1–163, arXiv:1003.3552 [hep-th].

[430] H. Ishimori, T. Kobayashi, H. Okada, Y. Shimizu, and M. Tanimoto, "Lepton Flavor Model from Delta(54) Symmetry," *JHEP* **0904** (2009) 011, arXiv:0811.4683 [hep-ph].

[431] B. Schwingenheuer, "Searches for neutrinoless double beta decay," *J.Phys.Conf.Ser.* **375** (2012) 042007, arXiv:1201.4916 [hep-ex].

[432] W. Rodejohann, "Neutrino-less Double Beta Decay and Particle Physics," *Int.J.Mod.Phys.* **E20** (2011) 1833–1930, arXiv:1106.1334 [hep-ph].

[433] **KATRIN Collaboration** Collaboration, A. Osipowicz *et al.*, "KATRIN: A Next generation tritium beta decay experiment with sub-eV sensitivity for the electron neutrino mass. Letter of intent," arXiv:hep-ex/0109033 [hep-ex].

[434] **WMAP Collaboration** Collaboration, E. Komatsu *et al.*, "Seven-Year Wilkinson Microwave Anisotropy Probe (WMAP) Observations: Cosmological Interpretation," *Astrophys.J.Suppl.* **192** (2011) 18, arXiv:1001.4538 [astro-ph.CO].

[435] L. Dorame, D. Meloni, S. Morisi, E. Peinado, and J. Valle, "Constraining Neutrinoless Double Beta Decay," *Nucl.Phys.* **B861** (2012) 259–270, arXiv:1111.5614 [hep-ph].

[436] J. Schechter and J. Valle, "Majorana Neutrinos and Magnetic Fields," *Phys.Rev.* **D24** (1981) 1883–1889.

[437] T. Schwetz, M. Tortola, and J. Valle, "Where we are on θ_{13}: addendum to 'Global neutrino data and recent reactor fluxes: status of three-flavour oscillation parameters'," *New J.Phys.* **13** (2011) 109401, arXiv:1108.1376 [hep-ph].

[438] **T2K Collaboration** Collaboration, K. Abe *et al.*, "Indication of Electron Neutrino Appearance from an Accelerator-produced Off-axis Muon Neutrino Beam," *Phys.Rev.Lett.* **107** (2011) 041801, arXiv:1106.2822 [hep-ex].

[439] S. B. Giddings and A. Strominger, "Loss of Incoherence and Determination of Coupling Constants in Quantum Gravity," *Nucl.Phys.* **B307** (1988) 854.

[440] T. Banks and N. Seiberg, "Symmetries and Strings in Field Theory and Gravity," *Phys.Rev.* **D83** (2011) 084019, arXiv:1011.5120 [hep-th].

[441] M. Kamionkowski and J. March-Russell, "Planck scale physics and the Peccei-Quinn mechanism," *Phys.Lett.* **B282** (1992) 137–141, arXiv:hep-th/9202003 [hep-th].

[442] R. Holman, S. D. Hsu, T. W. Kephart, E. W. Kolb, R. Watkins, *et al.*, "Solutions to the strong CP problem in a world with gravity," *Phys.Lett.* **B282** (1992) 132–136, arXiv:hep-ph/9203206 [hep-ph].

[443] E. Masso, F. Rota, and G. Zsembinszki, "Planck-scale effects on global symmetries: Cosmology of pseudo-Goldstone bosons," *Phys.Rev.* **D70** (2004) 115009, arXiv:hep-ph/0404289 [hep-ph].

[444] E. K. Akhmedov, Z. Berezhiani, R. Mohapatra, and G. Senjanovic, "Planck scale effects on the majoron," *Phys.Lett.* **B299** (1993) 90–93, arXiv:hep-ph/9209285 [hep-ph].

[445] V. Berezinsky and J. Valle, "The KeV majoron as a dark matter particle," *Phys.Lett.* **B318** (1993) 360–366, arXiv:hep-ph/9309214 [hep-ph].

[446] V. Berezinsky, A. S. Joshipura, and J. Valle, "Gravitational violation of R-parity and its cosmological signatures," *Phys.Rev.* **D57** (1998) 147–151, arXiv:hep-ph/9608307 [hep-ph].

[447] I. Rothstein, K. Babu, and D. Seckel, "Planck scale symmetry breaking and majoron physics," *Nucl.Phys.* **B403** (1993) 725–748, arXiv:hep-ph/9301213 [hep-ph].

[448] C. Burgess, M. Pospelov, and T. ter Veldhuis, "The Minimal model of nonbaryonic dark matter: A Singlet scalar," *Nucl.Phys.* **B619** (2001) 709–728, arXiv:hep-ph/0011335 [hep-ph].

[449] J. McDonald, "Gauge singlet scalars as cold dark matter," *Phys.Rev.* **D50** (1994) 3637–3649, arXiv:hep-ph/0702143 [HEP-PH].

[450] G. Belanger, F. Boudjema, A. Pukhov, and A. Semenov, "MicrOMEGAs 2.0: A Program to calculate the relic density of dark matter in a generic model," *Comput.Phys.Commun.* **176** (2007) 367–382, arXiv:hep-ph/0607059 [hep-ph].

[451] **Fermi-LAT collaboration** Collaboration, M. Ackermann *et al.*, "Constraining Dark Matter Models from a Combined Analysis of Milky Way Satellites with the Fermi Large Area Telescope," *Phys.Rev.Lett.* **107** (2011) 241302, arXiv:1108.3546 [astro-ph.HE].

[452] T. Cohen, J. Kearney, A. Pierce, and D. Tucker-Smith, "Singlet-Doublet Dark Matter," *Phys.Rev.* **D85** (2012) 075003, arXiv:1109.2604 [hep-ph].

[453] **Planck Collaboration** Collaboration, R. Adam *et al.*, "Planck intermediate results. XXX. The angular power spectrum of polarized dust emission at intermediate and high Galactic latitudes," arXiv:1409.5738 [astro-ph.CO].

[454] J. Amos, "Cosmic inflation: BICEP2 and Planck to share data,". http://www.bbc.com/news/science-environment-28127576.

[455] A. H. Guth, "The Inflationary Universe: A Possible Solution to the Horizon and Flatness Problems," *Phys.Rev.* **D23** (1981) 347–356.

[456] A. D. Linde, "Inflationary Cosmology," *Lect.Notes Phys.* **738** (2008) 1–54, arXiv:0705.0164 [hep-th].

[457] A. A. Starobinsky, "A New Type of Isotropic Cosmological Models Without Singularity," *Phys.Lett.* **B91** (1980) 99–102.

[458] S. Antusch and D. Nolde, "BICEP2 implications for single-field slow-roll inflation revisited," *JCAP* **1405** (2014) 035, arXiv:1404.1821 [hep-ph].

[459] J. Ellis, M. A. Garca, D. V. Nanopoulos, and K. A. Olive, "Resurrecting Quadratic Inflation in No-Scale Supergravity in Light of BICEP2," *JCAP* **1405** (2014) 037, arXiv:1403.7518 [hep-ph].

[460] S. Ferrara, A. Kehagias, and A. Riotto, "The Imaginary Starobinsky Model," *Fortsch.Phys.* **62** (2014) 573–583, arXiv:1403.5531 [hep-th].

[461] K. Harigaya, M. Ibe, K. Schmitz, and T. T. Yanagida, "Dynamical Chaotic Inflation in the Light of BICEP2," *Phys.Lett.* **B733** (2014) 283–287, arXiv:1403.4536 [hep-ph].

[462] N. Okada, V. N. enouz, and Q. Shafi, "Simple Inflationary Models in Light of BICEP2: an Update," arXiv:1403.6403 [hep-ph].

[463] R. Kallosh, A. Linde, and A. Westphal, "Chaotic Inflation in Supergravity after Planck and BICEP2," *Phys.Rev.* **D90** (2014) 023534, arXiv:1405.0270 [hep-th].

[464] Y. Chikashige, R. N. Mohapatra, and R. Peccei, "Are There Real Goldstone Bosons Associated with Broken Lepton Number?," *Phys.Lett.* **B98** (1981) 265.

[465] R. Kallosh and A. D. Linde, "Testing String Theory with CMB," *JCAP* **0704** (2007) 017, arXiv:0704.0647 [hep-th].

[466] M. U. Rehman and Q. Shafi, "Higgs Inflation, Quantum Smearing and the Tensor to Scalar Ratio," *Phys.Rev.* **D81** (2010) 123525, arXiv:1003.5915 [astro-ph.CO].

[467] M. U. Rehman, Q. Shafi, and J. R. Wickman, "GUT Inflation and Proton Decay after WMAP5," *Phys.Rev.* **D78** (2008) 123516, arXiv:0810.3625 [hep-ph].

[468] N. Okada and Q. Shafi, "Observable Gravity Waves From $U(1)_{B-L}$ Higgs and Coleman-Weinberg Inflation," arXiv:1311.0921 [hep-ph].

[469] M. Lattanzi and J. Valle, "Decaying warm dark matter and neutrino masses," *Phys.Rev.Lett.* **99** (2007) 121301, arXiv:0705.2406 [astro-ph].

[470] K. Nakayama, F. Takahashi, and T. T. Yanagida, "Chaotic Inflation with Right-handed Sneutrinos after Planck," *Phys.Lett.* **B730** (2014) 24–29, arXiv:1311.4253 [hep-ph].

[471] R. Kallosh, A. D. Linde, D. A. Linde, and L. Susskind, "Gravity and global symmetries," *Phys.Rev.* **D52** (1995) 912–935, arXiv:hep-th/9502069 [hep-th].

[472] M. Lattanzi, S. Riemer-Sorensen, M. Tortola, and J. W. F. Valle, "Updated CMB and x- and γ-ray constraints on Majoron dark matter," *Phys.Rev.* **D88** no. 6, (2013) 063528, arXiv:1303.4685 [astro-ph.HE].

[473] M. Frigerio, T. Hambye, and E. Masso, "Sub-GeV dark matter as pseudo-Goldstone from the seesaw scale," *Phys.Rev.* **X1** (2011) 021026, arXiv:1107.4564 [hep-ph].

[474] D. Kazanas, R. Mohapatra, S. Nasri, and V. Teplitz, "Neutrino mass, dark matter and inflation," *Phys.Rev.* **D70** (2004) 033015, arXiv:hep-ph/0403291 [hep-ph].

[475] M. Fukugita and T. Yanagida, "Baryogenesis Without Grand Unification," *Phys.Lett.* **B174** (1986) 45.

[476] G. Lazarides and Q. Shafi, "Origin of matter in the inflationary cosmology," *Phys.Lett.* **B258** (1991) 305–309.

[477] D. Aristizabal Sierra, M. Tortola, J. Valle, and A. Vicente, "Leptogenesis with a dynamical seesaw scale," *JCAP* **1407** (2014) 052, arXiv:1405.4706 [hep-ph].

[478] S. R. Coleman and E. J. Weinberg, "Radiative Corrections as the Origin of Spontaneous Symmetry Breaking," *Phys.Rev.* **D7** (1973) 1888–1910.

[479] **BICEP2 Collaboration** Collaboration, P. Ade *et al.*, "Detection of B-Mode Polarization at Degree Angular Scales by BICEP2," *Phys.Rev.Lett.* **112** (2014) 241101, arXiv:1403.3985 [astro-ph.CO].

[480] **Planck Collaboration** Collaboration, P. Ade *et al.*, "Planck 2013 results. I. Overview of products and scientific results," arXiv:1303.5062 [astro-ph.CO].

[481] V. N. Senoguz and Q. Shafi, "Chaotic inflation, radiative corrections and precision cosmology," *Phys.Lett.* **B668** (2008) 6–10, arXiv:0806.2798 [hep-ph].

[482] N. Okada, M. U. Rehman, and Q. Shafi, "Tensor to Scalar Ratio in Non-Minimal ϕ^4 Inflation," *Phys.Rev.* **D82** (2010) 043502, arXiv:1005.5161 [hep-ph].

[483] N. Okada, M. U. Rehman, and Q. Shafi, "Non-Minimal B-L Inflation with Observable Gravity Waves," *Phys.Lett.* **B701** (2011) 520–525, arXiv:1102.4747 [hep-ph].

[484] J. Martin, C. Ringeval, and V. Vennin, "Encyclopedia Inflationaris," *Phys.Dark Univ.* (2014) , arXiv:1303.3787 [astro-ph.CO].

[485] D. Salopek, J. Bond, and J. M. Bardeen, "Designing Density Fluctuation Spectra in Inflation," *Phys.Rev.* **D40** (1989) 1753.

[486] F. L. Bezrukov and M. Shaposhnikov, "The Standard Model Higgs boson as the inflaton," *Phys.Lett.* **B659** (2008) 703–706, arXiv:0710.3755 [hep-th].

[487] Y. Hamada, H. Kawai, K.-y. Oda, and S. C. Park, "Higgs inflation still alive," *Phys.Rev.Lett.* **112** (2014) 241301, arXiv:1403.5043 [hep-ph].

[488] P. Ramond, "Group theory: A physicist's survey," Cambridge University Press, 2010.